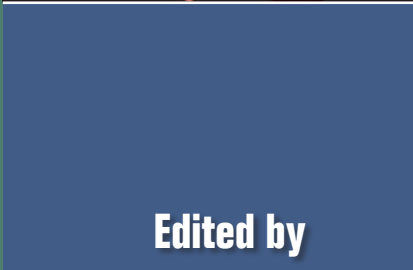
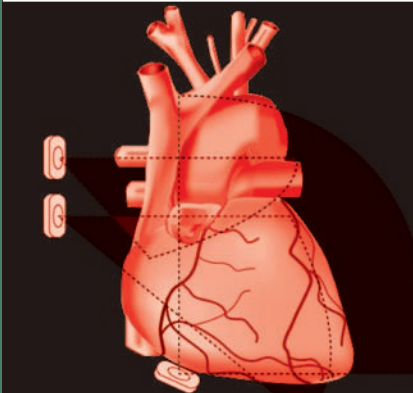
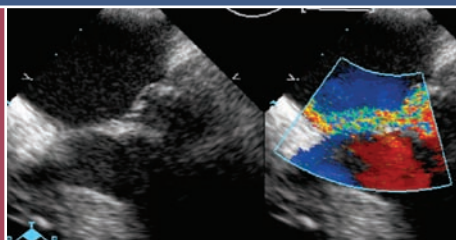
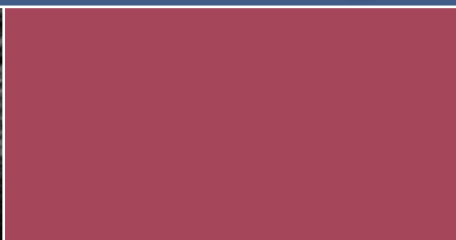
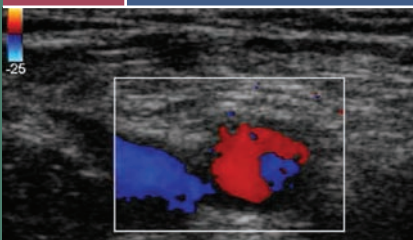
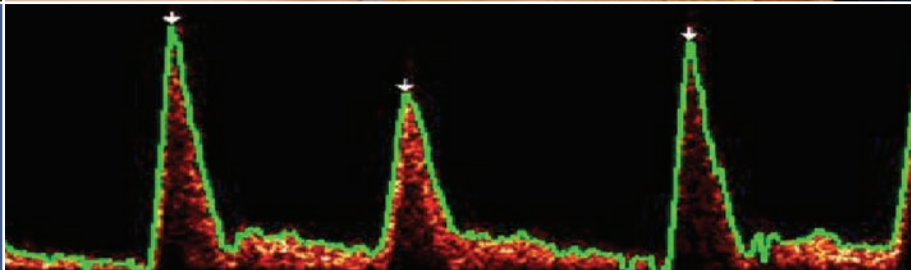


Practical Ultrasound in Anesthesia for Critical Care and Pain Management



Edited by



Philip M. Hopkins • A. R. Bodenham • Scott T. Reeves

informa
healthcare

Practical Ultrasound in Anesthesia for Critical Care and Pain Management

Practical Ultrasound in Anesthesia for Critical Care and Pain Management

Edited by

Philip M. Hopkins

*University of Leeds
Leeds, UK*

A. R. Bodenham

*Leeds General Infirmary
Leeds, UK*

Scott T. Reeves

*Medical University of South Carolina
Charleston, South Carolina, USA*

informa

healthcare

New York London

Informa Healthcare USA, Inc.
52 Vanderbilt Avenue
New York, NY 10017

© 2008 by Informa Healthcare USA, Inc.
Informa Healthcare is an Informa business

No claim to original U.S. Government works
Printed in the United States of America on acid-free paper
10 9 8 7 6 5 4 3 2 1

International Standard Book Number-10: 0-8247-2886-6 (Hardcover)
International Standard Book Number-13: 978-0-8247-2886-1 (Hardcover)

This book contains information obtained from authentic and highly regarded sources. Reprinted material is quoted with permission, and sources are indicated. A wide variety of references are listed. Reasonable efforts have been made to publish reliable data and information, but the author and the publisher cannot assume responsibility for the validity of all materials or for the consequence of their use.

No part of this book may be reprinted, reproduced, transmitted, or utilized in any form by any electronic, mechanical, or other means, now known or hereafter invented, including photocopying, microfilming, and recording, or in any information storage or retrieval system, without written permission from the publishers.

For permission to photocopy or use material electronically from this work, please access www.copyright.com (<http://www.copyright.com/>) or contact the Copyright Clearance Center, Inc. (CCC) 222 Rosewood Drive, Danvers, MA 01923, 978-750-8400. CCC is a not-for-profit organization that provides licenses and registration for a variety of users. For organizations that have been granted a photocopy license by the CCC, a separate system of payment has been arranged.

Trademark Notice: Product or corporate names may be trademarks or registered trademarks, and are used only for identification and explanation without intent to infringe.

Library of Congress Cataloging-in-Publication Data

Practical ultrasound in anesthesia for critical care and pain management / edited by Philip M. Hopkins, Andrew R. Bodenham, Scott T. Reeves.

p. ; cm.

Includes bibliographical references and index.

ISBN 978-0-8247-2886-1 (hb : alk. paper) 1. Ultrasonic imaging.
2. Anesthesia. 3. Critical care medicine. 4. Analgesia. I. Hopkins, Philip M. II. Bodenham, Andrew. III. Reeves, Scott T.

[DNLM: 1. Anesthesia—methods. 2. Critical Care—methods. 3. Pain—therapy.
4. Ultrasonography, Interventional—instrumentation. 5. Ultrasonography, Interventional—methods. WO 200 P8955 2008]

RC78.7.U4P733 2008

616.07'543—dc22

2008025112

For Corporate Sales and Reprint Permissions call 212-520-2700 or write to: Sales Department, 52 Vanderbilt Avenue, 7th floor, New York, NY 10017.

Visit the Informa Web site at
www.informa.com

and the Informa Healthcare Web site at
www.informahealthcare.com

To

My Savior, Jesus Christ, who gives me strength...

My wife, Cathy, who loves and puts up with me...

My children, Catherine, Carolyn, Townsend, who give me great joy...

My patients, who inspire me to do my best daily!

Scott T. Reeves, MD

Preface

The uses and applications of medical ultrasound are increasing, particularly outside traditional areas of radiology practice. Anesthesiology critical care and pain management are no exception. Just about every invasive procedure in the body can potentially be enhanced by the use of ultrasound. The introduction of small, portable, easy-to-use, and relatively inexpensive ultrasound machines has accelerated the use of such devices at the bedside by specialists in anesthesiology and related disciplines. Similar changes are occurring in other specialties such as surgery, accident and emergency medicine, and gastroenterology. Nevertheless, the use of such devices outside radiology has not met with universal approval. Issues of competency, training, and accreditation have all been raised and are clearly important as these techniques enter mainstream practice.

In this book, we provide core knowledge of how to use ultrasound devices safely. We then explain practical applications of these devices. The main areas where such techniques are to be used include the vascular system, the nervous system, the heart, the respiratory system, and miscellaneous other areas of the body. This will be of value to anesthesiologists and critical care physicians. Pain specialists will be interested in applications for nerve blocks. The book is not meant to be the definitive reference for ultrasound in these areas; rather it is aimed to provide a useful introduction combined with detailed practical information on the more commonly used applications. While catering to the needs of trainees in anesthesiology, critical care, and pain medicine who would want to apply the latest techniques from the outset, we also hope to assist accredited and certified specialists in these areas to introduce ultrasound techniques safely into their routine practice.

*Philip M. Hopkins
A. R. Bodenham
Scott T. Reeves*

Contents

| | |
|--|------------|
| <i>Preface</i> | v |
| <i>Contributors</i> | ix |
| | |
| 1. Applied Physics of Medical Ultrasound | 1 |
| <i>J. A. Evans</i> | |
| | |
| 2. Practical Applications—Getting the Best Out of Your Ultrasound Machine | 13 |
| <i>Heather Venables</i> | |
| | |
| 3. Assessment of Needle, Catheter, and Guidewire Position Using Ultrasonography | 27 |
| <i>G. A. Chapman and A. R. Bodenham</i> | |
| | |
| 4. Teaching, Training, and Accreditation | 47 |
| <i>Heather Venables</i> | |
| | |
| 5. Ultrasound-Guided Vascular Access | 57 |
| <i>A. R. Bodenham</i> | |
| | |
| 6. Ultrasound-Guided Peripheral and Regional Nerve Block | 71 |
| <i>Pawan K. Gupta and Philip M. Hopkins</i> | |
| | |
| 7. Transesophageal and Transthoracic Echocardiography: Examination Techniques and Views | 85 |
| <i>Bryan May, Kim Payne, and Scott T. Reeves</i> | |
| | |
| 8. Perioperative Transesophageal Echocardiography of the Heart Valves . . | 111 |
| <i>David A. Zvara, Daniel D. Amitie, Jason J. Baggett, and Christopher E. Beck</i> | |
| | |
| 9. Basic Echo Doppler | 147 |
| <i>Mary Beth Brady</i> | |

10. Transesophageal Doppler 167
Mark Hamilton and Monty Mythen

11. Transcranial Doppler Ultrasonography 179
Alet Jacobs and Ravi P. Mahajan

12. The Respiratory System 195
Daniel A. Lichtenstein

Index 217

Contributors

Daniel D. Amitie Section on Cardiothoracic Anesthesiology, The Wake Forest University School of Medicine, Winston-Salem, North Carolina, U.S.A.

Jason J. Baggett Section on Cardiothoracic Anesthesiology, The Wake Forest University School of Medicine, Winston-Salem, North Carolina, U.S.A.

Christopher E. Beck Section on Cardiothoracic Anesthesiology, The Wake Forest University School of Medicine, Winston-Salem, North Carolina, U.S.A.

A. R. Bodenham Academic and Clinical Departments of Anaesthesia and Intensive Care Medicine, Leeds General Infirmary, Leeds, U.K.

Mary Beth Brady Department of Anesthesiology and Critical Care Medicine, Johns Hopkins Medical Institutions, Johns Hopkins Medical Center, Baltimore, Maryland, U.S.A.

G. A. Chapman Academic and Clinical Departments of Anaesthesia and Intensive Care Medicine, Leeds General Infirmary, Leeds, U.K.

J. A. Evans Division of Medical Physics, Leeds Institute of Genetics Health and Therapeutics, University of Leeds, Leeds, U.K.

Pawan K. Gupta Leeds Teaching Hospitals NHS Trust, Leeds, U.K.

Mark Hamilton Department of Intensive Care, St. George's Hospital and Medical School, London, U.K.

Philip M. Hopkins University of Leeds, Leeds, U.K.

Alet Jacobs Department of Anaesthesia, Nottingham University Hospital, Queen's Medical Centre, Nottingham, U.K.

Daniel A. Lichtenstein Medical Intensive Care Unit, Hôpital Ambroise-Paré, Faculté Paris-Ouest, Boulogne, France

Ravi P. Mahajan University Division of Anaesthesia and Intensive Care, Queen's Medical Centre, Nottingham, U.K.

Bryan May Department of Anesthesia & Perioperative Medicine, Medical University of South Carolina, Charleston, South Carolina, U.S.A.

Monty Mythen Anaesthesia and Critical Care, Institute of Child Health, University College London, London, U.K.

Kim Payne Department of Anesthesia & Perioperative Medicine, Medical University of South Carolina, Charleston, South Carolina, U.S.A.

Scott T. Reeves Department of Anesthesia & Perioperative Medicine, Medical University of South Carolina, Charleston, South Carolina, U.S.A.

Heather Venables Education, Health & Sciences, University of Derby, Derby, U.K.

David A. Zvara Section on Cardiothoracic Anesthesiology, The Wake Forest University School of Medicine, Winston-Salem, North Carolina, U.S.A.

1

Applied Physics of Medical Ultrasound

J. A. Evans

*Division of Medical Physics, Leeds Institute of Genetics Health and Therapeutics,
University of Leeds, Leeds, U.K.*

INTRODUCTION

The Pulse-Echo Principle

Ultrasound imaging is deceptively simple in principle. At its core is the concept of echo formation. It can be illustrated as in Figure 1 by considering what happens when we shout in a confined space and listen for echoes. We quickly realize that the farther away the reflector is, the longer is the gap between our making the noise and the echo returning to us.

The distance D from the source to the wall can be estimated if we measure the time that elapses between the noise leaving us and the echo being received. If the speed at which the sound travels is c , then the time T is simply

$$T = 2D/c$$

Exactly the same principle applies in ultrasound imaging. The key components are as follows:

- A source
- A receiver
- A reflector
- A timer

We also need to know the speed at which the sound travels.

There are some further subtleties to consider, and these require us to look from above (Fig. 2). If the source of the noise spreads out as shown, although the distance to the reflector can be worked out, its direction is very uncertain. We cannot know where on the arc of the circle the reflector is situated, and we have no way of distinguishing echoes from positions a, b, and c.

To overcome this limitation, a narrow beam is needed. In fact, the narrower the beam is, the more certain we can be about the location of the reflector that caused any specific echo to be created. We should also note that we are assuming throughout that the sound travels in straight lines.

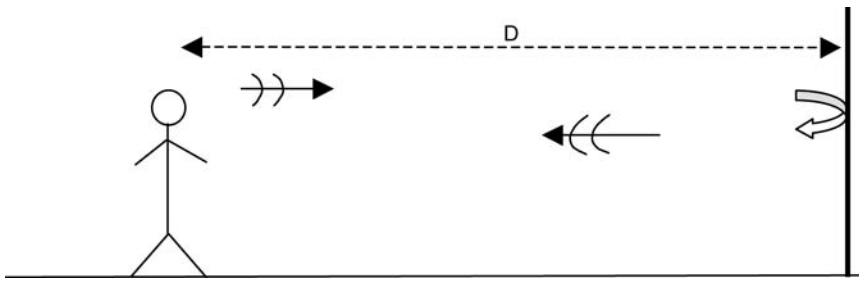


Figure 1 Pulse-echo principle.

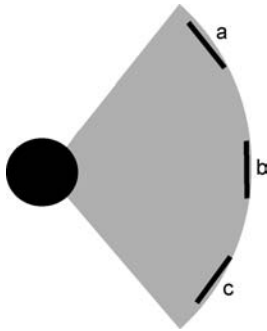


Figure 2 Reflectors at a, b, and c are indistinguishable if the beam diverges.

So we make the following extra assumptions:

- Sound travels in straight lines (rectilinear propagation).
- The sound beam is a thin pencil shape.

We will see later that there are circumstances in which these assumptions are invalid and give rise to image artifacts.

Pulse-Echo Ultrasound

So far everything has been considered in terms of a sound beam. We can translate these principles to ultrasound directly by making some changes. First, we recognize that ultrasound is no more than high-pitched sound. This does not mean louder; it means having a frequency that is above human hearing. Conventionally this is defined as being above 20,000 cycles per second, or 20 kHz. However, this definition should not be taken as meaning that there is a sharp cutoff. Some people's hearing will limit at lower frequencies, and some animals, such as bats, dogs, and dolphins, can create and detect higher frequencies. For medical imaging we go well beyond this point. The range of frequencies used clinically lie largely between 3 MHz and 15 MHz. There are no naturally occurring sources or detectors of such waves. Second, we need to recognize that the luxury of having only a single reflector is not one that is realistic in the body. There will be many reflectors of different shapes and sizes creating many different echoes. So to go to ultrasound, we replace the individual's voice and ears with a device called a transducer, and we replace the single reflector with multiple structures. This is illustrated in Figure 3.

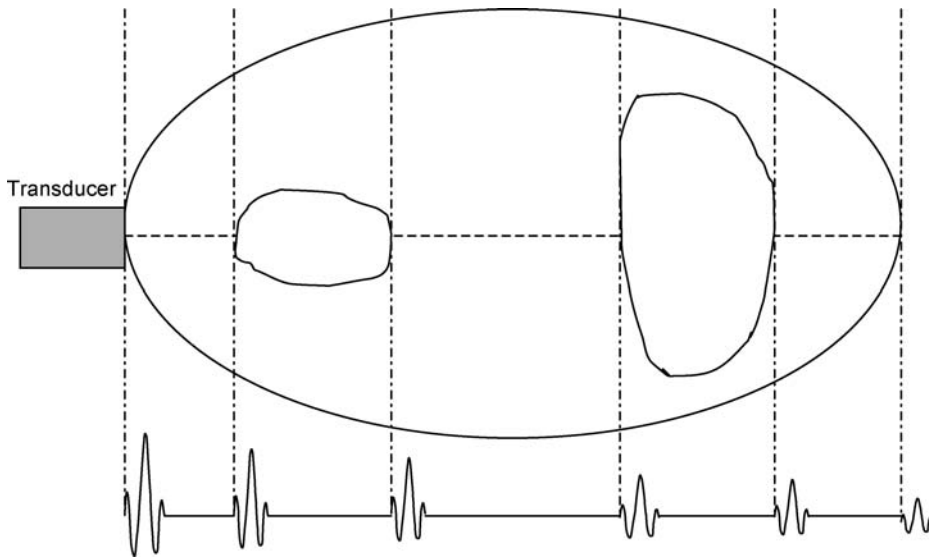


Figure 3 Echoes arising from a body section.

There are a number of aspects to note:

- A single ultrasound pulse can result in many echoes being generated.
- It is possible to tell the depth of the reflectors from their arrival time, subject to the assumptions identified above.
- In general, the echoes get smaller as the depth increases.

It is therefore important that the speed of sound be known. Potentially this is a problem because we would need to use different values when scanning different tissues. In practice, as can be seen from Table 1 below, the speed of sound in different soft tissues is remarkably similar.

This sound speed similarity is good news because it means that we can guess the value before we know the nature of tissue and be reasonably confident. In fact, all scanners are programmed in the factory to assume a value of 1540 m/sec, which is a good overall average for soft tissue. It is also clear that bone and lung, or indeed any gas collection, could potentially give large errors. However, as we shall see later, we never scan these for other reasons.

TGC

In order to transform the raw echo signals as illustrated in Figure 3 into a useful two-dimensional (2-D) image, two additional steps are needed. First, the size or amplitude of each individual echo is translated into a brightness or gray level. This brings with it a problem: as it stands, all of the echoes from nearby reflectors will be large and hence close to white, whereas those from great depths will be almost black. This does not represent the nature of the reflectors but simply their depth. To overcome this problem, scanners are fitted with a control called time gain compensation (TGC) or sometimes 'Swept Gain'. This control allows the operator to intervene and award more boost or gain to echoes from some depths than others. If this is correctly used, the result is that echoes from similar reflectors are represented as the same shade of gray regardless of their depth of origin. This is illustrated in Figure 4.

Table 1 Values for the Speed of Sound in Various Tissues

| Tissue | Speed of sound (m/sec) | Ref. |
|------------------|------------------------|------|
| Connective | 1613 | 1 |
| Muscle | 1547 | 1 |
| Fat | 1478 | 1 |
| Adipose | 1450 | 2 |
| Blood | 1584 | 2 |
| Brain | 1560 | 2 |
| Breast | 1510 | 2 |
| Kidney | 1560 | 2 |
| Liver | 1595 | 2 |
| Muscle, cardiac | 1576 | 2 |
| Muscle, skeletal | 1580 | 2 |
| Blood plasma | 1543 | 3 |
| Spinal cord | 1542 | 3 |
| Spleen | 1567 | 3 |
| Testis | 1595 | 3 |
| Lung | 600–1400 | 4 |
| Cortical bone | 4125 | 5 |

Source: From Refs. 4–8.

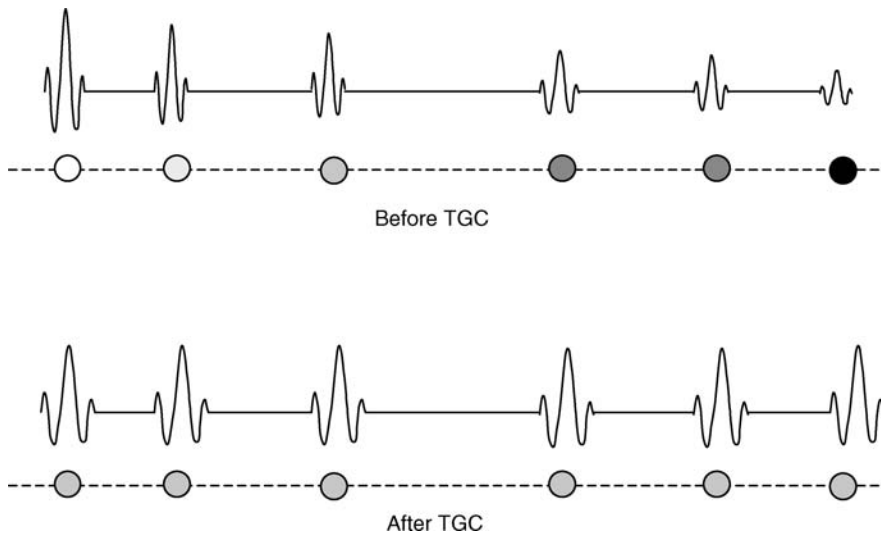


Figure 4 Use of TGC to equalize echo brightness. *Abbreviation:* TGC, time gain compensation.

IMAGE CREATION

The second step necessary to create an image is to acquire more sections. This could be done by mechanically moving the transducer so that it points in different directions at different times. This mode of operation is normally referred to as B mode (B for brightness). However, it is actually more convenient to have more than one transducer. These are frequently assembled into a single device called an array. Confusingly, the array is itself often called a transducer, whereas in fact it contains many small transducers.

We shall adopt that practice here and refer to the smaller component parts as transducer elements, or simply elements. This is illustrated in Figure 5.

The shape and size of arrays vary considerably since they are tailored to different clinical needs. The operator needs to select the best array in each case. However, arrays can be broadly categorized under three headings:

- Depth of penetration
- Field-of-view shape
- Contact length (footprint)

The depth of penetration is largely governed, as we shall see later, by the frequency of the transducer. Higher-frequency transducers penetrate less well but give better quality images.

There are fundamentally three types of arrays: linear, curvilinear, and phased. However, this terminology is not universally adopted by all manufacturers. Figure 6 shows these schematically.

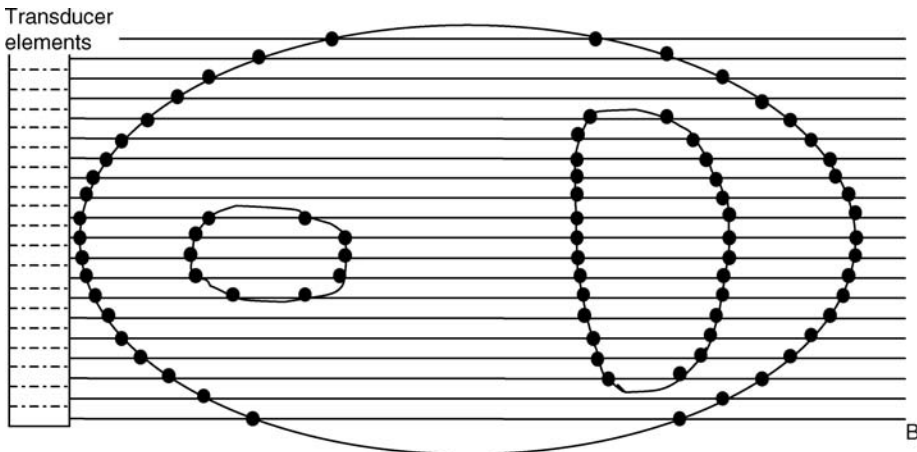


Figure 5 Use of an array transducer to create a 2-D image.

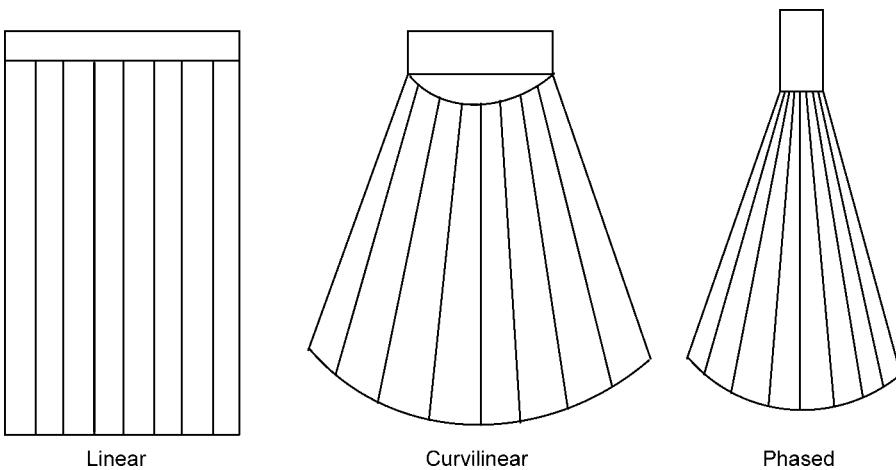


Figure 6 Array types.

Linear arrays have a rectangular field of view and are well suited to applications with reasonable access and a need to cover a lot of tissue close to the surface. Curvilinear arrays rely on being able to apply some pressure to the skin surface in order to make it deform to their shape. However once contact is established, a very wide field of view can be obtained. Phased arrays are ideally suited to applications with small access windows, e.g., scanning the heart while avoiding the lung field.

We now need to consider how long the image takes to create. Let us assume that the array in Figure 5 begins the process by sending a pulse from the top element at A. The system waits for echoes to come back from this line before sending out a pulse from the next line and so on until the last element is fired and the echoes from B have finally arrived. If successive lines are sent out too quickly, there is a danger that echoes will be misinterpreted as being associated with the wrong element, and ambiguity and artifacts will result. A single complete slice or frame therefore takes longer if more lines or elements are involved and also if a greater depth is selected. Once a slice is acquired, the process can begin again with a new pulse being sent out at A. In this way, a series of slices or frames is acquired, and these are presented to the display. In virtually all machines, the operator requires a real-time moving display and so the frames must be presented to the eye quickly enough for them to seem like a continuous moving image. In practice, this requires at least 20 frames per second. The implication of this for the operator is that the operator must avoid selecting a depth that is greater than that needed clinically. Any time that the machines uses to scan depths that are not relevant has to be paid for either by having a slower frame rate or by having fewer lines on the image and hence a poorer-quality display.

An alternative method of displaying the data is to retain its one-dimensional nature and use the other dimension to show time. This is illustrated in Figure 7. Let us assume that the structures at A and B are static, while those at C and D are moving. If we look at the line of dots representing the dashed section, we will see that the dots corresponding to A and B are static and those from C and D are backward and forward along the line of the display. This form of display is known as M-mode (M for motion) and is popular in cardiac applications.

Let us now turn our attention to what happens to the ultrasound pulse as it passes into the body. There are four processes that will concern us:

- Beam spreading
- Reflection
- Scatter
- Absorption

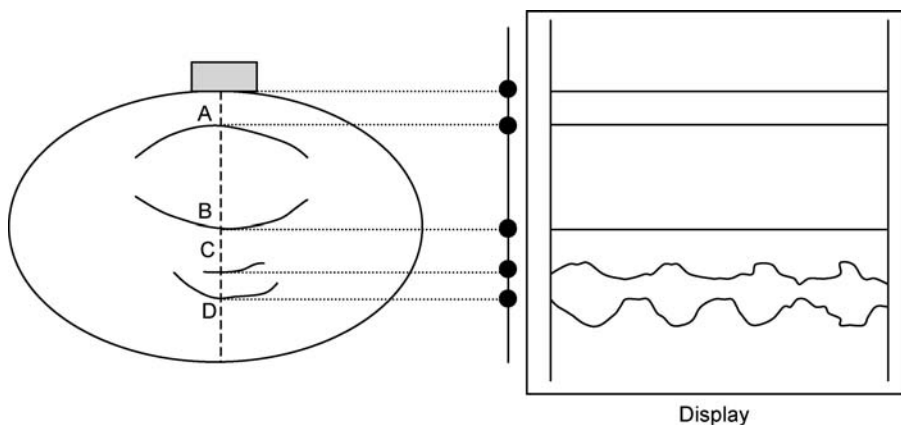


Figure 7 Principle of M-mode display.

Beam Spreading and Focusing

In the section “The Pulse-Echo Principle,” the need for the beam to be as narrow as possible was identified. The ideal beam is a thin pencil shape since this reduces the possibility of echoes from two different reflectors overlapping and causing ambiguity. Unfortunately, left to their own devices, beams from the transducer elements of the sort described above would diverge rapidly. A typical but somewhat idealized schematic of the beam shape is shown in Figure 8.

In Figure 8 the region close to the transducer, which is known as the near field, comes close to being the shape we need for imaging. The region beyond that, the far field, is very different, exhibiting rapid divergence and bringing with it degradation in image quality and resolution. For small transducer elements, the near field is very short (a few mm), and therefore most of the imaged region would be in the far field. In modern arrays, this problem is overcome by the use of electronic focusing, which has the effect of introducing a virtual lens. The effect is shown in Figure 9.

As is illustrated, the effect of using a focus is to improve the beam width at the selected depth and at depths close to it. However, the penalty is that away from the focal region, things have actually deteriorated and the divergence has increased. The operator normally has the freedom to select the focal depth by using the front panel controls of the scanner and so it is

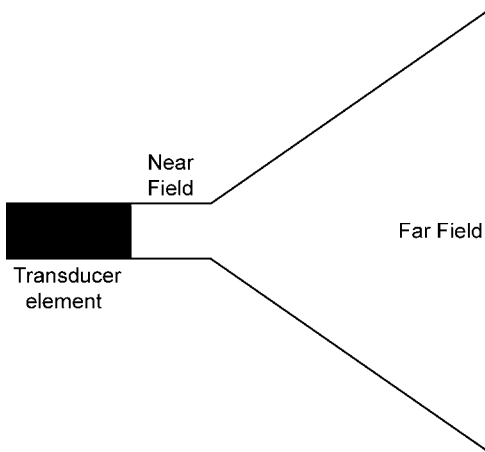


Figure 8 Idealized shape of an ultrasound beam from a small source.

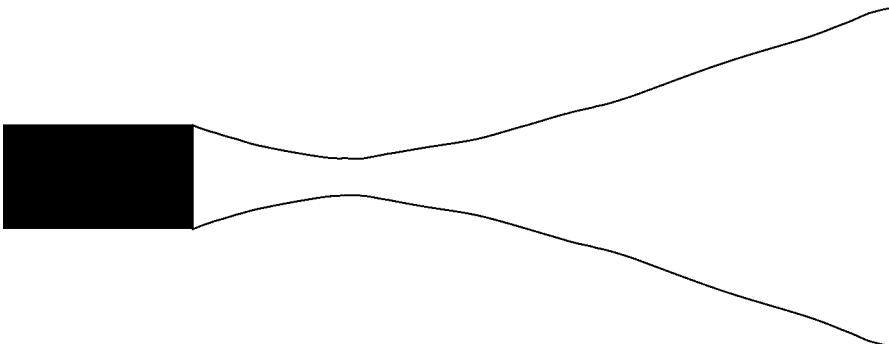


Figure 9 Effect of focusing on the beam shape.

important that the selected depth corresponds to the depth of clinical importance. An additional consideration is that the quality (narrowness) of the focus is better at higher frequencies. This is one reason for using as high a frequency as possible in each case.

Most scanners offer the possibility of using more than one focal depth. In effect the region is scanned repeatedly, with each repetition having the focus set to a different depth. This multiple zone focusing option certainly improves image quality. However because it requires several pulses per line instead of just one, there is a penalty to be paid, and this often manifests itself as a drop in the frame rate.

Reflection

There is a curious ambivalence about the identification of the ideal reflector. In order for it to be readily detectable, a reflector should send back a large echo to the sending transducer. That suggests that strong reflectors are ideal. However, as Figure 3 illustrates, we normally expect there to be many reflectors lying behind each other in a real body section. If the first reflector is a strong one, then there will be correspondingly less energy in the signal when it reaches subsequent reflectors, and hence our ability to detect them is reduced. In summary, we need weak reflectors for ideal imaging using pulse-echo techniques.

We can see reflections as arising at interfaces between different tissues or materials, e.g., muscle-blood or fat-liver. To predict the strength of the echo, we need a quantity known as acoustic impedance and often denoted by the symbol Z . This can be defined for a particular material as the product of two quantities, the density, ρ , and the speed of sound, c . So

$$Z = \rho c$$

It turns out that the fraction of energy, R , reflected at an interface depends on the difference in the Z values of the two materials. In fact

$$R = \frac{(Z_1 - Z_2)^2}{(Z_1 + Z_2)^2}$$

If we refer to Table 1, we can see that the values of c for soft tissues are very similar, and we would expect their densities also to be close. We would therefore predict that the Z values for all soft tissues would be much the same, and this turns out to be true. In other words the passage of an ultrasound beam from one soft tissue to another results in a modest-size echo being generated, which is exactly what we want.

The major exceptions are bone and gas. An interface between soft tissue and either of these will create a very strong echo. In case of gas, the interface presents as a near-perfect ultrasound mirror. This defines precisely where in the body ultrasound imaging will work and where it will fail. Behind such an interface, there will be a profound shadow from which little or no useful information can be gleaned.

It is also useful to recognize that both bone and gas collections have the same effect. Both will give strong white echoes on the display and create shadows. It is difficult to distinguish bone from gas by using ultrasound.

A practical point arising from this is the need to use coupling gels or oils. These obviously help lubricate the movement of the transducer over the patient, but crucially, they displace air from the transducer-skin interface, making scanning possible.

Another feature of reflection is the angular dependence of the reflected beam. If the interface is flat and smooth, then it behaves much like an optical mirror, as shown below in Figure 10.

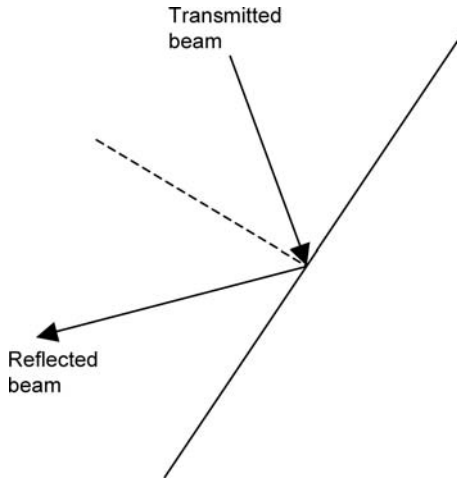


Figure 10 Reflection at a flat, smooth interface.

This potentially creates a problem. If the transducer is located at the top of the picture along the line of the transmitted beam, then it is expecting echoes along this same direction. As drawn, the echoes (no matter how strong) will not be detected. Fortunately, the body has very few large, flat, smooth interfaces and so there is no practical problem. However, there remains a significant angle dependency in real tissue. The consequence is that if the operator makes even a small change in the orientation of the transducer on the skin surface, the image will change. This leads, in part, to ultrasound's infamous operator dependency.

Scatter

The opposite end of the spatial scale is scatter. In this case, the target is assumed to be very small—much smaller than the beam or the wavelength. The idealized scatterer interacts only weakly with the beam but has the effect of redirecting the energy in all directions. In contrast to the ideal reflector, the scatterer can be detected from virtually all angles with equal facility. One example in the body is the erythrocyte, and this is critical as being the source of Doppler signals for blood flow measurement. Having said that, even this situation is not simple because of the presence of many other erythrocytes nearby. This turns the process into a complex multiple scattering one.

In general, real-life tissue interfaces do not behave exactly as ideal reflectors or scatterers but instead exhibit some properties of both. Fortunately, this actually works very well in practice even though it defies rigorous analysis.

Absorption

Unlike reflection and scatter, absorption is a nuisance with few redeeming features. It can be defined as the direct conversion of ultrasound energy into heat, and as such it is undesirable. In the absence of major reflecting interfaces, the ultrasound intensity drops off with increasing depth in an exponential manner.

In Figure 11 the upper trace shows the passage of a low-frequency wave through tissue. The lower trace is a wave at a higher frequency. It can be seen that the higher-frequency wave penetrates less well. The problem is that higher-frequency waves give

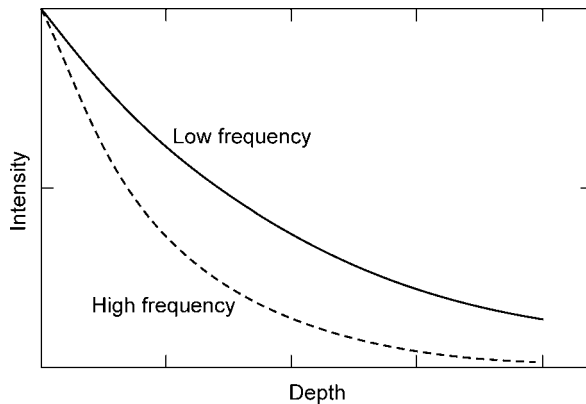


Figure 11 Exponential absorption.

better resolution, and hence we would always want to use as high a frequency as possible. This leads to the requirement for scanners to be equipped with a range of transducers working at different frequencies. The operator needs to make an educated guess at the start of the examination about how high a frequency can be used and select the appropriate transducer. Many modern transducers are capable at working at different frequencies, and if one of these is being used, then it should be set initially to as high a value as possible. So absorption not only causes unwanted patient heating but also limits the frequency and hence the resolution that can be achieved.

SAFETY

Ultrasound is generally considered a safe imaging modality. This is largely because it does not involve any of the problems associated with ionizing radiation, which constrain the use of modalities such as X ray, computed tomography (CT), positron emission tomography (PET), and nuclear medicine. Even magnetic resonance imaging (MRI) users have to give some thought to the possible risks of working close to a very strong magnetic field. However, despite an impeccable safety record, it is not appropriate to ignore the biological effects of ultrasound.

It is well known that ultrasound can cause biological effects in cells and certain animals. Furthermore the users of ultrasonic surgery, lithotripsy, and ultrasound physiotherapy would all testify to the fact that in some circumstances ultrasound can have quiet profound effects on living systems. There is a need to establish a safety gap between the levels used for these therapeutic applications and those used diagnostically. To establish these levels, we need to look at the mechanisms by which ultrasound can cause biological change.

There are three mechanisms by which ultrasound is known to cause biological damage:

- Cavitation
- Microstreaming
- Heating

This does not exclude the possibility that there might be other mechanisms, but it goes a long way toward explaining the observations so far in the literature.

Cavitation

Cavitation is concerned with the activity of bubbles. These will be small gas collections, normally pre-existing, in either the bloodstream or possibly interstitial spaces in tissue. Under the influence of an ultrasound wave, bubbles tend to oscillate. Since the wave consists of alternating positive and negative pressure phases, the bubbles will alternately be compressed and stretched. If the two processes (compression and rarefaction) were equally efficient, we would confidently expect equal reductions and increases in bubble size during these phases and no net change after the wave had passed. In fact this is not strictly what happens, and it turns out that the compressive process is somewhat less effective than the expansive one, and the net effect after several cycles is bubble growth. This is illustrated in Figure 12.

As a result the bubble steadily grows and oscillates. Its final size is limited by one of two processes. If the pressures are high, the bubble may eventually reach a size that cannot be supported and it will implode. This is called transient or inertial cavitation. It is associated momentarily with very high pressures and temperatures and is to be avoided. At lower pressures, a limiting size is reached at which the bubble stabilizes and oscillates. This is called stable or noninertial cavitation. It is likely to cause some local agitation, which may lead to biological change but on the whole is relatively benign. It is not surprising that cavitation is promoted by high negative pressures and low frequencies.

Microstreaming

It has been observed that the passage of an ultrasound wave through a liquid can cause a flow or stirring action, called microstreaming. It is not clear how significant this is, but it has been speculated that it may cause alteration in the permeability of the membranes of nearby cells.

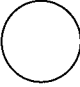

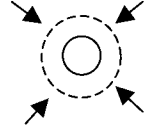

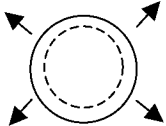
| Pressure | Bubble | Note |
|---|---|---|
| |  | Rest size |
|  |  | Compression phase – gas is driven into bubble |
|  |  | Rarefaction phase – gas pulled out of bubble |

Figure 12 Bubble oscillation while cavitating.

Heating

By far the mechanism that is currently causing most concern is heating. There is no doubt that all ultrasound exposures cause some heating due to the absorption process mentioned earlier. The issue is to minimize this and to find a method for predicting what the temperature rise will be in any specific situation. There is some helpful guidance from a number of bodies. For example, the World Federation for Ultrasound in Medicine and Biology (WFUMB) has published a number of safety statements, including:

A diagnostic exposure that produces a maximum in situ temperature rise of no more than 1.5°C above normal physiological levels (37°C) may be used clinically without reservation on thermal grounds.

This raises two questions. How can the operator know what the temperature rise is for any particular examination? Are temperature rises in excess of the value quoted necessarily harmful?

In order to provide some useful information to the operator, the National Electrical Manufacturers Association (NEMA) has agreed to adopt a system of providing on-screen labeling. This includes two indices, the mechanical index (MI) and the thermal index (TI). Their purpose is to advise the operator of the risk of damage due to either mechanical or thermal damage under any specific set of conditions. It is generally agreed that if the MI is less than 0.3, then the risk of cavitation damage is negligible. A TI value of 1 indicates that the worst-case temperature rise under the conditions prevailing at the time will be 1°C. Of course, the calculation on which this prediction is based has to assume certain tissue properties, and hence if there are particularly sensitive tissues involved, extra care is needed. Two specific examples are when scanning close to a bone interface, in which case the term used is the bone TI (TIB), and when working intracranially, in which case the term cranial TI (TIC) is used.

Of course, none of this advises the operator of what constitutes safe practice. It is left to professional bodies to do this. One useful source of such advice is the Web site administered by the British Medical Ultrasound Society (www.BMUS.org), which provides much more detail, practical advice, and help.

REFERENCES

1. Zagzebski JA. Essentials of Ultrasound Physics. St. Louis: Mosby, 1996.
2. Hoskins P, Thrush A, Martin K, et al. Diagnostic Ultrasound: Physics and Equipment. London: Greenwich Medical Media, 2003.
3. Hedrick WR, Hykes DL, Starchman DE. Ultrasound Physics and Instrumentation. 4th ed. St. Louis: Mosby, 2005.
4. Duck FA. Physical Properties of Tissue: A Comprehensive Reference Book. London: Academic Press, 1990.
5. Dunn F. Attenuation and speed of ultrasound in lung. J Acoust Soc Am 1986; 80(4):1248–1250.
6. International Commission on Radiation Units and Measurements. ICRU Report No. 61. Tissue substitutes, phantoms and computational modelling in medical ultrasound. Bethesda, MD: ICRU Publications, 1998.
7. Mast TD, Hinkelman LM, Orr MJ, et al. Simulation of acoustic pulse propagation through the abdominal wall. J Acoust Soc Am 1997; 102:1177–1190 (Erratum J Acoust Soc Am 1998; 102: 1122–1125).
8. McCarthy RN, Jeffcott LB, McCartney RN. Ultrasound speed in equine cortical bone: effects of orientation, density, porosity and temperature. J Biomech 1990; 23(11):1139–1143.

2

Practical Applications—Getting the Best Out of Your Ultrasound Machine

Heather Venables

Education, Health & Sciences, University of Derby, Derby, U.K.

INTRODUCTION

Recently, there has been an explosion in the use of ultrasound outside the confines of the conventional imaging department. Many specialties are waking up to the huge potential for focused ultrasound and ultrasound guidance for interventions. Unfortunately, to date, very few formal ultrasound courses are available or accessible to specialist groups. The result is, in some cases, the purchase and use of ultrasound equipment by individuals with little or no training.

The aim of this chapter is to provide clinicians who are new to ultrasound with some basic guidance on what to look for when purchasing a machine; it gives an overview of key equipment controls and indicates how these can be optimized. This is inevitably nothing more than an introduction, and readers are strongly encouraged to read further (see chap. 1 recommended texts).

HOW TO CHOOSE THE RIGHT MACHINE

In any area of ultrasound practice, both the specification of the equipment used and the operator's use of relevant equipment controls have a significant effect on the quality of images produced.

As computer-driven devices have become smaller, more powerful, and less expensive, there has been a shift towards the production of portable/handheld ultrasound systems. However, there is still a bewildering array of ultrasound equipment in the market, ranging in price from a few thousand pounds up to state-of-the-art cart-based machines in the region of Approx \$400,000.

It is not always easy to define which features of a machine are essential for a specific application, and it can sometimes be difficult to justify anything more than the most basic units in a nonconventional imaging setting. The Royal College of Anaesthetists, Critical Care and Pain Societies, and other relevant organizations have, to date, provided very little guidance.

BASIC COMPONENTS OF AN ULTRASOUND SYSTEM

Any ultrasound machine is composed of a transducer to transmit and receive ultrasound, a computer for storage and manipulation of the acquired data, and a monitor to display the image. Some form of image storage or hard copy device is needed to provide a permanent record of each examination.

The quality of the displayed data is determined by the skill of the operator and the inherent quality of each of the above components.

CART-BASED OR HANDHELD SYSTEMS

Many departments within the United Kingdom will have already purchased equipment to comply with guidelines from the National Institute for Health and Clinical Excellence (1) on the use of ultrasound in the placement of central venous catheters (CVCs). The most basic of these “palm top” devices (Fig. 1) are adequate for CVC placement but are of limited value in other applications such as the assessment of deep vein thromboses (DVTs) or focused cardiothoracic examinations. This is largely due to poor monitor quality, limited system resolution, and a limited choice of compatible transducers. Where there is enthusiasm to expand the use of ultrasound into other areas, this may be hindered by the limitations of existing equipment, and it may be difficult to justify early replacement. The choice of a very limited handheld system might therefore be a false economy.

In general, a mid-range, cart-based system with two transducers will be adequate for most anesthesia and critical care applications including limited cardiac imaging. There are now a number of hybrid systems available that convert easily from cart based to handheld and offer the benefits of both at reasonable cost. A key consideration when evaluating these is the quality of the monitor. For existing equipment where monitor quality is limited, it



Figure 1 SonoSite iLook device designed for vascular access applications.

may be worth considering the use of a separate, high-resolution monitor through which the image is viewed when the handheld equipment is used as a cart-based unit.

If more complex cardiac examinations including transesophageal echocardiography (TEE) are to be performed, a much more expensive, high-specification system is required (2,3).

One of the positive effects of the “handheld” ultrasound revolution is that market forces have prompted manufacturers of higher-specification cart-based equipment to lower the cost of their entry-level systems. These pieces of equipment can provide very good value for money; however, it is worth considering the availability of upgrade options.

Some manufacturers now offer a maintenance package as part of the initial capital purchase. This offer recognizes that equipment that is located outside of a conventional imaging department may not be covered by local equipment maintenance contracts. This factor is certainly worth exploring at the time of purchase. However, liaison with radiology over inclusion of equipment into trust-wide maintenance and quality assurance agreements is to be encouraged.

ERGONOMICS

It is estimated that more than 80% of ultrasound professionals sustain some level of work-related injury during their professional careers; 20% of sonographers ultimately retire from their profession because of physical incapacity directly related to musculoskeletal injury (4). Sonographers complain of pain, discomfort, tenderness, swelling, aching, and stiffness particularly in the shoulder joints and the neck (5).

Although personnel within anesthesia and critical care use ultrasound infrequently, this is likely to increase; so it is worth considering ergonomics as the service evolves.

Any ultrasound equipment purchase should be made with reference to current guidance on optimal ergonomic features (4,6). In particular, good ergonomic design should encourage a balanced, upright operator posture and minimize the strain on the joints of the neck and upper limb.

Most ultrasound examinations within anesthesia and critical care will be performed with the operator standing. The most important ergonomic feature of the equipment is therefore the ability to adjust the height of the monitor and control panel.

Vascular examinations and some interventional procedures often require the transducer to be held in one position while applying minimal pressure. Transducers therefore need to be lightweight and easy to grip.

On higher-specification systems, voice activation packages are available that allow the operator to perform hands-free adjustment of key controls. This can be particularly useful for interventional procedures. Although rarely used in the nonconventional setting, this feature is likely to become more commonplace as cost decreases. A summary of relevant ergonomic features is given in Table 1.

Helpful guidelines on ultrasound equipment procurement have been produced by a number of agencies and professional bodies (7,8).

Cost is usually the predominant factor affecting choice of equipment (5). An understanding of imaging objectives and how these are met by equipment performance will help justify significant financial outlay.

When selecting ultrasound equipment for any clinical context, there are a number of general factors that need to be considered. The Royal College of Radiologists Document, *Standards for Ultrasound Equipment* (2005) provides helpful guidance. This is summarized in Table 2.

Table 1 Summary of Ergonomic Features

| | |
|--|--|
| Scanning practice | Equipment features to consider |
| Most ultrasound examinations within anesthesia and critical care are performed with the operator standing | <ul style="list-style-type: none"> • Adjustable height of control panel • Adjustable height and tilt monitor (adjustable height patient couch/bed) |
| If seated | <ul style="list-style-type: none"> • Adjustable height chair |
| Importance of reducing transducer pressure | <ul style="list-style-type: none"> • lightweight transducer and cables |
| <ul style="list-style-type: none"> • during Doppler examinations • reduce operator fatigue | <ul style="list-style-type: none"> • adequate size and shape to allow a dynamic grip • cable tidy/arms supports |
| Need for hands-free manipulation of controls | <ul style="list-style-type: none"> • voice activation software |
| <ul style="list-style-type: none"> • undertaking interventional procedures | |

Table 2 General Considerations When Purchasing Ultrasound Equipment

- Clinical application(s) for which equipment will be used
- Relative workload in (each) application
- Transducer requirements
- Scanning capabilities required
- Measurement and analysis facilities required
- Physical size and maneuverability
- Ultrasound controls/settings—availability, ease of location, and operation
- Annotation and documentation—availability, ease of operation
- Facility for permanent recording of images
- Safety compliance, quality assurance
- Equipment trials and training
- Equipment review and replacement

Source: From Ref. 8.

CHOICE OF TRANSDUCER

Transducers come in a wide range of designs. They vary in size, shape, field of view, and transmit frequency (Fig. 2). Each of these criteria needs to be matched to the area of the body that is to be examined. As outlined in the previous chapter, high-frequency transducers provide better resolution but limited penetration (Table 3).

TRANSDUCER CLEANING

Numerous studies have identified the potential for the spread of infection from ultrasound transducers (9,10). This is particularly important in a high-dependency setting. Cleaning the transducer between patients is therefore essential. Most equipment manufacturers recommend a nonalcohol-based cleaning fluid. Over time, alcohol-based solutions will damage the seal on the transducer scanning surface. It is also worth noting that the thin protective covering on the scanning surface of a transducer can be damaged over time by use of abrasive paper towels.

GETTING STARTED

Using an ultrasound machine is a little like driving a car or using a home PC. In a car, there are a number of basic controls that are common to all models, some of which are in a



Figure 2 SonoSite probes; from left to right transvaginal, curved array larger footprint (abdominal/general), linear array (small parts/vascular), curved array small footprint (echocardiography), curved array small footprint (pediatric).

Table 3 Choice of Transducer

| Structures to be imaged | Transducer requirements |
|---|---|
| Abdominal organs (liver, kidneys, etc.) | <ul style="list-style-type: none"> 3–5 MHz required for adequate penetration to deep structures. Curved array gives good intercostal/subcostal access with a wide field for both deep and superficial structures |
| Vascular | <ul style="list-style-type: none"> Linear array for superficial vessels. Allows good skin contact and wide field of view for superficial, linear structures, 5–12 MHz |
| Nerves | <ul style="list-style-type: none"> 10–15 MHz, small footprint linear array for superficial structures such as the median nerve/brachial plexus. Lower frequency (4–7 MHz) may be required for deeper structures such as the adult sciatic nerve and infraclavicular brachial plexus |
| Cardiac | <ul style="list-style-type: none"> Small footprint phased array. Ease of access via limited intercostal/parasternal spaces. Wide field of view (adults 1.5–4 MHz, pediatric 3.5–8 MHz) Transesophageal imaging requires specialist transducer. Adults 3–10 MHz, pediatric 4–10 MHz |

standardized position within the vehicle. There are numerous additional controls that are either used rarely or may be hard to locate.

Unfortunately, with ultrasound equipment, there is no clear convention for the labeling and position of even the most commonly used controls, and even highly

experienced users can be confused by the layout of a new machine. To reduce the number of keys/tabs/dials, etc. on the control panel, some manufacturers use symbols or letters rather than text to label controls. To the new or infrequent user, these “hieroglyphics” can be confusing. Individual tabs/keys often have multiple functions depending on the mode of operation selected, and settings are often accessed via hidden on-screen menus.

Despite this apparent complexity, there are a small number of key equipment controls that are common to virtually all ultrasound systems. Once the function of these is understood and they are located on the control panel, it is relatively easy for the inexperienced user to produce good quality, diagnostic images.

This section will attempt to explain the function of each of these basic controls, where it is likely to be located and how it can be optimized.

Before using or evaluating any ultrasound equipment for the first time, the most useful starting point is to find a “co-pilot” who is familiar with the specific system.

This may be an experienced colleague from the same specialty, a Radiologist or a Sonographer. At the time of purchase, companies provide technical support from their highly experienced teams of application specialists. If it is not practical for them to spend time with all users of the equipment, planned “cascading” of information between colleagues is helpful. In practice, this does not always happen, and new users may be left to fend for themselves (chap. 4).

BASIC EQUIPMENT SETTINGS

Switching On/Off

An ultrasound machine is essentially a computer and, just as a home PC undergoes a start up process, it may take a few minutes to power up. Similarly, the user should switch off at the control panel, not at the plug on powering down.

New Patient (ID/Patient/Data)

Before scanning, patient details including name and hospital number should be entered. The relevant key is normally located on the control panel, often in either the top right or left corner (Fig. 3).

Transducer Selection

Basic handheld systems will have one transducer attached, and there may be no choice. On a higher-specification machine, once patient details are entered, an on-screen menu may appear giving options of transducer and application. Up to four transducers may be plugged in at any one time, and the operator will need to select the correct transducer from the menu to match the area to be examined.

Once the transducer is selected, a further menu may offer a choice of application presets matched to specific body areas.

Application Presets

When the relevant body area is selected, the machine will default to a range of settings that are optimized by the manufacturer for that target area. This will include B-mode settings affecting penetration, resolution, frame rate, etc. and Doppler settings.



Figure 3 Key to enter patient details.

It is important to choose the correct transducer/preset combination. It is not uncommon to observe inexperienced operators struggling to image deep into a large patient with these initial settings optimized for superficial structures. Inevitably, image quality will be poor and may be nondiagnostic.

Although presets provide a very useful starting point, there is no such thing as a standard patient. The operator will still need to adjust specific controls to compensate for patient size and condition and throughout the course of an examination.

The Control Panel

The layout of the control panel will vary considerably between machines and manufacturers. Individual controls will also vary in appearance as well as location. Simple controls such as focus or depth may be a soft key, a dial, a paddle, or on-screen. Individual tabs/keys may have multiple functions depending on the mode of operation selected.

It is for this reason that a co-pilot who is familiar with the specific system is such a useful ally when using a machine for the first time.

Manufacturers tend to group controls depending on function and to minimize operator movement and reach. For example, Doppler controls will normally be grouped together, as are calipers/measurement controls (Fig. 4).

Freeze

Freeze allows the operation to produce a static image for archiving and from which measurements can be taken. This is normally a soft key. Typically, it is situated toward the right hand side of the control panel to be reached easily with the left hand while scanning with the right. The key is normally labeled “freeze.” (Some of the more imaginative manufacturers use a snowflake.)



Figure 4 Calipers/measurement controls.

Tracker Ball

This is probably the only control on an ultrasound keyboard that is common to virtually all manufacturers. This is the equivalent of the computer mouse and is used to move the cursor around the screen when entering patient details, selecting transducer or typing on-screen text. The lap top equivalent tracking pad has replaced the tracker ball on handheld systems.

Depending on the scan mode that is operating, the tracker ball is used to move on-screen graphics such as calipers, position of the Doppler sample gate, box location for high-resolution zoom or color Doppler. The function changes as each application is selected or the select/set/priority tool is used (see below).

As one of the most commonly used controls, the layout of the control panel is often centered around the tracker ball. Other frequently used settings such as calipers, select, gain, etc. can often be located by their close proximity (Fig. 5).

Cine-Loop

On most equipment, the track ball also controls the cine-loop facility. This is a feature that allows the operator to scroll back through several seconds worth of captured frames once the image has been frozen. This is particularly useful when imaging noncooperative patients.

Select (Set/Priority)

This is a generic key that is used to activate functions such as caliper placement. On some machines, this changes the function of the tracker ball (Fig. 6).

Overall Gain

This controls the magnitude of amplification given to all returning echoes regardless of the depth from which they have returned. The overall gain control is normally a large dial.

Altering the overall gain will make everything in the image appear brighter or darker. Overall gain should be used in conjunction with time gain compensation (TGC)

Most inexperienced users tend to set the gain too high. There is almost a tendency to “turn up the lights” so that everything looks brighter. It is, however, more difficult to appreciate anatomical boundaries and subtle differences in reflectivity, if the gain is high. This is particularly important when searching for free fluid. With the gain set too high, amplified noise and artifactual echoes may obscure small pockets of fluid.

In the critical care/anesthetics setting, there is the further complication of high-ambient lighting. There may be little the operator can do to remedy this other than shading the monitor. A possible alternative is to use a pair of high-quality “virtual reality” video goggles that can be purchased from PC gaming outlets. These are used routinely in veterinary ultrasound where lighting conditions and safe positioning of equipment may be problematic. There is evidence that their use can help facilitate interventional procedures in humans (11) and reduce patient perceptions of pain and anxiety (12).

Video glasses form a virtual image in front of the user that is viewed, as the operator looks straight ahead. By looking downward, below the level of the glasses, the operator can see the patient and view the site of intervention. Although the quality of image is limited in comparison with most monitors, Pedersen et al. (11) conclude that it is adequate for most interventional procedures.

Time Gain Compensation

This usually consists of a number of sliders/paddles that correspond to specific depths within the patient (Fig. 7). TGC is used to compensate for increasing attenuation with depth. On the smaller handheld systems, TGC is often replaced by independent near and far gain controls. The operator should aim for an image where similar structures appear at the same brightness level regardless of depth.

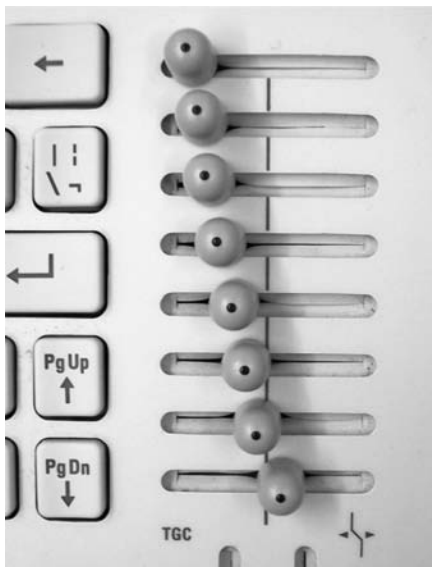


Figure 7 Time gain compensation (TGC) controls: a number of sliders that correspond to specific depths within the patient.

Depth/Zoom

The depth control should be set to demonstrate the whole region of interest during an initial survey of the area. During interventions that may be guided by ultrasound, such as CVC placement, it is often more important that the needle tip misses “innocent bystanders” than that the target structure is reached on first pass. Initial depth settings should therefore be set to demonstrate all of the relevant anatomy, not just the most superficial structures. This will give a better appreciation of the relative location of anatomical structures. Magnification can then be increased as the examination is focused to a specific depth. If high-resolution zoom (see below) is used on a real time image, it is important to recognize that the top edge of the image no longer represents the skin surface. Clearly this is critical for intervention guidance.

High-Resolution Zoom

This may be used to provide an expanded view of small structures. A region is selected by placing an on-screen box over the structure of interest. The location of the box is, normally, controlled by the tracker ball. Zoom is then activated to provide a high-resolution image of this small, defined area.

Focus

As the depth of interest changes from one structure to another, the depth to which the ultrasound beam is focused needs to be altered. This will improve lateral resolution, making it easier to delineate small structures. This is particularly important when imaging structures, such as nerves, that may be similar in brightness level to surrounding tissues.

The homogeneous speckle pattern characteristic of many solid organs is, in part, a product of the effective beam width. As beam width is reduced, contrast resolution will improve and structures, such as nerves, will be better visualized. Focus may need to be adjusted throughout the examination.

On some handheld systems, focus is optimized for the entire depth of view and is altered automatically as the depth setting is changed. On these systems, focus cannot be altered independently.

Frequency

Modern transducers utilize broad bandwidth technology and transmit over a range of frequencies. If the correct transducer/preset combination has been selected, it is rarely necessary to change frequency.

On some equipment, it is possible for the operator to optimize the image for deep or superficial structures (or for slender or challenging patients). By selecting general, penetration or high-resolution settings, a number of parameters are altered, including the range of frequencies from which the image is generated. This means that a single transducer can be used for a broad range of patient size and depth of interest.

Tissue Harmonic Imaging

This is an optional scan mode available on most equipment. Tissue harmonic imaging utilizes the second harmonic signal that is generated within the tissues because of

nonlinear propagation of the sound pulses. The frequency of the second harmonic is twice the transmit frequency. For example, a transducer with a central transmit frequency of 3 MHz would produce a harmonic signal of 6 MHz.

Key advantages of harmonic imaging are the reduction of artifacts and improvement in lateral resolution. Only the central portion of the main beam is of a high enough intensity to generate a harmonic signal. The result is a reduction in beam width and hence an improvement in lateral resolution. Grating lobe artifacts are essentially eliminated, and clutter within the image is markedly reduced.

Compound Imaging

In conventional B-mode imaging, each frame of information is generated by firing groups of piezoelectric elements in a single sweep across the face of the transducer. Each pulse of sound is fired at 90° to the array.

Compound imaging techniques (such as SonoCT) use electronic beam steering to fire pulses from between three and nine separate transmit angles (13). Real time imaging is then achieved by combining the data from multiple lines of sight to generate successive frames. By scanning from a number of different angles artifacts such as speckle, clutter, noise, and shadowing are reduced and real structures are reinforced.

The key drawback of this technique is that the system is unable to distinguish between artifacts that reduce image quality and “helpful” artifacts that may alert the operator to the presence of pathology or help characterize a lesion. Compound imaging effectively removes or reduces the appearance of all shadowing (Fig. 8).

Doppler Controls

Most manufacturers group Doppler controls together in one area of the control panel. However, frequently, they are adjusted via an on-screen menu.

In whatever context Doppler is used, correct setting of a number of equipment variables is vital. Understanding of these controls and a good awareness of the limitations of the equipment will enable the operator to make an accurate interpretation of blood flow. As with other applications, for vascular ultrasound imaging, manufacturers provide a

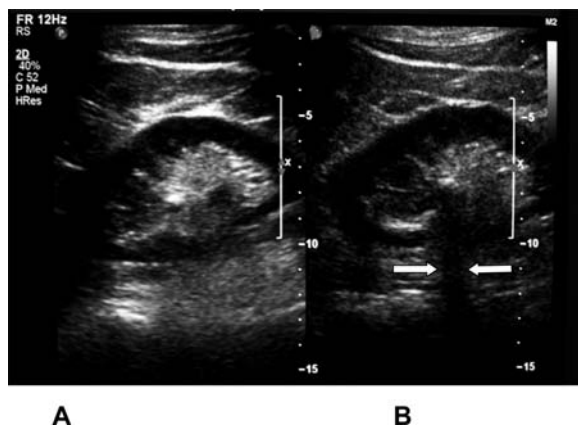


Figure 8 (A) Compound imaging on—shadowing from renal calculus is markedly reduced. (B) Compound imaging off—shadowing from calculus visible (*arrows*).

number of examination-specific presets. These generally include arterial and venous options. Although these provide an excellent starting point, a number of adjustments will need to be made to optimize demonstration of both normal hemodynamics and pathology.

As with other soft tissue structures, selection of transmit frequency, focal depth, and gain are equally applicable in both B-mode and Doppler assessment of vessels (14).

Velocity Scale (Pulse Repetition Frequency)

This setting determines the range of blood flow velocities that can accurately be displayed. In simple terms, if investigating high-velocity flow, the pulse repetition frequency (PRF) needs to be high. For low-velocity flow, PRF needs to be reduced. This applies to both color and spectral Doppler.

The scale is visualized as velocity range on the vertical axis of the spectral trace in pulsed wave Doppler and as a color bar in color flow mapping.

Wall Filter

This is used to remove the high amplitude, low frequency signal from vessel walls. If set too high, this can result in the appearance of loss of low velocity flow. Although wall filter settings generally change automatically as the PRF is altered, it may be worth checking, if very slow flow is suspected.

Color Gain

This controls the amount of overall amplification given to the color Doppler signal. At the start of the examination, increase the color gain so that color artefact can be seen throughout the soft tissue structures. The gain should then be backed off until the color artifact just disappears from the soft tissue and color filling remains within any vessels.

PUTTING IT ALL INTO PRACTICE

In the same way that it takes time to master the art of driving a car, use of an ultrasound machine can feel cumbersome and, at times irritating, during the early stages of learning. Uptake of ultrasound guidance for line placement and the growing range of applications within anesthesia and critical care are influenced by the provision of adequate training and support. Education and training issues are considered in chapter 4.

REFERENCES

1. National Institute for Clinical Excellence. Guidance on the use of ultrasound locating devices for placing central venous catheters. *NICE technical report number 49*. September 2002.
2. Vignon PF, Mickael BJ, Lesage J, et al. Hand-held echocardiography with Doppler capability for the assessment of critically-ill patients: is it reliable? *Intensive Care Med* 2004; 30(4): 718–723.
3. Spevack DM, Tunick PA, Kronzon I. Hand carried echocardiography in the critical care setting. *Echocardiography* 2003; 20(5):455–461 (review).
4. SDMS. Industry Standards for the Prevention of Work-Related Musculoskeletal Disorders in Sonography. Plano, Texas: Society of Diagnostic Medical Sonography, 2003.

5. Miles J. Work Related Upper Limb Disorders in Sonographers. London: Synergy, Society of Radiographers, 2005:6–11.
6. Dodgeon J, Newton-Hughes A. Enabling sonographers to minimise work related musculoskeletal disorders. In: BMUS Bulletin (11)3. London: British Medical Ultrasound Society, 2003.
7. NHS PASA. 2005. Ultrasound: radiology (online) Reading, NHS Purchasing and Supply Agency. Available at: <http://www.pasa.nhs.uk/dme/radiology/ultra.stm>. Accessed March 8, 2006.
8. RCR. Standards for Ultrasound Equipment BFCR(05)01. London: Royal College of Radiologists, 2005.
9. Fowler C, McCracken D. Ultrasound probes. Risk of cross infection and ways to reduce it—comparison of cleaning methods. *Radiology* 1999; 213(1):299–300.
10. Karadeniz YM, Kılıç D, Altan SK, et al. Evaluation of the role of ultrasound machines as a source of nosocomial and cross-infection (technical report). *Invest Radiol* 2001; 36(9):554–558.
11. Pedersen JF, Vedsted-Jacobsen A, Andresen N. The use of video glasses at ultrasound-guided interventions. *Acta Radiol* 2002; 43(5):539–540.
12. Bentsen B, Svensson P, Wenzel A. Evaluation of effect of 3D video glasses on perceived pain and unpleasantness induced by restorative dental treatment. *Eur J Pain* 2001; 5(4):373–378.
13. Philips (2005). SonoCT Real Time Compound Imaging. Available at: <http://www.medical.philips.com/us/products/ultrasound/technology/gi/sonoct.asp>. Accessed June 24, 2007.
14. Thrush A, Hartshorn T. *Peripheral Vascular Ultrasound: How, When, Why*. 2nd ed. Churchill Livingstone, 2005.

3

Assessment of Needle, Catheter, and Guidewire Position Using Ultrasonography

G. A. Chapman and A. R. Bodenham

Academic and Clinical Departments of Anaesthesia and Intensive Care Medicine, Leeds General Infirmary, Leeds, U.K.

INTRODUCTION

Anesthetists, pain specialists, and intensivists spend a considerable proportion of their working time performing invasive, needle-based interventions. To access deeper structures like central veins and nerves, they have traditionally relied upon surface-based landmarks to guide the needle into the correct position. Patients, however, are not uniform and present challenges due to wide variability, e.g., anatomical abnormalities, obesity, children, and anticoagulation status. Regardless of experience, there is the ever-present risk of needle misplacement with damage to adjacent structures, including arteries, nerve bundles, and pleura. Occasionally, such damage may have devastating implications for both the patient and the practitioner.

Historically, radiologists have used ultrasound to guide needle, catheter, and guidewire placement for various diagnostic and therapeutic purposes. The recent introduction of portable, affordable, high-resolution ultrasound scanners has accelerated interest in its use for interventional procedures in anesthesia, pain, and intensive care medicine.

Ultrasound guidance is now commonly used to assist invasive procedures, including vascular access (1), nerve blockade (2,3), and drainage of pleural or ascitic fluid collection. The advantages of ultrasound guidance include a greater likelihood of success, fewer complications, and less time spent on the procedure. This may result in increasing patient satisfaction and favor a modest financial benefit in the long term (4–6). Yet, despite the potential benefits that routine ultrasound guidance brings, there has been resistance to its use (7).

Ultrasound enables identification of a suitable target vessel and provides visualization of the surrounding anatomy, allowing a planned approach. The pathway to, and the site of, vessel puncture can be determined and viewed in real time to avoid specific surrounding structures.

Visualization of catheters and guidewires within target structures promotes safe practice and may avoid the use of X rays (8). Ultrasound has its limitations in that it will not easily show a central position of the catheter tip, which requires a chest X ray, electrocardiogram (ECG), or transesophageal echo verification. However, even this has been challenged (8).

We believe that many practitioners fail to take full advantage of ultrasound guidance during interventional procedures. A lack of understanding of how to assess the position of invasive devices and in particular the location of the needle tip is a major obstacle to optimum performance. This is particularly important when inserting needles into, or adjacent to, deeper structures, which may be in close proximity to at-risk structures such as vessels, nerves, and pleura. Such applications are likely to become more demanding as clinicians move to access deeper structures (previously considered inaccessible) with small-gauge needles. The theory and practice of needle visualization with ultrasound is well described in radiology texts (9–11) and only recently in the anesthetic literature (12).

PHYSICS OF ULTRASOUND

The physics of ultrasound is covered elsewhere. In this chapter we restrict the discussion to a few physical principles particularly related to needle, guidewire, or catheter visualization. A basic understanding of the relevant physics and instrumentation related to medical ultrasound is required in order to fully appreciate the merits and pitfalls of needle (device) visualization.

ACOUSTIC IMPEDANCE, REFLECTION, REFRACTION, AND SCATTERING

A tissue interface is formed where tissues of different acoustic impedances lie adjacent to one another. The tissue interface causes an ultrasound wave to be reflected, refracted, or scattered. The principles detailed below apply to both artificial devices and biological tissues.

Reflection of a sound wave occurs when it strikes the boundary between two media. The incoming wave is referred to as the incident wave, and the wave that is bounced from the surface is called the reflected wave. Depending on the angle of reflection, sound waves can return to the transducer probe to provide a signal. Optimum echoes are provided by ultrasound waves reflected back at 90° . Thus needles placed perpendicular to the beam are easier to visualize than those placed parallel or at a less acute angle to the beam. From the laws of reflection, the angle of incidence of the ultrasound beam equals the angle of reflection. Unless the ultrasound beam strikes at right angles to the interface, most of the ultrasound will be reflected away from the probe.

The amount of sound reflected by an object is highly dependent on the texture of its surface. When surface imperfections are smaller than the wavelength of the incident sound, virtually all of the sound is reflected. However, in reality, most objects have convoluted surfaces that scatter incident sound. Thus, the reflection of sound can be simply categorized into two types. The first, defined as sound reflected from a smooth surface (diaphragm) at a definite angle, is called specular reflection. The second, known as diffuse reflection, is produced by rough surfaces that tend to reflect sound in all directions (red blood cells). Typically, there are far more occurrences of diffuse reflection than specular reflection (Fig. 1).

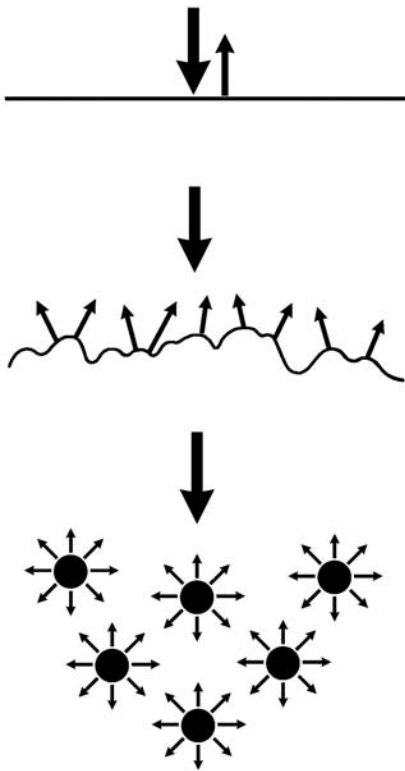


Figure 1 The amount of sound reflected by an object is highly dependent on the texture of its surface. Virtually all of the sound is reflected from large, smooth surfaces (diaphragm) and is called specular reflection (*upper image*). However, most objects have rough (*middle image*) or convoluted surfaces (red blood cells) that scatter incident sound producing diffuse reflection.

Reverberation is caused by multiple reflections of ultrasound between two closely spaced interfaces. The multiple echoes thus created reach the transducer before the next pulse transmission and give rise to multiple copies of the anatomy at the interface. The copies are displaced to greater depths in the image, depending on the number of back and forth reflections of the corresponding echoes. The echoes of the deepest copies will have travelled the longest distance and will therefore have the lowest amplitude (Fig. 2).

The artifact appears as a series of closely spaced, discrete echoes, which, because of its appearance, may be referred to as a comet tail. When separate echoes cannot be identified and the emission of sound from the origin appears continuous, the artifact is known as a ring-down artifact. This “ringing” is caused by a resonance phenomenon typically associated with the presence of a collection of gas bubbles. Reverberation artifacts are commonly seen at soft tissue-to-gas interfaces (the gall bladder). Thus the instrument detects sufficiently strong echoes, and reflectors that are not real are displayed. This may cause confusion on the display.

Refraction occurs when the transmitted beam is deviated from the path of the incident beam. Refracted sound travels through the interface to be reflected or refracted at deeper structures. This can lead to distortion or image artifacts. When the sound wave strikes a small irregular surface and is reflected in many different directions, scattering occurs. Some scattered sound waves will return to the probe and produce a signal (Fig. 3).

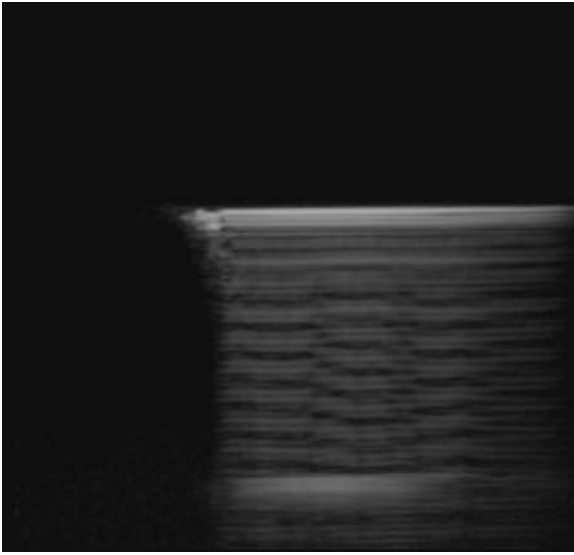


Figure 2 24G Sprotte spinal needle in longitudinal axis of probe in a water bath. The side hole near the tip is uppermost with an air bubble within it. There is a marked reverberation artifact inferiorly.

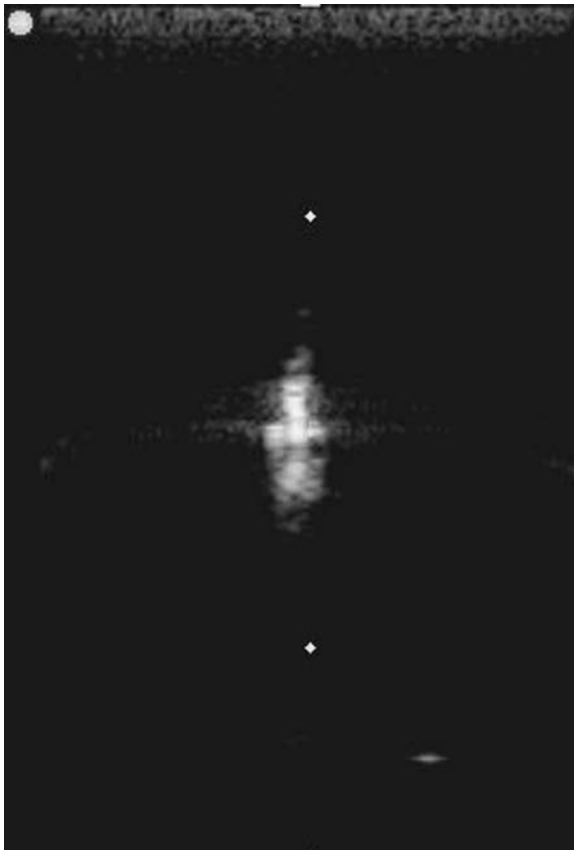


Figure 3 An 18G vascular access needle in a water bath, crossing the ultrasound beam in cross section. The needle tip is surrounded by a scattering artifact. Principles of needle visualization are easier to demonstrate in a water bath where the needle shaft and tip are not obscured by heterogeneous body tissues.

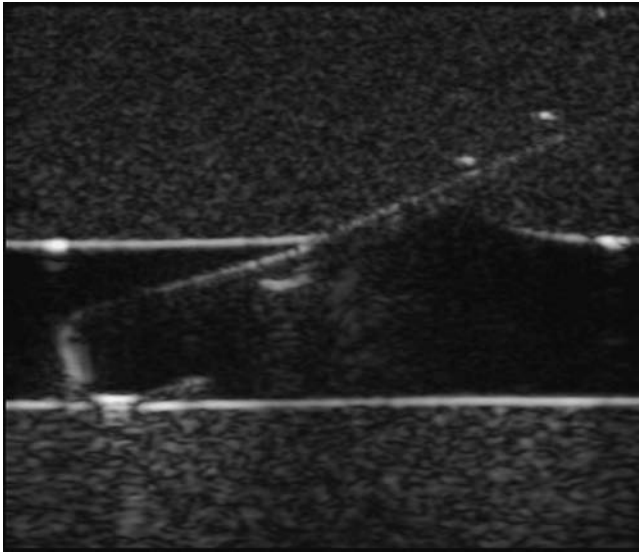


Figure 4 Agar phantom with a fluid-filled cavity. A standard 18G vascular access needle has been inserted into the fluid-filled cavity, with a J-guidewire passed through, seen in a longitudinal section. The machined needle tip appears brighter than the shaft, with an associated scattering artifact. Also noticeable are air bubbles in the agar preparation above the needle and in the fluid cavity (white spots). The interface between the fluid and agar is bright due to enhancement.

Tissue acoustic impedance is a product of tissue density and the speed of sound in that tissue and is measured in rayls. Since the speed of sound in soft tissues is assumed to be constant, acoustic impedance is generally altered only by a change in the density of the tissue. In other words, reflection of an ultrasound wave occurs at the interface of tissues of differing densities. Importantly, only very small differences in the density of adjacent tissues are required to form a tissue interface. Fortunately, soft biological tissues all have densities sufficiently different to create tissue interfaces enabling ultrasound to distinguish between them and their adjacent structures.

The intensity of sound that is reflected at an interface is determined by the difference between the acoustic impedances (or the densities) of the two tissues. If the difference is small, only a small percentage of the sound will be reflected. If the difference is large, most of the sound will be reflected. The intensity of the reflected sound is portrayed by the brightness of the image on the gray-scale display.

When compared with soft tissue, needles, catheters, and guidewires have markedly different acoustic impedances ensuring that the majority of the ultrasound beam is likely to be reflected and scattered from the tissue device interface. As such, invasive devices should be easily seen with ultrasound, but other factors are also relevant (Fig. 4).

ATTENUATION, ACOUSTIC SHADOWING, AND ENHANCEMENT

The decrease in signal strength (amplitude) of a soundwave as it passes through a medium is known as attenuation. This results from a combination of absorption, scattering, reflection, and divergence of the ultrasound beam.

If the acoustic impedances of the tissues forming an interface are sufficiently different, then most or all of the ultrasound will be reflected. Highly reflective surfaces

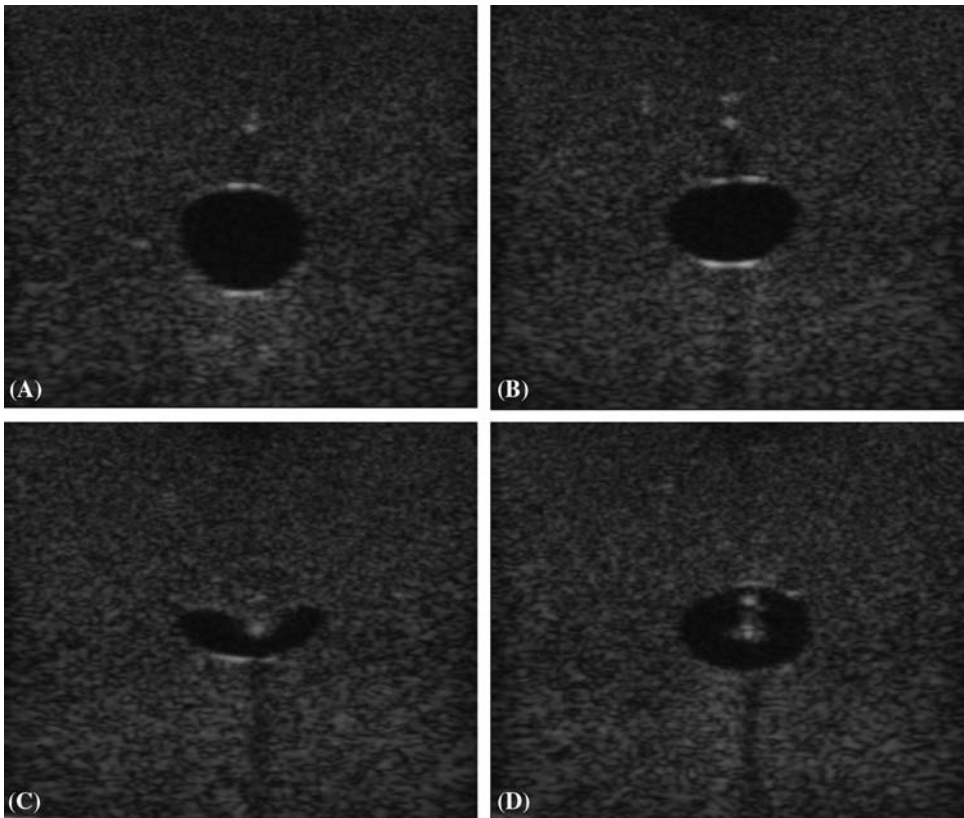


Figure 5 Agar phantom in a water bath with a fluid-filled cavity (black hole in the center of the picture) in a transverse section. A standard 18G vascular access needle is advanced toward the target “vessel.” (A) The needle tip (white dot at the 12 o’clock position) approaches the vessel. (B) More of the needle tip and shaft enter the beam with a progressively increasing artifact (double dot and acoustic shadow). (C) The superior wall of the agar fluid-filled interface becomes indented. (D) The agar-filled tube (vessel) re-expands with the needle tip seen within the fluid-filled cavity.

reflect almost the entire ultrasound beam. The area behind this interface will appear black and is termed an acoustic shadow. This shadow, corresponding to the width of the interface, fills the area behind the interface down to the lower border of the image and explains why it is not possible to image structures deeper to bone or gas using ultrasound.

A needle passing through the ultrasound beam in transverse section causes an acoustic shadow seen as a black stripe, the approximate width of the needle, passing downward on the display (Fig. 5). This artifact may be used to ascertain where the needle is crossing the beam but importantly does not accurately represent the future path of the needle.

Excessive reflection of the ultrasound beam in the superficial tissues may obscure deeper structures, resulting in an unsatisfactory image and making needle visualization difficult.

Ultrasound echoes of interfaces behind or within a structure of low attenuation (low reflectivity) appear enhanced and explain why ultrasonographers request a full bladder for pelvic examination. Vessel walls are typically enhanced due to the presence of blood. This effect can be seen when the needle is within a fluid-filled space (Fig. 6), and injection of fluid into tissues through a needle will also help enhance its tip (13).

The opposite is true of air. Ultrasound will not pass through air and may result in artifact (Fig. 7) or picture whiteout. It is not possible to visualize through or into air-filled cavities.

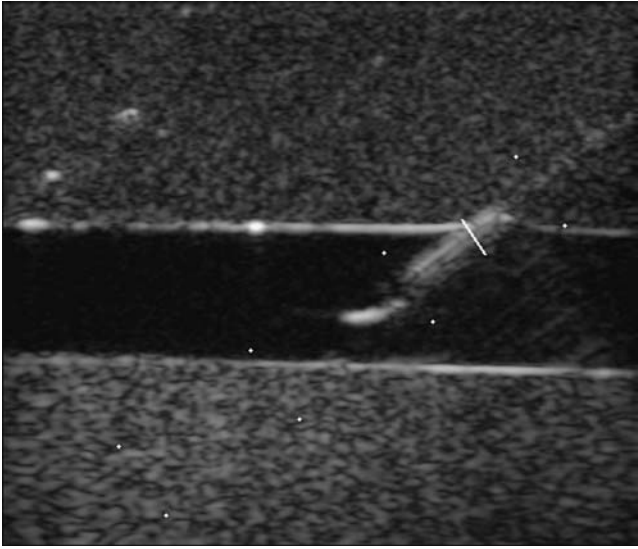


Figure 6 Agar phantom with a fluid-filled cavity in a longitudinal section. An 18g echotip needle (Cook USA) vascular access needle has been introduced at about 30° to the longitudinal plane. Only the roughened section (echo tip) of the needle can be easily visualized. The needle shaft within the agar is seen only weakly. Acoustic shadowing causes the agar below the needle to appear darker. In this case, a needle-guide device has been used with electronically generated tram lines displayed, which serve as a guide to the intended direction of the needle (white dots) and provide an indication of the length of the needle required to reach a given position (white line).

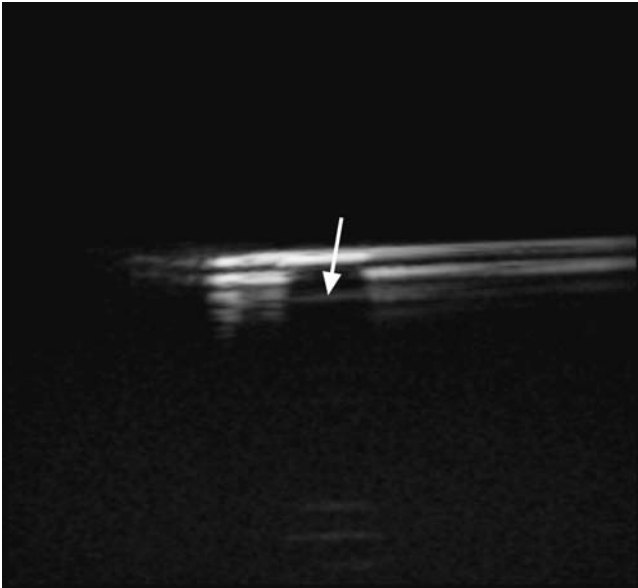


Figure 7 A fluid filled 20g intravenous cannula with tapered tip (needle withdrawn) in a water bath in a longitudinal section, with an air bubble (*arrow*). Most of the ultrasound waves are reflected at the air-liquid interface so obscuring the inferior wall of the cannula in this section. Elsewhere, the two walls of the cannula are easily visualized.

Images of certain tissues are highly dependent on their angle in relation to the ultrasound beam at which they are viewed. This is known as anisotropy, and nerves are weakly anisotropic.

TRANSDUCER PROBES

A general-purpose, small parts, vascular linear array probe that operates between 7 and 12 MHz is generally used for vascular access and nerve blockade, giving high-resolution images to a depth of 6 to 8 cm. Color Doppler imaging is useful to identify blood flow in vessels and has been used to aid needle visualization (14). Doppler imaging reduces the displayed image quality and as a result is not normally used for this purpose.

Resolution is the ability to discriminate between two points and can be described in three planes: axial, transverse, and slice thickness.

Axial resolution is the resolution along the direction of the beam and is limited by the duration of the ultrasound pulse. The higher the frequency of ultrasound, the shorter the pulse duration, which results in better axial resolution. Transverse (lateral) resolution is that at right angles to the beam direction and is limited by the beam width at the point of reflection. It depends on the probe design and in particular the density of crystals. Lateral resolution is poorer than axial resolution and may be improved by focusing the ultrasound beam. The beam width is reduced by mechanical or electronic means, improving lateral resolution, but this is restricted to the focal zone of the transducer. Slice thickness refers to the out-of-imaging plane beam thickness (Fig. 8). Slice thickness affects the region

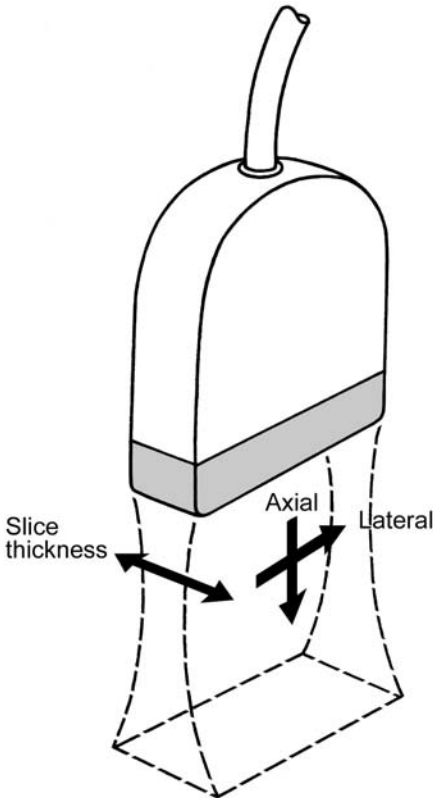


Figure 8 Axial and lateral resolution and slice thickness. Slice thickness refers to the out-of-imaging plane beam thickness and affects the region perpendicular to the scan plane over which the returning echoes will be obtained.

perpendicular to the scan plane over which the returning echoes will be obtained and should preferably be as small as possible to maintain image quality.

Thus a needle may appear to be within or adjacent to the desired target structure but in reality lies above or below it. The clinician should be aware of the limitations of two-dimensional imaging while manipulating the needle tip in the three planes.

Temporal resolution refers to the ability to locate the position of a moving structure at a specific time point and is dependent on the frame rate. This is of importance in echocardiography but of little consequence to anesthetists performing needle-based interventions on relatively immobile structures.

DISPLAY SETUP

Probe orientation is important to avoid the need to manipulate needles in the mirror image of that displayed on the screen. Machine settings can be adjusted or changed electronically, and so it is important to check the machine setup before proceeding. A palpable orientation marker is usually present on the side of the transducers, which corresponds to a marker on the display. Touch one side of the probe or move the probe on the patient, and observe the image to establish the correct orientation.

By convention in radiology, when imaging the body in the transverse plane (right angles to the long axis), the right side of the patient corresponds to the left side of the ultrasound image (i.e. the same as looking from the feet, as is the convention with CT images). If imaging in the longitudinal plane (along the long axis of the patient's body or limb), convention dictates that the left side of the image be orientated toward the patient's head. The top of the display corresponds to the transducer face (in contact with the skin), while the bottom represents the lower extent of tissue visualized by the device. We would suggest that the operator, when using ultrasound for needle visualization, set up the orientation in the correct anatomical orientation, as it would be viewed from where the operator is positioned. Needle movements by the operator will then correspond anatomically to that on the display.

Depth control adjusts the depth of the field of view of the ultrasound image. It is indicated on the display as a distance in millimeters and corresponds to the distance from the transducer face to the bottom of the image. If this is set too deep, all areas of interest will be small and compressed into the top half of the image. If this setting is too superficial, the structures of interest will not be viewed in their entirety. There are usually depth markers (in centimeters) on the side of the screen, and the depth control should be adjusted until the structures of interest are close to the center of the screen. This enables important collateral structures to be visualized in relation to the target tissues and avoided.

Gain control enables amplification of the received ultrasound signal. If gain is increased, the image becomes brighter; if it is reduced, the image becomes darker. Gain controls are typically divided into overall, near, and far. Overall gain changes the amplification of the whole display, near gain changes the amplification adjacent to the transducer, i.e., the top half of the display, and far gain changes the amplification of the image farthest away from the transducer.

The gain should be adjusted to produce the best possible image. A relatively dark image may allow easier identification of the white dots generated by a needle passing through tissues. Increasing the gain control may increase the amount of artifact, making needle visualization more difficult.

Ultrasound gel is required for acoustic coupling between the transducer-skin interfaces providing an air-free contact with the skin. The gel is also a lubricant enabling the operator to move and manipulate the probe. For interventional purposes, the gel needs to be sterile both inside and outside the protective sheath.

For invasive, needle-based procedures, a sterile field is required. Transducers cannot be autoclaved without damage but should be cleaned with proprietary disinfectant solutions designed for this purpose (check with the manufacturer's instructions for suitable solutions).

A sterile plastic or latex sheath of sufficient length is used to cover the probe and cable. The operator bunches the sterile sheath up and places sterile ultrasound gel into the sheath. With the help of an assistant, the probe is placed directly onto the gel within the sheath, and the operator telescopes the sheath along the transducer cable, taking care to maintain sterility. The sheath is then tightly applied to the gel and probe and any air bubbles smoothed away to leave a thin film of gel across the face of the transducer. Elastic bands applied over the sheath help keep it tightly applied to the transducer face. Sterile gel is then placed on the skin over the area of interest and the transducer used in the usual way.

PHANTOMS

A phantom mimics the properties of biological tissue with respect to sound transmission (i.e., has similar acoustic impedance) and may be used to test the physical properties of ultrasound imaging devices and as a substitute for patients for clinical practice (15,16).

Phantoms can be homemade from agar, vegetable, and meat products (17). Basic commercial products consist of an agar block containing fluid-filled tubes designed to simulate blood vessels. Advanced models come complete with blood-mimicking fluid intended for use in phantoms with flow mechanisms. This simulates the acoustic and physical characteristics of blood, providing a stable and reliable fluid for Doppler studies and system evaluations.

Phantoms are useful to demonstrate principles of needle visualization plus ultrasound probe and needle orientation but are generally expensive (£200–£300) and deteriorate quickly with use. Unfortunately, even commercial products do not closely resemble the feel or visual effects of real body tissues and vessel walls; however, we believe that they should be used together with a simple water bath prior to attempting needle visualization in patients.

ASSESSMENT OF NEEDLE POSITION

The importance of real-time assessment of needle position cannot be overstated. Without accurate identification of the position of the needle, it is possible that damage to collateral structures may occur, even if the target structure has been correctly visualized using ultrasound before starting and the initial starting position of the needle is correct. If such skills can be developed, the success rate of correct needle placement will be increased.

The images shown in this chapter were obtained using SonoSiteTM TITAN and iLook ultrasound machines (SonoSite, Hitchin, U.K.), a commercial agar phantom, and a water bath. Similar devices are available from multiple other manufacturers. They serve to demonstrate the principles of ultrasound needle visualization and its limitations. Background signals and artifacts from body tissues that mask needle imaging are avoided by the use of phantoms and serve to illustrate the potential benefits of practicing on such aids before approaching patients.

Unfortunately there is no universally accepted nomenclature for what constitutes transverse or longitudinal in relation to the ultrasound beam. We describe the needle as longitudinal when it is in line with the long axis of the ultrasound probe. If the needle

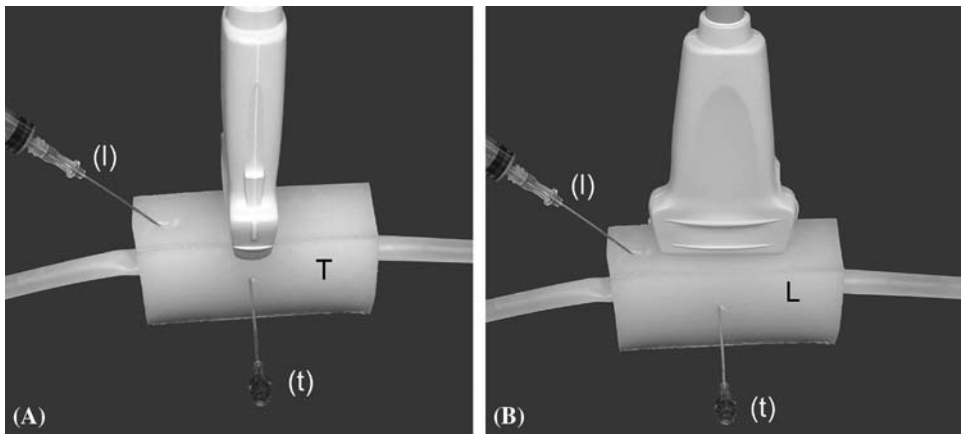


Figure 9 Agar phantom with a plastic fluid-filled pipe. The ultrasound probe may be aligned in transverse (A) or longitudinal section (B) in relation to the target “vessel.” The needle may also be introduced in either a transverse or a longitudinal section.

is inserted adjacent to the longest side of the probe and is seen in relation to the short axis of the probe, the needle is transverse (Fig. 9).

A number of factors influence the assessment of needle position:

- The use of larger needles with a guidewire in their lumen provides the best ultrasound visibility (18). However, standard 18G needles used in Seldinger vascular techniques are easily visualized. Smaller-gauge needles may produce fewer artifacts.
- Needles placed perpendicular to the beam are easier to visualize than needles placed parallel or at a less acute angle to the beam (18). When the ultrasound beam strikes at right angles to the interface, most of the ultrasound is reflected back toward the probe. However this is only the case for some of the reflected sound waves. Reflection at other angles may result in a distorted image or artifact.
- The needle tip may be visualized even when the shaft cannot. The needle tip has a machined cutting bevel with an irregular surface. The portion of the beam that interacts with this interface is “scattered” in all directions. Thus some of the beam will be reflected back to the transducer even when the shaft of the needle is nearly parallel to the ultrasound beam.
- “Scattering” can also be utilized to improve visualization of the needle shaft. The inner or outer aspect can be scratched or roughened, increasing scattering and producing an echo (19,20). Extrareflective needles specifically designed for ultrasound are commercially available (Fig. 10). Such modifications may not be all that useful in clinical practice (21). Some needles may be better visualized with the inner trocar in situ. However, most needles are sufficiently “visible” sonographically, provided the correct alignment is maintained.
- Introducing the needle in a short “in-and-out, side-to-side” motion causes deflection of the adjacent soft tissues and makes the trajectory of the needle more discernible within the otherwise stationary field. This may be compared to finding a moving needle as opposed to a static needle in a haystack.
- If using a focused transducer, needles are seen best when they are within the focal zone.

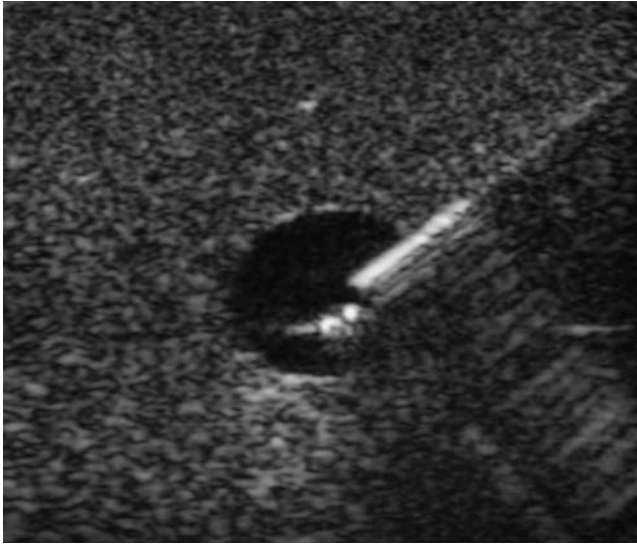


Figure 10 An 18g echotip vascular access needle (Cook USA) has been inserted into an agar block. Injection of saline through the needle to produce a fluid bubble which enhances the image of the tip. There is acoustic shadowing beneath the needle, and a reverberation artefact from the machined section of the needle which produces an enhanced area of reflection for sound waves.

- Rocking the transducer into the path of the needle, if it has deflected out of the image plane, will improve needle visualization.
- When the needle shaft crosses the ultrasound beam, an acoustic shadow forms, which may be used to indirectly assess needle position.
- Priming the needle with sterile water increases needle shaft and tip brightness (22). Likewise, the injection of fluid may improve needle and catheter tip visualization (13). With the needle or catheter placed in a solid organ, there is an increase in echogenicity at the needle tip when fluid is injected (enhancement). This may be useful in nerve blockade, when it is helpful to confirm the site and spread of local anesthetic fluid injection (Fig. 10).

However, the injection of a small bolus of saline or air through the needle is not advisable if the plan is to subsequently use nerve stimulation to reposition the needle tip. During electrical stimulation, the ability to elicit a motor response with a low current (<0.5 mA) is lost after the injection of even a small amount of normal saline or air (the Raj test) (23). However, the injection of a nonconducting solution (dextrose 5% in water) through an insulated needle has recently been demonstrated, albeit in a porcine model, to sustain and even enhance a motor response by decreasing the conductive surface area and increasing the current density at the needle tip (24).

- A small bolus injection of air or macro bubbles may highlight the location of the needle tip, but the acoustic shadow it produces spoils further visualization of deeper structures. This may be relevant with ultrasound-guided injection of local anesthetic solutions. Prewarming local anaesthetic solutions may help prevent bubble formation seen when cold solutions warm up to body temperature. It is sensible to use fluid-filled needles and the minimum number of syringes necessary to avoid inadvertent air deposition in tissues.

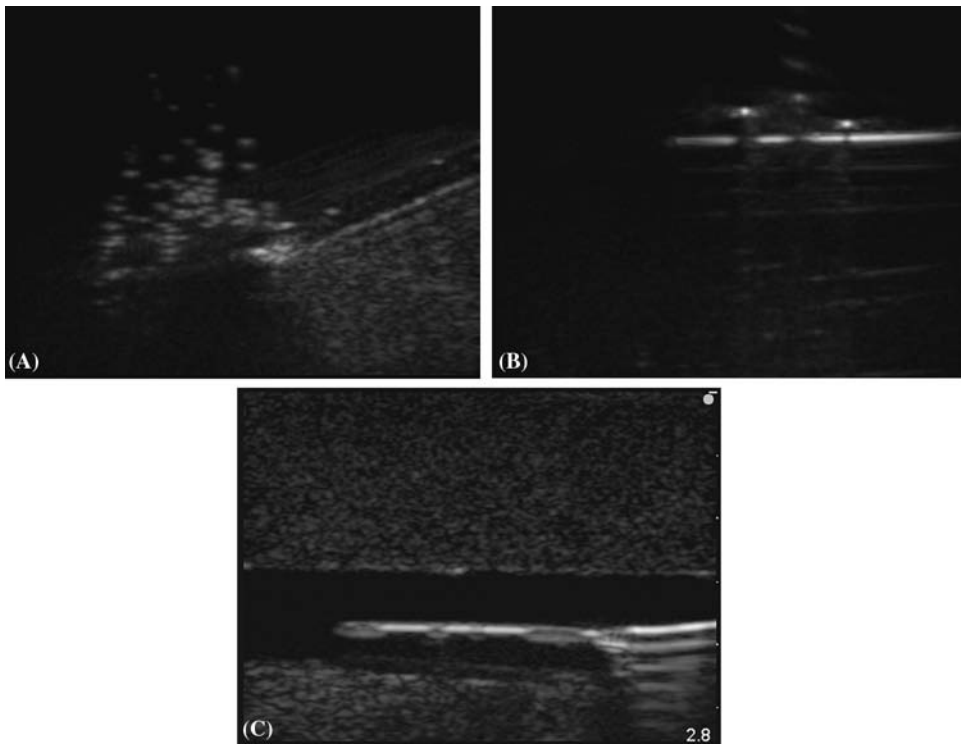


Figure 11 (A) A 16G Tuohy needle seen in a longitudinal section with injection of microbubbles. The machined needle tip appears brighter than the shaft. Also noticeable is the reverberation artifact inferior to the shaft. (B) An 18G plastic three-holed epidural catheter in a water bath with slow injection of air. Bubbles are seen escaping through the three holes in the epidural catheter. The bubbles cast an acoustic shadow below, obscuring a section of the catheter. (C) Agar phantom with a fluid-filled cavity in a water bath. An 18G Tuohy needle with an epidural catheter is seen in a longitudinal section. A reverberation artifact inferior to the needle and air bubbles within the catheter are demonstrated.

- Injection of solutions, containing microbubbles, from the needle into a vein can be seen with ultrasound, and this is the basis of one type of ultrasound contrast media (25,26). Any solution injected from a syringe will have some microbubbles in it. This can be dramatically increased by agitation (Fig. 11).
- Power Doppler ultrasound may be used to localize the needle tip by detecting physical vibrations. Rotating a stylet, whose tip is slightly bent, inside a stationary cannula while the stylet is completely within the cannula creates lateral vibrations. The minute deflection at the needle tip when rotated causes tissue motion. In contrast, extending and retracting a straight stylet inside a stationary cannula produces axial vibration. The stylet's tip makes contact with the tissue and causes it to move. The lateral vibration method appears to perform better than the axial vibration method under approximately the same variety of configurations (e.g., different insertion angles and depths). Tissue stiffness affects the performance of the lateral vibration method although good images can be obtained through proper tuning of the ultrasound machine.

NEEDLE GUIDANCE TECHNIQUES

There are two main ways that needles can be guided through the tissues, direct and indirect methods.

Indirect Ultrasound Guidance

The target structure is localized prior to puncture using ultrasound. The skin is marked, and the angle and depth of the needle course are estimated. Imaging is then abandoned and the needle directed toward the predicted target tissue. Indirect ultrasound guidance is likely to be safer than pure landmark techniques as it identifies the approximate position of a suitable target structure, e.g., a large patent and nonthrombosed vein. However, it is only really suitable where there is a widespread collection to be drained, e.g., ascitic fluid or a pleural effusion, which requires neither precise needle placement nor avoidance of collateral structures apart from the inferior epigastric and intercostal vessels, respectively.

Direct Ultrasound Guidance

Ultrasound identifies the target structure and then is used to visualize the needle in real time as it traverses through the tissues and guide it to precisely penetrate or lie alongside this, as necessary. Collateral structures can be deliberately avoided.

Real-time scanning techniques produce a rapid series of images, which are displayed sequentially to depict motion giving a real-time, two-dimensional image of a three-dimensional structure. With the introduction of the needle, a dynamic operator machine feedback loop is formed, and with practice, control of the probe and needle is accomplished. Self-aspiration devices may free up the operator's hand and enable the needle to be directed with more control and confidence.

The practitioner is required to concentrate on the image on the screen as well as the patient. Hence it is important to have the patient's anatomical area of interest and the ultrasound screen in the same line of vision and to have the correct anatomical orientation between the two (see above). Usually this means placing the display at eye level on the opposite side of the patient to where the operator is standing.

Direct ultrasound guidance may be divided into two techniques, needle guidance devices and free-hand punctures.

Needle Guidance Devices

Needle guides direct the needle in a fixed, predetermined direction to various depths from the transducer surface, depending on the selected angle of the guide relative to the transducer (27–29). These vary between manufacturers and may be a fixed part of the transducer or detachable, sterile, single-use plastic, or reusable metal devices. Fixed guides lie within the sterile sheath, while sterile, detachable guides are attached onto the probe over the sterile sheath (Fig. 12). Guides are designed to be used in either the transverse or the longitudinal plane. Tram lines can be generated electronically on the display to show the approximate path of the needle as seen in Figure 6. These guides are particularly useful for directing needles into deeper structures like the kidney. Longer needles will be required to compensate for the less acute angle of trajectory and the section of needle held in the guide. The direction of the bevel and the flexibility of the shaft may alter the trajectory, particularly with long needles.

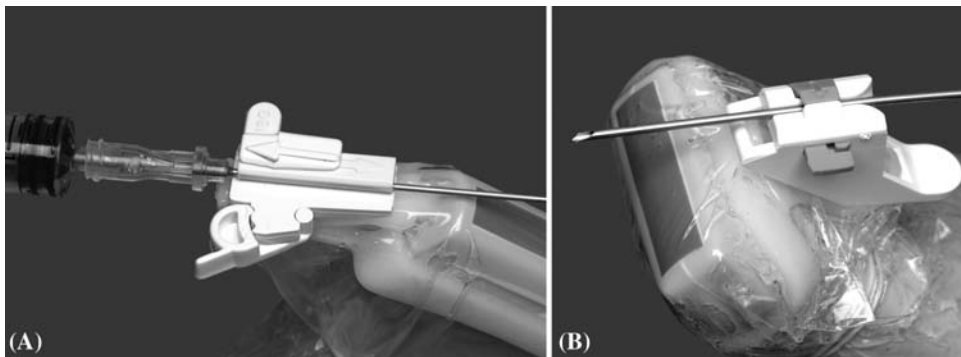


Figure 12 Needle guides can be aligned either along the long axis or the short axis (transverse configuration) of the probe. (A) The sterile disposable needle guide is mounted along the long axis over the sterile plastic sheath and ultrasound probe. (B) The needle guide is mounted along the transverse axis. CISCO guide and Sonosite probes.

The target structure is identified and positioned in the tram lines on the display and the probe held still. The depth from the skin can be estimated or formally measured. The needle is clamped in the guide and passed through tissues either to a predetermined depth or until needle tip position in the target structure can be identified by direct visualization or other means (e.g., aspiration of blood). Needle guides present an additional cost but may be helpful for the novice or occasional user, in more difficult cases or as a teaching aid to provide valuable insight into needle visualization.

Free-Hand Puncture

Many ultrasound practitioners prefer the “free-hand” approach. The needle is inserted through the skin directly into the view of the transducer without the use of a guide (17,30). This provides greater flexibility without additional equipment and allows for subtle adjustments compensating for improper trajectory or patient movement. The probe may also be more easily positioned to ensure satisfactory contact with the skin. The operator holds the transducer with one hand and inserts the needle with the other. The needle may be inserted parallel (longitudinal) to the transducer or perpendicular (transverse) to it. The target structure may be imaged in longitudinal or cross section and the needle then introduced either transverse or longitudinal to the beam. The choice will depend on the applied anatomy, desired direction of needle insertion, ease of visualization of structures with ultrasound, and operator skill and experience. For example, a cross-sectional view of central veins may be easier to interpret and may give a better view of collateral structures such as the artery or chest wall. We would argue that for central venous catheterization, it is more important to miss collateral structures than to hit the internal jugular than access the vein on the first pass.

TECHNIQUES OF NEEDLE VISUALIZATION

The importance of ultrasound-guided insertion of central lines for vascular access is well recognized (6,31,32). A recent review has illustrated the techniques of ultrasound guidance used during nerve blockade (33). Irrespective of the technique that is being performed, some verification of needle tip placement in the target structure is required, e.g., aspiration of blood or fluid or the vein reopening following collapse due to the pressure of the advancing needle. The needle may appear to be in the vessel

sonographically but still be covered by adherent tissues because of the large, relatively blunt needles. The same considerations would apply during regional nerve block techniques when relatively blunt needles need to penetrate the fascial sheath encasing the neurovascular bundle. Confirmation of position could be established by the click as the needle enters the sheath, visualization of the needle tip in the tissues, a positive low-threshold signal from a nerve stimulator, or visualization of the injected local anesthetic in the area of interest. If the injected local anesthetic does not appear as a fluid-filled collection in the area of injection, then it is likely that it is entering an incorrect location, e.g., the pleural space or vascular system.

Transverse and longitudinal approaches are described below in relation to central venous access.

Transverse Approach

In the transverse approach, the needle is inserted steeply, nearly parallel to the ultrasound beam. Typically, vessels are viewed in cross section, enabling adjacent structures to be easily visualized, but this approach gives poorer visualization of the needle because, first, the angle of approach of the needle is out of necessity more parallel to the ultrasound beam, and second, only one short segment of the needle is visible as an echogenic area on the display at any one time. What is thought to be the tip of the needle may actually be the needle shaft. Rocking the transducer back and forth or withdrawing the needle slightly and realigning it in a more vertical plane can establish the position of the needle tip at this point. The needle tip is seen as a highly echogenic (white) spot, which disappears as soon as the transducer is angled distal to it and moves with the operator. The sequence is shown in Figure 5.

Despite the above disadvantages, a study on residents who attempted to cannulate a synthetic arm showed that novice ultrasound users obtain vascular access much faster using a short-axis (transverse) approach than a long-axis (longitudinal) approach (34).

Longitudinal Approach

The longitudinal view allows much better needle visualization because the needle is more perpendicular to the ultrasound beam and multiple dots build up the image of the needle. However, the needle course is seen only in relation to the vessel of interest and not in relation to adjacent structures. If the needle approach is made steeper the image will degrade.

The target vessel is scanned using the transverse view to establish its position in relation to the skin and the surrounding tissues. The transducer is then rotated through 90° so that it overlies the vessel along its length. The position over the vein can be confirmed, as it is easily compressible and nonpulsatile. The needle is inserted at an angle of approximately 45° to the skin and directed beneath the transducer along its length. The needle must be kept within the image plane and care taken to avoid the probe inadvertently moving from over the target vein to the adjacent artery. The needle is visualized clearly as it approaches, then indents, and then enters the vein. The position of the needle within the vein is then confirmed with free aspiration of blood, and the guidewire is inserted and visualized within the vein after the needle is withdrawn as before.

Hybrid Approach

In this approach, structures are visualized in cross section, but the needle approach is in the longitudinal axis. Care needs to be taken to ensure that the guidewire passes in the correct direction centrally. Again, as in the cross-sectional approach, guidewires are less likely to travel in the direction intended.

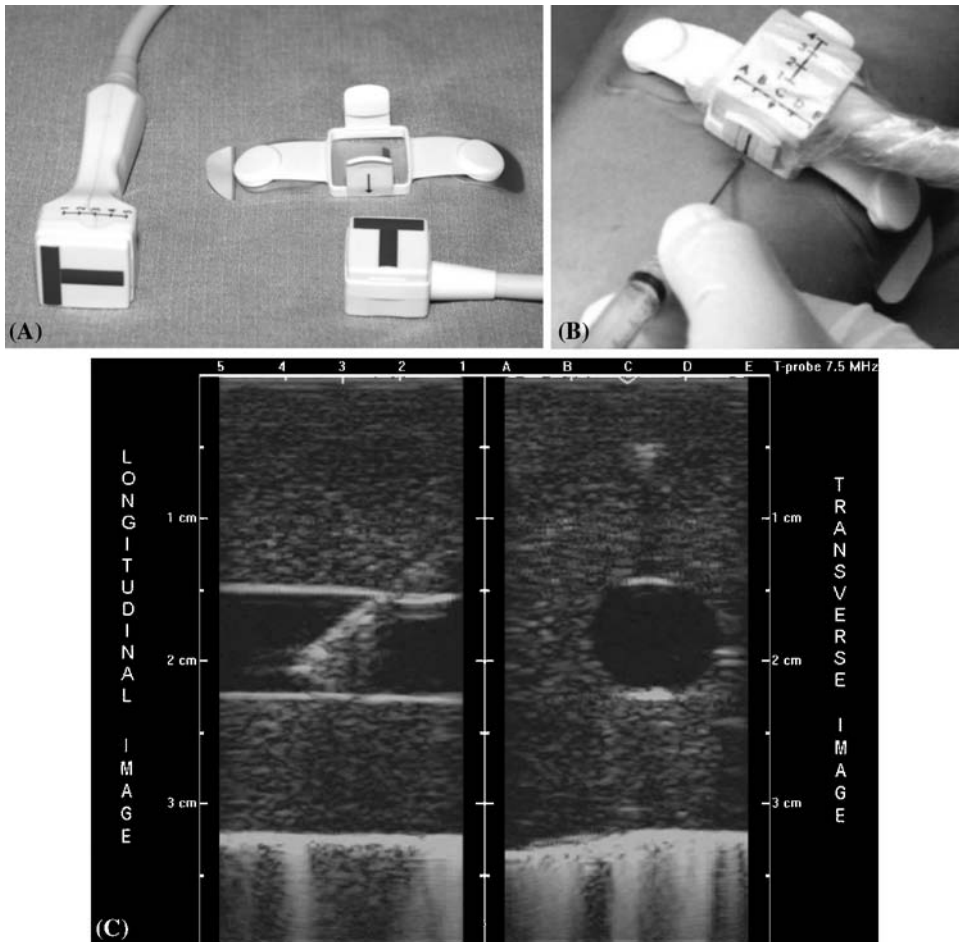


Figure 13 (A) A “Punctsure” ultrasound probe (PunctSURE ultrasound, Inceptio Medical Technologies, Kaysville, Utah, U.S.) contains two linear array transducers aligned perpendicular to each other. This provides simultaneous imaging in both a longitudinal and a transverse plane using a single handheld (*left*) or hands-free securable probe with an adhesive securing device (*right*). (B) A “Punctsure hands-free” probe secured using a bracelet strap with the needle introduced initially into the transverse beam and then passed into the longitudinal beam. (C) The “Punctsure” ultrasound machine displays both longitudinal (*left*) and transverse (*right*) ultrasound images on the same screen. The needle is passing into the fluid-filled agar phantom. This picture illustrates how the needle tip is located within the vessel in the longitudinal view (*left*). However it appears to be outside the vessel on the image on the right (transverse view) as it is the shaft rather than the tip of the needle that is being visualized.

Future Developments

Academic and commercial interest in this area is increasing with a number of new developments including the following:

1. Hands-free ultrasound probes
2. Probes with both transverse and longitudinal arrays, allowing simultaneous visualization of needle position in both planes (Fig. 13)
3. Three-dimensional probes
4. Needle tips which emit an ultrasound signal that is detected by the probe and visualized as a pulsating spot

5. Mirror-type systems, e.g., the sonic flashlight, merging real-time images from ultrasound with direct human vision (real-time tomographic reflection)
6. Echo-tip needles
7. Robot-assisted devices

The value of the above systems has yet to be proven, and all are likely to be more expensive than standard needles and ultrasound devices.

CONCLUSION

Ultrasound techniques demands detailed knowledge of the regional anatomy to identify surrounding structures and interpret images when seeking out target vessels and nerves. A measure of hand-to-eye coordination is necessary, and the ability to process two-dimensional images while thinking and working in a three-dimensional environment requires patience and practice.

Time spent understanding and practicing the applied physics of needle visualization with ultrasound will be repaid many times over when performing invasive procedures. The operator's skill in aligning the ultrasound probe and needle is arguably the most important variable influencing needle visualization, and considerable real-time scanning experience remains the key factor to the successful performance of ultrasound-guided interventions.

ACKNOWLEDGMENTS

We thank Dr. J. A. Evans (senior lecturer in medical physics) and Dr. M. J. Darby (consultant radiologist), both based in Leeds, U.K., for reviewing the text and medical photography and illustrations.

REFERENCES

1. Sharma A, Bodenham AR, Mallick A. Ultrasound-guided infraclavicular axillary vein cannulation for central venous access. *Br J Anaesth* 2004; 93(2):188–192.
2. Sandhu NS, Capan LM. Ultrasound-guided infraclavicular brachial plexus block. *Br J Anaesth* 2002; 89(2):254–259.
3. Chan VW, Perlas A, Rawson R, et al. Ultrasound-guided supraclavicular brachial plexus block. *Anesth Analg* 2003; 97(5):1514–1517.
4. Scott DH. Editorial II: The king of the blind extends his frontiers. *Br J Anaesth* 2004; 93(2): 175–177.
5. Scott DH. It's NICE to see in the dark. *Br J Anaesth* 2003; 90(3):269–272.
6. Calvert N, Hind D, McWilliams R, et al. Ultrasound for central venous cannulation: economic evaluation of cost-effectiveness. *Anaesthesia* 2004; 59(11):1116–1120.
7. Chalmers N. Ultrasound guided central venous access. NICE has taken sledgehammer to crack nut. *BMJ* 2003; 326(7391):712.
8. Maury E, Guglielminotti J, Alzieu M, et al. Ultrasonic examination: an alternative to chest radiography after central venous catheter insertion? *Am J Respir Crit Care Med* 2001; 164(3): 403–405.
9. Caspers JM, Reading CC, McGahan JP, et al. Ultrasound-guided biopsy and drainage of the abdomen and pelvis. In: Rumack CM, Wilson SR, Charboneau JW, eds. *Diagnostic Ultrasound*. USA: Mosby, 1997.
10. Merritt CR. Physics of ultrasound. In: Rumack CM, Wilson SR, Charboneau JW, ed. *Diagnostic Ultrasound*. USA: Mosby, 1998.

11. Kremkau FW. *Diagnostic Ultrasound: Principles and Instruments*. Philadelphia: Saunders, 2002.
12. Chapman GA, Johnson D, Bodenham AR. Visualisation of needle position using ultrasonography. *Anaesthesia* 2006; 61(2):148–158.
13. McGahan JP. Laboratory assessment of ultrasonic needle and catheter visualization. *J Ultrasound Med* 1986; 5(7):373–377.
14. Wang HC, Yu CJ, Chang DB, et al. Transthoracic needle biopsy of thoracic tumours by a color Doppler ultrasound puncture guiding device. *Thorax* 1995; 50(12):1258–1263.
15. McNamara MP Jr., McNamara ME. Preparation of a homemade ultrasound biopsy phantom. *J Clin Ultrasound* 1989; 17(6):456–458.
16. Fornage BD. A simple phantom for training in ultrasound-guided needle biopsy using the freehand technique. *J Ultrasound Med* 1989; 8(12):701–703.
17. Matalon TA, Silver B. US guidance of interventional procedures. *Radiology* 1990; 174(1):43–47.
18. Schafhalter-Zoppoth I, McCulloch CE, Gray AT. Ultrasound visibility of needles used for regional nerve block: an in vitro study [see comment]. *Reg Anesth Pain Med* 2004; 29(5):480–488.
19. Reading CC, Charboneau JW, Felmler JP, et al. US-guided percutaneous biopsy: use of a screw biopsy stylet to aid needle detection. *Radiology* 1987; 163(1):280–281.
20. Heckemann R, Seidel KJ. The sonographic appearance and contrast enhancement of puncture needles. *J Clin Ultrasound* 1983; 11(5):265–268.
21. Jandzinski DI, Carson N, Davis D, et al. Treated needles: do they facilitate sonographically guided biopsies? *J Ultrasound Med* 2003; 22(11):1233–1237.
22. Perlas A, Chan VW, Simons M Brachial plexus examination and localization using ultrasound and electrical stimulation: a volunteer study. *Anesthesiology* 2003; 99(2):429–435.
23. Raj PP, de Andres J, Grossi P, et al. Aids to localization of peripheral nerves. In: Raj PP, ed. *Textbook of Regional Anesthesia*. New York, NY: Churchill Livingstone, 2002:251–284.
24. Tsui BC, Wagner A, Finucane B. Electrophysiologic effect of injectates on peripheral nerve stimulation.[see comment]. *Reg Anesth Pain Med* 2004; 29(3):189–193.
25. Lindner JR, Lewis C. Contrast echocardiography: clinical utility for the evaluation of left ventricular systolic function. *Am Heart Hosp J* 2004; 2(1):16–20.
26. Feinstein SB. The powerful microbubble: from bench to bedside, from intravascular indicator to therapeutic delivery system, and beyond. *Am J Physiol Heart Circ Physiol* 2004; 287(2): H450–H457.
27. Rizzato G, et al. Aspiration biopsy of superficial lesions: ultrasonic guidance with a linear-array probe. *AJR Am J Roentgenol* 1987; 148(3):623–625.
28. Buonocore E, Skipper GJ. Steerable real-time sonographically guided needle biopsy. *AJR Am J Roentgenol* 1981; 136(2):387–392.
29. Reid MH. Real-time sonographic needle biopsy guide. *AJR Am J Roentgenol* 1983; 140(1): 162–163.
30. Reading CC, Charboneau JW, James EM, et al. Sonographically guided percutaneous biopsy of small (3 cm or less) masses. *AJR Am J Roentgenol* 1988; 151(1):189–192.
31. National Institute for Clinical Excellence. *Guidance on the use of ultrasound locating devices for central venous catheters (NICE technology appraisal, No. 49)*. London: NICE, 2002.
32. Alderson PJ, Burrows FA, Stemp LI, et al. Use of ultrasound to evaluate internal jugular vein anatomy and to facilitate central venous cannulation in paediatric patients. *Br J Anaesth*, 1993; 70(2):145–148.
33. Marhofer P, Greher M, Kapral S Ultrasound guidance in regional anaesthesia. *Br J Anaesth* 2004; 26:26.
34. Blaiwas M, Brannam L, Fernandez E. Short-axis versus long-axis approaches for teaching ultrasound-guided vascular access on a new inanimate model. *Acad Emerg Med* 2003; 10(12): 1307–1311.

4

Teaching, Training, and Accreditation

Heather Venables

Education, Health & Sciences, University of Derby, Derby, U.K.

INTRODUCTION

There has been a significant increase in the use of ultrasound in anesthesia, critical care, and pain management in recent years. Within the United Kingdom, this has been driven, in part, by the publication of guidelines from the National Institute for Health and Clinical Excellence (1) on the use of ultrasound in the placement of central venous catheters (CVCs). Many departments have already purchased equipment in order to comply with these guidelines. However, there remains no clear strategy for training and accreditation.

The development of an agreed national training and accreditation program for ultrasound in anesthesia, critical care, and pain management in the United Kingdom may be hindered by the fact that multiple professional bodies are involved and that there is no mandatory requirement for formal training.

The Royal College of Anaesthetists, the Pain Society, and the Critical Care Society each have within their stated remit a commitment to training and education. However, to date they have offered little guidance.

One exception to this is the Association of Cardiothoracic Anaesthetists. In collaboration with the British Society of Echocardiography, the association has issued an agreed curriculum and formal examination (see www.bsecho.org). Cardiac ultrasound is a highly specialized area, requiring a level of expert practice that exceeds what would be expected for most other applications under discussion.

The NICE guidelines (2002) recommend that “*all those involved in placing CVCs using 2D imaging ultrasound guidance should undertake appropriate training to achieve competence.*” However, this document makes no attempt to define competence and does not define or quantify what may be considered “appropriate” training.

In the United Kingdom, the Royal College of Radiologists (RCR) has issued recommendations for training nonimaging specialists in ultrasound techniques (2). The document can be viewed in full at www.rcr.ac.uk.

The RCR recognizes the need for a range of specialties to develop ultrasound skills and outlines a proposed curriculum for each area, including both intensive care and focused emergency ultrasound. The document provides a reasonably comprehensive syllabus for critical care ultrasound, but there is no specific mention of anesthetics or pain

management. The range of examinations likely to be undertaken by these groups spans a number of disciplines, including emergency ultrasound, vascular and musculoskeletal applications.

This chapter seeks to highlight the need for a robust training and assessment strategy for ultrasound in anesthesia, critical care, and pain management. It explores some of the barriers to this and outlines how other professional groups have responded. For those with an interest in the provision of local training, some of the practical issues that need to be considered are highlighted.

WHY TRAINING IS IMPORTANT

It is widely recognized that ultrasound is highly operator dependent. Users are both ethically and legally vulnerable when they use equipment without adequate training (2). However, equipment is available in many departments, and there may be no clear regulation of its use.

There are many positive publications in the literature to support the use of ultrasound in anesthesia and critical care, and these have led to recommendations such as those issued by NICE. Key perceived benefits include a reduction in complications for procedures such as CVC placement (3–6). However, there is also sporadic evidence to suggest that the use of ultrasound may increase rather than decrease complications through operator inexperience or the use of unsuitable equipment (7).

Initial use of ultrasound has developed as an aid to interventional procedures rather than as a diagnostic tool. There is, however, an element of diagnosis inherent in any ultrasound examination, and this will grow as operator skills and experience develop. For example, if a thrombosed central vein is noted during venous access, referral for more formal imaging and the need for short- or long-term anticoagulation should be considered. It would be inappropriate to simply ignore this and move to an alternative puncture site (8,9).

However limited the intended use of ultrasound, it is essential that users be aware of how the equipment can be manipulated so as to avoid diagnostic confusion and to be able to interpret ultrasound images beyond simple recognition of normal anatomy.

In addition to the use of ultrasound to guide venous access, there has been a rapid increase in the range of diagnostic and interventional procedures undertaken by anesthetists and intensivists. In the future it is envisaged that procedures such as arterial access, diagnosis of pleural collections, echocardiography, regional nerve blocks, and other techniques are likely to be performed routinely by anesthetists using ultrasound (8,10–13).

Thoracic imaging by specialists is rapidly evolving to include assessment of the size and nature of pleural effusions and detection of pneumothoraces, peripheral pulmonary emboli, and other lung pathologies, all of which are diagnostic in intent (14–17).

There is growing acceptance among imaging specialists of a legitimate clinical need for ultrasound services to be provided by nonradiologists. The evidence for the development of point-of-care imaging is compelling (18–20). The training recommendations issued by the RCR are a direct response to this evidence (2) (www.rcr.ac.uk).

These include an outline syllabus for urological, gynecological, gastrointestinal, vascular, breast, thoracic, focused emergency, musculoskeletal, and intensive care applications. The training implications of this shift of service provision are huge, and it is against this background that training for anesthetists, intensivists, and pain management specialists needs to be considered.

WHAT SHOULD TRAINING INVOLVE?

The European Federation of Societies for Ultrasound in Medicine and Biology (EFSUMB) has proposed minimal training requirements for the practice of medical ultrasound in Europe (2005) (<http://www.efsumb.org/>). These are supported by the RCR and the British Medical Ultrasound Society. The EFSUMB recommendations make no specific mention of anesthesia, critical care, or pain management, but form the basis of the RCR guidelines.

Both documents define an appropriate level of training in ultrasound as “one that allows for the provision of a safe and effective ultrasound service” (2). On this basis, training requirements are divided into three levels of competency. These are summarized in Table 1.

Level 1 Training

Level 1 training is seen as the standard of knowledge and practice that most nonimaging specialists, including anesthesiologists and intensivists, are likely to require. Some may then extend their practice to Level 2, with a small number including those undertaking the transesophageal echocardiogram (TEE) and perhaps more complex nerve blocks] functioning at Level 3 (2,8).

The boundaries between these three levels are difficult to define with any precision and are the subject of debate. However, they provide a useful framework within which the

Table 1 Levels of Training

Level 1

Practice at this level would usually require the following abilities:

- To perform common examinations safely and accurately.
- To recognize and differentiate normal anatomy and pathology.
- To diagnose common abnormalities within certain organ systems.
- To recognize when a referral for a second opinion is indicated.
- To understand the relationship between ultrasound and other imaging.

Within most medical specialties, training would be gained during parent specialist training programs.

Level 2

Practice at this level would usually require *most or all* of the following abilities:

- To manage referrals from level 1 practitioners.
- To recognize and diagnose almost all abnormalities in the relevant organ system.
- To perform common noncomplex ultrasound-guided invasive procedures.
- To teach ultrasound to trainees and level 1 practitioners.
- To conduct some research in ultrasound.

The training up to this level would be gained during a period of subspecialty training either within or after completion of the parent specialist training.

Level 3

This is an advanced level of practice, which includes *some or all* of the following abilities:

- To accept tertiary referrals from level 1 and level 2 practitioners.
- To perform specialized examination and guided invasive procedures.
- To conduct substantial research and development in ultrasound.
- To teach ultrasound at all levels.

In the United Kingdom, this would equate to a consultant radiologist with a subspecialty practice that includes a significant commitment to ultrasound.

breadth and level of practice in any specialty can be defined. However, some areas such as musculoskeletal ultrasound do not fit easily into progressive “levels” of training. In this case, the RCR recommends an alternative “modular” approach. This may be a more helpful model when considering the range of different body areas that may be of interest in anesthetics, critical care, and pain management.

The College of Emergency Medicine (CEM) has recently endorsed the development of ultrasound within the specialty and has issued guidelines on the introduction of Level 1 ultrasound training and assessment as part of its formal credentialing for specialist registrars. This training provides a helpful model for the introduction of training and assessment at a national level that could assist in the development of training and accreditation for other specialties. The CEM recommendations are based on EFSUMB and RCR guidelines. However, these have been adapted to include a more flexible approach to practical training and the assessment of competence.

The CEM proposals for training are summarized below but can be viewed in full at <http://www.emergencymed.org.uk/CEM> under specialist training. It is envisaged that all specialist registrars in emergency medicine will have acquired the relevant knowledge and skills by the end of their fourth year of training.

Theoretical Training

It is useful to consider the theoretical and practical aspects of ultrasound training as distinct components.

Preliminary theoretical training should cover relevant anatomy, the physics of ultrasound, levels and sophistication of equipment, image recording, reporting, artifacts, and the relevance of other imaging modalities to ultrasound (2). This element of training may be best delivered by linking with some of the excellent courses run by university departments accredited by the Consortium for the Accreditation of Sonographic Education (CASE). Although these modular courses were aimed initially at radiographers, they are now accessed by a growing number of clinicians from a range of specialties. As a result, course providers are becoming more aware of the need for increased flexibility. Within these programs of study, trainees are able to work toward negotiated learning outcomes that focus on their own area of clinical practice. This has replaced the “all-or-nothing” approach that was designed primarily for imaging specialists.

There are numerous short courses provided nationally and regionally that are aimed at nonimaging specialists. Although, to date, few of these are aimed specifically at anesthetists or intensivists, the basic principles of ultrasound are relevant and transferable between specialties, and these may contribute to the provision of theoretical training.

Some trusts have introduced modular training in the clinical setting. Delivered through Specialist Registrar training afternoons, these may include didactic and practical ultrasound sessions. It is also likely that e-learning will play an important part in the dissemination of theoretical knowledge (Table 2).

Practical Training

Practical experience should be gained under the guidance of a named supervisor who has been trained in ultrasound, within a training department (2). The RCR recommends that this should be a department of clinical radiology; however, this raises some significant issues.

NICE predicts the need for radiology input of approximately 0.5 of a consultant radiologist in the first year of implementation of ultrasound-guided CVC placement

Table 2 Summary of Recommended Theoretical Syllabus for Level 1

| |
|--|
| Anatomy—relevant to area of ultrasound practice |
| Physics and instrumentation—basic components of an ultrasound system |
| <ul style="list-style-type: none"> • Types of transducers, production of ultrasound, and use of ultrasound controls • Frequency, image quality, and penetration • Interaction of ultrasound with tissue, including biological effects • Safety of ultrasound • Basic principles of real-time and Doppler ultrasound • Recognition and explanation of common artifacts • Image recording systems |
| Ultrasound techniques |
| <ul style="list-style-type: none"> • Patient information and preparation • Indications for examinations • Relevance of ultrasound to other imaging modalities • The influence of ultrasound results on the need for other imaging • Scanning techniques, including the use of spectral Doppler and color Doppler |
| Administration |
| <ul style="list-style-type: none"> • Image recording, storing, and filing • Reporting • Medicolegal aspects • Requirements for training • Consent • Departmental protocols • Resource implications of ultrasound use |

Source: From Ref. 2.

within each trust, with the expectation that this will decrease as skills are cascaded downward (1).

The practical implications of training a large number of staff are formidable, including cost, training time, and access to equipment. It is unrealistic to expect clinical radiology departments to be able to provide this level of input when they are often struggling to meet the training needs of their own staff. They have existing commitments to established programs, such as the joint RCR/Royal College of Obstetricians and Gynaecologists (RCOG) training initiative (www.rcog.org.uk), and are swamped by requests for training from an ever-increasing group of specialists. This is further exacerbated by a national shortage of radiologists and sonographers.

If formal ultrasound training and accreditation are to be established in anesthesia, critical care, and pain management, they will need to be adequately funded and these costs will need to be met by the relevant departments.

HOW MUCH TRAINING IS REQUIRED?

Ultrasound is essentially a practical skill that requires excellent hand-eye coordination, spatial awareness, and pattern recognition, as well as a good grasp of underlying theory. Individual trainees will acquire these skills at widely different rates. Any training program that is too prescriptive is likely to be unhelpful.

It is also important to acknowledge that some individuals do not have a natural aptitude to undertake ultrasound examinations. Intensive training and support may be

required in some cases. Despite this, a small number of individuals may remain unable to practice independently at the required level of competence.

The RCR-recommended minimum number of examinations in each area is high and the subject of some debate. In emergency medicine, there is a growing body of evidence to suggest that focused ultrasound skills can be acquired without the need for extensive periods of practical training. For highly focused examinations, such as focused assessment with sonography in trauma (FAST), published studies have used widely differing training schedules. These range from a minimum of one-hour didactic and one-hour practical sessions (21) to more than 500 supervised examinations (22).

A key guiding principle of many applications of ultrasound in the emergency medicine setting is the concept of a “rule-in” approach. Negative or equivocal ultrasound findings are noncontributory. Positive findings are documented and are used to inform clinical decision making as part of an agreed algorithm. However, no attempt is made to exclude pathology or confirm normal findings. It is therefore possible to develop technical and interpretive skills to undertake a “rule-in” examination far quicker than would be expected if the user were required to undertake a thorough examination to exclude pathology. This can lead to some degree of confusion and, on occasion, disagreement between professional groups where there is a misunderstanding of the “rule-in” approach.

The use of ultrasound in anesthesia, critical care, and pain management includes examinations that fall into both the “rule-in” and exclusion categories. This can be a helpful distinction to make when planning rollout of initial training. Ultrasound is a beguiling tool once basic competence is acquired and equipment is purchased. By clarifying the exclusion value of each examination, trainees can be encouraged to develop a better awareness of their own limitations and the limitations of the technique.

Assessment of Competence

A simplistic requirement for minimum numbers as an indicator of implied competence is educationally unsound. The end point of training should be judged by an assessment of competence. It is therefore essential that the required competencies be clearly defined. The relevant colleges and specialist societies will need to engage in this.

The RCR recommendations provide a useful starting point and have been used by the CEM in the development of a Level 1 training and assessment document. The CEM has produced a competency-based triggered assessment document that is similar to those used in surgical training (23). This moves away from the concept of absolute number of scans or hours training and promotes self-assessment of competence by the individual prior to final assessment of skills.

Trainees must pass a module of theoretical learning, undertake a period of training under the supervision of a named supervisor (a Level 2 or Level 1 practitioner with one-year experience), and keep a log of their experience.

When the trainees feel that they have reached a suitable level of competence, an assessment is triggered. This is then undertaken by the supervisor in a real-life situation and enables assessment of the trainees’ judgment in action, as well as individual skill elements.

If the assessment criteria are met, the trainees are “signed off” as competent in that specific examination [e.g., FAST and abdominal aortic aneurysm (AAA)] and no further exit examination is required. If the trainees fail to meet any of the criteria, feedback is given and a date for the next assessment is agreed.

Further assessments will be triggered as the trainees gain competence in each new area of ultrasound practice. A similar model would apply well to the use of ultrasound in a range of examinations in anesthesia, critical care, and pain management.

WHO SHOULD PROVIDE SUPERVISION AND ASSESSMENT?

The RCR recommends that trainees be supervised by a Level 2 practitioner, or a Level 1 practitioner with a minimum of two years of experience, from the same specialist area. The CEM has reduced this requirement to a Level 1 practitioner with a minimum of one year's experience. This was in part a pragmatic solution to the limited number of suitably experienced staff members available to train a "first generation" of Emed Ultrasound practitioners. However, this also recognizes the straightforward "rule-in" nature of most initial applications. It is envisaged that training for more complex investigations will be undertaken by Level 2 practitioners in each trust.

Any ultrasound training initiative for nonimaging specialists should foster close relationships with radiology. This will ensure that mutual support continues beyond the initial role out of training. Ideally a radiologist should act as mentor and regular clinicoradiology meetings should be established (2).

It is likely that there will be significant local and regional variation in the level of support offered by existing imaging services. In some trusts, there is strong radiology support, and structured in-house training is already in place. Sonographers also provide an excellent training resource and should be encouraged to contribute to both planning and implementation of local training.

In anesthesia, critical care, and pain management, a compounding problem is the nature of the examinations that will be undertaken. Some of these fall outside the remit of traditional imaging specialists. For example, few radiologists or sonographers have any practical experience of ultrasound imaging of nerves, pneumothoraces, etc (24).

The provision of adequate training for the first cohort of practitioners in any trust will be challenging and will require commitment within each department. National agreement on suitable training and assessment as a requirement by the relevant colleges and professional bodies could act as a driver for change. This would undoubtedly make it easier for each trust to justify the need to commit significant financial and human resources.

Setting Up a Local Training Program

In the absence of national guidance, individual departments will need to consider how best to provide training for their staff and prevent risk to patients from imprudent use of equipment.

As with many other medical training initiatives, the presence of a "local champion" is key (25–27). Ideally this should be someone who is senior, is on the permanent staff, is good at motivating others, has time allocated to this role, and has experience of the relevant ultrasound techniques.

The CEM has established a network of regional coordinators to oversee the implementation of ultrasound training. These experienced practitioners have the overall responsibility for the development of local courses and to cascade training within each deanery.

A number of practical considerations that may have an impact on the successful rollout of training are summarized in Table 3.

Table 3 Practical Considerations When Setting Up a Local Ultrasound Training Program

| | |
|--|--|
| Who will provide initial training? | Level 2/level 1 practitioner with experience to act as trust-wide lead. Who will provide funding for back fill? |
| Whom to train first? | Senior staff/middle grade. Can then cascade to juniors. Staff turnover may be an issue. |
| When will training be delivered? How often? | Availability of staff. Can be difficult to gather staff because of clinical commitments/leave. |
| Supervision of trainees | Experienced staff not always available to supervise when ultrasound examination is indicated. |
| Protocols | Clear protocols need to be agreed upon, including restrictions on unsupervised use of equipment and referral of incidental findings. |
| Record keeping/audit | Essential, if the impact of training is to be monitored and evaluated. The output of any ultrasound examination should be a written report. |
| Loss of landmark skills for intervention | Concern regarding loss of landmark skills is well documented in relation to CVC insertion. This will need to be evaluated as the use of ultrasound increases. |
| Provision/organization of disposables/security | Who will be responsible for ordering disposables such as ultrasound gel, transducer covers, etc.? Who is responsible for the secure storage of the equipment? |
| Equipment purchase and maintenance/cleaning | How many machines? Where should they be located? Is maintenance/warranty included in the initial purchase cost/covered by the local trust? Risk of cross-infection from ultrasound equipment is well documented. |

Maintenance of Skills

Once trainees are deemed competent, there will be a need for continuing professional development and maintenance of practical skills. For critical care, the RCR recommends that a Level 1 practitioner undertake a minimum of 100 examinations per year with no more than one month elapsing between periods of practice (2).

The CEM stipulates that no more than three months should elapse without the trainees using their scanning skills. If more than three months elapses, the trainees must be reassessed with direct observation of procedural skills by a trainer.

Both RCR and CEM recommend that all practitioners should

- have regular meetings within the department to ensure appropriate ultrasound use,
- have a named “ultrasound mentor,”
- include ultrasound in their ongoing CME,
- audit their practice,
- participate in multidisciplinary meetings, and
- keep up to date with relevant literature.

Regular contact between the department lead for ultrasound practice and radiological colleagues is encouraged.

THE GRANDFATHER CLAUSE

Within anesthesia, critical care, and pain management, there may be a significant number of senior staff members who have considerable experience of ultrasound but no formally

recognized training. This is similar to emergency medicine where focused ultrasound has been used in the United Kingdom since the early 1990s.

The CEM has stated that “practitioners who have used Ultrasound in Level 1 practice for some time, but have never been through an assessment process may be deemed to be ‘Level 1 competent’ for the purposes of appraisal if they have a letter from a Consultant Radiologist or a Consultant in EM with extensive ultrasound experience confirming their competence. This letter should be held within their appraisal folder, and the Regional Ultrasound Co-ordinator should be made aware.” It is anticipated that this “grandfather clause” will be withdrawn in the future when robust training capacity exists.

THE WAY FORWARD

Ultrasound meets all of the requirements of a first-line investigative tool. It is safe, cheap, available, and repeatable. It has a proven record in guidance of interventional procedures, and there is now compelling evidence that point-of-care ultrasound by adequately trained practitioners can reduce risk, improve patient care, and save cost.

If these expectations are to be realized in anesthesia, critical care, and pain management, there is a clear need for the relevant colleges and specialist societies to agree on a national framework for training, assessment, and continuing professional development. The Royal College of Radiologists has published recommendations that provide useful generic guidance. However, the use of ultrasound in these areas differs significantly from current traditional imaging practices. Future training and education initiatives will need to reflect this in both content and method of delivery.

Neri et al. (28) have proposed a curriculum for ultrasound in critical care that outlines training requirements for Levels 1, 2, and 3. This identifies core competencies at each level and stresses an outcome-based approach that is tailored to setting-specific training needs.

The requirement for widespread ultrasound education is a significant challenge. In emergency medicine, the inclusion of ultrasound in fellowship and resident training has now been established. However, this has left many qualified practicing physicians to fend for themselves (29). High-quality interactive online learning materials that include challenging cases are likely to be an important way of supporting this group.

There is tremendous interest worldwide in the expansion of point-of-care ultrasound, and there is a growing sense of urgency in the need for training and education. Until this is established, all clinicians have an obligation to practice within and not beyond their own limitations.

REFERENCES

1. National Institute for Clinical Excellence. Guidance on the use of ultrasound locating devices for placing central venous catheters. *NICE technical report number 49*. September 2002.
2. Royal College of Radiologists. Recommendations for training non-imaging specialists in ultrasound techniques. Royal College of Radiologists 2005.
3. Hatfield A, Bodenham A. Portable ultrasound for difficult central venous access. *Br J Anaesth* 1999; 82(6):822–826.
4. Miller AH, Roth BA, Mills TJ, et al. Ultrasound guidance versus the landmark technique for the placement of central venous catheters in the emergency department. *Acad Emerg Med* 2002; 9(8): 800–805.

5. Marhofer P, Greher M, Kapral S. Ultrasound guidance in regional anaesthesia. *Br J Anaesth* 2005; 94(1):7–17.
6. Milling TJ Jr., Rose J, Briggs WM, et al. Randomized, controlled clinical trial of point-of-care limited ultrasonography assistance of central venous cannulation: the Third Sonography Outcomes Assessment Program (SOAP-3) Trial. *Crit Care Med* 2005; 33(8):1764–1769.
7. Grebenik CR, Boyce A, Sinclair ME, et al. NICE guidelines for central venous catheterization in children. Is the evidence base sufficient? *Br J Anaesth* 2004; 92(6):827–830.
8. Bodenham AR. Editorial II: Ultrasound imaging by anaesthetists: training and accreditation issues. *Br J Anaesth* 2006; 96(4):414–417.
9. Sutin KM, Schneider C, Sandhu NS, et al. Deep venous thrombosis revealed during ultrasound-guided femoral nerve block. *Br J Anaesth* 2005; 94(2):247–248.
10. Sandhu NS, Manne JS, Medabalmi PK, et al. Sonographically guided infraclavicular brachial plexus block in adults: a retrospective analysis of 1146 cases. *J Ultrasound Med* 2006; 25(12):1555–1561.
11. Wiebalck A, Grau T. Ultrasound imaging techniques for regional blocks in intensive care patients. *Crit Care Med* 2007; 35(suppl 5):S268–S274 (review).
12. Susti A. Role of ultrasound in the airway management of critically ill patients. *Crit Care Med* 2007; 35(suppl 5):S173–S177 (review).
13. Marhofer P, Chan VW. Ultrasound-guided regional anesthesia: current concepts and future trends. *Anesth Analg* 2007; 104(5):1265–1269 (review).
14. Lichtenstein DA. Ultrasound in the management of thoracic disease. *Crit Care Med* 2007; 35(suppl 5):S250–S261 (review).
15. Bouhemad B, Zhang M, Lu Q, et al. Clinical review: bedside lung ultrasound in critical care practice. *Crit Care (London, UK)* 2007; 11(1):205 (review).
16. Balik M, Plasil P, Waldauf P, et al. Ultrasound estimation of volume of pleural fluid in mechanically ventilated patients. *Intensive Care Med* 2006; 32(2):318–321.
17. Beaulieu Y, Marik PE. Bedside ultrasonography in the ICU: Part 2. *Chest* 2005; 128:1766–1781.
18. Langlois S. Focused ultrasound training for clinicians. *Crit Care Med* 2007; 35(suppl 5):S138–S143.
19. Kirkpatrick AW. Introduction to the use of ultrasound in critical care medicine. *Crit Care Med* 2007; 35(suppl 5):S162–S172.
20. Beaulieu Y. Specific skill set and goals of focused echocardiography for critical care clinicians. *Crit Care Med* 2007; 35(suppl 5):S144–S149.
21. Ma OJ, Mateer JR, Ogata M, et al. Prospective analysis of a rapid trauma ultrasound examination performed by emergency physicians. *J Trauma* 1995; 38(6):879–885.
22. Glaser K, Tschmelitsch J, Klingler P, et al. Ultrasonography in the management of blunt abdominal and thoracic trauma. *Arch Surg* 1994; 129:743–747.
23. Fish D. The educational thinking behind The Royal College of Surgeons of England's first curriculum framework. *Ann R Coll Surg Engl* 2004; 86(4):312–315.
24. Chan SSW. Emergency bedside ultrasound to detect pneumothorax. *Acad Emerg Med* 2003; 10:91–94.
25. Freedman VA, Calkins M, DeRosiers R, et al. (Eds.) *Barriers to Implementing Technology in Residential Long-Term Care Settings*. Polisher Research Institute. Washington, DC: U.S. Department of Health and Human Services, 2005.
26. Smith D, Madden K, DeGraba T, et al. Current perspectives on interventional stroke treatment. *The stroke interventionalists*. 1998
27. Cook DJ, Montori VM, McMullin JP, et al. Improving patients' safety locally: changing clinician behaviour. *Lancet* 2004; 363(9416):1224–1230.
28. Neri L, Storti E, Lichtenstein D. Toward an ultrasound curriculum for critical care medicine. *Crit Care Med* 2007; 35(suppl 5):S290–S304.
29. Blaivas M, Kirkpatrick A, Sustic A. Focused applications of ultrasound in critical care medicine. Future directions and conclusions. *Crit Care Med* 2007; 35(suppl 5):S305–S307.

5

Ultrasound-Guided Vascular Access

A. R. Bodenham

*Academic and Clinical Departments of Anaesthesia and Intensive Care Medicine,
Leeds General Infirmary, Leeds, U.K.*

INTRODUCTION

Ultrasound-guided vascular access has been used for many years in difficult cases by radiologists who have had ready access to devices. Recently the commercial development of small, portable ultrasound machines has widened the application for this technology for venous access and other procedures by multiple specialties. The rationale for the use of such devices is to provide fast, reliable, safe guidance for needle placement both in routine and in more difficult cases. The role for ultrasound guidance in arterial puncture is less well established than in venous access, but likely to follow similar trends.

THE VENOUS SYSTEM

Is There a Clinical Need?

Most clinicians will have seen occasional severe morbidity or mortality from central venous access, and reported complications represent only the tip of the iceberg. Most published studies quote complications for central venous access between 1% and 10%, dependent on clinical case mix and the skill and experience of the operator (1–3). Such figures are generally quoted for routine venous access and are likely to be considerably higher for the more difficult case or novice operator. In the author's experience most operators tend to underestimate the frequency of complications, in their own and others' practice. There is good evidence that the risk of early complications is clearly related to the number of needle passes (1). Such procedural complications are well recognized, and those obviously related to needle puncture are listed in Table 1 (further information and illustrations on the accompanying CD).

To date, clinicians and patients have tended to accept that procedural complications are an inevitable and acceptable consequence of such techniques. The advent of the widespread use of ultrasound with documented reductions in complication rates makes such tenets increasingly unsupportable, and henceforth there will be increasing medicolegal scrutiny of this area of practice. It can be questioned, in a capacity as an expert witness, For how much longer can colleagues be defended who choose not to learn

Table 1 Some Procedural Complications of Venous Access

| |
|---|
| (Related to needle damage) |
| Inadvertent arterial puncture leading to <i>Bleeding, hematoma, false aneurysm, thrombosis, hemothorax, and AV fistula</i> |
| Pneumothorax |
| Chylothorax |
| Venous tear leading to <i>Bleeding, hematoma, thrombosis, and hemothorax</i> |
| Venous thrombosis |
| Nerve damage |
| Catheter related sepsis |

Abbreviation: AV, arteriovenous.

or use ultrasound and then have serious complications during central venous catheter procedures? It should be appreciated that ultrasound will only help with needle placement and give limited information on guidewire or catheter placement. It will not protect against great vessel damage from dilators, catheters, or guidewires, but it is intuitive that accurate central placement of guidewires in the correct patent vessel is fundamental to subsequent safe catheter placement.

In addition to the above complications, other issues are commonly ignored, but are likely to be significant. These include pain and discomfort, delayed or cancelled surgery, delayed administration of intravenous fluids/medications, and delayed discharge from hospital. Reported studies tend only to record rates of eventual catheter placement success, which may require multiple needle passes. It is likely that multiple punctures, even if eventually successful, will lead to an increased risk of subsequent venous thrombosis and catheter-related sepsis (3).

THE RATIONALE FOR ULTRASOUND

The wide variability in vascular anatomy is well recognized, even in otherwise healthy individuals, (Fig. 1) with multiple patterns of dominant, absent, duplicate, or other variant vessels. There is a wide range in patient size and shape, from the neonate to the morbidly obese. Patients who have had longer-term venous access frequently have diseased vessels with thrombosis (Fig. 2) and later stenosis and obstruction (Fig. 3). These factors demonstrate flaws in the concept of blind landmark-based techniques. The value of ultrasound in the recognition and management of problem cases has been documented (4,5).

Ultrasound can provide the following:

1. Evidence of a large suitable patent vein. The presence of respiratory variation in vein size and antegrade flow with a normal Doppler signal suggest direct continuity with the vena cava and right atrium (6). The presence of a thrombus or a small scarred contracted vessel or multiple collaterals should prompt operators to reconsider and move elsewhere (Fig. 2). Valves are frequently seen in the lower internal jugular vein, subclavian vein, and femoral veins and should be avoided by moving the intended puncture site slightly more proximally or distally.
2. Cannulation procedures. A collapsed vein with marked collapse in inspiration suggests hypovolemia. Cannulation procedures may be helped by a steep head-down tilt, volume loading, positive pressure ventilation, a Valsalva maneuver, and timing of the vein puncture with respiration. Operators should be able to visualize when the needle has transfixated the vein, to alert them to go no deeper and pull back until blood is aspirated.

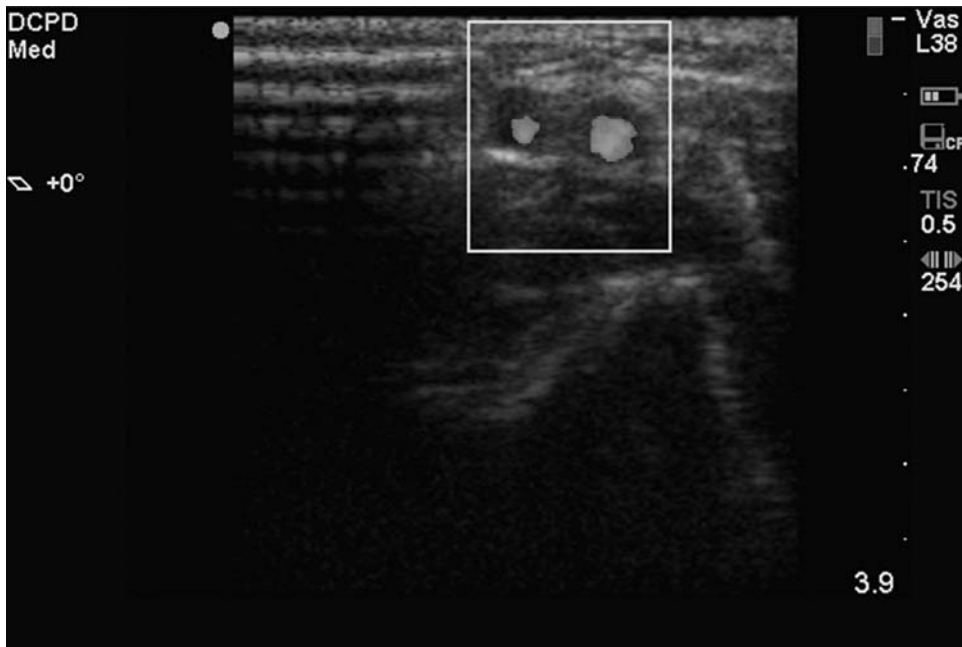


Figure 1 The author’s antecubital fossa in front of the elbow with color Doppler on. There are two brachial arteries due to high bifurcation of the radial and ulnar arteries, a common normal variant in about 1/15 of the population. Only one pulsation can be felt.



Figure 2 Difficult central venous access. Patent subclavian and internal jugular veins on the left were initially easily demonstrated and punctured with ultrasound guidance but did not allow central passage of guidewires or catheters. More detailed ultrasound examination showed retrograde venous flow up the left IJV with color Doppler and multiple collaterals in the neck. A later venogram, with X-ray contrast injected up both arms, demonstrates a blocked left brachiocephalic/innominate vein, following long-term central venous access. *Abbreviation:* IJV, internal jugular vein.



Figure 3 Noncompressible thrombus completely blocking the right subclavian vein. Less complete thrombosis may be seen in cross section as a crescent of noncompressible echogenic material in the vein.

3. Cannulation of central veins. Conversely, ultrasound guidance will help in cannulation of central veins in the head-up position, if required, due to brain injury or in the breathless patient (Fig. 4) (7).
4. First-pass venipuncture, in most cases, into the center of the vessel. Often in a well-filled vein, only the front wall of the vessel requires puncture, avoiding transfixion, due to the improved control of the needle.
5. Visualization of collateral structures to avoid, e.g., arteries, nerves, and pleura. The approach of the needle can be orientated so that the vein is not overlying the artery, pleura, or other vital structures.
6. Limited visualization of needle/guidewire/catheter in the vein.
7. Some evidence of catheter tip misplacement. Has it migrated up into the neck or to the contralateral side?

Limitations of Ultrasound Guidance

1. Ultrasound guidance will not allow first-time users instant success. There is a definite learning curve, with some individuals finding ultrasound concepts, three-dimensional visualization of body structures, and needle guidance easier than others (8).



Figure 4 Difficult central venous access. A Hickman line was tunneled from the left chest wall to the insertion site in the left internal jugular vein. The morbidly obese patient (body mass index 55) had pneumonia and gastrointestinal leak after gastric stapling and could not lie flat due to dyspnea. The procedure was done under local anesthesia, in the sitting position, with the vein identified and punctured using ultrasound guidance. No surface landmarks were available, and the carotid artery was very difficult to palpate.

2. Standard probes cannot easily visualize the superior vena cava (SVC) and right atrium (RA) because of the sternum and air-filled lung to confirm that catheters have passed centrally into the correct position. Transesophageal probes are required to visualize the SVC.
3. Damage to other collateral structures will still occur unless operators can visualize the needle tip to guide it accurately into the target vessel. This is, I believe, a major limitation for many operators (see chap. 3) (9). Initial correct vessel puncture may not avoid subsequent damage from guidewire, catheter, or dilator insertion.

WHAT IS THE EVIDENCE THAT ULTRASOUND IS HELPFUL?

There have been a number of studies comparing ultrasound to so-called landmark techniques. In the United Kingdom, the National Institute of Clinical Excellence (NICE) commissioned an analysis of this area of practice (10,11). An analysis of all randomized trials showed that there was insufficient evidence to comment on routes other than via the internal jugular vein. For this route, the study showed that the use of ultrasound provided a lower failure rate overall and a lower failure rate on first pass of the needle. There was decreased time for cannulation, a lower frequency of complications, and potential cost savings overall. An earlier analysis showed similar findings (12). NICE suggests that ultrasound guidance is used for elective cannulation of the internal jugular vein. However, similar advantages are seen for cannulation of veins and arteries at other sites in both elective and acute situations. More recently there have been a number of other supportive papers (3), including those cited elsewhere in this chapter.

In addition there have been a large number of observational studies in patients with “normal” and “abnormal” anatomy. The ability to visualize vessels and collateral structures and avoid unsuitable vessels, thereby choosing the optimal puncture site, have been demonstrated in a number of surveys. The high frequency of thrombosis and blocked veins

in the hospital population requiring total parenteral nutrition and dialysis has been noted (4,5). There have been calls for study of the use of ultrasound for all routes of access to establish benefit. I believe it is impractical and probably unethical to attempt to take patients to the point of serious complications with a blind puncture just to prove the efficacy of ultrasound at another anatomical site. A few case series and reports have suggested that ultrasound is unhelpful or makes the frequency of complications higher. In my opinion this represents operator inexperience, a lack of training, or the use of inadequate devices in the more challenging case, e.g., a very small child, rather than a fundamental weakness of the technology (13). Other studies may have used ultrasound to only establish the presence of the vein rather than real-time guidance of needle insertion (14).

Ultrasound guidance had developed more quickly in adult practice than in pediatrics. However, similar benefits in children are starting to be realized (15,16), but the size of vessels in neonates challenges current nonspecialized equipment.

There are costs involved in securing ready access to ultrasound devices in all areas where vascular procedures are performed (17,18). Equally there are costs associated with training and accreditation of a large pool of operators to perform such procedures (19) (see chap. 4 for further information). Overall in the longer term, the improved safety and efficacy of procedures should easily outweigh such considerations, and the skills learned should be easily transferable to other areas of practice.

APPLIED PHYSICS

Optimum visualization of superficial vessels is usually provided by a small-parts linear probe with a frequency between 5 and 12 MHz. There are small-purpose ultrasound devices specifically designed for venous access or alternatively more general-purpose machines with a range of probes. More expensive devices will have color and other Doppler facilities, which will allow differentiation of arterial and venous blood flow and the direction of flow within vessels. Whether such Doppler is required for routine central venous access is debatable. If the vessel is so small and deep as to require Doppler to differentiate it from other structures, it can be questioned whether it should be cannulated in the first place. Features which distinguish arteries and veins are summarized in Table 2.

Vessels can be visualized in transverse or longitudinal section. Size, depth, and patency of vessels can be assessed with ultrasound. The presence of valves, thrombus, or other anatomical abnormalities can also be assessed. The optimum site for venipuncture in any individual patient can then be decided.

Table 2 Distinguishing Features of Veins and Arteries

Real-time images are required because of these dynamic changes.

Arteries

Pulsatile, resistant to compression, round shape, visibility improving with compression through the probe, and characteristic Doppler signal

Veins

Elliptical shape, easily compressed, respiratory variation in size, increased size with Valsalva, IPPV or dependent position, and characteristic Doppler signal

Abbreviation: IPPV, intermittent positive pressure ventilation.

There are also other devices that provide only an audible signal by using a Doppler probe. There is conflicting evidence for their usefulness, but they were not recommended in the recent U.K. NICE appraisal (10,11).

APPLIED ULTRASOUND ANATOMY

Veins

Internal Jugular Vein

The vein lies surprisingly superficial (1–2 cm deep) and close alongside or partially overlapping the carotid artery (Fig. 5), but there is a wide variability in their relationship (20), in part dependent on the orientation of the ultrasound probe. Some patients will have a dominant venous drainage on one or other side of the neck, and in occasional patients, one vein will be congenitally absent. Associated structures, such as the thyroid and trachea, are easily visualized.

Axillary/Subclavian Vein

The presence of the clavicle restricts ultrasound visualization of the subclavian vein. Access can be achieved by a supraclavicular approach, but it is more usual to move a short distance laterally over the deltopectoral triangle to visualize the axillary artery and vein and branches, in particular the cephalic vein (Fig. 6). The chest wall and pleura are easily visualized and identified by the characteristic appearances of ribs in transverse section and the echogenic pleura with the sliding lung sign (21). On moving further laterally, overlap of the artery and vein decreases, and the chest wall and pleura falls away from the vein (a misplaced needle

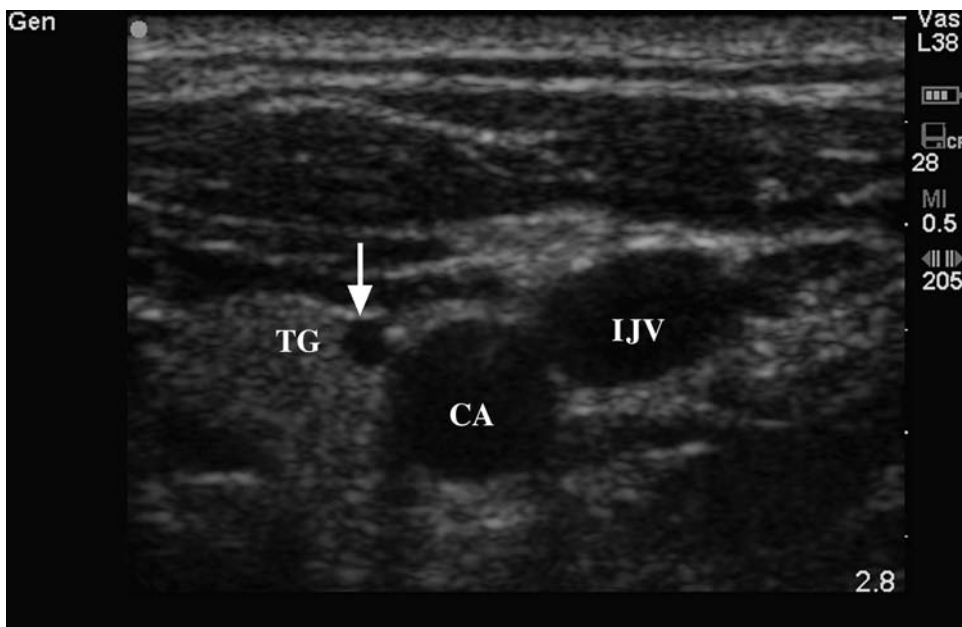


Figure 5 Cross-sectional images of the right IJV, partially overlying the right CA next to the TG. The center of the IJV is only 1.5 cm deep to the skin. Images are orientated to be seen from the patient’s head. *Abbreviations:* IJV, internal jugular vein; CA, carotid artery; TG, thyroid gland, Arrow, thyroid artery.

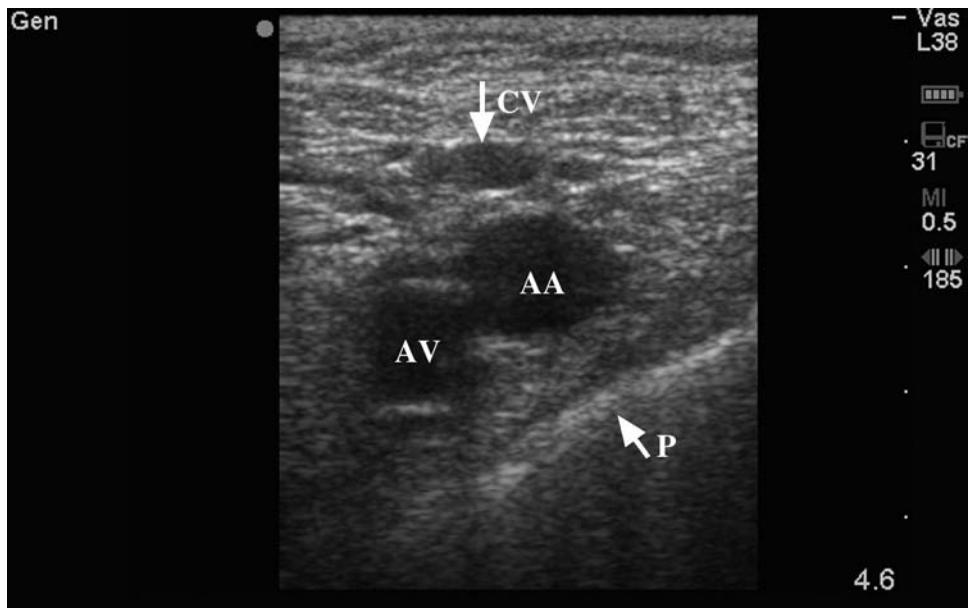


Figure 6 Cross-sectional images of the right axillary vein (AV), just lateral to the SV. The CV lies anteriorly, and the AA is seen deeper and more cranial. The pleura (P) and chest wall are easily visualized. The ultrasound probe is placed just lateral to the medial section of the clavicle, with the image orientated to be seen from the patient's right side. *Abbreviations:* SV, subclavian vein; CV, cephalic vein; AA, axillary artery.

transfixing the vein does not hit vital structures). However, the vein becomes smaller and deeper based. The brachial plexus is just cephalad to the artery (22).

Surface landmark approaches via the infraclavicular routes to the axillary vein have been described previously but have never achieved widespread popularity due to the difficulty of identifying such landmarks unless the patient is very thin. Ultrasound offers easy access to this site except in the very obese or muscular patient, and a large clinical experience of this approach is developing (23).

Femoral Vein

The femoral vein is traditionally identified by palpating the femoral artery and then directing a needle medially, assuming there is only one major vein and artery lying in a side-by-side position. However, the reality is more complex (Fig. 7). Often it is the superficial branch of the femoral artery that is most easily palpated, and the level of the inguinal ligament is difficult to identify even in thin subjects.

Traditional anatomical teaching suggests that the superficial femoral artery does not cross the femoral vein until several centimeters below the inguinal ligament, but this is not the case. Computed tomography (CT) and ultrasound studies have shown that crossover is much higher than is commonly appreciated (24,25). This is one reason why an inadvertent arterial puncture is common via this route. In addition the femoral vein receives several branches high in the groin, notably the long saphenous vein, which may approach the size of the femoral vein at the junction. If the puncture is too high, then there are risks of retroperitoneal hemorrhage if vessels are damaged.

The use of ultrasound allows accurate verification of applied femoral anatomy and an accurate first-pass puncture of the common femoral vein immediately below the

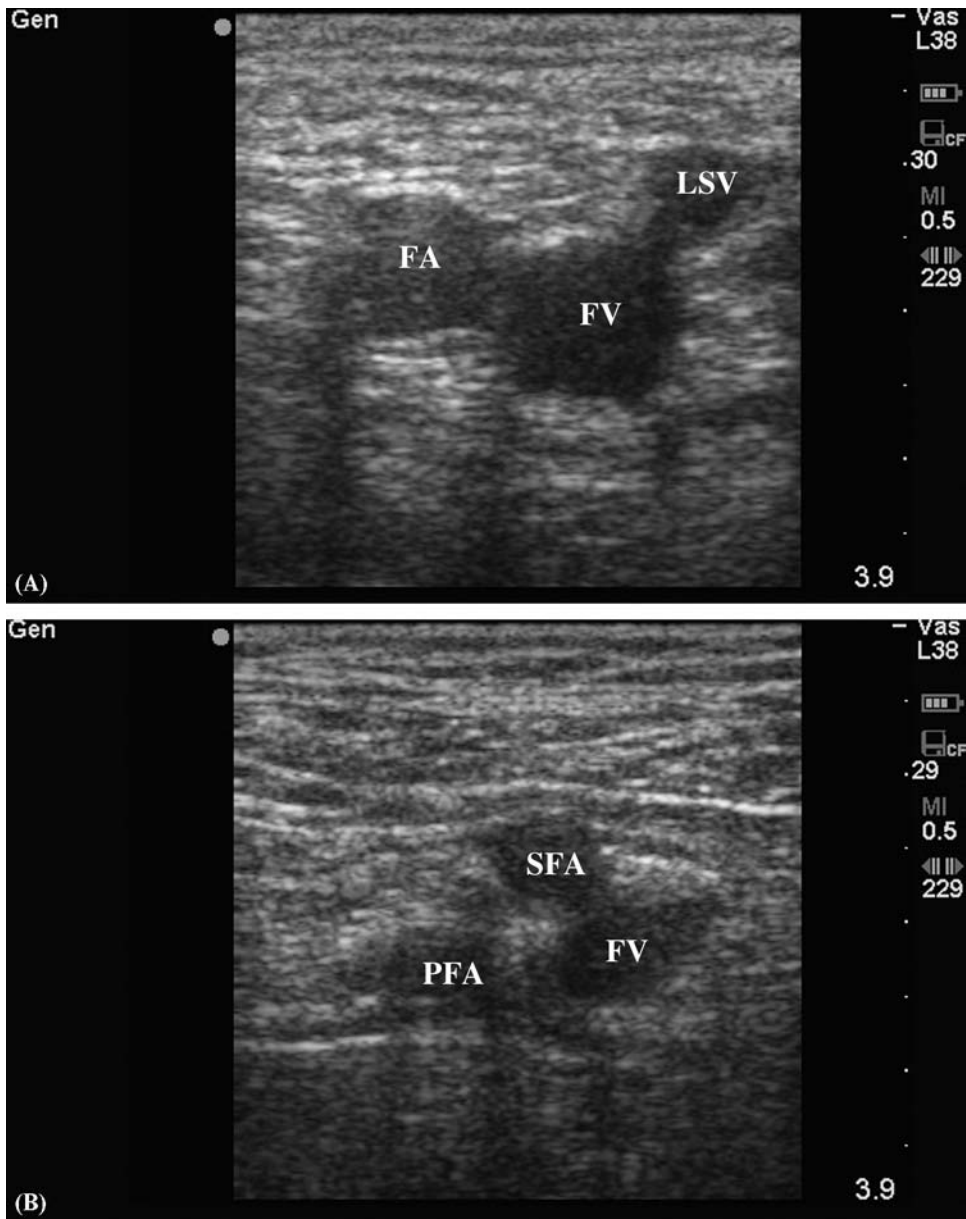


Figure 7 (A) Cross-sectional images of the right femoral vessels approximately 3 cm below the inguinal ligament, orientated to be seen from the patient’s feet. The superficial femoral artery partially overlaps the femoral vein. The profunda femoris artery is deeper. (B) Cross-sectional images of the right femoral vessels just below the inguinal ligament, orientated to be seen from the patient’s feet. The common femoral artery lies alongside the FV at the saphenofemoral junction, where the long saphenous vein joins it.

inguinal ligament. Ultrasound does not allow easy visualization anteriorly above the inguinal ligament due to the gas-filled bowel in the peritoneal space. The larger vessels can be followed down into the thigh, and there have been limited reports of access via these lower routes.

Arm and Leg

Deeper veins in the arm can be used when they cannot be palpated or visualized by eye from the skin surface. Techniques have been described both for short- and longer-term access, in particular the use of peripherally inserted central catheters from the antecubital fossa (26) or higher in the upper arm above the elbow flexure (27). These approaches may be particularly useful in the obese patient whose superficial veins are obscured by fat or the IV drug abuser with thrombosed superficial veins. Leg veins can be used in a similar fashion.

More Unusual Routes of Access

Multiple different sites of access, such as the inferior vena cava, portal vein, azygous system, and collaterals following great vessel obstruction, have been described utilizing ultrasound to guide puncture, but are beyond the scope of this chapter.

Lymphatics

Lymph nodes can be easily visualized with ultrasound as round structures with low echogenicity (Fig. 8). As a result of their presence close to major arteries and veins, they may be mistaken for vessels. They do not pulsate or cycle in size with respiration and are not easily compressible. Scanning along vascular trunks will demonstrate the characteristic shape of nodes. Larger lymphatic vessels are visible with ultrasound and are likely to be difficult to distinguish from vessels except by the lack of a Doppler signal (28).

Arteries

There have been fewer studies on the use of ultrasound to facilitate arterial access. Nevertheless, all the cited advantages for venous access are likely to be equally relevant to arterial access both for peripheral and for more central access. It is commonly cited, "Why use it when you can palpate the vessel?" Palpation gives only the approximate location of a deeper vessel and gives no indication about the presence of duplication (Fig. 1), atheroma, tortuosity, narrowing, dissection, or thrombus, all of which would be relative contraindications to the use of that site for access. All these findings are easily visible with ultrasound.

In the known arteriopath it seems intuitive that suitable sites (e.g., both groins) should be scanned prior to arterial puncture to choose the least diseased vessel. In addition ultrasound can guide puncture of the common femoral artery rather than the often more easily palpable superficial femoral artery (SFA) (Fig. 7). Anecdotally, most cannulation-induced problems requiring arterial surgical reconstruction in the groin are related to puncture of the SFA rather than the common femoral artery. Studies to date have been small but have suggested benefit from using ultrasound if the pulses are difficult to feel or in the obese subject (29).

Peripheral arteries can easily be visualized with a high-frequency probe (Fig. 9). The use of ultrasound has been reported to increase the success of radial artery cannulation at the wrist in both adults and neonates (30,31).

Ultrasound allows identification of arteries away from the classical palpable puncture sites at the wrist, antecubital fossa, and ankle. It should be appreciated that these traditional access sites were chosen not because they were necessarily the ideal site for cannulation but rather because they were the only consistent superficial palpable sites. Their position over joints with a wide range of movements is not ideal, leading to kinking, vessel trauma, thrombosis, dislodgement, and discomfort. Other less mobile sites may be

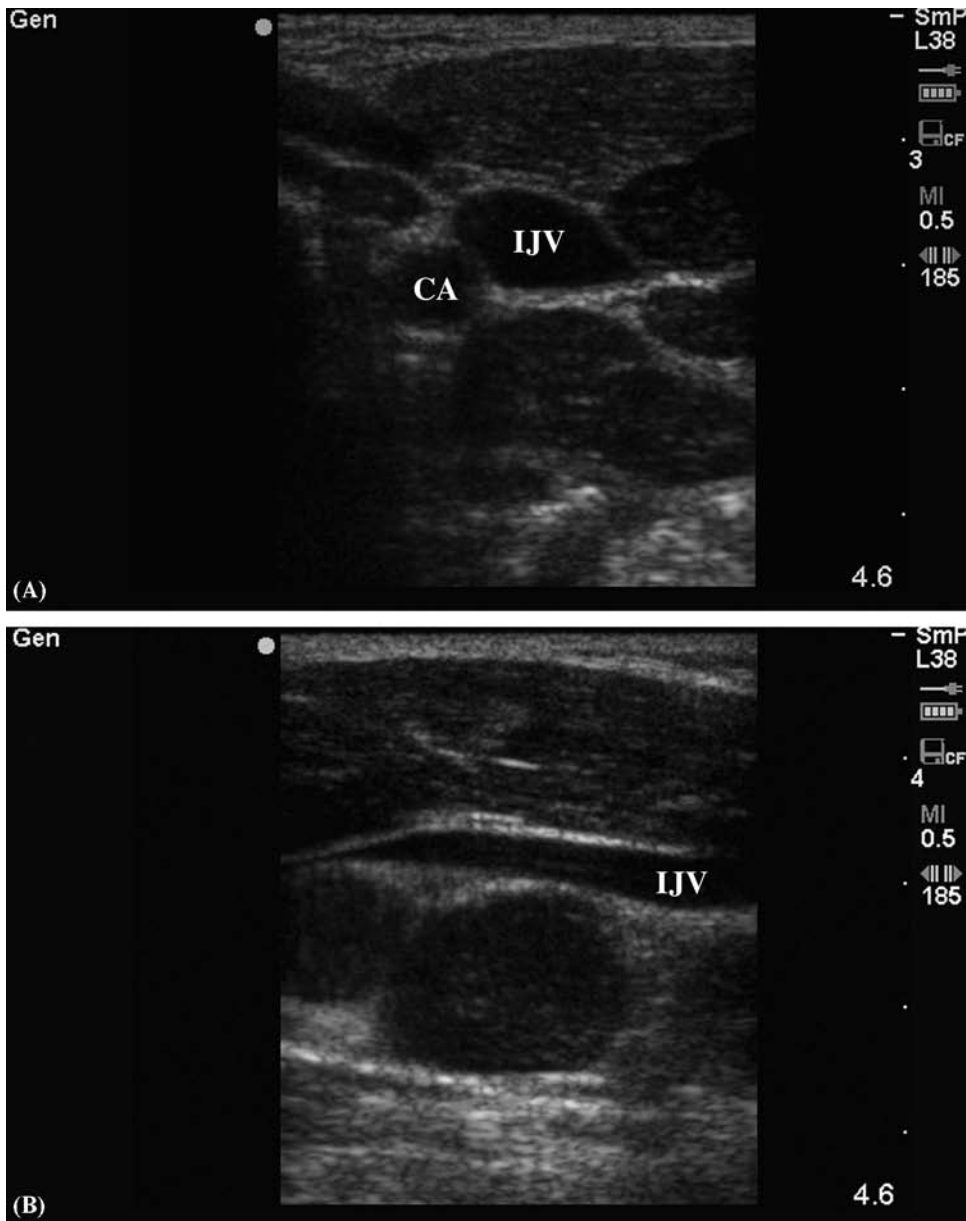


Figure 8 (A) Cross-sectional image of the right IJV in a patient with massive lymphadenopathy from hematological malignancy. The nodes resemble vessels on initial viewing but are slightly more echogenic and have none of the other characteristics of vessels (Table 2). (B) Transferring the probe to the long axis of the IJV further demonstrates the round outlines of the nodes. *Abbreviation:* IJV, internal jugular vein.

more attractive in these respects. We have been using the impalpable section of the radial artery in the forearm as an alternative site for cannulation in anesthesia and critical care when conventional sites have been exhausted (Fig. 9). Further work on the relative success and safety of such sites is required.

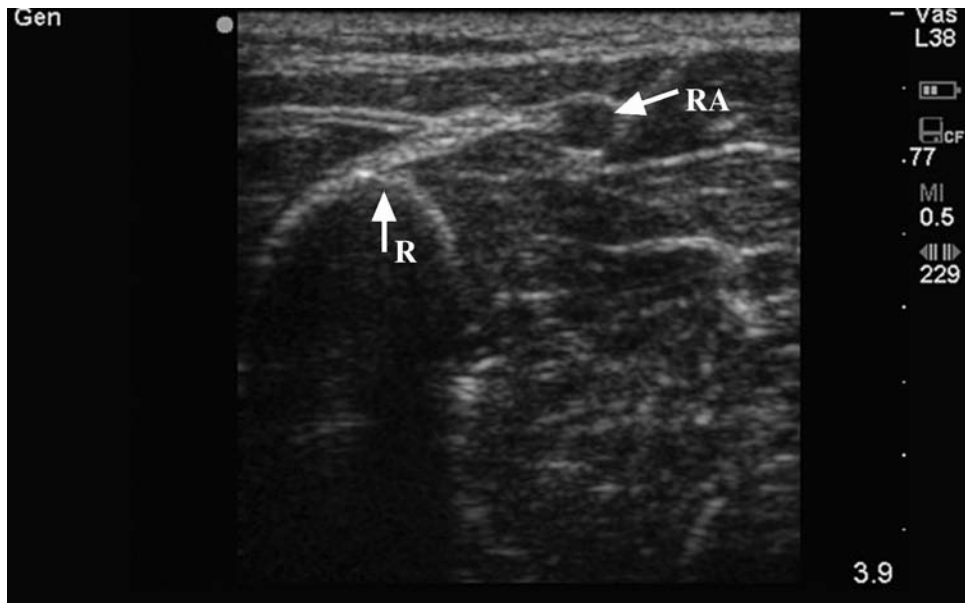


Figure 9 The radial artery (RA) 8 cm above the wrist joint. The artery is difficult to palpate higher in the forearm as it lies below muscle and fascia. The radial artery is easy to visualize with a high-resolution probe and the anterior surface of the radius bone (R) is also seen. Such sites provide an alternative route for arterial cannulation but require ultrasound guidance to identify the vessels.

PRACTICALITIES OF VASCULAR ACCESS UTILIZING ULTRASOUND

If possible, explain the risk benefits of the procedure, proposed site of access, and potential complications to the patient. Obtain verbal or written consent if practical. Check for the presence of an appropriate vessel with ultrasound before starting. Monitor the patient with pulse oximetry, electrocardiography, and noninvasive blood pressure measurement. Establish peripheral intravenous access, and offer conscious sedation if appropriate. Place the patient 15° head down for jugular or subclavian vein access. Ensure the field is aseptic, image the vessel at the chosen site with ultrasound, and infiltrate the skin and subcutaneous tissues with local anesthetic.

Transducer and Display Setup

Touch one side of the probe and observe the image to allow orientation. A palpable marker is often present on the side of the transducer corresponding to a marker on the display. Adjust the depth to ensure structures are visualized in the center of the screen. Alter the gain to create a relatively dark image that allows discrimination of the white dots generated by the needle. Use sterile ultrasound gel inside and outside the protective sterile sheath.

Position the ultrasound display at eye level to the operator on the opposite side of the patient. Place the probe lightly on the skin (veins will collapse easily). Choose a site and probe orientation where the vein lies side by side with the artery (rather than anterior to it), as the vein will often need to be transfixed to puncture its anterior wall. If the vein is

transfixed, successful aspiration then occurs on gentle withdrawal of the needle. Similar considerations apply for arterial access.

Needle Visualization

This is covered elsewhere in this book (see chap. 3 for further information) and other reviews. I believe this is a weakness of many operators who have no difficulty in visualizing the target vessel but fail to understand needle tip visualization and hence still risk needle damage during insertion procedures (9).

Verification of Needle Tip Placement

The vein wall may occlude the needle tip that appears to lie within the vessel lumen on ultrasound. Irrespective of the technique used, verify needle tip placement by either aspirating blood or noting the vein to reopen following collapse due to the pressure of the advancing needle. The needle tip may require further fine adjustment to allow passage of the guidewire as traditionally learned with conventional surface landmark-based techniques.

CONCLUSION

Ultrasound guidance is a useful technique to aid central venous and arterial access. It is effective in routine and difficult cases, improves success rates of cannulation, and reduces complications. Orientation of the ultrasound probe and needle is a skill that takes some practice, but the time spent understanding and practicing the technique will be repaid many times over when performing invasive procedures.

REFERENCES

1. Mansfield PF, Hohn DC, Fornage BD, et al. Complications and failures of subclavian-vein catheterization. *N Engl J Med* 1994; 331:1735–1738.
2. Sznajder JI, Zveibil FR, Bitterman H, et al. Central vein catheterization. Failure and complication rates by three percutaneous approaches. *Arch Intern Med* 1986; 146:259–261.
3. Karakitsos D, Labropoulos N, De Groot E, et al. Real-time ultrasound guided catheterization of the internal jugular vein: a prospective comparison to the landmark technique in critical care patients. *Crit Care* 2006; 10:R162.
4. Forauer AR, Glockner JF. Importance of US findings in planning jugular vein haemodialysis catheter placements. *J Vasc Interv Radiol* 2000; 11:233–238.
5. Hatfield A, Bodenham A. Portable ultrasound for difficult central venous access. *Br J Anaesth* 1999; 82:822–826.
6. Conkbayir-Isik, Men-Süleyman, Yanik-Bahar, et al. Color Doppler sonographic finding of retrograde jugular venous flow as a sign of innominate vein obstruction. *J Clin Ultrasound* 2002; 30:392–398.
7. Brederlau J, Greim C, Schwemmer U, et al. Ultrasound-guided cannulation of the internal jugular vein in critically ill patients positioned in 30 degrees dorsal elevation. *Eur J Anaesthesiol* 2004; 21:684–687.
8. Sites-Brian D, Gallagher JD, Cravero J, et al. Learning curve associated with a simulated ultrasound-guided interventional task by inexperienced anesthesia residents. *Reg Anesth Pain Med* 2004; 29:544–548.
9. Chapman GA, Johnson D, Bodenham AR. Visualisation of needle position using ultrasoundography. *Anaesthesia* 2006; 61:148–158.

10. Hind D, Calvert N, McWilliams R, et al. Ultrasonic locating devices for central venous cannulation: meta-analysis. *BMJ* 2003; 327:361.
11. National Institute for Clinical Excellence. Guidance on the use of ultrasound locating devices for central venous catheters (NICE technology appraisal, No. 49.). London: NICE, 2002.
12. Randolph AG, Cook DJ, Gonzales CA, et al. Ultrasound guidance for placement of central venous catheters: a meta-analysis of the literature. *Crit Care Med* 1996; 24:2053–2058.
13. Grebenik CR, Boyce A, Sinclair ME, et al. NICE guidelines for central venous catheterization in children. Is the evidence base sufficient? *Br J Anaesth* 2004; 92:827–830.
14. Hayashi H, Amano M. Does ultrasound imaging before puncture facilitate internal jugular vein cannulation? Prospective randomized comparison with landmark-guided puncture in ventilated patients. *J Cardiothorac Vasc Anesth* 2002; 16:572–275.
15. Chuan WX, Wei W, Yu L. A randomised controlled study of ultrasound prelocation vs anatomical landmark guided cannulation of the internal jugular vein in infants and children. *Pediatr Anaesth* 2005; 15:733–738.
16. Leyvi G, Taylor D, Reith, et al. Utility of ultrasound-guided central venous cannulation in pediatric surgical patients; a clinical series. *Pediatr Anesth* 2005; 15:953–958.
17. Scott DHT. Its NICE to see in the dark. *Br J Anaesth* 2003; 269–272.
18. Calvert N, Hind D, McWilliams RG, et al. The effectiveness and cost effectiveness of ultrasound locating devices for central venous access: a systematic review and economic evaluation. *Health Technol Assess* 2003; 7:1–84.
19. Bodenham A. Editorial II: Ultrasound imaging by anaesthetists: training and accreditation issues. *Br J Anaesth* 2006; 96:414–417.
20. Denys BG, Uretsky BF. Anatomical variation of the internal jugular vein. *Crit Care Med* 1991; 19:1516–1519.
21. Galloway S, Bodenham A. Ultrasound imaging of the axillary vein—anatomical basis for central venous access. *Br J Anaesth* 2003; 90:589–595.
22. Klaastad-Øivind, Smith-Hans-Jørgen, Smedby-Orjan, et al. A novel infraclavicular brachial plexus block: the lateral and sagittal technique, developed by magnetic resonance imaging studies. *Anesth-Analg* 2004; 98:252–256.
23. Sharma A, Bodenham AR, Mallick A. Ultrasound-guided infraclavicular axillary vein cannulation for central venous access. *Br J Anaesth* 2004; 93:188–192.
24. Hughes P, Scott C, Bodenham A. Ultrasonography of the femoral veins, implications for vascular access. *Anaesthesia* 2000; 55:1199–1202.
25. Baum PA, Matsumoto AH, Teitelbaum GP, et al. Anatomic relationship between the common femoral artery and vein: CT evaluation and clinical significance. *Radiology* 1989; 173:775–777.
26. Sandhu NS, Sidhu DS. Mid arm approach to basilic and cephalic vein using ultrasound guidance. *Br J Anaesth* 2004; 93:292–294.
27. Sofocleous CT, Schur I, Cooper SG, et al. Sonographically guided placement of peripherally inserted central venous catheters. *Am J Roentgenol* 1999; 170: 1613–1616.
28. Zironi G, Cavalli G, Casali A, et al. Sonographic Assessment of the distal end of the thoracic duct in healthy volunteers and patients with portal hypertension. *Am J Radiology* 1995; 165:863–866.
29. Dudeck O, Teichgraeber U, Podrabsky P, et al. A randomized trial assessing the value of ultrasound-guided puncture of the femoral artery for interventional investigations. *Int J Cardiovasc Imaging* 2004; 20:363–368.
30. Schwemmer-U, Arzet-H-A, Trautner-H, et al. Ultrasound-guided arterial cannulation in infants improves success rate. *Eur J Anaesthesiol* 2006; 23:476–480.
31. Levin-Phillip-D, Sheinin-Olga, Gozal-Yaacov. Use of ultrasound guidance in the insertion of radial artery catheters. *Crit Care Med* 2003; 31:481–484.

6

Ultrasound-Guided Peripheral and Regional Nerve Block

Pawan K. Gupta

Leeds Teaching Hospitals NHS Trust, Leeds, U.K.

Philip M. Hopkins

University of Leeds, Leeds, U.K.

With the increasing availability of relatively inexpensive portable, high-quality ultrasound equipment, the use of ultrasound for needle guidance in local and regional anesthetic techniques has become increasingly popular (1). Prior to this, nerve block techniques relied on the use of surface anatomical landmarks to guide the introduction of the needle with its course being gauged by the “feel” of the needle passing through fascial planes. Confirmation of the proximity of the needle to the target nerve structures was assessed initially by needle-evoked paresthesia but more recently by evoked muscle responses to electrical stimulation of the nerve through the nerve block needle. However, these techniques are “blind” and make no allowance for interindividual anatomical variability not only in the position of the target nerves themselves but also in vital structures that are either in direct anatomical relation with the nerve or that lie potentially in the path of the needle. Furthermore, neither paresthesia nor nerve stimulation are a particularly sensitive guide to needle position. The result of these deficiencies in regional anesthetic techniques was an inevitable incidence of failure to produce sufficient analgesia and complications related to either needle damage of the nerve or related structures or intravascular injection of local anesthetic. In other words, even in the best hands, without the use of imaging there is always an element of luck in regional anesthetic techniques.

The use of ultrasound, with appropriate experience and training, enables the regional anesthesiologist to identify the target injection site for local anesthetic and its adjacent structures along with all structures in the potential path of the needle from skin to target. Real time imaging during injection of the local anesthetic allows the operator to assess its spread and adjust the position of the needle tip as necessary to ensure placement of local anesthetic solution around all the appropriate nerves (2). Table 1 lists advantages that have been proposed for ultrasound-guided regional anesthetic blockade.

Table 1 Proposed Advantages of Ultrasound

| | |
|-----|---|
| 1. | Real-time direct visualization of nerves and surrounding anatomical structures |
| 2. | Direct visualization of the spread of local anesthetic during injection |
| 3. | Avoidance of complications (e.g., intraneuronal or intravascular local anesthetic injection) |
| 4. | Avoidance of painful muscle contractions during nerve stimulation |
| 5. | Reduction of the dose of local anesthetic |
| 6. | Faster sensory onset time |
| 7. | Improved quality of block |
| 8. | Increased success rate |
| 9. | Safe to perform under general anesthesia |
| 10. | Close supervision possible during training |
| 11. | Steeper learning curve |
| 12. | Cheaper compared with other imaging modalities, can be performed in the operating theater department, and carries no radiation risk |

We should of course reiterate that these potential advantages only apply if appropriate equipment is used by appropriately trained and experienced individuals.

EQUIPMENT

The physical principles of ultrasound have been outlined in Chapter 1. Superficial structures including superficial nerves are best visualized using a high-frequency (greater than or equal to 10 MHz) linear-array probe. With increasing depth of target structure, visualization requires a lower frequency probe. The most deeply placed nerves, for example, the sciatic nerve, are best visualized using a curvilinear probe with low frequency (2–5 MHz).

There is a variety of suitable portable systems available. It is strongly recommended that a color Doppler imaging facility is included for best identification of vascular structures. The capturing and storing of still and moving images is also highly recommended and indeed may become a requirement for medicolegal purposes in the future.

ULTRASOUND IMAGING OF NERVES

Nerve trunks and their peripheral branches are composed of parallel bundles of nerve fibers organized in groups as fascicles. Fascicles vary in size and can contain from a few to several hundred axons. Within a fascicle, the axons are separated by a delicate layer of connective tissue (endoneurium). In turn, the fascicles are enclosed with a thicker layer of connective tissue (the perineurium) and the whole nerve by the thickest outer layer of connective tissue (epineurium). Sonographically, neural tissue appears hypoechoic (dark), but the perineurium and, especially, the epineurium are hyperechoic (white). Skeletal muscles also appear as structures with hypoechoic and hyperechoic areas but they can usually be distinguished from nerves because of their size and their relative lack of density of the hypoechoic areas and by a knowledge of anatomy. The hyperechoic reflection of the epineurium is also usually brighter than that of the epimysium, although this distinction becomes less clear as the epimysium of muscles thickens toward tendonous insertions.

In conclusion, therefore, positive identification of nerve structures can be difficult. It is aided by a sound knowledge of the anatomy of the region of interest and the three-dimensional course of the nerves themselves, and their surrounding structures. Because the sonographic appearance of nerves is sometimes difficult to distinguish from that of other structures, it is worth spending time adjusting the angle of the probe, the pressure

applied through the probe to the skin, and the settings on the ultrasound machine to optimize the visualization.

NEEDLE VISUALIZATION

Needle visualization has been covered in detail in Chapter 3. It is our opinion that the needle should be inserted in the plane of the array of the ultrasound probe. We cannot emphasize too highly the narrowness of the ultrasound beam and therefore the importance of maintaining the needle in the plane of the middle of the long axis of the probe. In-plane alignment of the needle permits visualization of its tip throughout the course of needle placement from skin penetration to targeted positioning. With optimal views, the needle can be visualized directly, but on other occasions, especially when deeper needle placement is required, one must rely on the real-time visualization of tissue displacement to identify the needle tip. At any stage, the position of the needle tip can be confirmed by the injection of a small volume of saline.

PRINCIPLES OF SAFE PRACTICE IN ULTRASOUND-GUIDED NERVE BLOCK

1. Ultrasound-guided nerve block should only be practiced under the supervision of an anesthetist with relevant experience.
2. The ultrasound machine and transducer should be appropriate for the procedure to be undertaken.
3. The patient should be appropriately starved, IV access secured, basic monitoring attached and resuscitation equipment and drugs available.
4. A skilled assistant should be present.
5. The procedure should be undertaken under aseptic conditions.
6. If the patient is awake, the site of needle insertion should be anesthetized with local anesthetic.
7. Prior to needle insertion, the target nerves, related structures, and intended path of needle insertion should be visualized.
8. During needle placement, the location of the needle tip should be identified at all times.
9. Aspirate through the needle before injection and at intervals during injection to minimize the risk of intravascular placement of local anesthetic.
10. Ensure spread of local anesthetic is visible during injection. If this is not the case, the needle tip is either out of the field of view or in a blood vessel and injection should be stopped.

ULTRASOUND-GUIDED REGIONAL ANESTHETIC TECHNIQUES

In theory, it is possible to use ultrasound guidance for any regional or peripheral nerve block technique. Table 2 lists the blocks that have been reported in the literature as being carried out under ultrasound guidance. However, owing to the confines of space, it is not possible to describe all of these. Instead, we will describe in detail a limited selection of blocks. These are plexus and relatively proximal peripheral nerve blocks most commonly employed in anesthetic practice. We will also discuss the potential for using ultrasound to guide epidural and paravertebral needle placement.

Table 2 Blocks Reported in the Literature to Have Been Performed Under Ultrasound Guidance

| |
|---|
| Head and neck: |
| Retrobulbar |
| Cervical plexus |
| Stellate ganglion |
| Glossopharyngeal nerve |
| Superior laryngeal nerve |
| Inferior alveolar nerve |
| Accessory nerve |
| Lesser occipital nerve |
| Upper limb: |
| Brachial plexus |
| Interscalene |
| Supraclavicular |
| Infraclavicular |
| Axillary |
| Musculocutaneous |
| Ulnar, median, and radial nerves at the elbow, wrist, and forearm |
| Thorax and abdomen: |
| Celiac plexus |
| Iliohypogastric and ilioinguinal |
| Transversus abdominus plane block |
| Posterior lumbar plexus |
| Lumbar facet nerve |
| Phrenic nerve |
| Psoas compartment |
| Paravertebral |
| Pudendal nerve |
| Central neuraxial: |
| Epidural |
| Lower limb: |
| Sciatic nerve |
| Femoral nerve |
| Popliteal fossa |
| Saphenous nerve |
| Ankle |

BRACHIAL PLEXUS BLOCKS

Anatomy

The brachial plexus provides the nerve supply to the upper limb. It is derived from the anterior rami of the fifth, sixth, seventh, and eighth cervical nerves and the first thoracic nerve. The plexus extends from the roots in the neck to the cords in the axilla. The roots (C5-T1) pass dorsal to the vertebral artery through the intervertebral foramina. They then lie between the anterior and middle scalene muscles in the neck and from there descend toward the first rib, converging to form superior, medial, and inferior trunks in the posterior cervical triangle. Behind the clavicle, the trunks bifurcate into anterior and posterior divisions as they cross the first rib before forming posterior, lateral, and medial cords, which subsequently form the terminal nerves in the axilla.

Approaches to the Brachial Plexus

Local anesthetic blocks at the level of the roots, trunks, divisions, cords, and terminal branches of the brachial plexus have been described. The approaches differ in terms of distribution of successful sensory block and potential for complications. For example, a block using the interscalene approach invariably fails to provide analgesia to the distribution of C8 and T1 while commonly producing ipsilateral phrenic nerve paralysis and Horner's syndrome. In contrast, a block performed using the axillary approach is most likely to fail to block the musculocutaneous and radial nerves, while there is risk of intravascular injection. The periclavicular approaches (infraclavicular and supraclavicular) are most likely to produce complete brachial plexus analgesia, but are associated with a risk of pneumothorax and intravascular injection. Of the periclavicular approaches, we strongly favor the supraclavicular approach when using ultrasound as the target structures, being more superficial than with the infraclavicular approach, are more easily identified. Indeed, with the advent of ultrasound, the supraclavicular approach is the preferred technique for upper limb surgery below the shoulder. For procedures on the shoulder, the interscalene approach is recommended.

Supraclavicular Brachial Plexus Block (3,4)

Patient position: Supine with head turned 45° to the contralateral side.

Equipment: High-frequency linear probe with color Doppler facility.

Position of probe: Coronal oblique plane in the supraclavicular fossa (Fig. 1).

Visualization of plexus (Fig. 2): The key landmark is the subclavian artery as it crosses the first rib. Apply sufficient pressure to the ultrasound probe to get a view down on to the rib behind the clavicle. In this location, the trunks have usually divided into anterior and posterior divisions, and these can be visualized superiorly and posterolaterally to the subclavian artery (Fig. 2A). One or more divisions of the lower trunk can often be visualized in the angle formed between the subclavian artery and the first rib. Indeed, if local anesthetic is injected between the artery and the rib, by lifting up the artery away from the rib, a nerve structure can sometimes be identified between them (Fig. 2B).



Figure 1 Position of the probe and needle insertion for supraclavicular brachial plexus block.

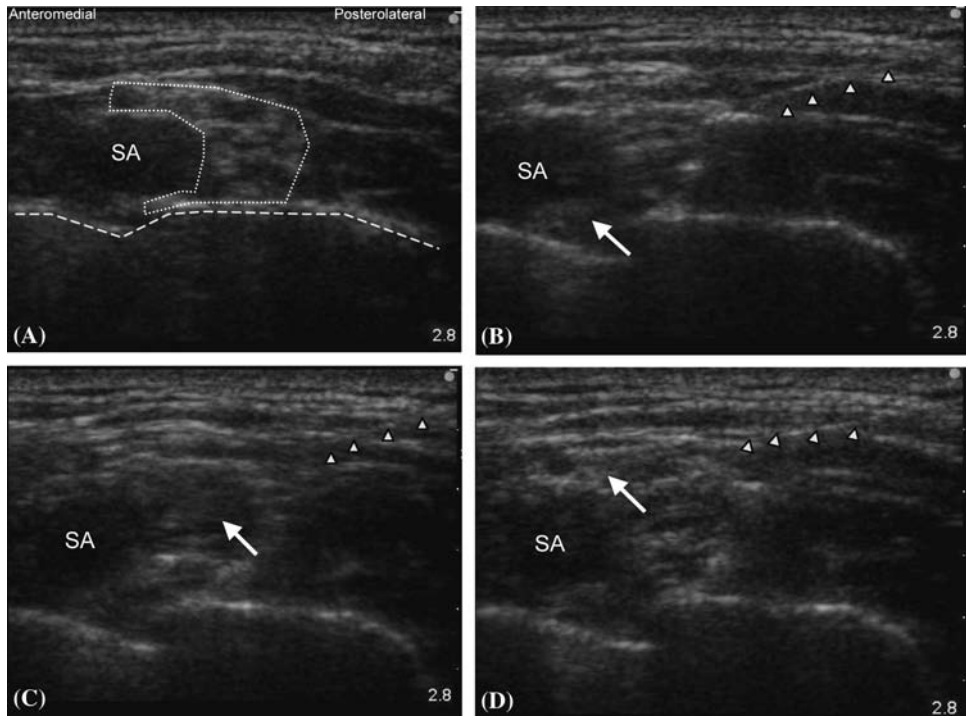


Figure 2 View of the supraclavicular brachial plexus obtained using a 10-MHz linear-array probe placed in an axial oblique position. (A) Prior to injection. The dashed line indicates the composite image formed by the first rib and cervical pleura; the dotted line encloses the divisions of the brachial plexus. (B) After injection of local anaesthetic in the angle between the rib and the subclavian artery. (C) At completion of a second injection of local anaesthetic. (D) During a third injection of local anaesthetic. In B, C, and D, the arrows point to nerves highlighted by surrounding local anaesthetic, while the triangles emphasize the position of the needle. *Abbreviation:* SA, subclavian artery.

Executing the block: The needle is passed medially from the posterolateral edge of the field of view in the plane of the long axis of the ultrasound probe (Fig. 1) toward the target structures. Care should be taken to avoid too deep an angle of insertion so as not to puncture the cervical pleura. After passing through the thick fascial layer covering the neurovascular structures, local anaesthetic can be injected adjacent to the nerve. It is apparent that in most people, there are distinct compartments within the neurovascular sheath, and so the needle would invariably need to be repositioned once or twice to ensure full spread around all the neuronal structures (Fig. 2B–D). In subjects where visualization of all the nerve structures is incomplete, successful block can invariably be achieved by ensuring spread of local anaesthetic adjacent to the posterolateral half of the circumference of the subclavian artery. Occasionally, branches of the subclavian artery can impinge on the path of the needle (Fig. 3).

Interscalene Brachial Plexus Block (5)

The patient is positioned as for the supraclavicular approach. In the authors' experience, it is best to initially visualize the plexus in the supraclavicular region around the subclavian artery and then trace the path of the trunks proximally by moving the probe toward the root of the neck, if necessary, superiorly, so that the probe lies in an axial oblique plain to

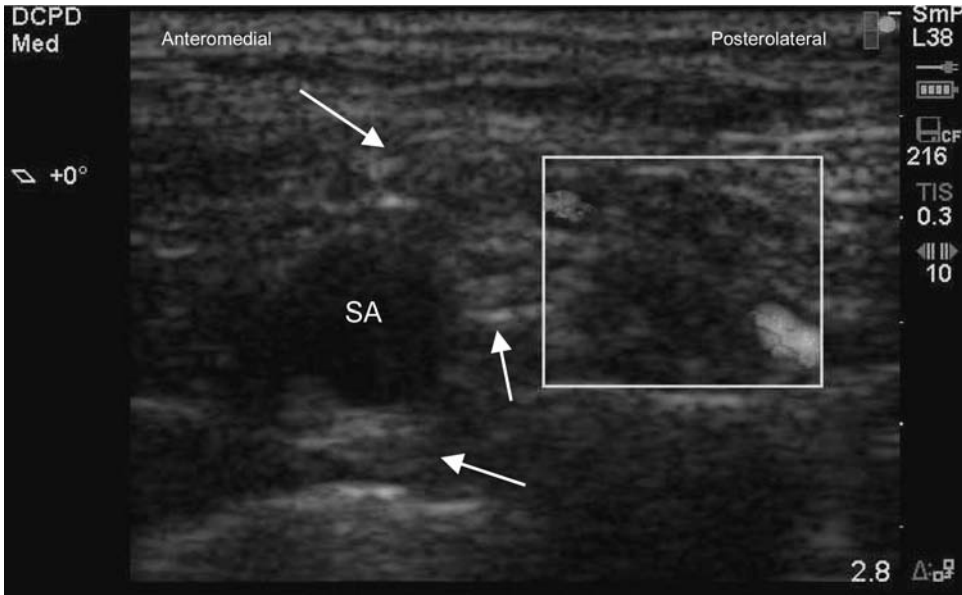


Figure 3 View of the supraclavicular brachial plexus with color Doppler to illustrate branches of the subclavian artery potentially in the path of the needle. The arrows point to major nerve components. *Abbreviation:* SA, subclavian artery.

the neck. The upper and middle trunks of the plexus are usually readily visualized between the anterior and middle scalene muscles (Fig. 4). Alternatively, the probe can be placed over the sternocleidomastoid muscle at the level of the cricoid cartilage and then moved laterally. Deep to the lateral border of the sternocleidomastoid, the anterior scalene muscle will be seen, and lying between it and the middle scalene will be the upper and middle trunks of the plexus.

In executing the block, the needle should be inserted in the plain of the long axis of the probe from posterior to anterior.

Infraclavicular Brachial Plexus Block (6)

Although this approach has no advantages over the supraclavicular approach when performed under ultrasound guidance, prior to the increasing availability of ultrasound equipment, it did gain popularity as the risk of pneumothorax is less than that with the supraclavicular approach. It produces a more reliably comprehensive block than the axillary approach.

Patient position: Supine with the arm to the side.

Equipment: Medium- to high-frequency linear probe with color Doppler facility.

Position of probe: Parasagittal plain medial to the coracoid process.

Visualization of plexus: Deep to the pectoralis major and minor muscles, locate the axillary artery and vein. Both of these vessels are hypoechoic but can be distinguished by the pulsatility of the artery and the compressibility of the vein. The cords of the brachial plexus appear hypoechoic with the lateral cord most commonly superior to the axillary artery and the posterior cord posterior to the artery. The medial cord can often be seen between the artery and the vein but is not always visible.

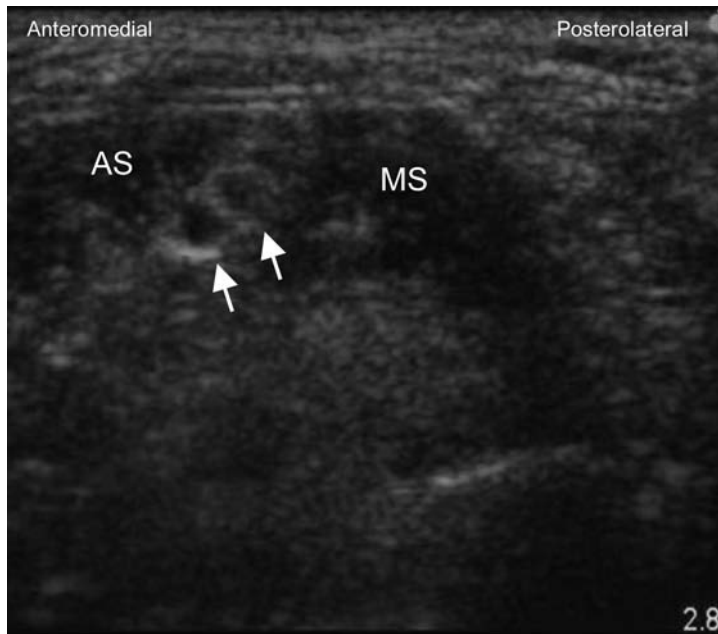


Figure 4 View of the interscalene brachial plexus obtained using a 10-MHz linear-array probe placed in an axial oblique position. The arrows point to the upper and middle trunks of the brachial plexus. *Abbreviations:* AS, anterior scalene muscle; MS, middle scalene muscle.

Executing the block: A 10-cm needle will be required. It should be introduced in the plane of the long axis of the probe and targeted initially adjacent to the posterior cord. The needle should be repositioned as required to ensure the spread of the local anesthetic to all three cords.

Axillary Approach to the Brachial Plexus (7)

Patient position: Supine with the arm abducted to 90° and the forearm flexed.

Equipment: High-frequency linear probe with color Doppler facility.

Position of the probe: The probe should be placed perpendicular to the long axis of the arm as close to the axilla as possible.

Visualization of the plexus: The dark, round, pulsatile axillary artery is easily identified in the axilla and is distinguished from the axillary veins that are nonpulsatile and readily compressed. The median and ulnar nerves are usually lateral and medial to the artery, respectively while the radial nerve is usually posterior or posteromedial to the artery. The musculocutaneous nerve usually branches off more proximally and can be seen as a hypoechoic structure between the biceps and coracobrachialis muscles for a short distance before entering the body of the coracobrachialis muscle.

Executing the block: The needle should be inserted in an anteroposterior direction in the long axis of the probe. It should be noted that the median and ulnar nerves are superficial, but to obtain access to the radial nerve, the needle will need to pass through the biceps muscle. The needle will need to be repositioned to ensure spread of local anesthetic around the circumference of the axillary artery and then further repositioned if block of the musculocutaneous nerve is required.

CERVICAL PLEXUS BLOCK (8)

The cervical plexus consists of superficial and deep components carrying sensory fibers from skin and superficial structures of the head, neck, and shoulder, and deeper structures of the neck with motor supply to the anterior neck muscles and the diaphragm. The plexus is formed by the anterior primary rami of the first four cervical nerves. It lies deep to the internal jugular vein and the sternocleidomastoid muscle on the surface of scalenus medius and levator scapuli.

The vertebral artery lies in close proximity to the second, third, and fourth cervical nerves. The artery arises from the first part of the subclavian artery and passes vertically through the foramina of the first six cervical vertebrae. At the level of the atlas, the artery winds behind the lateral mass of the vertebra and enters the skull through the foramen magnum. Between the first and second cervical vertebrae, the artery makes a prominent loop allowing it to pass from the foramen of the axis to the more laterally placed foramen of the atlas. This loop is a prominent landmark for the transverse process of the second cervical vertebrae and second cervical nerve, which are immediately inferior and posterior to the artery.

Cervical plexus block may lead to serious complications such as hematoma, phrenic nerve blockade, and intrathecal or intravascular injection.

Position of the patient: Supine with the head turned to the contralateral side.

Equipment: High-frequency linear probe with color Doppler facility.

Position of probe: Axial oblique plane to the neck.

Executing the block: At the level of the carotid bifurcation, the deep cervical plexus can be blocked by a single injection. The needle should be directed in the plane of the long axis of the probe behind the posterior border of the sternocleidomastoid muscle to penetrate the fascia overlying the scalenus muscles before the injection is made. To block the superficial cervical plexus, an additional subcutaneous injection at this level must be made.

FEMORAL NERVE BLOCK (9)

The femoral nerve lies in the femoral triangle lateral to the femoral artery and vein, respectively. The nerve is most superficial, and therefore most accessible for ultrasound-guided nerve block, below the level of the skin crease in the groin. At this level, the femoral nerve divides principally into major anterior and posterior divisions. At this level, the femoral artery may or may not have given off its major branch, the profunda femoris artery. The posterior division of the femoral nerve may lie posterior or lateral to the femoral artery and occasionally will be visualized between the femoral and the profunda femoris arteries. The lateral circumflex femoral artery, which usually arises from profunda femoris but may arise from the femoral artery, can sometimes be seen passing between the divisions of the femoral nerve (Fig. 5D).

Patient position: Supine.

Equipment: High-frequency linear probe with color Doppler facility.

Position of probe: The probe is placed over the femoral pulse parallel and just distal to the skin crease of the groin.

Executing the block (Fig. 5A–C): The needle is inserted in the long axis of the ultrasound probe and directed from lateral to medial. The needle tip should be placed in the femoral triangle lateral to the artery, and the spread of local anesthetic observed. Spread of solution is usually compartmentalized, and therefore, the block is

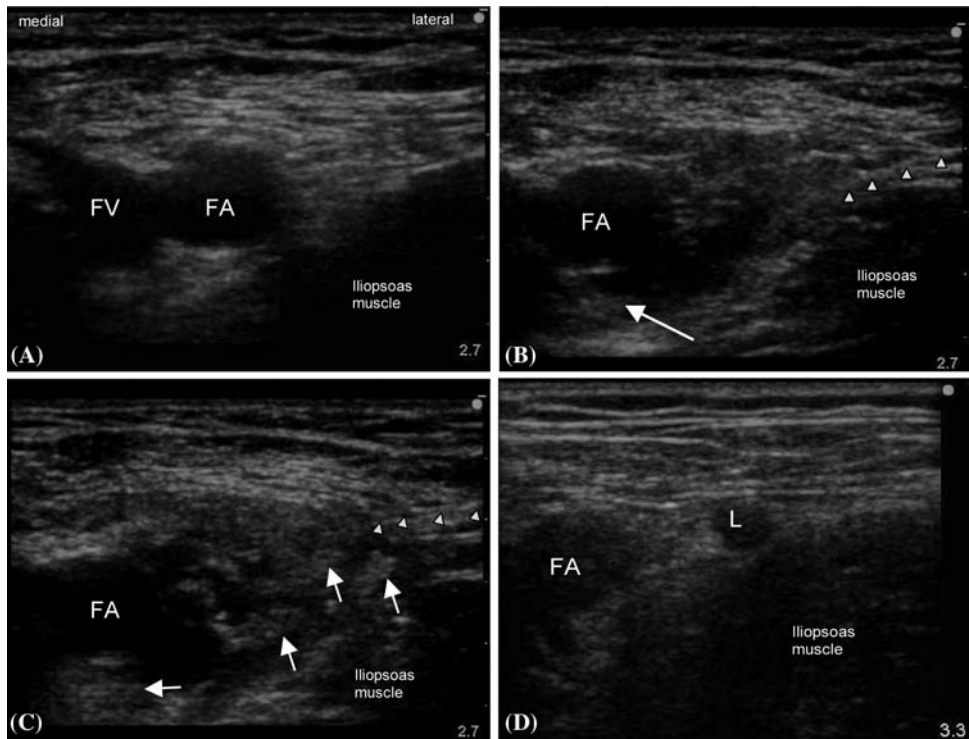


Figure 5 Femoral nerve block. In **A–C**, a 13.5-MHz linear-array probe is placed in the groin crease. (**A**) Prior to injection. At this level, the femoral nerve is branching with individual branches obscured within the femoral triangle. (**B**) During first injection of local anaesthetic below the femoral artery. (**C**) During second injection of local anaesthetic more superficially and laterally within the femoral triangle. In **B** and **C**, the arrows point to nerves highlighted by surrounding local anaesthetic, while the triangles emphasize the position of the needle. (**D**) A different patient imaged with a 10-MHz linear-array probe. In this case, the lateral circumflex femoral artery (*L*) passes between the branches of the femoral nerve. *Abbreviations:* FA, femoral artery; FV, femoral vein.

improved by separate, deep (Fig. 5B) and superficial (Fig. 5C) injections. Injection of a larger volume of local anaesthetic (20–30 ml) improves the chances of cephalad spread to also block the lateral cutaneous nerve of the thigh.

SCIATIC NERVE BLOCK

The sciatic nerve is the largest nerve in the body. It arises from the lumbar sacral plexus (L4–S3) and provides sensory innervation to all the joints of the lower limb and the posterior thigh and, with the cutaneous branch of the femoral nerve, to the leg, ankle, and foot regions. The nerve leaves the pelvis through the posterior sciatic foramen, lying between the fascial planes of obturator internus and inferior gemellus muscles anteriorly and the gluteus maximus muscle posteriorly. The nerve then passes between the ischial tuberosity and the greater trochanter. At the inferior border of gluteus maximus, the sciatic nerve becomes superficial and then continues in the posterior thigh toward the superior aspect the popliteal fossa. At a variable distance above the popliteal crease, the nerve divides into the common peroneal and tibial nerves.

The sciatic nerve is most superficial and therefore accessible for ultrasound-guided block in the subgluteal region, while it, or its branches, can be blocked in the popliteal fossa.

Subgluteal Sciatic Nerve Block (10)

Patient position: Supine with an assistant supporting the patient's leg with hip and knee flexed approximately 90°. Alternatively, the patient can be placed in the lateral position, with the leg to be blocked uppermost—the hip and knee are flexed approximately 90°.

Equipment: Low- to medium-frequency curved-array probe.

Position of probe: Perpendicular to the long axis of the femur in the crease of the buttock. In this position, the sciatic nerve lies midway between the greater trochanter of the femur laterally and the ischial tuberosity medially. These bones can be identified by their hyperechoic periosteum and hypoechoic shadow beneath. The nerve appears as a round or elliptical structure, approximately 5 to 8 mm in diameter, medial to the biceps femoris muscle. The nerve is surrounded by adipose tissue creating a very good echo interface with the aponeurosis of the surrounding muscles, giving the muscles a well-defined border.

Executing the block: A 10-cm short-bevelled needle can be inserted in the long axis of the plane of the ultrasound probe, and its tip guided into the sciatic nerve canal. The needle may need repositioning to ensure spread of the local anesthetic solution around the circumference of the nerve.

Popliteal Fossa Block

Patient position: Supine with an assistant supporting the patient's leg, with hip and knee flexed approximately 90°. Alternatively, the patient can be placed in the lateral position, with the leg to be blocked uppermost—the hip and knee are flexed approximately 90°.

Equipment: Medium- to high-frequency linear probe with color Doppler facility.

Position of probe: Perpendicular to the long axis of the femur, approximately 8 cm proximal to the popliteal skin crease. In this position, the nerve is superficial, lying between the biceps femoris muscle laterally and the semitendinosus/semimembranosus muscles medially (Fig. 6A). The popliteal artery and vein lie deep and medial to the sciatic nerve.

Executing the block: The needle is inserted in the long axis of the probe on the lateral side, and its tip is located to ensure the spread of the local anesthetic around the nerve. It should be noted that the sciatic nerve sometimes divides into its terminal branches proximal to this level, in which case, the common peroneal nerve will lie lateral to the tibial nerve (Fig. 6B).

EPIDURAL ANALGESIA (11–13)

The end point for correct needle placement within the epidural space is different from the traditional techniques of the blocks described above. The end point utilizes the fact that the needle has to be inserted through the tough ligamentum flavum before entering the epidural space, which transmits the low pressures of the thoracic cavity. There is thus a marked loss of resistance as the epidural space is entered if continuous pressure is applied to the plunger of a syringe attached to the needle. Identification of the epidural space using ultrasonography is perhaps more difficult than that with the superficial structures

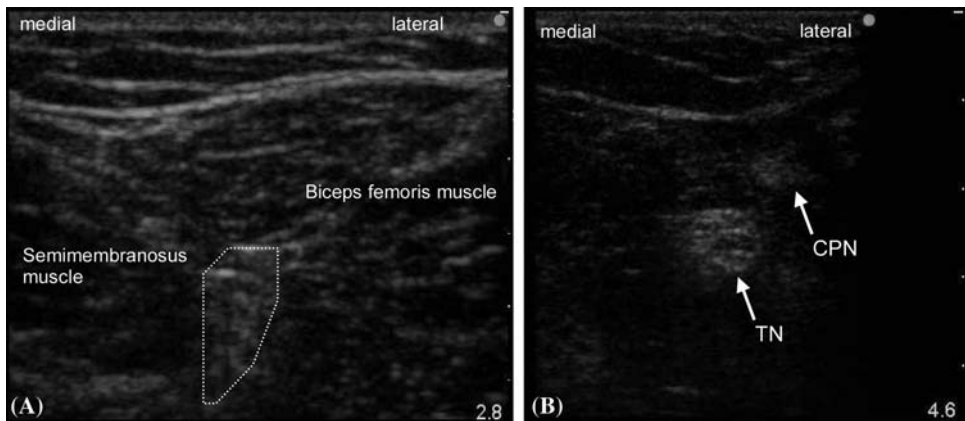


Figure 6 Views of the sciatic nerve and its branches in the popliteal fossa obtained using a 10-MHz linear-array probe aligned perpendicular to the femur on the posterior surface of the thigh. (A) View when probe placed 8 cm proximal to the popliteal skin crease: the dotted line follows the margin of the sciatic nerve. (B) View when probe placed just proximal to the popliteal skin crease; the arrows point to the tibial (TN) and common peroneal (CPN) branches of the sciatic nerve.

described in the preceding sections of this chapter. For these reasons, it is likely that the use of ultrasound guidance in epidural analgesia will be adopted less enthusiastically. However, especially in difficult cases, ultrasound can already aid in identification of the precise level of needle insertion, the midline structures, and the depth of injection.

VISUALIZATION OF THE EPIDURAL SPACE

Probes in the range of 4 to 7 MHz are best suited for imaging the space, although in thin subjects, a higher-frequency probe may be optimal. The patient is in sitting or in lateral position with the posterior convexity of the spine maximized. The probe is placed transversely to the long axis of the spine over the sacrum, seen as a continuous hypoechoic band. The probe is then moved cephalad in the midline to identify the L5-S1 intervertebral space. Further cephalad midline movement of the probe will identify in turn the ascending intervertebral spaces. Movement of the probe will laterally identify the anatomy of the posterior vertebral arch and the facet joints. In the intervertebral spaces, the first echogenic structure encountered is the ligamentum flavum, beyond which lies the dura mater (Fig. 7), separated from the ligamentum flavum by the epidural space. The ligamentum flavum and dura mater appear hyperechoic, with the epidural space and the cerebrospinal fluid beyond the dura appearing hypoechoic.

THORACIC PARAVERTEBRAL BLOCK (14)

As with epidural injections, most anesthesiologists use a loss of resistance technique for identification of the thoracic paravertebral space. The technique is used to block the spinal nerves as they pass through the intervertebral foramina. As with the epidural technique, it is likely to be initially used to assess the depth of the space and identification of landmarks prior to the conventional technique being used. However, as anesthesiologists become increasingly skilled with ultrasound needle visualization, we expect transition to ultrasound-guided techniques over the next few years.

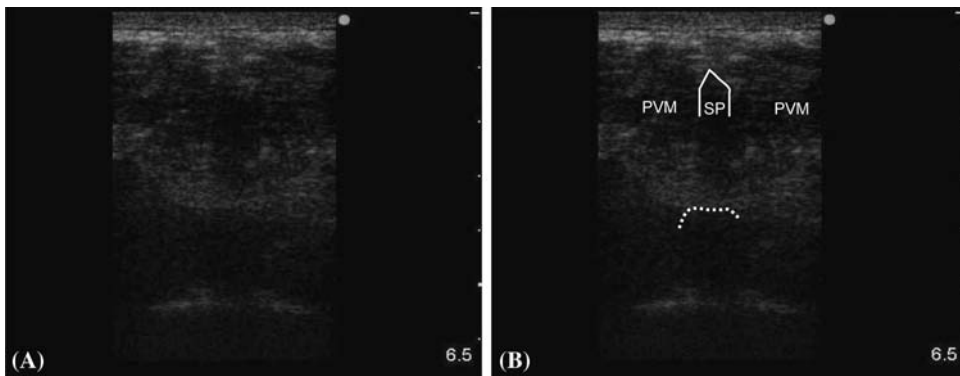


Figure 7 Intervertebral views at the level of L3/4. A 5-MHz linear array probe is placed transversely in the midline. **B** is the same image as **A** but with the paravertebral muscles (PVM), the spinous process (SP), and the ventral dura (*dotted line*) marked.

To visualize the paravertebral space, first place the ultrasound probe in the midline to identify the spinous process, seen as a superficial hyperechoic surface with a deeper hypoechoic component. The probe is then moved laterally 2 to 3 cm to visualize the transverse process of the vertebra. Deep to the transverse process, the pleura can be seen as a hyperechoic shadow that moves with respiration. The paravertebral space is entered above the transverse process medial to the pleura.

CONCLUSION

The introduction of ultrasound guidance for regional anesthetic techniques has gathered pace over the past 10 years and is one of the most important advances of recent years in anesthesia. It is likely that ultrasound guidance will become the gold standard for regional anesthesia (1).

REFERENCES

1. Hopkins PM. Ultrasound guidance as a gold standard in regional anaesthesia. *Br J Anaesth* 2007; 98:299–301.
2. Marhofer P, Greher M, Kapral S. Ultrasound guidance in regional anaesthesia. *Br J Anaesth* 2005; 94:7–17.
3. Chan VWS, Perlas A, Rawson R, et al. Ultrasound guided supraclavicular brachial plexus block. *Anesth Analg* 2003; 97:1514–1517.
4. Williams SR, Chouinard P, Arcand G, et al. Ultrasound guidance speeds execution and improves the quality of supraclavicular block. *Anesth Analg* 2003; 97:1518–1523.
5. Perlas A, Chan VWS. Ultrasound guided interscalene brachial plexus block. *Tech Reg Anesth Pain Manag* 2004; 8:143–148.
6. Sandhu NS, Capan LM. Ultrasound-guided infraclavicular brachial plexus block. *Br J Anaesth* 2002; 89:254–259.
7. Retzl G, Kapral S, Greher M, et al. Ultrasonographic findings of the axillary part of the brachial plexus. *Anesth Analg* 2001; 92:1271–1275.
8. Sandeman DJ, Griffiths MJ, Lennox AF. Ultrasound guided deep cervical plexus block. *Anaesth Intensive Care* 2006; 34:240–244.

9. Marhofer P, Schrogendorfer K, Koinig H. Ultrasonographic guidance improves sensory block and onset time of three-in-one blocks. *Anesth Analg* 1997; 85:854–857.
10. Sukhani R, Candido KD, Doty R, et al. Infragluteal parabiceps sciatic nerve block: an evaluation of a novel approach using a single injection technique. *Anesth Analg* 2003; 96:868–873.
11. Grau T, Leipold RW, Horter J, et al. The lumbar epidural space in pregnancy: visualization by ultrasonography. *Br J Anaesth* 2001; 86:798–805.
12. Grau T, Leipold R, Delorme S, et al. Ultrasound imaging of the thoracic epidural space. *Reg Anesth Pain Med* 2001; 27:200–206.
13. Grau T, Leipold R, Horter J, et al. Paramedian access to the epidural space: the optimum window for ultrasound imaging. *J Clin Anesth* 2001; 13:213–217.
14. Naja MZ, Gustafsson AC, Ziade MF, et al. Distance between the skin and the thoracic paravertebral space. *Anaesthesia* 2005; 60:680–684.

7

Transesophageal and Transthoracic Echocardiography: Examination Techniques and Views

Bryan May, Kim Payne, and Scott T. Reeves

Department of Anesthesia & Perioperative Medicine, Medical University of South Carolina, Charleston, South Carolina, U.S.A.

INTRODUCTION

Transesophageal and transthoracic echocardiography have become critical diagnostic tools for the evaluation of cardiac disease. As such, physicians need to be familiar with the image planes acquired from these techniques. This chapter will present the common echocardiographic imaging planes of both transthoracic echocardiography (TTE) and transesophageal echocardiography (TEE) as well as certification requirements in the expanding field of intraoperative TEE.

SAFETY AND COMPLICATIONS

Although TEE is considered to be a minimally invasive and relatively safe procedure when performed by an experienced echocardiographer, there are several absolute and relative contraindications that one must be aware of before beginning any examination (Table 1). Absolute contraindications to TEE include esophageal obstruction (tumor or stricture), diverticula, and recent esophageal or gastric surgery. Relative contraindications are more numerous and include esophageal varices, odynophagia, dysphagia, gastro-esophageal reflux disease, and unstable cervical spines.

Overall, complications associated with TEE are uncommon. Numerous case reports and large multicenter studies have been conducted, showing that the insertion and manipulation of the TEE probe may cause oral, pharyngeal, esophageal, or gastric trauma in only 0.18% to 2.4% of surgical patients.

PATIENT PREPARATION

TEE can be performed as an outpatient or inpatient procedure, with sedation ranging from light sedation to general anesthesia. To optimize the ultrasonographic examination in an

Table 1 Contraindications to Transesophageal Echocardiography

| |
|---|
| Absolute contraindications to TEE |
| <ul style="list-style-type: none"> • Active gastrointestinal bleed • Perforated viscus • Unwilling or uncooperative patient • Esophageal obstruction (mass or stricture) |
| Relative contraindications to TEE |
| <ul style="list-style-type: none"> • Esophageal stricture • Esophageal varices • Esophageal diverticula • Odynophagia • Dysphagia • Severe gastroesophageal reflux disease • History of gastrointestinal bleed • History of esophageal or gastric surgery • Severe cervical arthritis • Unstable cervical spine • Hiatal hernia • Severe oropharyngeal pathology • History of head, neck, or mediastinal radiation • Recent oral intake |

awake patient, the patient must be both cooperative and calm. The patient should be kept nil per os (NPO) for a minimum of six hours prior to examination, and all dentures should be removed. Topical anesthesia of the oro-hypopharynx is recommended prior to TEE probe insertion, and providing adequate sedation is very important to avoid discomfort. Frequently used sedative agents include intravenous midazolam, fentanyl, Demerol, and propofol. A drying agent such as glycopyrolate may be useful to decrease oral secretions. A bite block should be used to prevent damage to both the patient's teeth and the ultrasound transducer during both probe insertion and manipulation.

The patient should be continuously monitored with pulse oximetry, blood pressure cuff, and continuous electrocardiogram. Suction, supplemental oxygen, and an emergency crash cart with airway and resuscitation drugs should always be readily available. An intravenous catheter should be placed even if sedation is not required, to allow immediate vascular access should the need arise.

Intraoperative TEE is performed in an anesthetized patient after induction of anesthesia and placement of an endotracheal tube. A bite guard should be placed prior to insertion of the TEE probe. An orogastric tube should be passed to evacuate any air or gastric contents that may otherwise interfere with the image quality.

PROBE INSERTION TECHNIQUES

TEE probe insertion is generally considered very safe if performed properly; however, cases of pharyngeal trauma, dental injuries, esophageal trauma, arrhythmias, respiratory distress, and hemodynamic effects have been reported. The well-lubricated TEE probe is most often inserted blindly into the esophagus by displacing the mandible anteriorly and inserting the probe gently in the midline. Most often, this insertion is accomplished by performing a jaw lift with the left hand and advancing the probe with the right hand while applying constant gentle pressure. A simple maneuver of rotating the probe slightly back

and forth during insertion may help locate the esophageal inlet. During probe insertion and manipulation, the control knobs must remain in the neutral position (nonlocked) to prevent esophageal damage. If more than minimal resistance is encountered during probe insertion, a different technique may be necessary to locate the esophagus.

In the intubated patient, the endotracheal tube tends to fall back and may rest against the posterior pharyngeal wall, thus minimizing access to the esophageal inlet. Direct laryngoscopy may be used to directly visualize and expose the glottis and permit direct passage of the probe posteriorly into the esophagus. A gloved-hand technique may also be employed by guiding the probe with your fingers while lifting the mandible anteriorly. This is the same technique that is often used when inserting an orogastric tube. Flexing the head forward may also be helpful as excessive extension of the head and neck is often a cause of encountered resistance. If all of these techniques fail or any unusual resistance is encountered, it is best to abandon the procedure. The risks of oropharyngeal or esophageal injury may outweigh the benefits of TEE. Alternatively, epicardial echocardiography may be utilized.

PROBE MANIPULATION

There are several possible manipulations of the TEE probe that will allow the ultrasonographer to alter the position and orientation of the ultrasound beam. The first technique is the advancement and withdrawal of the probe itself within the esophagus and stomach to obtain different levels of imaging (Fig. 1). The depth of insertion can be determined by the markings on the shaft of the probe. The beam's orientation may also be adjusted by rotating the shaft of the probe toward the patient's left (counterclockwise from the ultrasonographer's perspective at the patient's head) or right (clockwise rotation).

The two control wheels on the handle of the probe permit further movement of the probe's tip. The larger wheel allows the ultrasonographer to flex the tip anteriorly

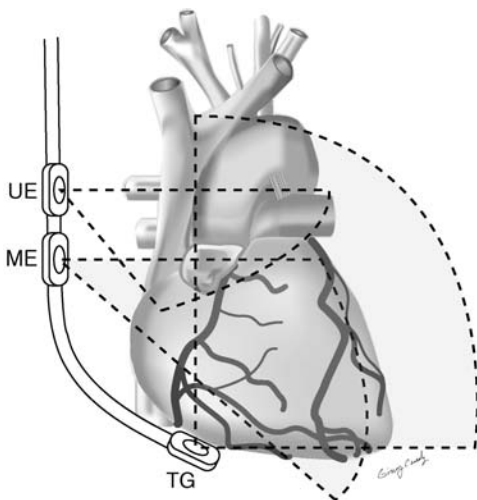


Figure 1 The three main imaging planes within the esophagus and their relationship to the heart. These include the UE, ME, and TG imaging planes. *Abbreviations:* UE, upper esophageal; ME, midesophageal; TG, transgastric.

(anteflex) toward the patient's sternum or posteriorly (retroflex) toward the spine (Fig. 2). The small wheel flexes the probe's tip toward the patient's left or right side (Fig. 3).

Finally, the imaging plane can be electronically rotated using the buttons located on the top of the probe handle (Fig. 4). This allows the transducer located within the probe's tip to be rotated from the 0° horizontal plane to its mirror image at 180°.



Figure 2 Anteflexion and retroflexion of the probe head is accomplished by rotation of the large knob on the TEE probe handle. *Abbreviation:* TEE, transesophageal echocardiography.



Figure 3 Leftward and rightward movement of the probe head is accomplished by rotation of the small knob on the TEE probe handle. *Abbreviation:* TEE, transesophageal echocardiography.

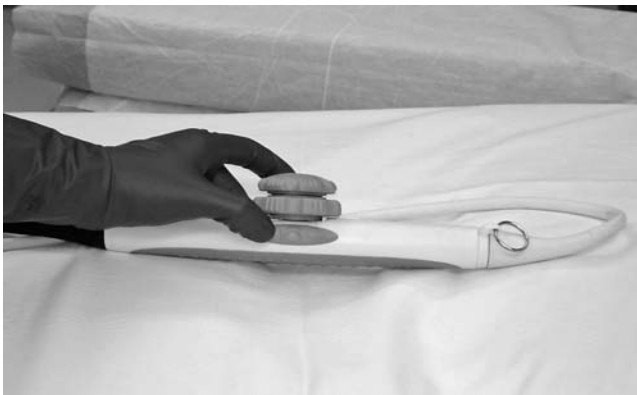


Figure 4 The imaging plane can be electronically rotated using the buttons located on top of the probe handle. This allows the transducer located within the probe's tip to be rotated from the 0° horizontal plane to its mirror image at 180°.

TRANSESOPHAGEAL ECHOCARDIOGRAPHY EXAMINATION TECHNIQUE

In 1999 the American Society of Echocardiography (ASE) and the Society of Cardiovascular Anesthesiologist (SCA) developed guidelines for performing a comprehensive intraoperative multiplane TEE examination. This chapter will discuss the 20 commonly found image views as published under those guidelines. It is important to note that the sequence in which these views are obtained is not nearly as important as actually performing a complete comprehensive examination. As such, I will utilize a technique developed at the Medical University of South Carolina, where the heart valves are first evaluated from the midesophageal (ME) imaging planes. This allows one to evaluate the mitral, aortic, tricuspid, and pulmonic valves prior to having to deal with surgical skin incision and Bovie interference. By having completely performed the examination of the valves with both two-dimensional (2D) and color flow Doppler, surgery does not need to be delayed to obtain this critical information. Using the technique described above, the examination is started at the ME level at the mitral valve (Fig. 1).

Midesophageal Four-Chamber View

The ME four-chamber view (Fig. 5) is obtained at an imaging angle of 0° . The TEE probe is advanced to approximately 35 cm from the incisors until the mitral and tricuspid valves are visualized. Occasionally the imaging angle needs to be rotated between 0° and 10° with some posterior flexion of the probe in order to optimize this view. In addition, all four chambers of the heart can be evaluated. The septal and lateral walls of the myocardium are well visualized, and regional wall motion can be determined. This view

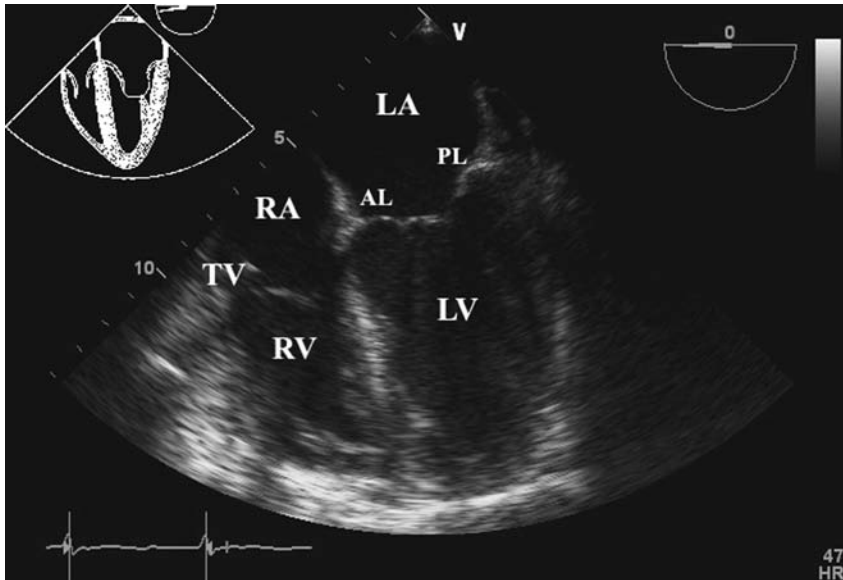


Figure 5 ME four-chamber view is obtained with an imaging angle between 0° and 10° . All four chambers of the heart as well as the TV and MV are clearly seen. The LA, LV, RA, RV, AL of the MV, and PL of the MV are also seen. *Abbreviations:* ME, midesophageal; TV, tricuspid valve; MV, mitral valve; LA, left atrium; LV, left ventricle; RA, right atrium; RV, right ventricle; AL, anterior leaflet; PL, posterior leaflet.

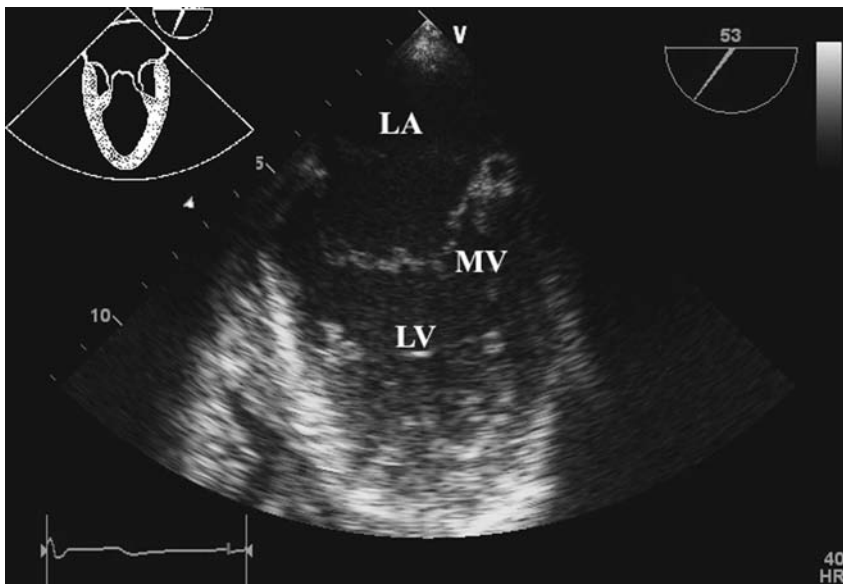


Figure 6 Midesophageal mitral commissural view is obtained by rotating the image angle to approximately 60° . *Abbreviation:* ME, midesophageal.

allows clear delineation of tricuspid and mitral valve pathology. With color flow and spectral Doppler, one can evaluate the degree of tricuspid and mitral valve insufficiency and/or stenosis. By slightly withdrawing the probe from the patient's mouth (1–2 cm), the left ventricular outflow track (LVOT) will come into view as well as a portion of the aortic valve. This view is commonly referred to as the ME five-chamber view; however, it is not part of the standard ASE/SCA published guideline views.

Midesophageal Mitral Commissural View

From the ME four-chamber view, rotating the image angle to approximately 60° will develop the ME mitral commissural view (Fig. 6). This view is useful for evaluating the posterior and anterior leaflets of the mitral valve. Specifically, the P1 and P3 scallops of the posterior leaflet of the mitral valve will clearly be visualized with the A2 segment of the anterior leaflet occupying the middle of the imaging plane. The anterior lateral and posterior medial papillary muscles and the subcordal apparatus can also be appreciated.

Midesophageal Two-Chamber View

From the ME mitral commissural view, rotating the image angle to approximately 60° to 90° will allow one to obtain the ME two-chamber view (Fig. 7). This view is identified by the presence of the left atrial appendage (LAA) and the absence of any right heart structures. The anterior and inferior walls of the left ventricle will be clearly visualized. LAA thrombus, ventricular thrombus, or regional wall motion abnormalities involving the left ventricular apex can best be appreciated in this view. By withdrawing the probe slightly out of the patient's mouth, the left upper pulmonary vein (LUPV) will be seen just above the LAA on the monitor.

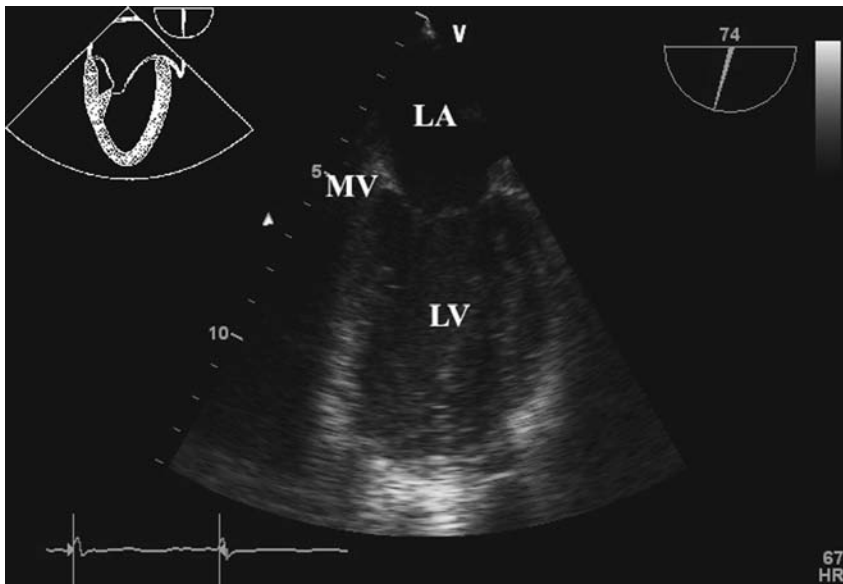


Figure 7 The ME two-chamber view is obtained from the ME mitral commissural view by rotating the image angle to approximately 60° to 90° . *Abbreviation:* ME, midesophageal.

Midesophageal Long-Axis View

From the ME two-chamber view, continued angle rotation will allow evaluation of the ME long-axis (LAX) view (Fig. 8). This view allows evaluation of the LVOT and the aortic valve as well as evaluation of the anterior leaflet of the mitral valve as it coadapts

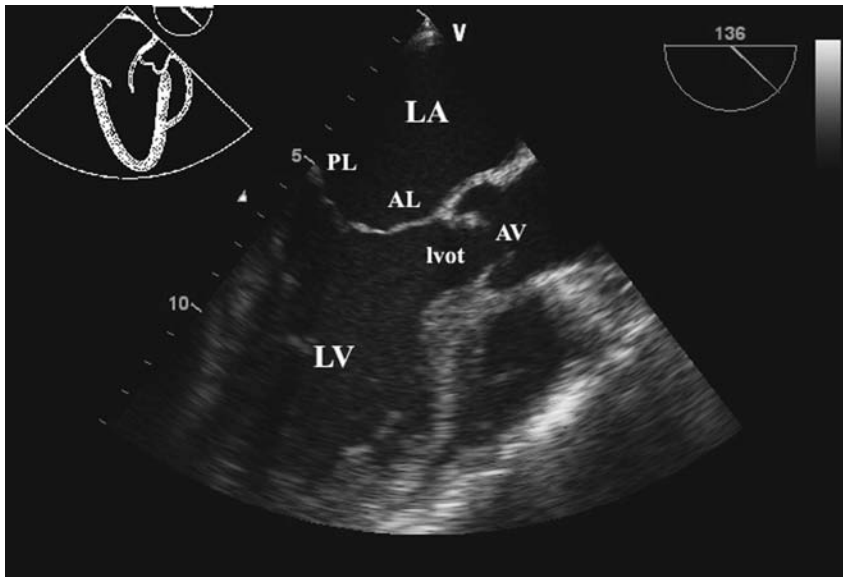


Figure 8 The ME LAX view is obtained at approximately 120° . The LA, LV, AV, AL of the MV, the PL of the MV, and the LVOT are also seen. *Abbreviations:* ME, midesophageal; LAX, long axis; LA, left atrium; LV, left ventricle; AV, aortic valve; AL, anterior leaflet; PL, posterior leaflet; MV, mitral valve; LVOT, left ventricular outflow tract.

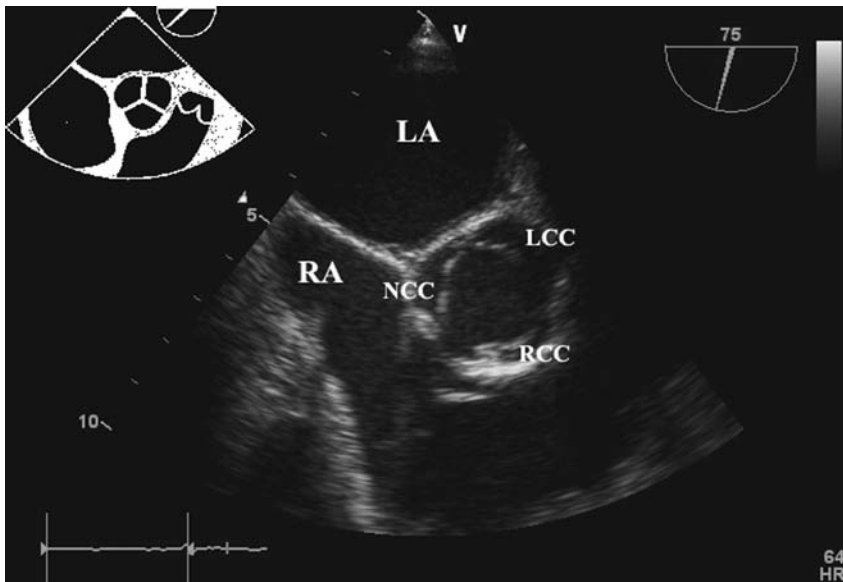


Figure 9 ME AV SAX view. The RCC, LCC, and NCC of the AV can clearly be seen. *Abbreviations:* ME, midesophageal; AV, aortic valve; SAX, short axis; RCC, right coronary cusp; LCC, left coronary cusp; NCC, noncoronary cusp.

with the P2 segment of the posterior leaflet. As one evaluates the mitral valve with color flow Doppler, it is important to have a clear understanding of 2D anatomy.

Midesophageal Aortic Valve Short-Axis View

From the ME LAX view, the imaging angle is returned back to 0° and the ME four-chamber view. The probe is slightly withdrawn out of the patient's mouth (1–2 cm) in order to visualize the aortic valve. From this imaging plane, the imaging angle is rotated to approximately 40° to 60° to obtain the ME aortic valve short-axis (SAX) view (Fig. 9). This view allows clear delineation of the three leaflets of the aortic valve and is best used for using planimetry to calculate aortic valve area.

Midesophageal Right Ventricular Inflow-Outflow View

From the ME aortic valve SAX view, the imaging angle is rotated to approximately 60° to 90° to obtain the ME right ventricular inflow-outflow track view (Fig. 10). This view will allow visualization of the tricuspid valve, the right ventricular outflow track (RVOT), and the proximal pulmonary artery.

Midesophageal Bicaval View

From the ME right ventricular inflow-outflow view, the imaging angle is rotated to approximately 90° with slight rotation of the handle of the TEE probe in order to obtain the ME bicaval view (Fig. 11). This view allows visualization of the superior vena cava and inferior vena cava as it enters the right atrium and the right atrial appendage. The fossa ovalis is easily seen, and this view is the preferred view for diagnosing the presence of a patent foramen ovale.

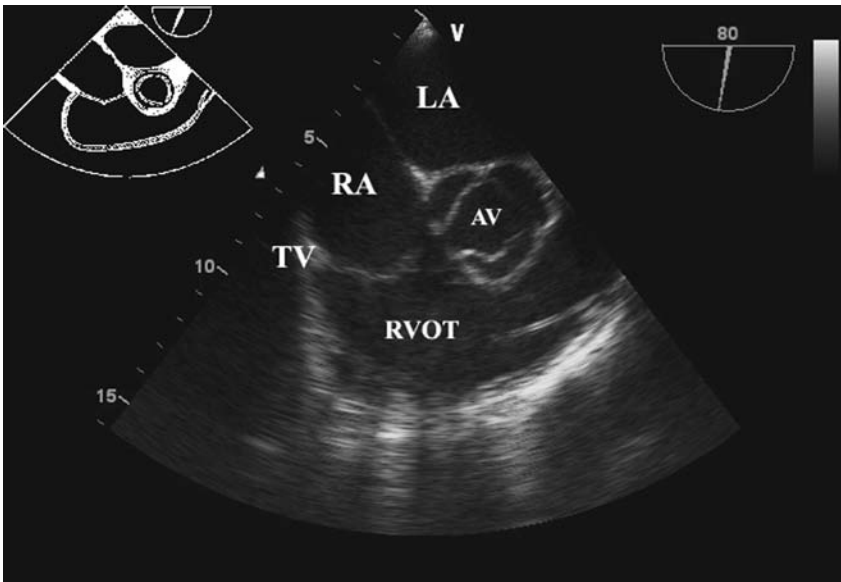


Figure 10 ME right ventricular inflow-outflow view will allow visualization of the RA and LA, the TV, the AV, the RVOT, and the proximal pulmonary artery can be seen. *Abbreviations:* ME, midesophageal; RA, right atrium; LA, left atrium; TV, tricuspid valve; AV, aortic valve; RVOT, right ventricular outflow track.

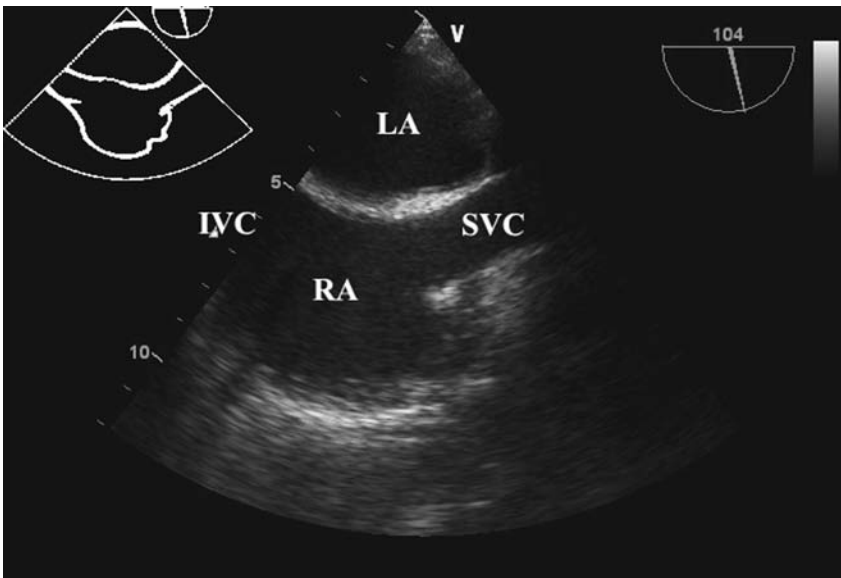


Figure 11 The ME bicaval view allows visualization of the SVC and IVC as it enters the RA. *Abbreviations:* ME, midesophageal; SVC, superior vena cava; IVC, inferior vena cava; RA, right atrium.

Midesophageal Aortic Valve Long-Axis View

From the ME bicaval view, the imaging angle is rotated further to approximately 110° to 130° with slight rotation of the handle in order to obtain the ME aortic valve LAX view (Fig. 12). The LVOT, aortic valve, proximal ascending aorta, and aortic root will be

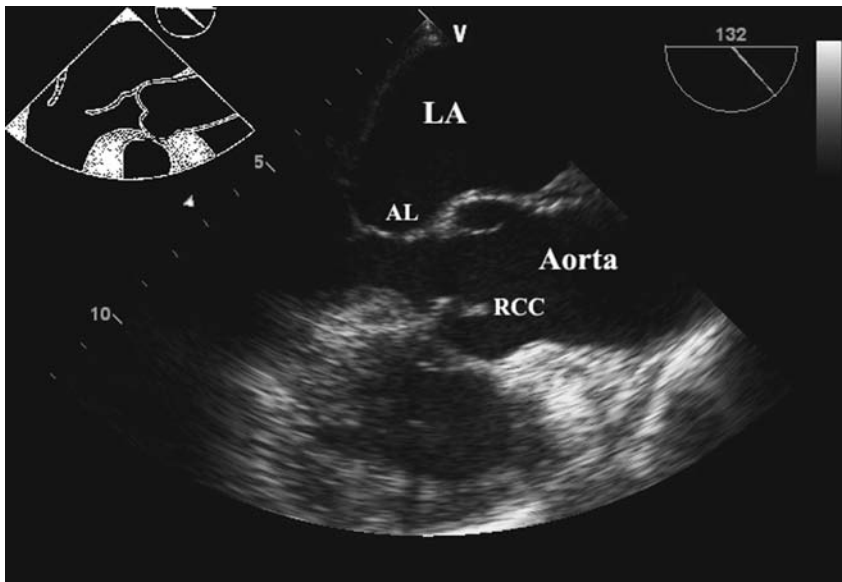


Figure 12 The ME AV LAX view allows visualization of the LVOT, AV, proximal Ao, and the aortic root. The RCC is also seen. *Abbreviations:* ME, midesophageal; AV, aortic valve; LAX, long axis; RCC, right coronary cusp; LVOT, left ventricular outflow tract; Ao, ascending aorta.

clearly visualized. This view is useful for determining the degree of aortic insufficiency with color flow Doppler using the jet width method.

This concludes the views imaged at this level from the midesophagus. However, there are two views, which are slightly higher in the esophagus, that need to be evaluated.

Midesophageal Ascending Aorta Short-Axis View

The imaging angle is returned to 0° , and the probe is slowly withdrawn from the patient's mouth until the ascending aorta is clearly visualized in the center of the imaging plane. This is the ME ascending aortic SAX view and is usually obtained between 0° and 10° (Fig. 13). This view allows evaluation of the ascending aorta, the superior vena cava, the main pulmonary artery, and the right main pulmonary artery.

Midesophageal Ascending Aorta Long-Axis View

From the ME ascending aortic SAX view, the imaging angle is rotated to 90° to get the ME ascending aorta LAX view (Fig. 14). The ME ascending aorta aortic LAX view is most useful for diagnosing type A aortic dissections.

Transgastric Mid-Short-Axis View

The TEE probe is now advanced into the patient's stomach with mild anteflexion in order to develop the transgastric (TG) mid-SAX view (Fig. 15). The posterior medial and anterior lateral papillary muscles should be clearly visualized in this view. This view is extremely useful because it allows evaluation of all three coronary artery distributions simultaneously. In addition, it is the preferred view for evaluating left ventricular preload and ejection fraction.

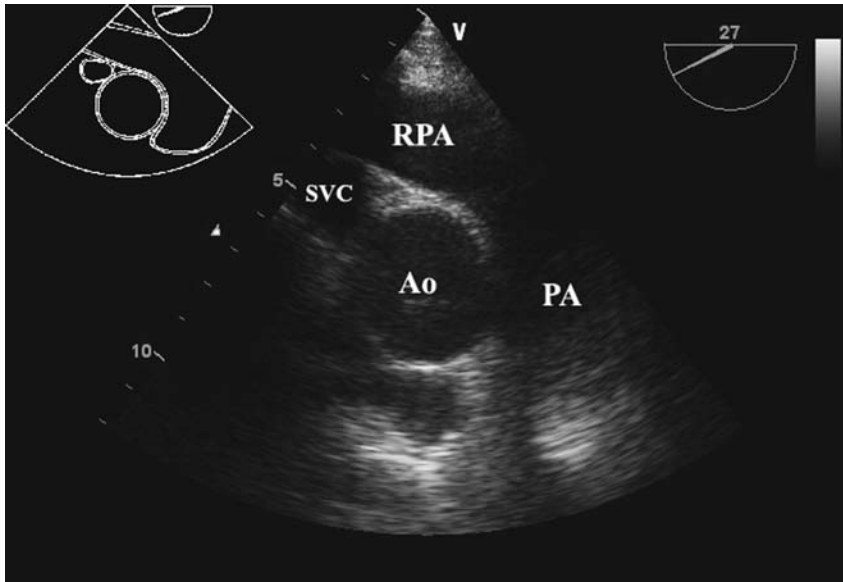


Figure 13 ME Ao SAX view allows evaluation of the Ao, the SVC, the main PA and the RPA. *Abbreviations:* ME, midesophageal; Ao, ascending aorta; SAX, short axis; SVC, superior vena cava; PA, pulmonary artery; RPA, right main pulmonary artery.

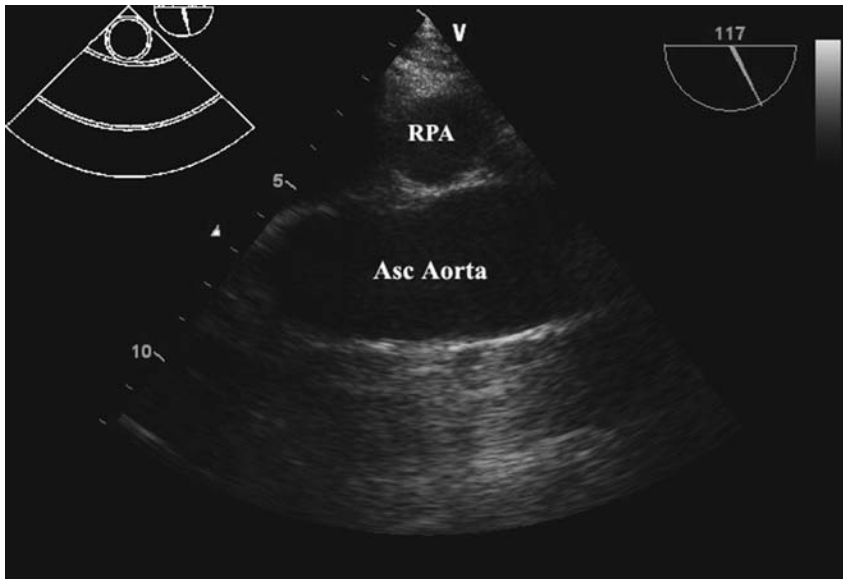


Figure 14 ME Ao LAX view is useful for diagnosing type A aortic dissections. *Abbreviations:* ME, midesophageal; Ao, ascending aorta; LAX, long axis.

Transgastric Two-Chamber View

By rotating the probe 90°, the TG two-chamber view will now be visualized (Fig. 16). The TG two-chamber view is useful for evaluating the mitral valve’s subvalvular apparatus (papillary muscles and the primary, secondary, and tertiary cordal attachments).

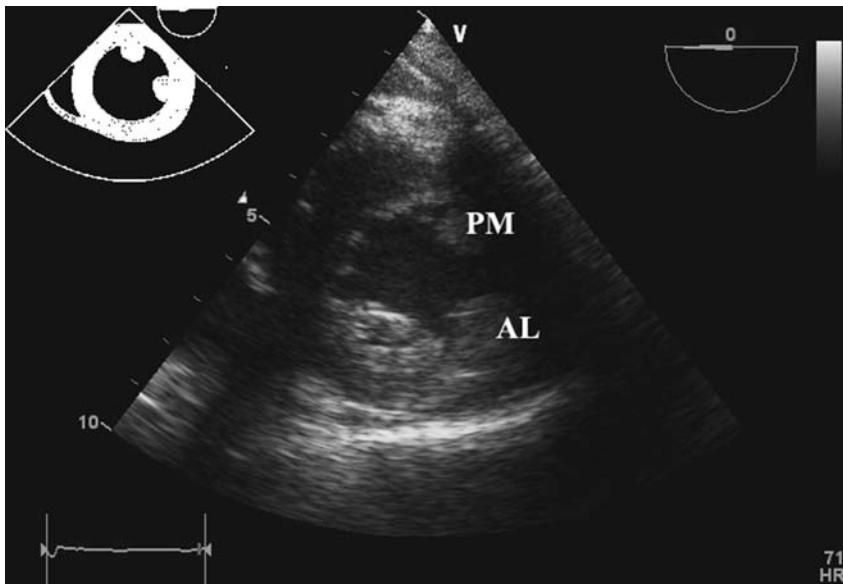


Figure 15 The TEE probe is advanced into the patient's stomach with mild anteflexion in order to develop the TG mid SAX view. The posterioriomedial and anteriolateral papillary muscles must be clearly visualized in this view. *Abbreviations:* TEE, transesophageal echocardiography; TG, transgastric; SAX, short axis.

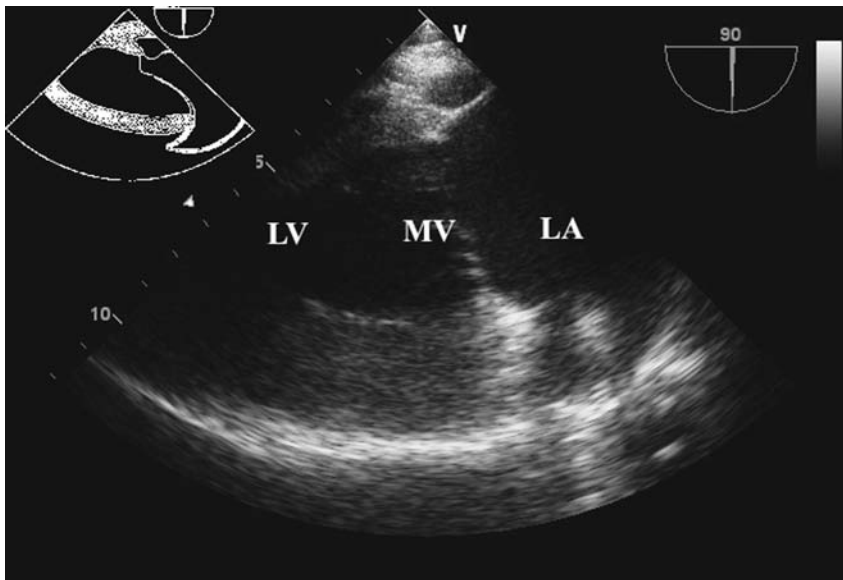


Figure 16 The TG two-chamber view is used for evaluating the MV's subvalvular apparatus (papillary muscles and the primary, secondary, and tertiary cordal attachments). *Abbreviations:* TG, transgastric; MV, mitral valve.

Transgastric Long-Axis View

From the TG two-chamber view, continuing rotation of the image angle to 110° to 130° allows evaluation of the TG LAX view (Fig. 17). In this view, the LVOT and aortic valve will be seen on the right side of the imaging screen. This view allows for parallel

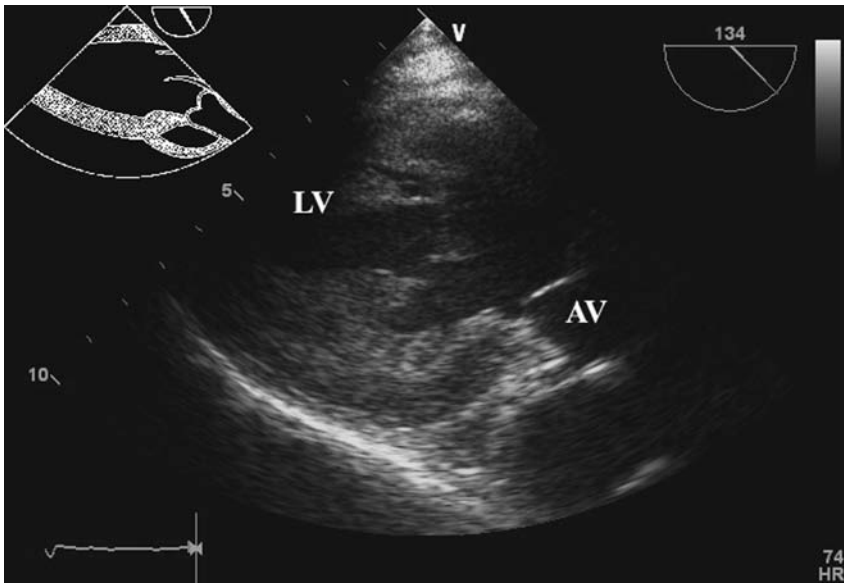


Figure 17 The TG LAX view is most commonly utilized to evaluate velocities and hence pressure gradients across the AV. *Abbreviations:* TG, transgastric; LAX, long axis; aortic valve, AV.

continuous-wave Doppler beam alignment, which is necessary to evaluate velocity and pressure gradients in a patient expected to have aortic stenosis.

Transgastric Right Ventricular Inflow View

Rotation of the probe shaft toward the patient's right will allow visualization of the right atrium and ventricle in the LAX (Fig. 18). This view is useful for evaluating the tricuspid valve chordal attachments.

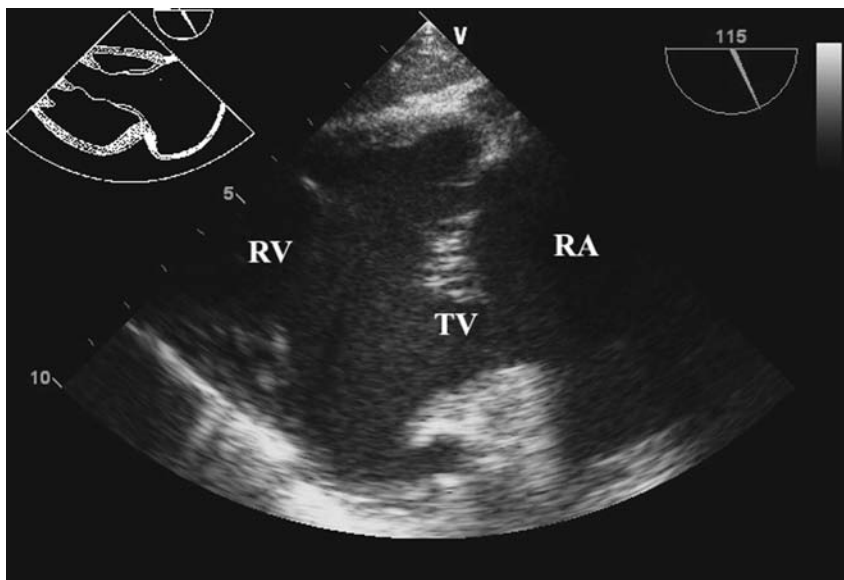


Figure 18 TG right ventricular inflow view. *Abbreviation:* TG, transgastric.

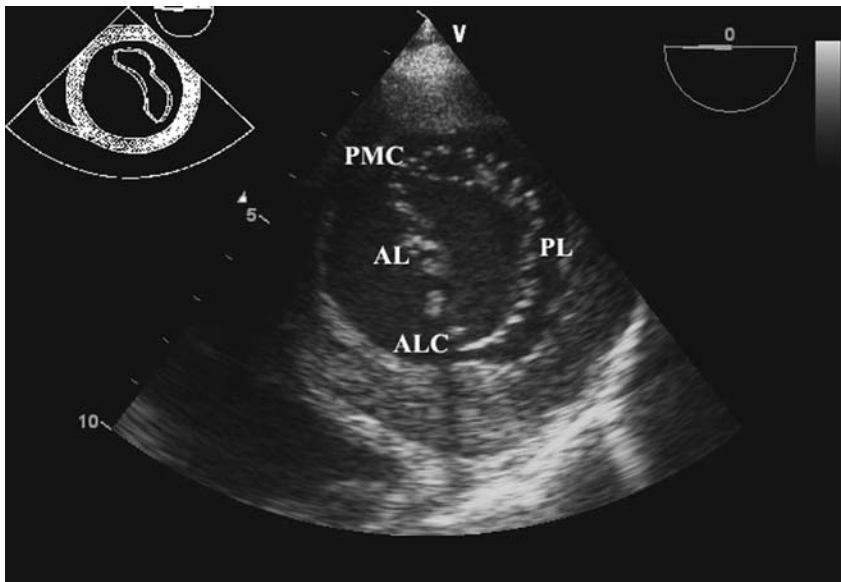


Figure 19 The TG Basal SAX view and is most useful for evaluating MV pathology as the complete AL and PL as well as the posteromedial and anteriolateral papillary muscles are well visualized. *Abbreviations:* TG, transgastric; SAX, short axis; AL, anterior leaflet; PL, posterior leaflet.

Transgastric Basal Short-Axis View

The imaging angle is then rotated back to 0° , and the probe is slightly withdrawn until the fish-mouth appearance of the mitral valve in the SAX is visualized (Fig. 19). This is the TG basal SAX view and is most useful for evaluating mitral valve pathology as the complete anterior and posterior leaflets are seen.

Deep Transgastric View

Following evaluation of the TG basal SAX view, the TEE probe is relaxed (hence no flexion) and then advanced deep into the stomach until no recognizable structures are visualized. This process usually requires advancement of 3 to 4 cm from the traditional TG views. At this depth, the probe is anteflexed (with the big knob) and rotated slightly toward the patient's left (slight turning of the little knob) until contact is made against the stomach wall. At 0° , typically the deep TG view will be visualized and will be very similar to the parasternal LAX view seen with TTE, which will be discussed later (Fig. 20). The left ventricle is at the top of the monitor, with the aortic valve and ascending aorta at the bottom of the monitor. Note that the left ventricle, the LVOT, and the aortic valve are directly parallel to the Doppler beam. This view is the best view for evaluating blood velocities and pressure gradients across the aortic valve.

Descending Thoracic Aorta Short-Axis View

Following the evaluation of the deep TG LAX view, the exam is now changed to focus on the thoracic aorta. The TEE probe is rotated 180° by turning the shaft of the probe to look at more posterior structures in the chest. The depth is decreased to approximately 6 cm in order to visualize the descending thoracic aorta in the SAX. The complete thoracic aorta is slowly visualized along its course as the probe is withdrawn (Fig. 21).

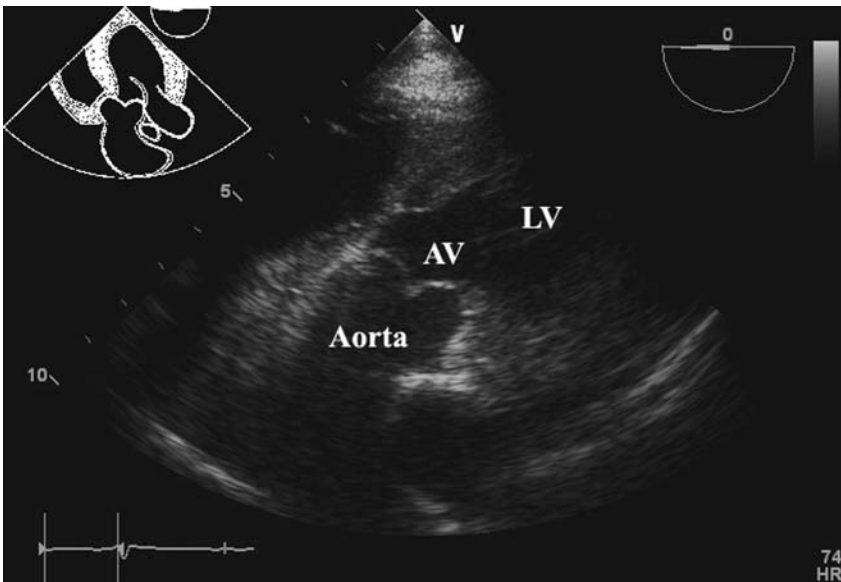


Figure 20 The deep TG view will demonstrate the LV at the top of the monitor with the AV and Ao at the bottom of the monitor. Note that the LV, the LVOT, and the AV are directly parallel to the Doppler beam. This is the best view for evaluating blood flow velocities and pressure gradients across the AV. *Abbreviations:* TG, transgastric; LV, left ventricle; AV, aortic valve; Ao, ascending aorta; LVOT, left ventricular outflow tract.

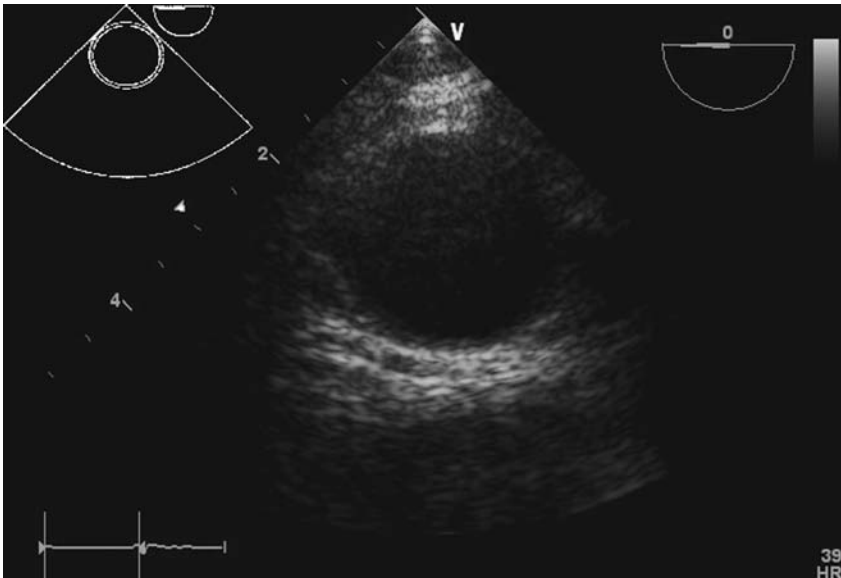


Figure 21 In order to evaluate the descending thoracic aorta SAX view, the TEE probe is rotated 180° by turning the shaft of the probe to look at more posterior structures in the chest. The depth is decreased to approximately 6 cm in order to visualize the descending thoracic aorta. *Abbreviation:* SAX, short axis.

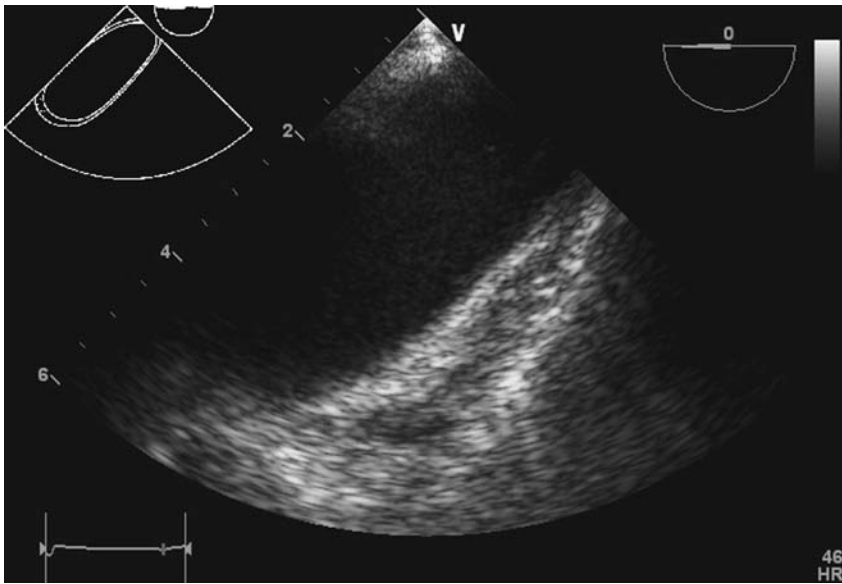


Figure 22 UE aortic arch LAX view. *Abbreviations:* UE, upper esophageal; LAX, long axis.

Upper Esophageal Aortic Arch Long-Axis View

When the aorta begins to appear elongated, the level of the aortic arch has been reached. This view is called the upper esophageal (UE) aortic arch LAX view (Fig. 22).

Upper Esophageal Aortic Arch Short-Axis View

The imaging angle is then rotated to 90° in order to get the UE aortic arch SAX view (Fig. 23).

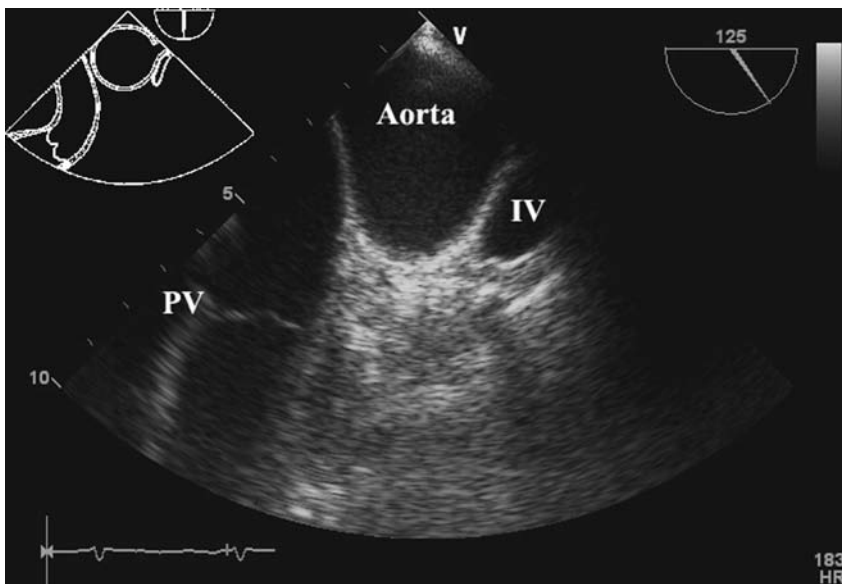


Figure 23 UE aortic arch SAX view allows excellent Doppler evaluation of the PV. The IV is also visualized. *Abbreviations:* UE, upper esophageal; SAX, short axis; pulmonic valve; IV, innominate vein.

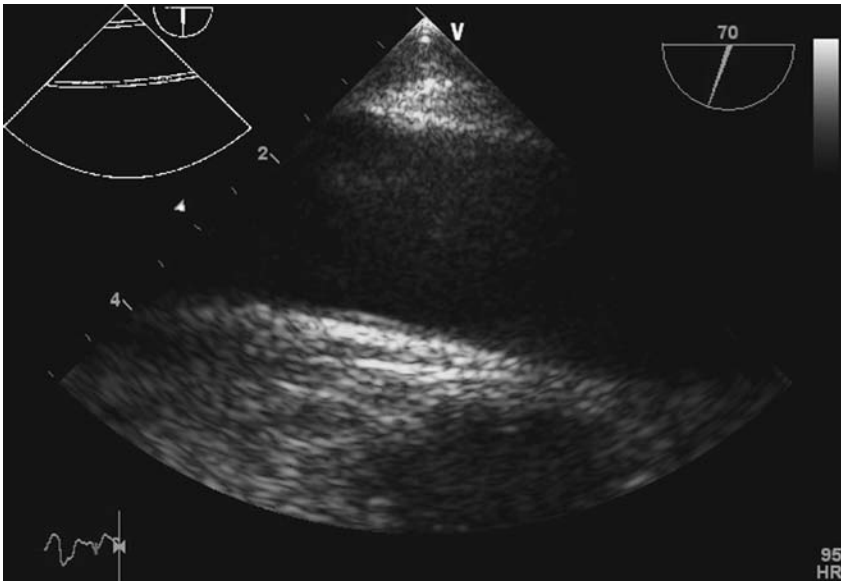


Figure 24 Descending aorta LAX view. *Abbreviation:* LAX, long axis.

Descending Aorta Long-Axis View

The probe is then slowly advanced into the patient, allowing visualization of the descending aorta (the descending aorta LAX view) (Fig. 24). The aorta is then visualized along its course as the probe is slowly advanced in this LAX plane until the stomach is again reached.

With practice, this complete 20-view TEE comprehensive examination can be performed within 10 to 20 minutes, depending on the patient's pathology. As one learns TEE, it is extremely important that as complete an examination as possible is performed in order to assist in learning normal from abnormal structures and to increase the speed and accuracy of the evaluation. Most anesthesiologists and critical care physicians will spend their careers evaluating patients via TEE. In the case of anesthesiologists, this will primarily be secondary to the inability to perform TTE secondary to interference with the surgical site or the surgical drapes. Critical care physicians will utilize TEE because of improved image resolution obtained from transesophageal compared with TTE windows in mechanically ventilated patients. Despite the overwhelming utilization of TEE, it is critical that TTE views be understood and appreciated. As such, the common 10 TTE views evaluated routinely in cardiology echocardiography labs will be discussed.

TRANSTHORACIC ECHOCARDIOGRAPHY

TTE views are most commonly obtained from the parasternal, apical, and subcostal windows. The transthoracic examination will begin at the parasternal LAX window.

Parasternal Long-Axis View

The transthoracic examination is begun in the parasternal position. With the patient in the left lateral decubitus position, the probe is placed in the left third or fourth intercostal space. The parasternal LAX view (Fig. 25) is performed with the transducer marker facing

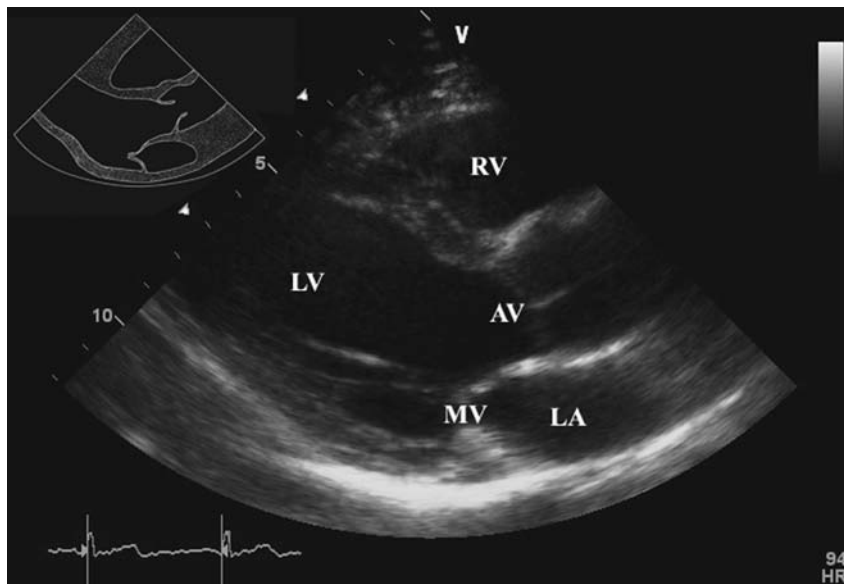


Figure 25 Parasternal LAX view is performed with the transducer indentation marker facing toward the patient's right flank and allows for visualization of the MV, LA, LV, and AV. *Abbreviations:* LAX, long axis; MV, mitral valve; LA, left atrium; LV, left ventricle; AV, aortic valve.

toward the patient's right flank and allows for visualization of the mitral valve, left atrium, left ventricle, and aortic valve. The degree of mitral or aortic insufficiency can be quantified in this view.

Parasternal Long-Axis View of the Right Ventricle

With the ultrasound transducer remaining in the third or fourth interspace, slight angulation inferomedial and with clockwise rotation of the transducer will visualize the LAX view of the right ventricle and right atrium (Fig. 26).

Parasternal Short-Axis View of the Right Ventricular Outflow Tract

From the parasternal LAX view, the ultrasound transducer is rotated by hand (clockwise) to approximately 90°, and the ultrasound beam is angulated superior and medial in order to obtain the parasternal SAX view (Fig. 27). This allows clear delineation of the tricuspid valve, the RVOT, the pulmonic valve, and the aortic valve. This view is useful for determining the degree of insufficiency of the aortic, tricuspid, or pulmonic valves.

Parasternal Short-Axis View of the Mitral Valve

From the parasternal SAX view of the RVOT, the ultrasound beam is progressively directed more inferior and lateral (toward the ventricular apex). The first view obtained is a SAX cut through the mitral valve, very similar to the TEE TG basal SAX view. This view is the parasternal SAX view of the mitral valve (Fig. 28) and allows evaluation of the anterior and posterior leaflets of the mitral valve.

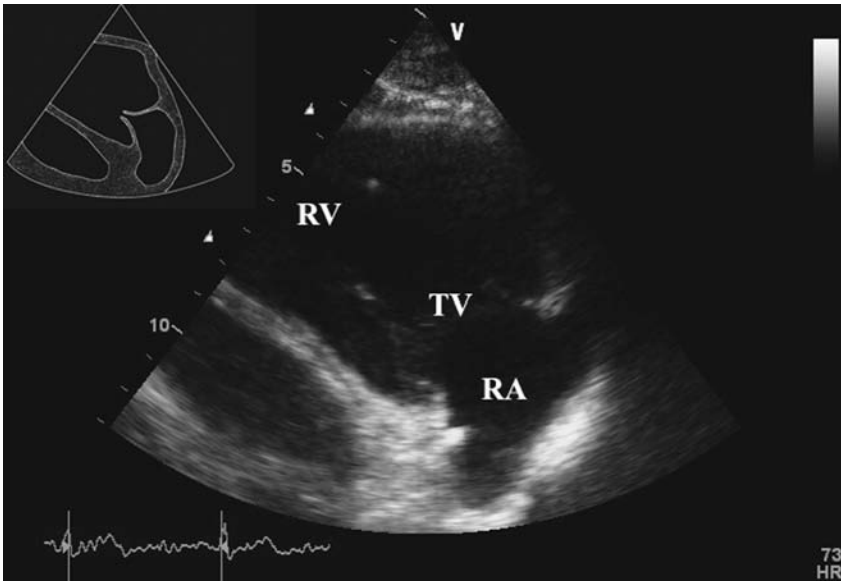


Figure 26 Parasternal LAX view of the RV allows evaluation of the TV for insufficiency or stenosis. *Abbreviations:* LAX, long axis; RV, right ventricle; TV, tricuspid valve.

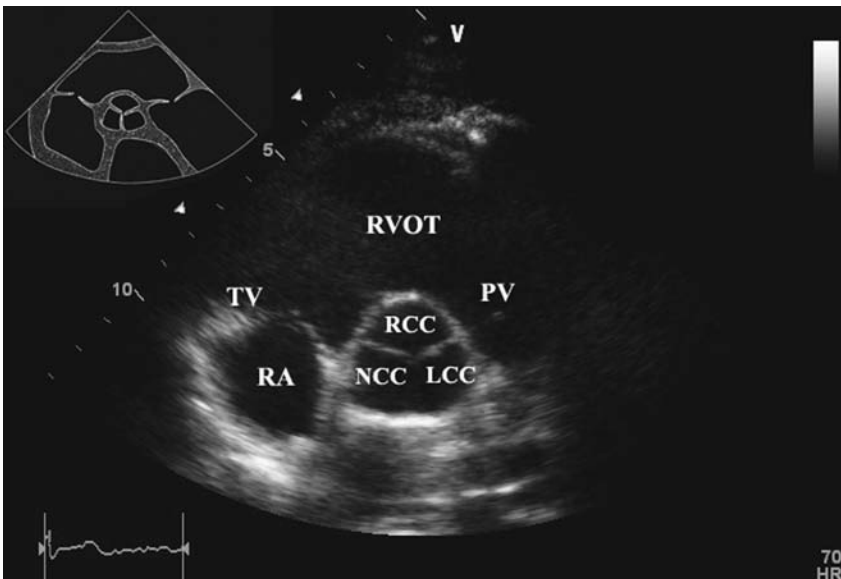


Figure 27 Parasternal SAX view of the RVOT allows clear delineation of the TV, the RVOT, the PV, and the AV. The AV's coronary cusp can be clearly delineated: RCC, LCC, and NCC. *Abbreviations:* SAX, short axis; RVOT, right ventricular outflow tract; TV, tricuspid valve; PV, pulmonic valve; AV, aortic valve; RCC, right coronary cusp; LCC, left coronary cusp, NCC, noncoronary cusp.

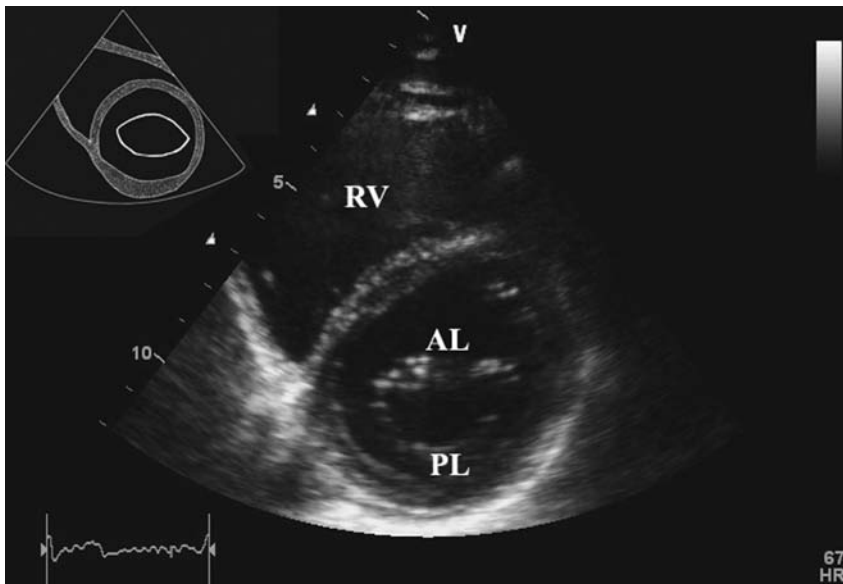


Figure 28 Parasternal SAX view of the MV demonstrates the AL and PL of the MV. *Abbreviations:* SAX, short axis; AL, anterior leaflet; PL, posterior leaflet; ML, mitral valve.

Parasternal Short-Axis View of the Left Ventricle

Further tilting of the transducer inferiorly from the parasternal SAX view of the mitral valve positioning will bring out a SAX view of the left ventricle. This parasternal left ventricular view (Fig. 29) is excellent for evaluating global and regional left ventricular function.

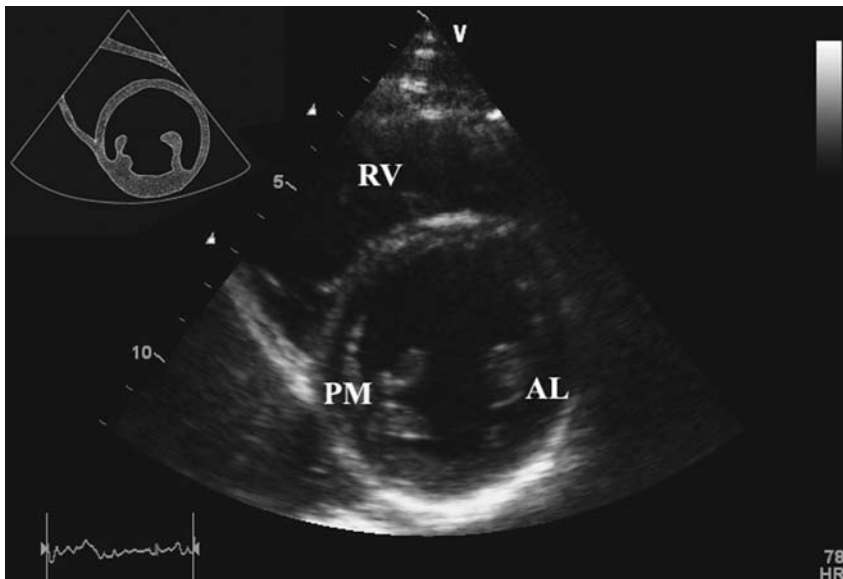


Figure 29 Parasternal SAX view of the LV allows one to easily evaluate global and regional left ventricular function. The anteriolateral and posteriomedial papillary muscles are easily seen. *Abbreviations:* SAX, short axis; LV, left ventricle.

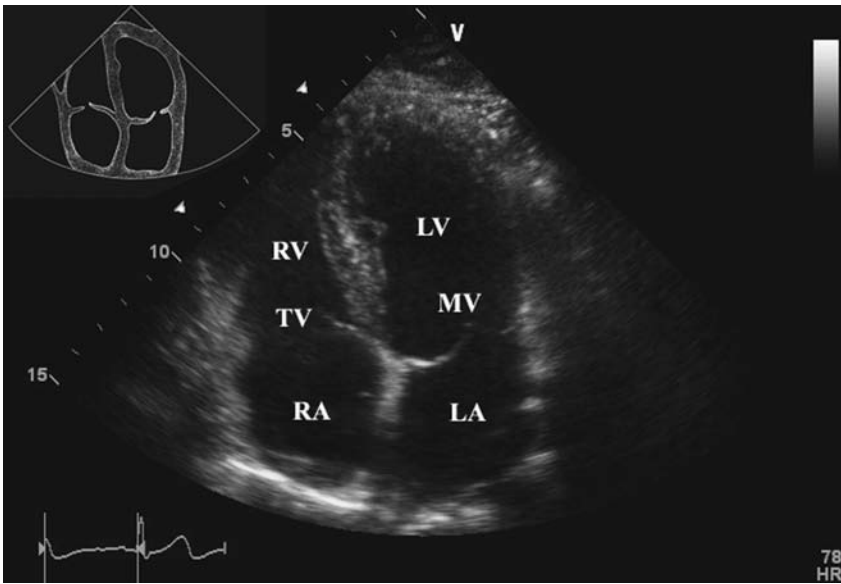


Figure 30 Apical four-chamber view allows evaluation of all four chambers of the heart in LAX. *Abbreviation:* LAX, long axis.

Apical Four-Chamber View

Following evaluation from the parasternal window, the transducer is moved to the apical window. The apical position is determined with the patient in the left lateral decubitus position. The apical impulse is found, and the transducer is placed in that position, with the indentation marker pointing up. The first view obtained is the apical four-chamber view (Fig. 30). In this view, all four chambers of the heart are clearly visualized, with the right ventricle, tricuspid valve, and right atrium seen to the left of the screen and the left ventricle, mitral valve, and left atrium seen to the right of the screen. Angulating the transducer anteriorly will allow the aortic valve and root to be seen in an oblique LAX view. This view is frequently referred to as the apical five-chamber view (Fig. 31).

Apical Two-Chamber View

From the apical four-chamber view, the transducer is rotated counterclockwise to about 60° in order to obtain the apical two-chamber view (Fig. 32) with visualization of the left atrium, mitral valve, and left ventricle. The apical two-chamber view is useful for evaluating the anterior and posterior walls of the left ventricle.

Apical Long-Axis View

By continuing to rotate the transducer from the apical two-chamber view, the apical LAX view is obtained (Fig. 33), which is similar to the parasternal LAX view. The aortic valve, LVOT, and mitral valve are well seen in this view.

Subcostal Four-Chamber View

The subcostal windows are evaluated with the patient supine and the legs occasionally bent in order to relax the abdominal musculature. The subcostal four-chamber view (Fig. 34)

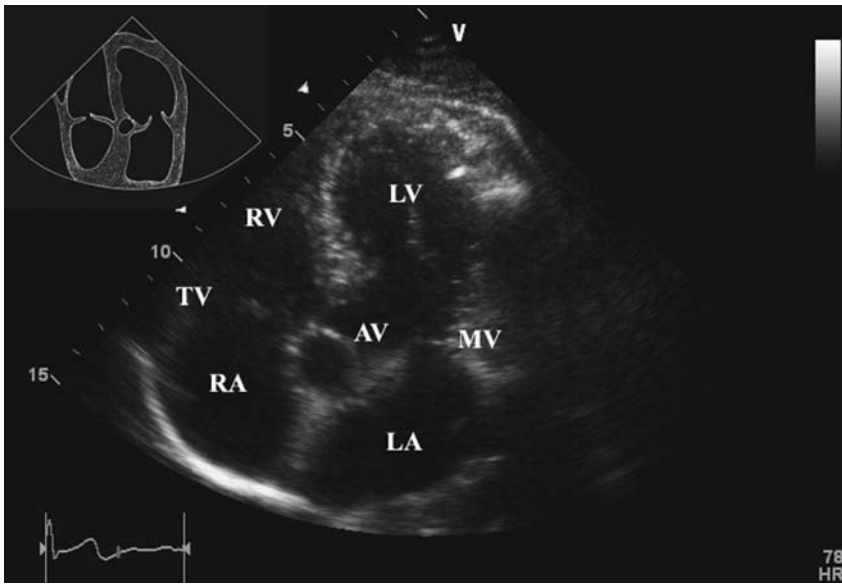


Figure 31 Apical five-chamber view allows evaluation of the AV and LVOT. *Abbreviations:* AV, aortic valve; LVOT, left ventricular outflow tract.

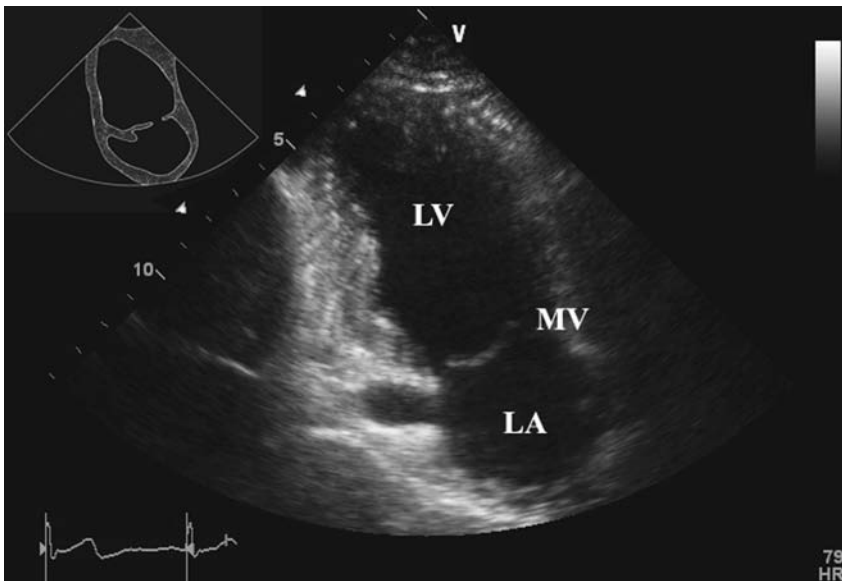


Figure 32 Apical two-chamber view is useful for evaluating the anterior and posterior walls of the LV. *Abbreviation:* LV, left ventricle.

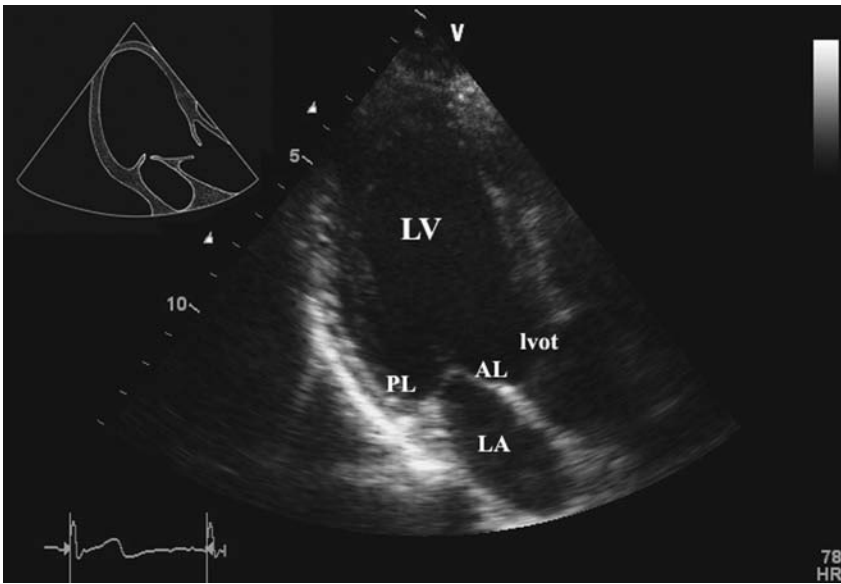


Figure 33 Apical LAX view is similar to the parasternal LAX view and allows further evaluation of the AV and LVOT. *Abbreviations:* LAX, long axis; AV, aortic valve; LVOT, left ventricular outflow tract.

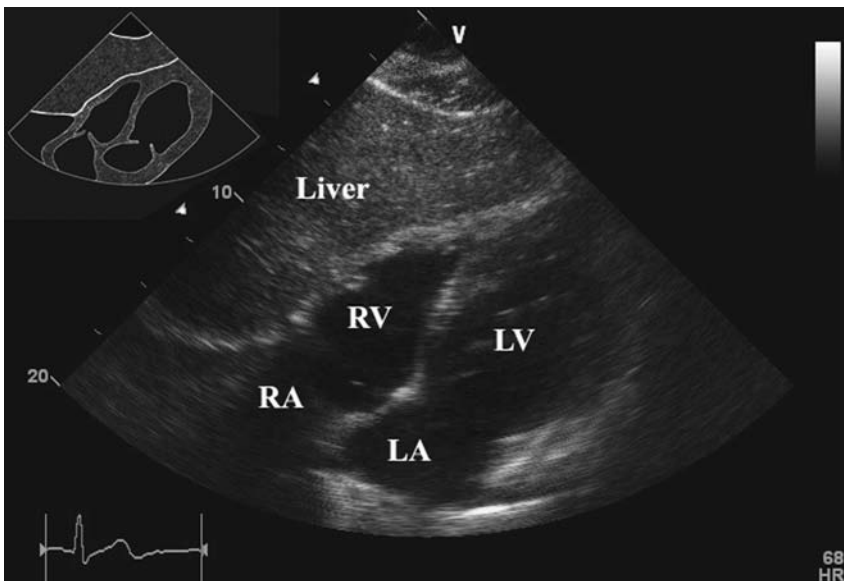


Figure 34 Subcostal four-chamber view allows evaluation of all four chambers of the heart and the interatrial septum.

allows evaluation of all four chambers of the heart and the interatrial septum. A portion of the liver is also seen.

CERTIFICATION

Board Certification in the United States

The U.S. requirements for board certification in perioperative TEE have been developed by the National Board of Echocardiography. Certification requirements include completion of a written examination, medical licensure, and medical board certification, along with specific training in the fields of perioperative care of patients with cardiovascular disease and echocardiography.

The initial requirement is successful completion of the Examination of Special Competence in Perioperative Transesophageal Echocardiography (PTEeXAM). Applicants must be board certified within their medical specialty and hold a current medical license.

Specific training or experience in the perioperative care of surgical patients with cardiovascular disease can be demonstrated via the fellowship pathway or the practice experience pathway. The fellowship pathway requires a minimum of 12 months of clinical fellowship training dedicated to the perioperative care of surgical patients with cardiovascular disease. The practice experience pathway requires 24 months of clinical practice dedicated to the perioperative care of surgical patients with cardiovascular disease. In the two years prior to the application, per year the applicant must have personally delivered care to at least 150 patients with cardiovascular disease.

Specific training in echocardiography must also be demonstrated via a supervised training pathway or a practice experience pathway. The supervised training pathway requires specific training or experience in perioperative TEE. A total of 300 complete perioperative TEE examinations with a wide spectrum of diagnoses are required. At least 150 examinations must be personally performed, interpreted, and documented by the applicant with appropriate supervision. The examinations that are not personally performed by the applicant must be acquired and analyzed in the applicant's training institution. Documentation of compliance with the supervised training pathway must be obtained from the institution and presented to the National Board of Echocardiography. The practice experience pathway can be utilized if training or clinical experience was completed prior to July 1, 2006. In the practice experience pathway, the physician must have performed at least 300 TEE examinations on surgical patients within the four years preceding the application, with no less than 50 exams in any year. This pathway also requires 50 hours of AMA Category I CME training devoted to echocardiography during the time of clinical experience in TEE.

Accreditation in Europe

In Europe, accreditation in adult TEE is run as a service jointly by the European Association of Echocardiography and the European Association of Cardiothoracic Anaesthesiologists. The goal of accreditation is to set a European standard for competency and excellence in TEE. While the European accreditation is designed to test the competency of an individual to be able to interpret and report routine TEE studies unsupervised, the right to perform and report TEE exams will be defined by national laws in each country.

The accreditation process includes a practical and a written component. Enrollment for the accreditation process is through the European Association of Echocardiography.

The written exam can be taken only after acceptance for enrollment and should be attempted within one year of enrollment. The written exam includes a section on theory and a section on echo reporting.

The practical assessment (log book) must be completed within a 24-month period or within 12 months of completing the written exam. Reports from 125 clinical TEE cases performed by the candidate are required. If the candidate holds an accreditation in TTE, only 75 cases are required. A letter from a supervisor is required that documents training, personal performance, and reports of the studies by the candidate and a review of the studies undertaken by the candidate for competence.

Accreditation in Europe is only granted for a period of five years, after which time a reaccreditation process is required that demonstrates continued practice and education in the field of TEE.

CONCLUSION

With a thorough understanding of ultrasound anatomy and practice, any anesthesiologist or critical care physician can become facile in TTE or TEE. The next two chapters will further expand upon the diagnostic capacity of echocardiography. Since the majority of readers will be utilizing TEE over TTE, these chapters will be presented from the transesophageal perspective.

SUGGESTED READINGS

1. Perrino AC, Reeves ST, eds. *A Practical Approach to Transesophageal Echocardiography*. Philadelphia: Lippincott Williams & Wilkins, 2003.
2. Oh JK, Seward JB, Tajik AJ, eds. *The Echo Manual*. 2nd ed. Philadelphia: Lippincott Williams & Wilkins, 1999.
3. Shanewise J, Cheung A, Aronson S, et al. ASE/SCA guidelines for performing a comprehensive intraoperative multiplane transesophageal echocardiography examination: recommendations of the American Society of Echocardiography Council for Intraoperative Echocardiography and Society of Cardiovascular Anesthesiologists Task Force for Certification in Perioperative Transesophageal Echocardiography. *J Am Soc Echocardiogr* 1999; 12:884–898.
4. Savage RM, Aronson S, eds. *Comprehensive Textbook of Intraoperative Transesophageal Echocardiography*. Philadelphia: Lippincott Williams & Wilkins, 2005.

8

Perioperative Transesophageal Echocardiography of the Heart Valves

David A. Zvara, Daniel D. Amitie, Jason J. Baggett, and Christopher E. Beck

Section on Cardiothoracic Anesthesiology, The Wake Forest University School of Medicine, Winston-Salem, North Carolina, U.S.A.

INTRODUCTION

The proximity of the transesophageal echocardiography (TEE) probe in the esophagus allows far superior imaging of the heart valves, in general, than transthoracic echocardiography (TTE). Hence, the echocardiographer can make easy assessments of both structure and function of all four heart valves. In this chapter, perioperative TEE of the heart valves is discussed. For each valve, there is a discussion of normal anatomy, standard TEE images, valvular stenosis, and regurgitation.

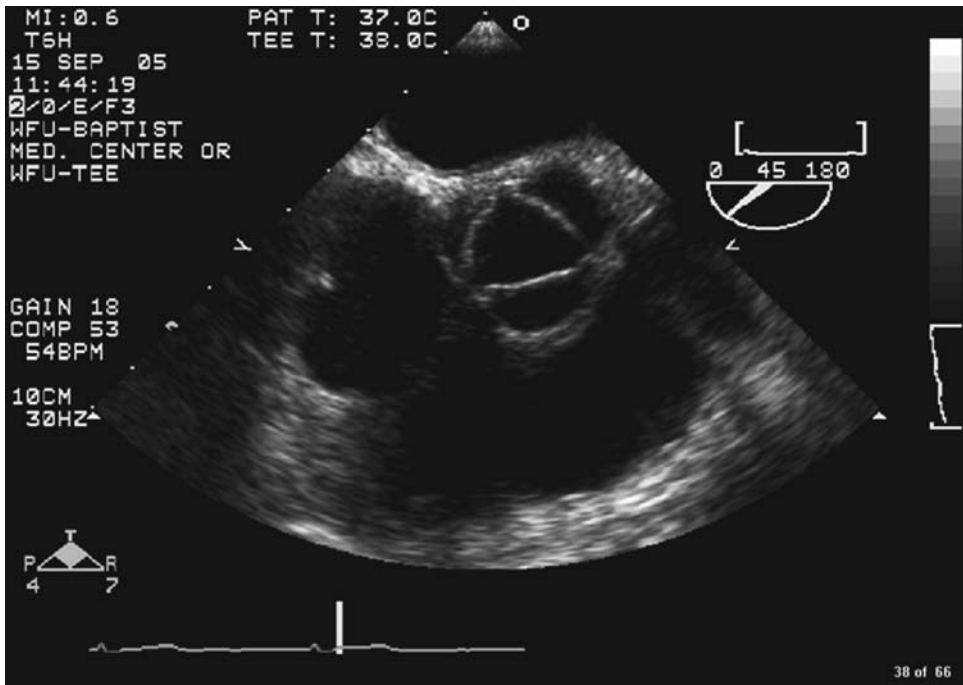
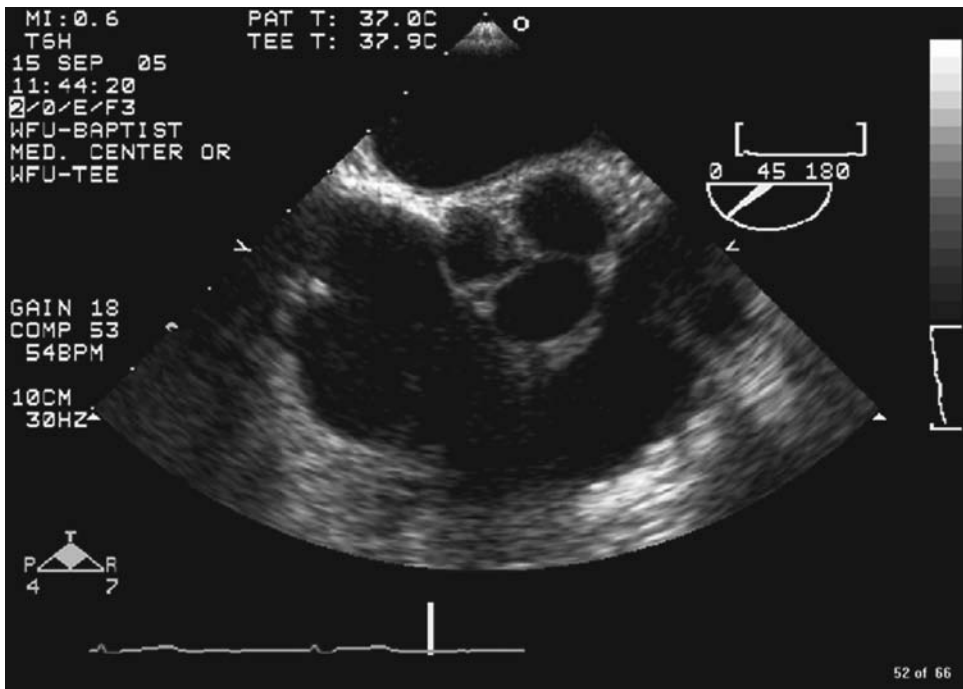
THE AORTIC VALVE

Unobstructed imaging planes allow complete assessment of the aortic valve by two-dimensional (2D) and Doppler echocardiography. Perioperative TEE is often vital in confirming a diagnosis, defining aortic valvular hemodynamics, and guiding surgical and perioperative care.

Aortic Valve Anatomy

The aortic valve consists of three semilunar valves named according to their relationship with the appropriate coronary arteries: the right coronary cusp, the left coronary cusp, and the noncoronary cusp. At the center of the free edge of each cusp is a tiny, elevated nodule commonly referred to as the nodule of Arantius. All three nodules of Arantius coapt at the center of a normal, closed aortic valve (Figs. 1 and 2). The lunulas are the free edges of the cusps and span from the nodule of Arantius to the wall of the aorta (1). When the lunulas of the cusps are apposed and the nodules of Arantius are coapted in a normal aortic valve, the valve is completely closed.

Figure 3 demonstrates normal subvalvular, valvular, and ascending aortic anatomy in the midesophageal (ME) aortic valve long-axis (LAX) view. In this image, the left



Figures 1 (above) and 2 (below) The ME aortic valve SAX image demonstrates the three cusps of the aortic valve closed (Figure 1) in diastole, and open in systole (Figure 2). Note the resemblance of the closed aortic valve to the peace or Mercedes-Benz symbol. The left coronary cusp is located at 2 o'clock, the right coronary cusp is located at 6 o'clock, and the noncoronary cusp is located at 10 o'clock. Planimetry of the open aortic valve will yield the AVA. *Abbreviations:* ME, midesophageal; SAX, short axis; AVA, aortic valve area.

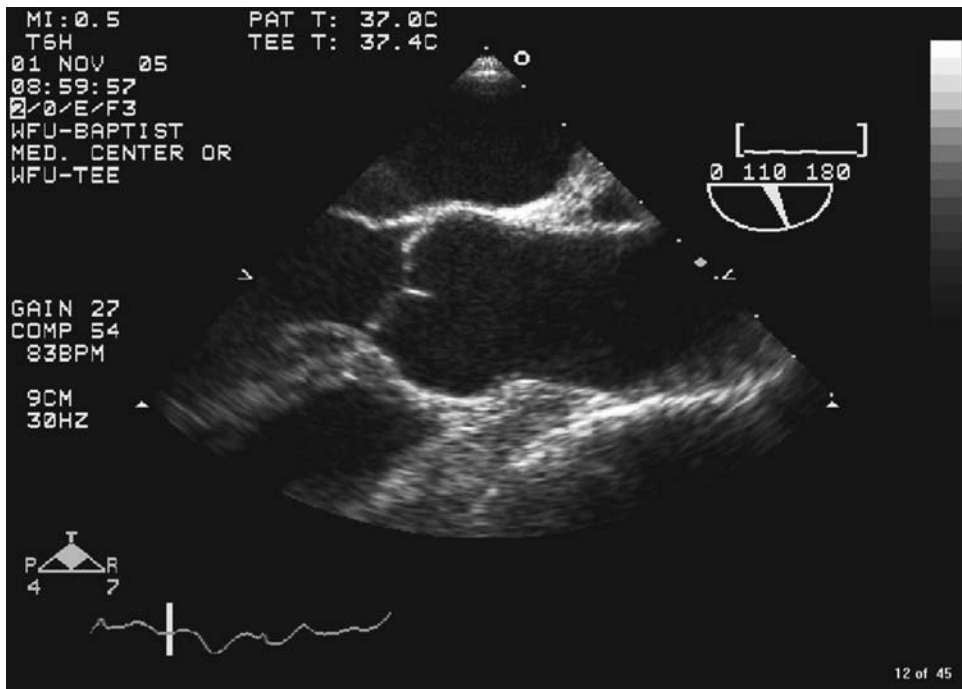


Figure 3 The ME aortic valve LAX image identifies the LVOT, the closed aortic valve, the aortic valve annulus, sinuses of Valsalva, the sinotubular junction, and the proximal ascending aorta. *Abbreviations:* ME, midesophageal; LAX, long axis; LVOT, left ventricular outflow tract.

ventricular outflow tract (LVOT), aortic valve annulus, sinuses of Valsalva, sinotubular junction, and proximal ascending aorta are well visualized. Measurements of these structures are part of a complete examination and are integral in determining annular dilatation and aortic aneurysm pathology. Aortic regurgitation can be quantified in this view. The aortic valve complex, including the junction of the aortic valve with the ventricular septum and the anterior mitral valve leaflet, is easily visualized in this imaging plane (2).

Standard TEE Views

There are six key TEE images relevant to the evaluation of the aortic valve. In a standard examination, all images should be obtained. The sonographer, however, must realize that this may not always be possible. In aneurysmal aortic malformations, for example, the anatomy is frequently distorted, altering the usual appearance or location of the anatomic structures. In any given patient, the echocardiographer may have to employ atypical windows in order to obtain the desired information. In a routine examination, however, the following images typically provide the basis of a complete examination of the aortic valve.

Midesophageal Four-Chamber View

After orally inserting the TEE probe, first confirm that the multiplane angle is 0° and then gently advance the probe until the ME four-chamber view appears. In order to maximize the image, it is sometimes necessary to manipulate the TEE probe and adjust the multiplane angle between 0° to 20° . Once the image is optimized, the left atrium, left ventricle, right atrium, right ventricle, intra-atrial wall, intraventricular wall, lateral

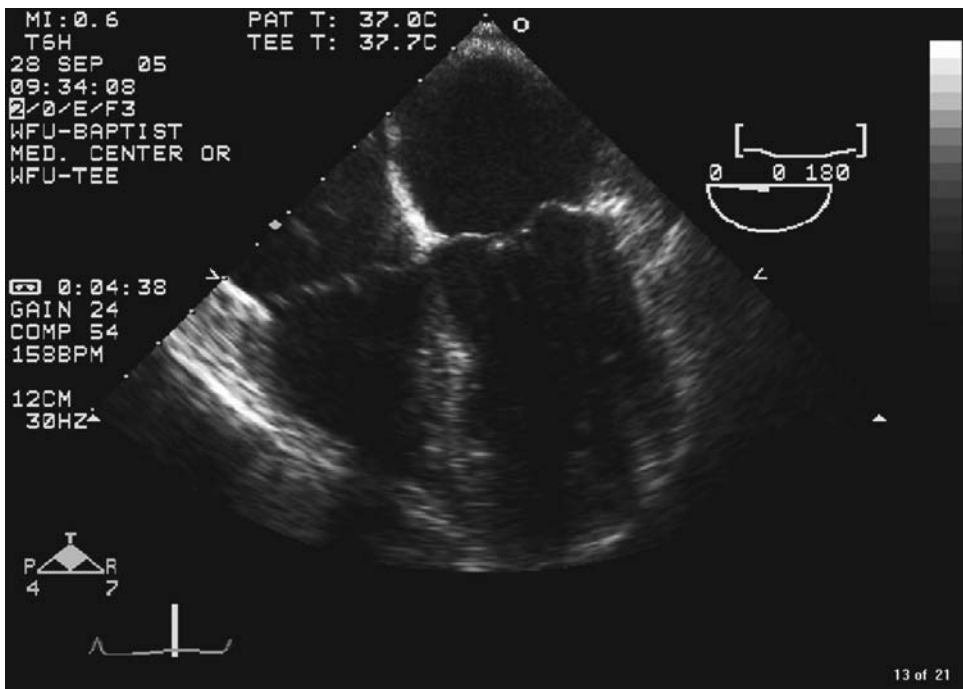


Figure 4 The ME four-chamber image demonstrates the right atrium, right ventricle, left atrium, left ventricle, tricuspid valve, and mitral valve. *Abbreviation:* ME, midesophageal.

ventricular wall, tricuspid valve, and mitral valve can be identified (Fig. 4). Although the aortic valve is not visualized with this image, this view is valuable because the effects of aortic valve disease on the left-heart cardiac chamber size, function, and ventricular wall thickness can be examined. By withdrawing, or gently retroflexing the TEE probe, the five-chamber view is visible, allowing assessment of the left ventricular (LV) septal wall thickness. Again, such information is important in grading aortic regurgitation and flow abnormalities in the LVOT (i.e., as seen with hypertrophic obstructive cardiomyopathy).

Midesophageal Aortic Valve Short-Axis View

From the ME four-chamber view, withdraw the TEE probe until the leaflets of the aortic valve can be visualized. Next, change the multiplane angle from 0° to 40° to 60° and visualize the aortic valve on the short axis (SAX) (Fig. 1). The aortic valve, left atrium, right atrium, and intra-atrial septum are easily identified. In some individuals, it is possible to identify the right ventricle, pulmonic valve, tricuspid valve, and right ventricular inflow and outflow tract in this image plane. In a normal aortic valve, the three cusps can be readily identified. The left main coronary artery and the right coronary artery are sometimes observed. Many structural components of the aortic valve, including orifice size (by planimetry), leaflet mobility, vegetations, and abscesses, can be visualized here. Congenital bicuspid aortic valves are relatively common and readily identified in this image plane (Fig. 5). When a bicuspid valve is noted, comprehensive measurements of the sinotubular junction and ascending aorta are critical to rule out an associated aneurysm. Color Doppler in this imaging plane can demonstrate a regurgitant jet, allowing both an assessment of the relative magnitude of jet size and the location of the jet origin (Fig. 6).

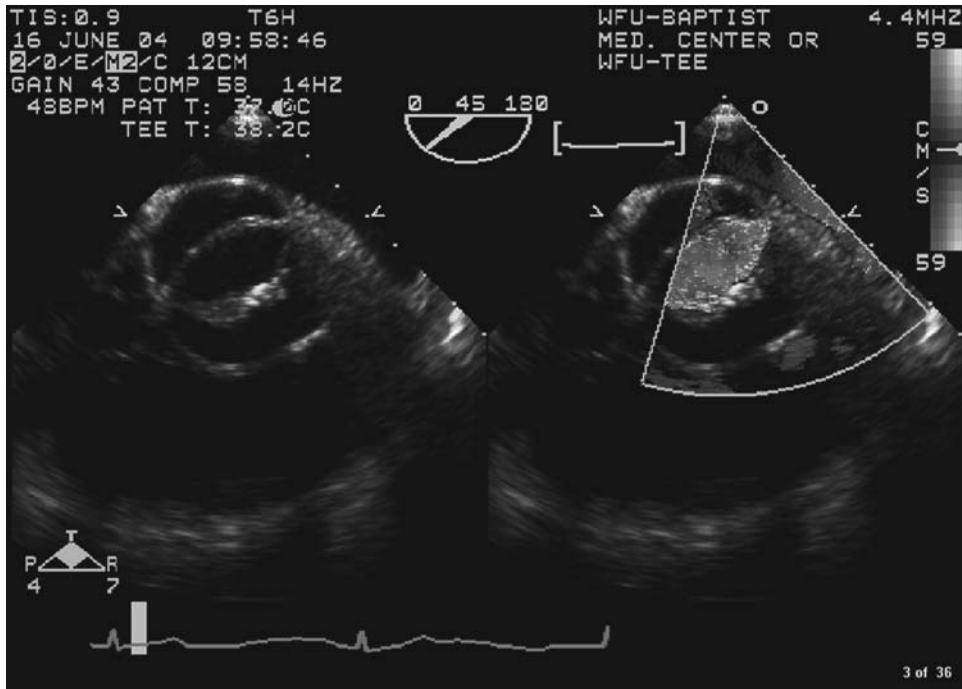


Figure 5 The color compare view of the ME aortic valve SAX image demonstrates the open bicuspid valve in the left frame and the blood flow across the bicuspid valve during systole in the right frame. *Abbreviations:* ME, midesophageal; SAX, short axis.

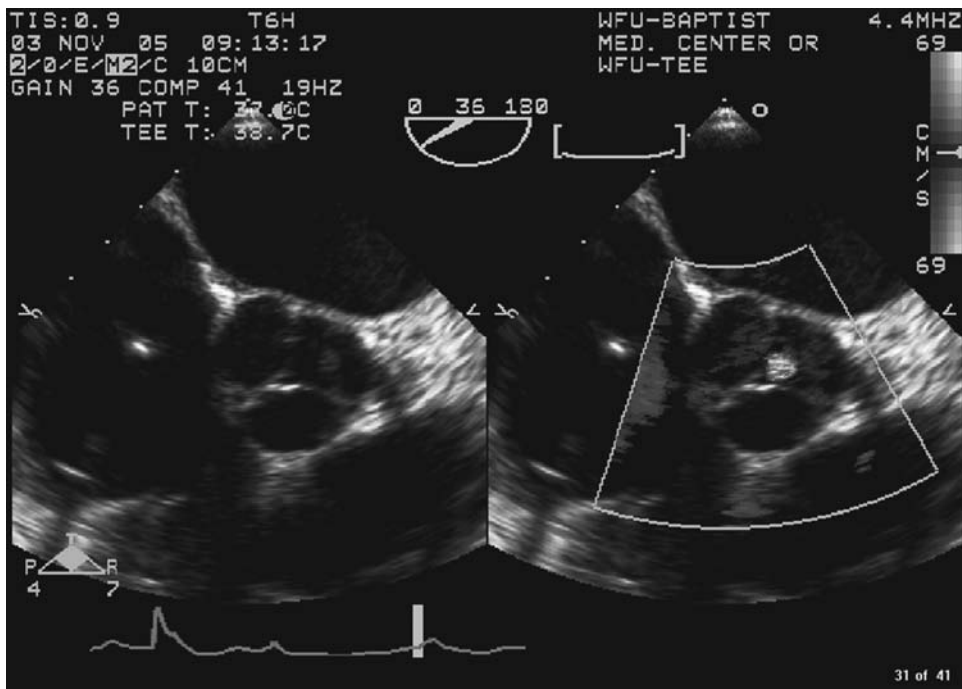


Figure 6 The color compare view of the ME aortic valve SAX image demonstrates the aortic valve at end diastole. The color on the right frame demonstrates the central jet of aortic regurgitation in this patient. *Abbreviations:* ME, midesophageal; SAX, short axis.

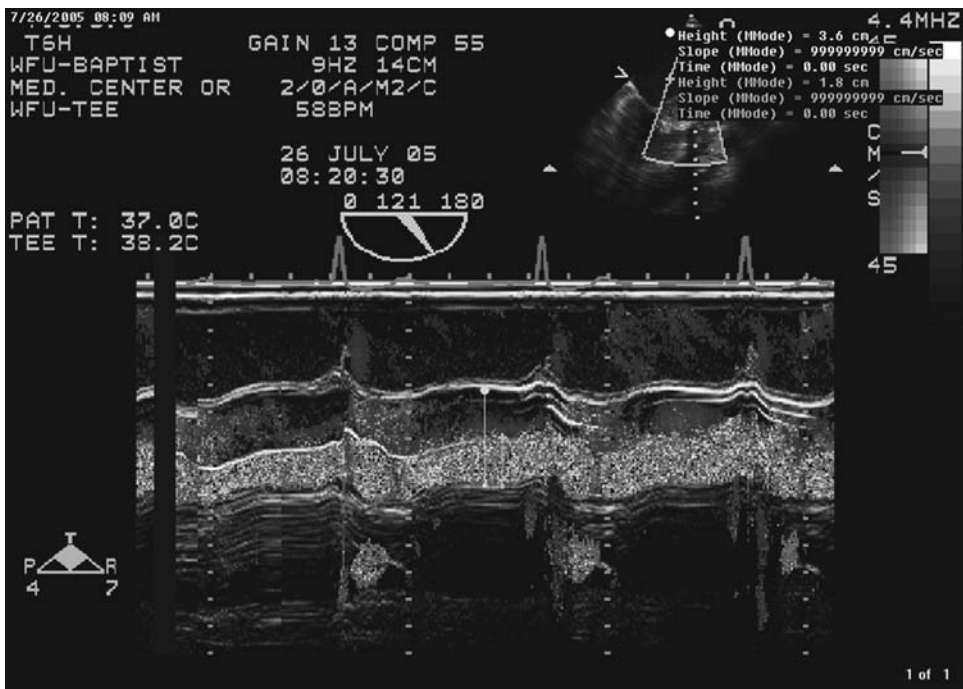


Figure 7 By using the color M-mode across the LVOT in the ME aortic valve LAX image, one can measure the aortic regurgitant jet height and compare it to the LVOT height. In this image the aortic regurgitant jet height is 1.8 cm and the LVOT height is 3.6 cm. Thus, the ratio is 50% and classifies the aortic regurgitation as moderate. *Abbreviations:* LVOT, left ventricular outflow tract; ME, midesophageal; LAX, long axis.

Midesophageal Aortic Valve Long-Axis View

After completing the ME aortic valve SAX view, rotate the multiplane angle approximately 90° and visualize the aortic valve in the LAX plane (Fig. 3). Structures of interest include the LVOT (measured 1 cm proximal to the aortic valve), ascending aorta (measured 1 cm distal to the aortic valve), aortic valve, annulus, sinus of Valsalva, sinotubular junction, and proximal ascending aorta. Color Doppler M-mode proximal to the aortic valve can be used to quantify aortic regurgitant flow relative to the size of the LVOT (Fig. 7), thereby allowing a qualitative grading of aortic regurgitation.

Upper-Esophageal Aortic Arch Long-Axis View

This view allows the echocardiographer to examine the direction of blood flow during the cardiac cycle with pulse-wave Doppler. It is very useful to detect reversal of flow during diastole commonly seen with aortic regurgitation. From the ME four-chamber view, rotate the probe to the left until the aorta is identified, then gradually withdraw the probe until the aortic arch is visible in the LAX view at 0°. Next, examine the blood flow in the aortic arch with pulse-wave Doppler. If holodiastolic reversal of blood flow is present, then this is an indication of severe aortic regurgitation. This information is primarily for confirmation of aortic regurgitation rather than diagnosis because other views of the aortic valve are superior. Many times, this view is difficult to obtain with TEE.

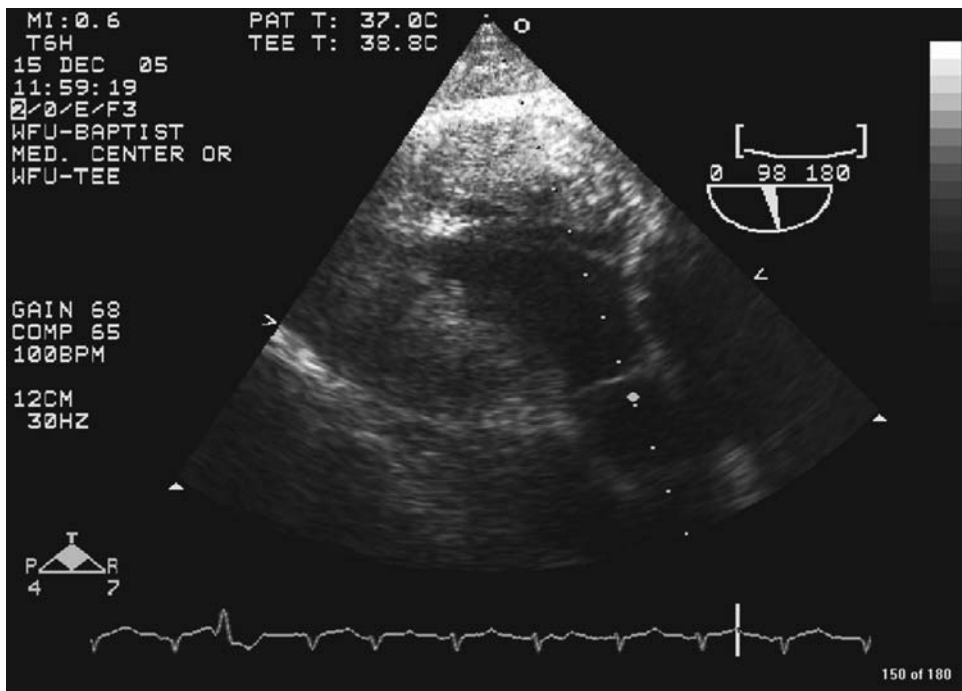


Figure 8 The TG LAX image demonstrates the left ventricle, the LVOT, and the aortic valve. This is important for aligning the Doppler beam parallel to the aortic valve and measure the velocities in the LVOT and the aortic valve. *Abbreviations:* TG, transgastric; LAX, long axis; LVOT, left ventricular outflow tract.

Transgastric Long-Axis View

From the standard ME four-chamber view, advance the probe until the transgastric (TG) midpapillary SAX view is seen, then rotate the multiplane angle from 0° to approximately 120° . From this view, the aortic valve, LVOT, and left ventricle can be identified (Fig. 8). The aortic valve may not be as clearly defined as with the previous views, but the alignment of the valve and the ultrasound beam are nearly parallel allowing valvular velocities to be measured with greater accuracy. It is possible to verify the aortic valve in this view by using the color Doppler mode to examine the blood flow and visualize flow direction. Once the view is located, pulse-wave Doppler ultrasound can be used to measure the velocity of the LVOT, and continuous-wave Doppler ultrasound can be used to measure the aortic jet velocity.

Deep Transgastric Long-Axis View

The deep TG LAX view is considered among the most challenging views of any of the standard 20 cross-sectional images to obtain because of the amount of manipulation to position the TEE probe. Starting from the TG midpapillary SAX view, advance and anteflex the probe until the transducer is adjacent to the apex of the heart. Color Doppler provides additional information on the extent and severity of aortic regurgitation (Fig. 9). Moreover, the velocities of the LVOT and the aortic valve, with same type of evaluation used for the TG LAX view, can be determined (Fig. 10).

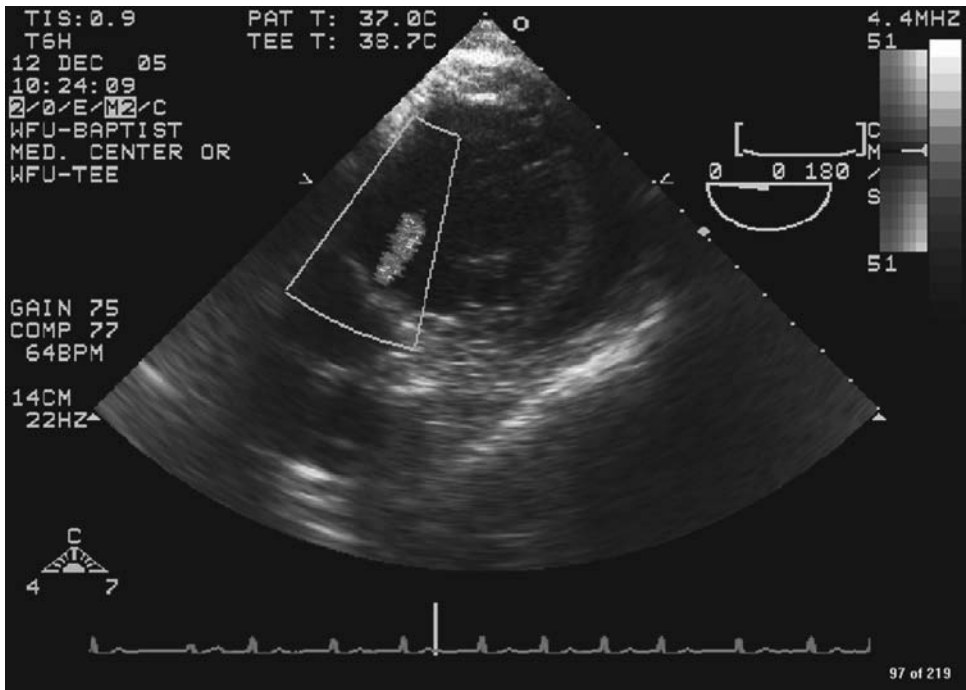


Figure 9 The deep TG image demonstrates a small aortic regurgitation jet coming back into the left ventricle across the aortic valve. *Abbreviation:* TG, transgastric.

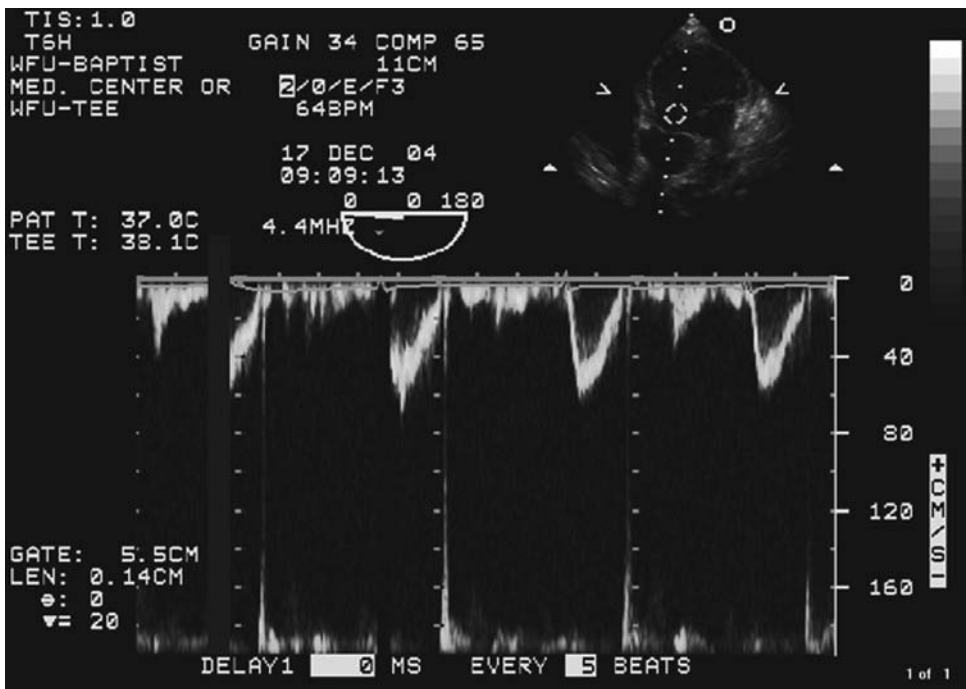


Figure 10 The deep TG image demonstrates the closed aortic valve in the left window, and the pulse-wave Doppler is properly aligned across the aortic valve to measure the velocity of blood flow in the LVOT in the right window. *Abbreviations:* TG, transgastric; LVOT, left ventricular outflow tract.

Aortic Regurgitation

TEE is essential when evaluating aortic regurgitation because it can identify the presence of regurgitation, quantify severity, determine the etiology, and examine the secondary effects on other heart structures (i.e., left ventricle, mitral valve). In general, the etiologies of aortic regurgitation are classified into two major groups, leaflet abnormalities and aortic root abnormalities. Leaflet abnormalities include congenital bicuspid valves; calcific, rheumatic, or myxomatous valve disease; endocarditis; and nonbacterial thrombotic endocarditis. Historically, rheumatic valve disease has been the leading cause of aortic regurgitation; however, aortic root abnormalities are now a more common cause. Aortic root abnormalities include annular dilatation, hypertensive aortic root dilation, cystic medial necrosis, Marfan syndrome, and aortic dissection (3). In addition to knowing the etiology, it is very important to understand the techniques used to evaluate and grade the severity of aortic regurgitation with TEE (Table 1).

Two reliable techniques to assess aortic regurgitation are color Doppler and color M-mode in the ME aortic valve LAX view. In either technique, the sonographer measures the maximum diameter of the aortic regurgitant jet relative to the LVOT during diastole (Fig. 7). These values are then compared as a ratio (aortic regurgitant jet diameter/LVOT diameter) and used to define the severity of aortic regurgitation as follows: trivial (1–24%), mild (25–46%), moderate (47–64%), and severe (>65%) (4). Color Doppler can estimate the severity of aortic regurgitation by showing the depth of penetration of the regurgitant jet into the left ventricle during diastole (Fig. 11). Aortic regurgitation severity can be quantified by the depth of regurgitant jet in relation to the following LV structures:

Table 1 Aortic Regurgitation Table

| Measurement | Echo view | Trivial (0–1+) | Mild (1+–2+) | Moderate (2+–3+) | Severe (3+–4+) |
|-------------------------------------|---|-------------------|-----------------------------------|-----------------------------------|--|
| AI area/ LVOT area | ME aortic valve SAX | <4% | 4–24% | 25–59% | >60% |
| AI jet height/ LVOT diameter | ME aortic valve LAX | 1–24% | 25–46% | 47–64% | >65% |
| Jet depth | ME aortic valve LAX | LVOT | Mid-anterior mitral leaflet | Tip anterior mitral leaflet | Papillary muscle head |
| Vena contracta | ME aortic valve LAX, ME aortic valve SAX | | | | Width >6 mm or area >7.5 mm ² |
| Aorta diastolic flow reversal | UE aortic arch LAX | | | | Holodiastolic retrograde flow in descending aorta |
| PHT | TG LAX, deep TG LAX | | >500 ms | 200–500 ms | <200 ms |
| AR jet decay slope | TG LAX, deep TG LAX | | | >2 m/sec | >3 m/sec |

Abbreviations: AI, aortic insufficiency; ME, midesophageal; LAX, long axis; SAX, short axis; UE, upper esophageal; TG, transgastric; PHT, pressure half-time; AR, aortic regurgitation.

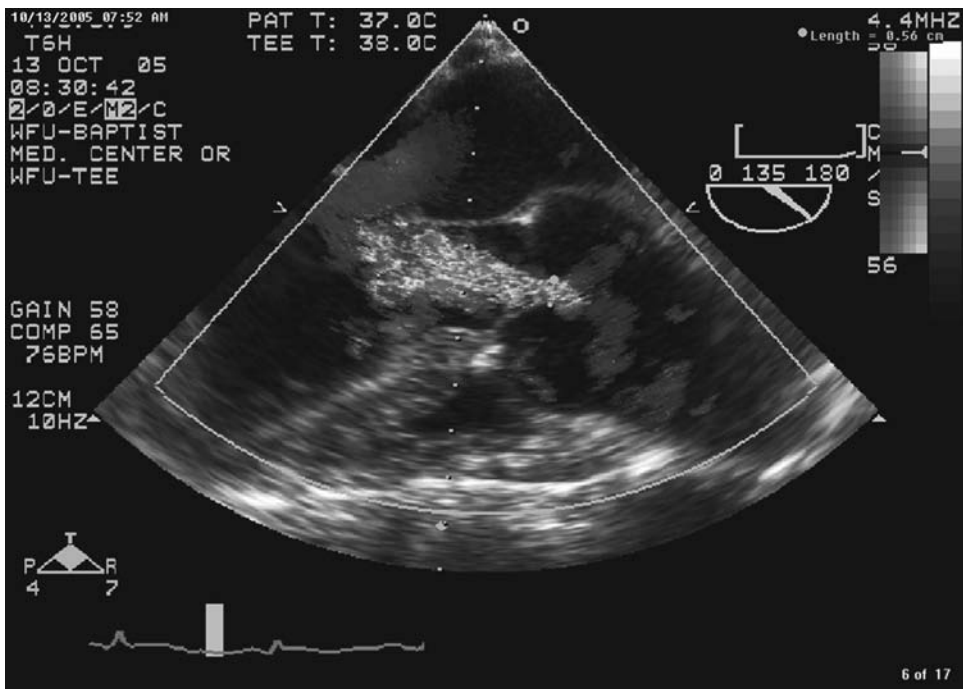


Figure 11 The plume of the aortic regurgitant jet stretches to the tip of the anterior mitral valve leaflet. This is consistent with moderate aortic regurgitation. The vena contracta is measured at the width of the aortic regurgitant jet at its origination in the aortic valve. The vena contracta in this image is measured at 0.56 cm.

the LVOT (trivial), the mid-anterior leaflet (mild), the tip of the anterior mitral leaflet (moderate), or the papillary muscle head (severe) (5).

Color Doppler can evaluate aortic regurgitation in the ME aortic valve SAX view. This method compares the ratio of the regurgitant jet area to the LVOT area during diastole (Fig. 12). The key factor with this measurement is the proper location of the image plane proximal to the aortic valve itself and identification of the maximum regurgitant jet diameter. It is imperative to manipulate the TEE probe to maximize the regurgitant jet area. Comparing the ratio of the regurgitant jet area to the LVOT area, the severity of aortic regurgitation is as follows: trivial (<4%), mild (4–24%), moderate (25–59%), and severe ($\geq 60\%$) (5).

The aortic regurgitant jet vena contracta can be measured and used as an assessment of aortic regurgitant severity. This measurement is obtained by measuring the width of the color Doppler flow at the aperture of the aortic valve in either the ME aortic valve SAX or the ME aortic valve LAX view (Fig. 11). If either the width is greater than 6 mm or the area is greater than 7.5 mm^2 , then the aortic regurgitation is severe (6).

Another means to examine aortic regurgitation and note its presence is by examining the aortic blood flow throughout systole and diastole with the aortic arch view. In a normal patient, blood flow in the aorta moves forward during systole and there is only a slight reversal of blood flow during diastole secondary to aortic recoil and filling of the branches of the aorta. However, if aortic regurgitation is severe, then there is a pathologic aortic retrograde blood flow observed throughout diastole because of the blood falling back through the regurgitant valve and into the left ventricle. By examining the aorta and its flow pattern, any evidence of hodiastolic retrograde blood flow suggests severe

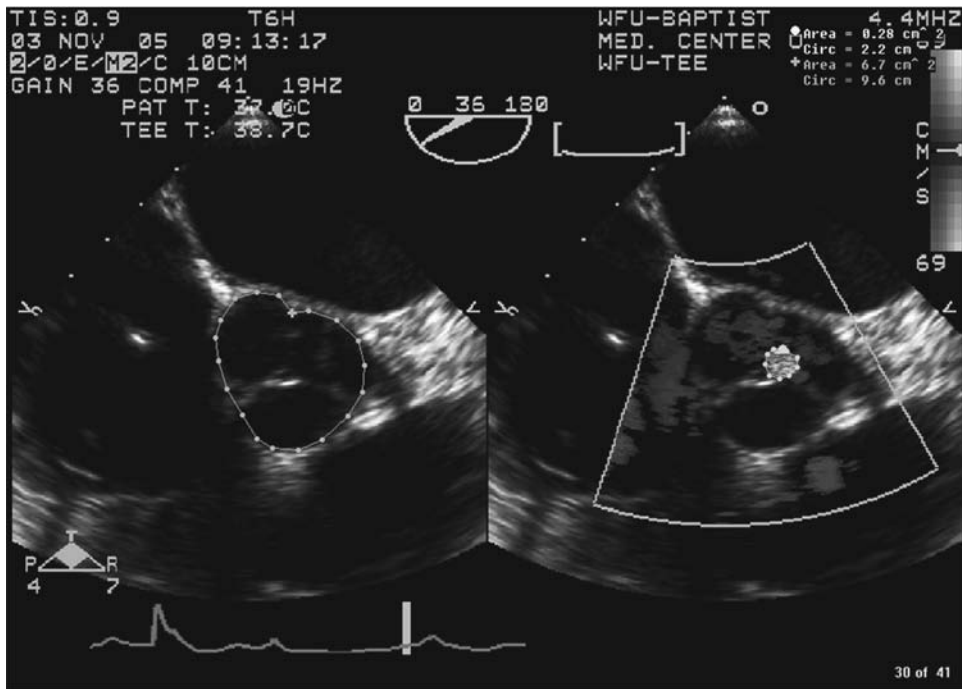


Figure 12 The area of the LVOT is 6.7 cm², and the area of the aortic regurgitation is 0.28 cm². The ratio of the areas is 4%. This indicates a small regurgitant orifice and may be consistent with mild aortic regurgitation. Other measures of aortic regurgitation are required to fully assess the functional impact of any regurgitant lesion. *Abbreviation:* LVOT, left ventricular outflow tract.

aortic regurgitation (7). This is, perhaps, the only view of the aortic valvular structure that is better visualized with TTE than with TEE.

In elderly patients, the aortic valve is sometimes poorly visualized secondary to shadowing from calcific degeneration of the aortic valve. In patients with previous prosthetic valve replacement, or other infiltrative or degenerative conditions, the aortic valvular images may be similarly compromised.

Continuous-wave Doppler flow in the deep TG LAX view is helpful when quantifying aortic valve regurgitation. The primary advantage is the alignment of the continuous wave being parallel to the blood flow through the aortic valve (Fig. 10). However, the limitation of this approach is the difficulty in obtaining a high-quality image to measure the slope of the aortic regurgitant jet and the pressure half-time (PHT). On the basis of the Bernoulli principle, the velocities of the aortic regurgitant jet decay and the PHT are related to the pressure difference between the left ventricle and the aorta. In severe regurgitation, the pressure gradients equalize much quicker, thereby reducing the PHT and accelerating the regurgitant jet decay slope. In order to accurately measure the slope of the aortic regurgitant jet and the PHT, first verify the aortic valve by examining the blood flow with color Doppler flow in the deep TG LAX view. After confirming the aortic valve and its blood flow, it is very important to align the continuous Doppler wave parallel to the aortic valve to obtain the most accurate measurements. Next, measure the slope of the aortic regurgitant jet decay. If it is 2 or 3 m/sec, then it suggests moderate or severe aortic regurgitation, respectively. Secondly, determine the PHT by measuring the time it takes for the maximum aortic transvalvular pressure to drop to half (Fig. 13).

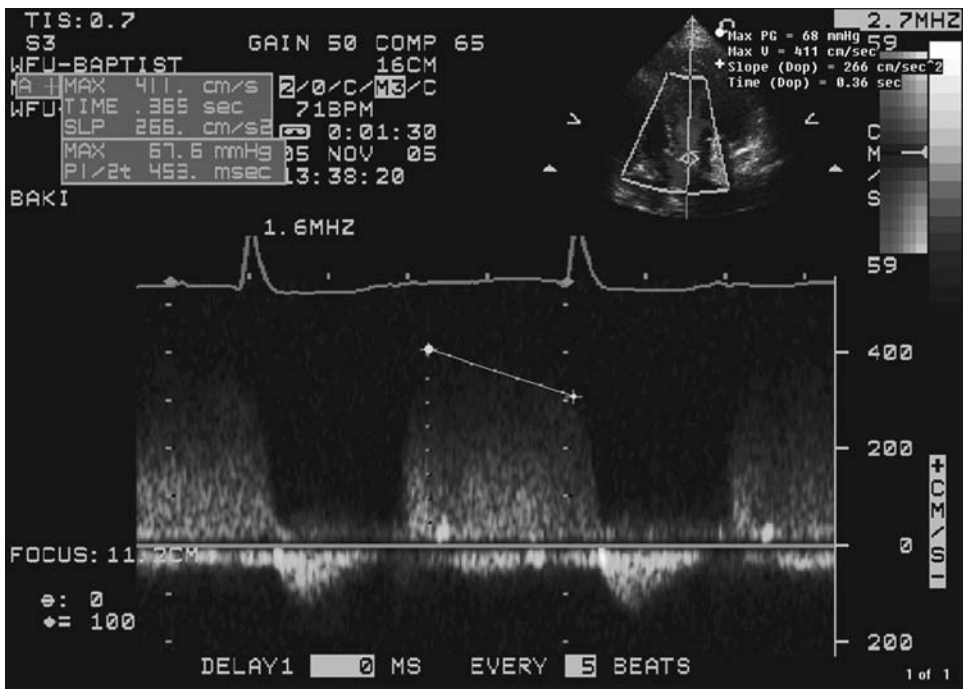


Figure 13 The deep TG image with a continuous-wave Doppler across the aortic valve measures the amount of aortic regurgitation across the aortic valve. The slope of the aortic regurgitation is 2.66 m/sec. The PHT is 453 milliseconds. Both measurements are consistent with moderate aortic regurgitation. *Abbreviations:* TG, transgastric; PHT, pressure half-time.

The severity of aortic regurgitation based on the PHT is greater than 500 milliseconds (mild), 200 to 500 milliseconds (moderate), or less than 200 milliseconds (severe) (5).

Aortic Stenosis

Aortic stenosis is divided into three broad categories: valvular, subvalvular, and supra-valvular. Valvular stenosis may be classified as either congenital or acquired. Acquired stenosis may be due to a variety of causes including commissural fusion with calcification, rheumatic or other infective etiologies. The bicuspid aortic valve is the most common congenital abnormality, and approximately 1% of the U.S. population is born with this disorder (8). Supra-valvular aortic stenosis is a congenital lesion, whereas subvalvular aortic stenosis is usually caused by fibromuscular or muscular obstruction to flow (hypertrophic obstructive cardiomyopathy). The TEE criteria for grading aortic stenosis are summarized in Table 2.

One of the easiest and most reliable methods to measure aortic stenosis is by planimetry in the 2D mode. The three leaflets of the aortic valve are readily identified by the aortic valve SAX view, and the TEE trace function allows the area of stenosis to be measured during systole (Fig. 14). Normal valve area is 2.5 to 3.5 cm². The severity of aortic stenosis is divided into three categories by valve area: mild (1.5–1.0 cm²), moderate (1.0–0.8 cm²), and severe (<0.8 cm²) (9). Limits of this technique include an inability to evaluate the stenotic valve in the correct plane and thereby underestimate the true area of valvular stenosis. Therefore, it is imperative to examine the valve until the narrowest area of opening is identifiable and the stenotic area is reproducible with multiple measurements.

Table 2 Aortic Stenosis

| Measurement | Echo | Normal | Mild | Moderate | Severe |
|----------------------------|---------------------|-------------------------|-------------------------|-------------------------|----------------------|
| AVA | ME aortic valve SAX | 2.6–3.5 cm ² | 1.0–1.5 cm ² | 0.8–1.0 cm ² | <0.8 cm ² |
| Peak velocity | TG LAX, deep TG LAX | 1.0–1.7 m/sec | | | >4.5 m/sec |
| Mean gradient | TG LAX, deep TG LAX | | <20 mmHg | 20–50 mmHg | >50 mmHg |
| Peak pressure gradient | TG LAX, deep TG LAX | | <36 mmHg | >50 mmHg | >80 mmHg |
| VTI LVOT/ VTI aortic valve | TG LAX, deep TG LAX | | | | <0.25 |

Abbreviations: AVA, aortic valve area; ME, midesophageal; LAX, long axis; SAX, short axis; TG, transgastric; VTI, velocity time integral; LVOT, left ventricular outflow tract.

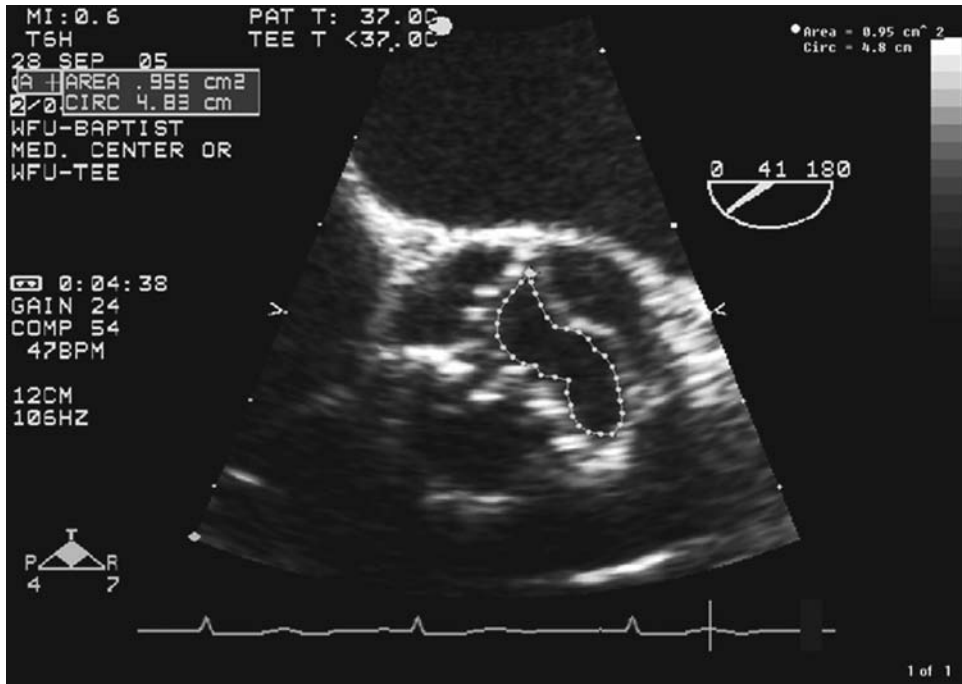


Figure 14 The ME aortic valve SAX image demonstrates the planimetry valve area of the aortic valve. The area of the traced AVA is 0.95 cm². *Abbreviations:* ME, midesophageal; SAX, short axis; AVA, aortic valve area.

As with aortic regurgitation, continuous-wave Doppler in the deep TG LAX view provides information on stenosis. From the continuous-wave Doppler profile, the peak aortic velocity can be determined by measuring the maximum height of the aortic wave envelope and the mean aortic velocity can be determined by tracing the aortic wave envelope (Fig. 15). If the peak aortic velocity is greater than 4.5 m/sec, then the aortic stenosis is severe (10). Either the peak or the mean aortic velocity can be substituted into the simplified Bernoulli equation, which is used to calculate the transvalvular pressure

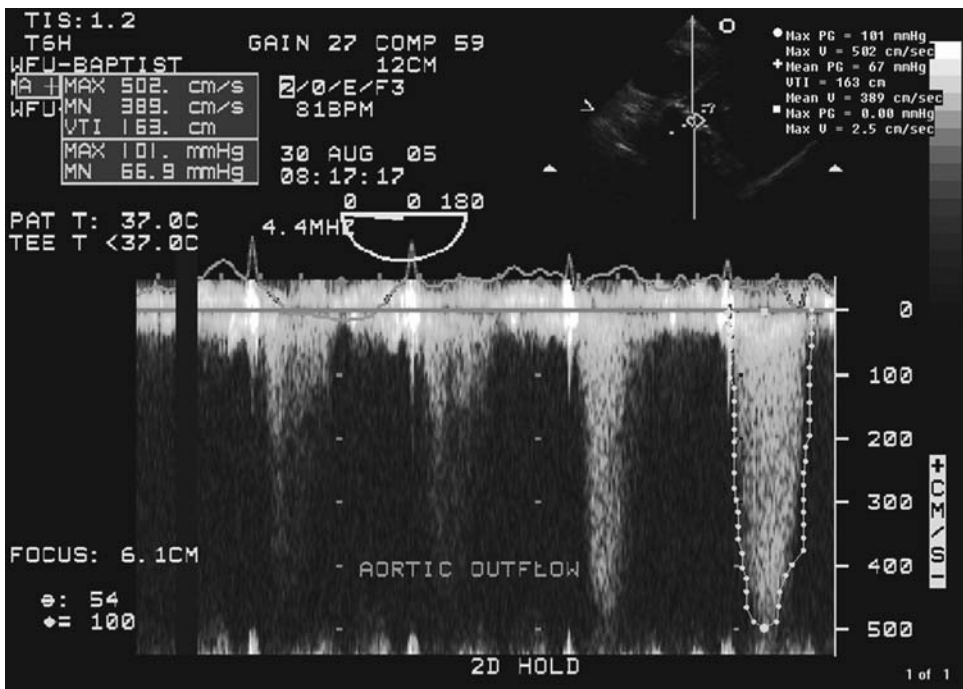


Figure 15 Placing the continuous-wave Doppler across the aortic valve in the deep TG image, it is possible to measure the maximum velocity and the peak and mean gradients across the aortic valve. Note how the secondary control is directing the cursor at an angle to the continuous-wave Doppler to align the beam parallel to the direction of blood flow across the aortic valve. The maximum velocity is 5.02 m/sec, and the peak and mean pressure gradients are 101 mmHg and 66.9 mmHg, respectively, indicating a severely stenotic valve. *Abbreviation:* TG, transgastric.

gradient and is another method to quantify the amount of aortic stenosis. The simplified Bernoulli equation for the peak gradient is as follows:

$$\text{Peak gradient (mmHg)} = 4(\text{Aortic peak velocity})^2$$

Based on the peak aortic gradient value, the severity of aortic stenosis is graded as mild (<36 mmHg), moderate (>50 mmHg), or severe (>80 mmHg). The simplified Bernoulli equation for the mean gradient is either of the following:

$$\text{Mean gradient (mmHg)} = 4(\text{Mean velocity})^2$$

$$\text{Mean gradient (mmHg)} = 2.4(\text{Maximum velocity})^2$$

The value of the mean aortic velocity grades the severity of aortic stenosis as mild (<20 mmHg), moderate (20–50 mmHg), or severe (>50 mmHg) (10). This technique is sometimes difficult as the deep TG LAX view can be difficult to acquire even for an experienced echocardiographer.

Finally, the continuity equation can be used to calculate the aortic valve area (AVA). The continuity equation assumes that a stroke volume of blood in one chamber of the heart is the same as a stroke volume of blood in the immediate next chamber of the heart. This stroke volume can be determined by multiplying the stroke distance as represented by the velocity time integral (VTI) by the cross-sectional area of the blood flow cylinder. Accordingly, the VTI multiplied by the area at point A must equal the VTI

multiplied by the area at point B (stroke volume A = stroke volume B). For the aortic valve, the LVOT diameter and VTI is used to compare and determine the area of the aortic valve. First, the LVOT diameter is measured by the aortic valve LAX view and its area is calculated. Next, the pulse-wave Doppler in the deep TG view is used to determine the VTI of blood flow at the LVOT. Lastly, the continuous-wave Doppler at the aortic valve determines the VTI of blood flow through the aortic valve. All of this information is applied with the following continuity equation to determine the AVA:

$$\begin{aligned} (\text{Volume of blood})_{\text{Aortic valve}} &= (\text{Volume of blood})_{\text{LVOT}} \\ (\text{Volume of blood})_{\text{Aortic valve}} &= \text{AVA} \times \text{VTI}_{\text{Aortic valve}} \\ (\text{Volume of blood})_{\text{LVOT}} &= \text{Area}_{\text{LVOT}} \times \text{VTI}_{\text{LVOT}} \end{aligned}$$

Therefore,

$$\text{AVA} \times \text{VTI}_{\text{Aortic valve}} = \text{Area}_{\text{LVOT}} \times \text{VTI}_{\text{LVOT}}$$

Finally,

$$\text{AVA} = \frac{\text{Area}_{\text{LVOT}} \times \text{VTI}_{\text{LVOT}}}{\text{VTI}_{\text{Aortic valve}}}$$

THE MITRAL VALVE

Anatomy

The mitral valve acquired its name in the sixteenth century because of its resemblance to a bishop’s miter. The valve is bicuspid with an anterior and posterior leaflet. The anterior leaflet is the larger of the two leaflets, accounting for two-thirds of the surface area of the valve. The anterior leaflet base-to-coaptation distance is longer than that of the posterior leaflet. The posterior leaflet wraps around the anterior leaflet, accounting for only one-third of the valve’s surface area and two-thirds of the annular circumference. The mitral annulus is a fibrous ring surrounding the mitral valve. The anterior leaflet portion of the annulus is part of the heart’s fibrous skeleton. This skeleton also has a common attachment to the left coronary and noncoronary cusps of the aortic valve. The coaptation points of the anterior and posterior leaflets at the annulus are called the anterolateral and posteromedial commissures. The leaflets themselves are attached to the anterolateral and posteromedial papillary muscles via the chordae tendineae. During ventricular systole, the contraction of the papillary muscles prevent mitral leaflet prolapse. The Carpentier classification of the mitral valve has been adopted by the American Society of Echocardiography and the Society of Cardiovascular Anesthesiologists (11,12). This classification divides the three scallops of the posterior leaflet into P1, P2, and P3. The anterior leaflet is similarly divided into the three segments A1, A2, and A3, which oppose the corresponding scallops of the posterior valve. The coaptation of A1/P1 at the annulus forms the anterolateral commissure. The coaptation of A3/P3 at the annulus forms the posteromedial commissure.

Standard TEE Views

Localization of mitral valve pathology is often important information for the surgeon. For example, in evaluating mitral regurgitation (MR), identification of prolapse of the posterior leaflet and annular dilation may lead to mitral valve repair rather than replacement. A systematic approach to interrogation of the mitral valve consists of seven views, which allow visualization of all six segments of the mitral valve.

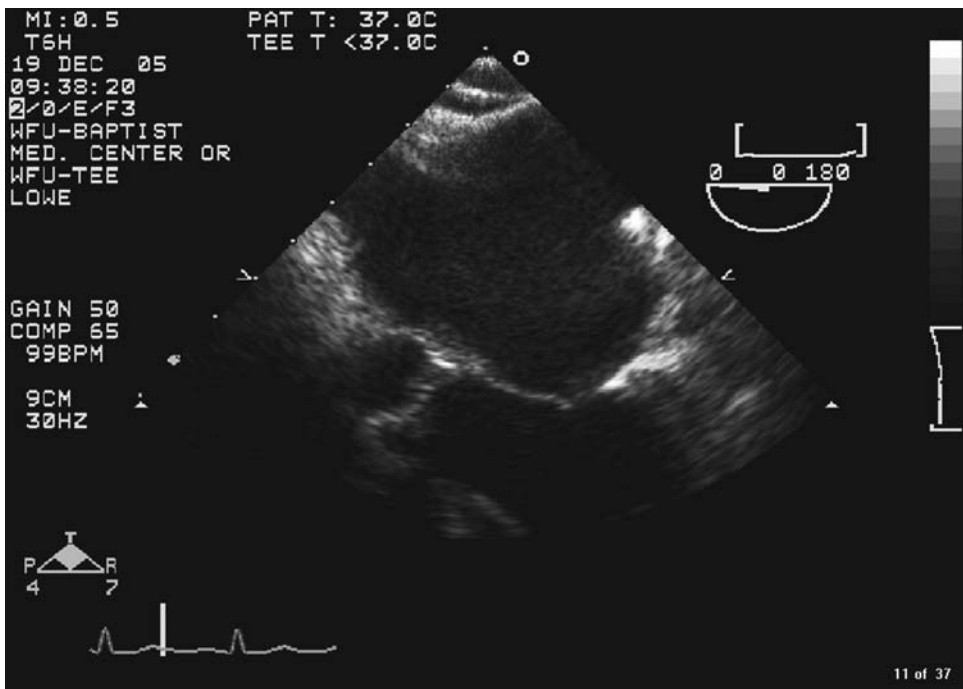


Figure 16 ME five-chamber view demonstrating the mitral valve. *Abbreviation:* ME, midesophageal.

Midesophageal Five-Chamber View

The probe is in the midesophagus with an imaging plane approximately 0° to 10° . This view allows visualization of the anterior segments of both the anterior and posterior leaflets of the mitral valve (Fig. 16).

Midesophageal Four-Chamber View

From the ME five-chamber view, this next image can be visualized by either pushing the echo probe in deeper or slightly retroflexing the probe. Here the posterior segments of both the anterior and posterior leaflets of the mitral valve are seen (Fig. 17).

Midesophageal Commissural View—Mid

The ME commissural view (mid) is viewed at an imaging plane of 45° to 70° . From the left to the right of the screen, usually segments P3-A2-P1 are seen (Fig. 18).

Midesophageal Commissural View—Right

Rotating the echo probe to the right yields the ME commissural view (right). This view brings more of the anterior leaflet into view: segments P3-A3-A2 (Fig. 19).

Midesophageal Commissural View—Left

Rotating left with the probe now reveals the ME commissural view (left). This image brings more of the posterior leaflet into view: segments P3-P2-P1 (Fig. 20).

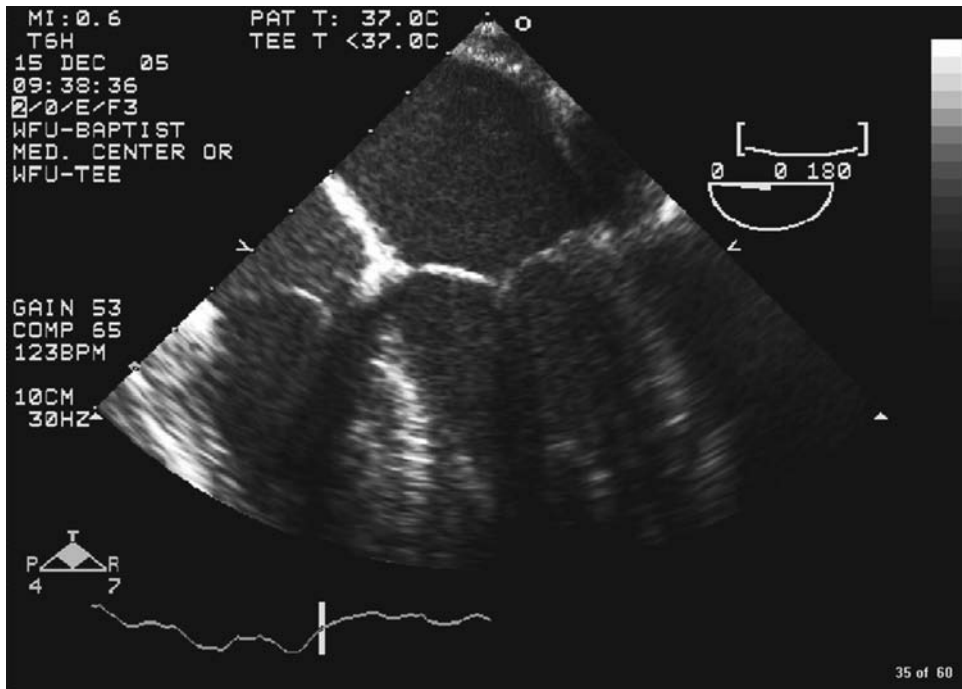


Figure 17 ME four-chamber view focusing on the mitral valve. *Abbreviation:* ME, midesophageal.

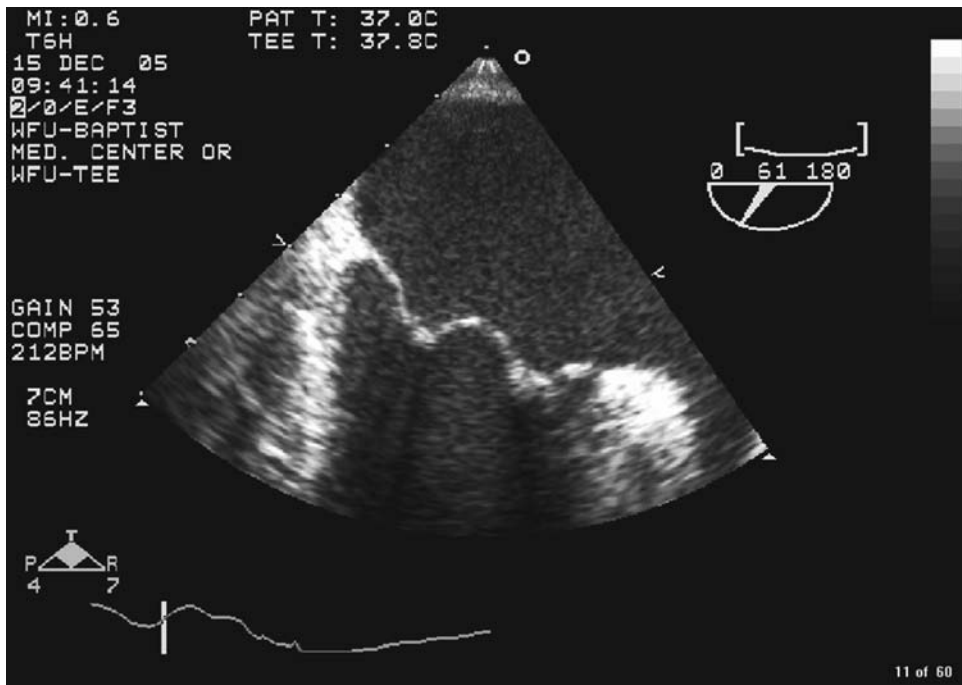


Figure 18 ME commissural view—mid (P3-A2-P1). *Abbreviation:* ME, midesophageal.

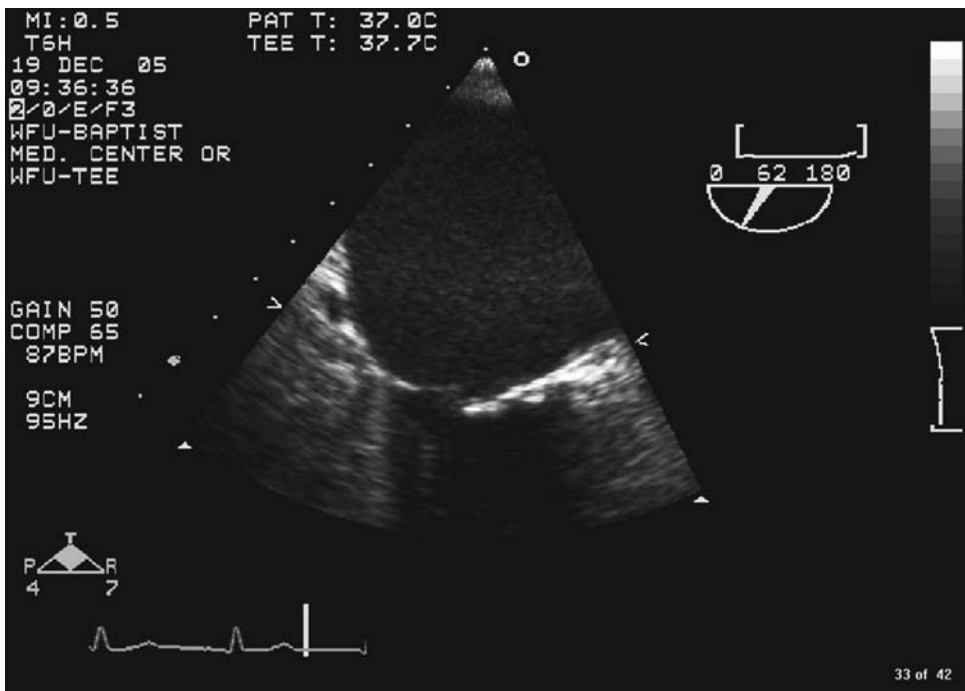


Figure 19 ME commissural view—right (P3-A3-A2). *Abbreviation:* ME, midesophageal.

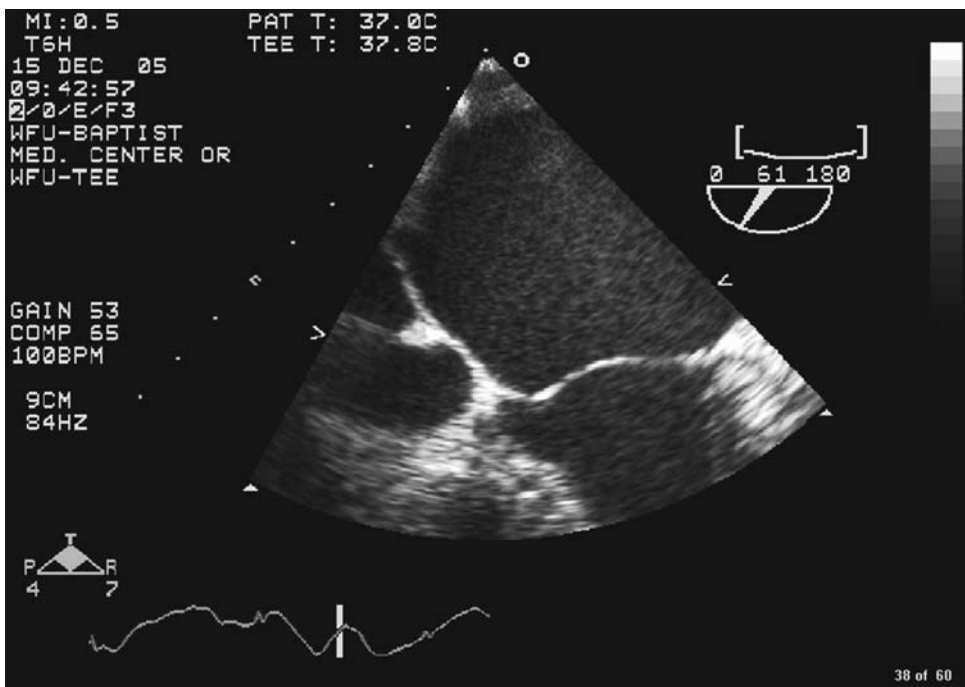


Figure 20 ME commissural view—left (P3-P2-P1). *Abbreviation:* ME, midesophageal.

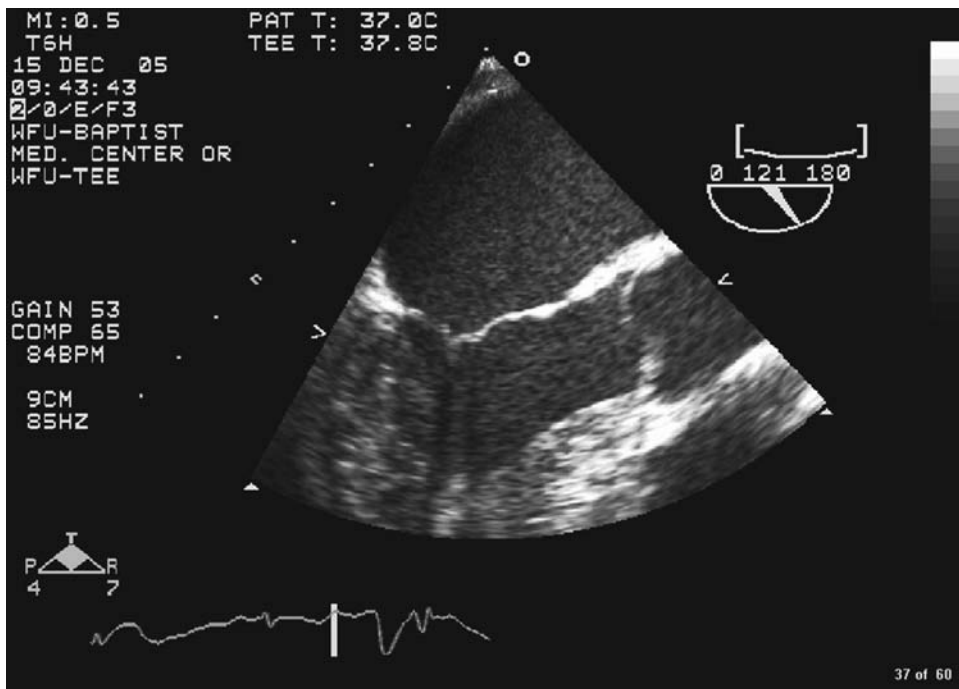


Figure 21 ME aortic valve LAX view highlighting the mitral valve (P2-A2). *Abbreviations:* ME, midesophageal; LAX, long axis.

Midesophageal Long-Axis View

The ME LAX view can be obtained by rotating the imaging plane to 110° to 150°, usually revealing a P2-A2 segment cross section (Fig. 21).

Transgastric Basal Short-Axis View

The seventh view is the TG basal SAX view (the “fish-mouth” view). Using color flow Doppler, this view is very helpful in determining the origin of the regurgitant jet as the whole valve can be seen *en face* (Fig. 22).

Mitral Stenosis

The normal mitral valve orifice area is 4 to 6 cm². Patients are typically symptomatic when the valve area is less than 1.5 cm². A valve area of less than 1.0 cm² is often associated with symptoms at rest. The major cause of mitral stenosis in adult patients is rheumatic heart disease. This disease process is characterized by commissural fusion with doming of the valve leaflets. Leaflet tip thickening and chordae tendineae thickening, fusion, and calcification result in restricted leaflet motion. Other uncommon causes of mitral stenosis include mitral annular calcification, active infective endocarditis (vegetation obstructing the mitral orifice), tumor (i.e., left atrial myxoma), systemic lupus erythematosus (verrucous vegetations), carcinoid, congenital defects, Fabry’s disease, and Whipple’s disease.

As the mitral valve area (MVA) progressively narrows, an increase in the transvalvular pressure gradient leads to increased left atrial (LA) pressures and LA

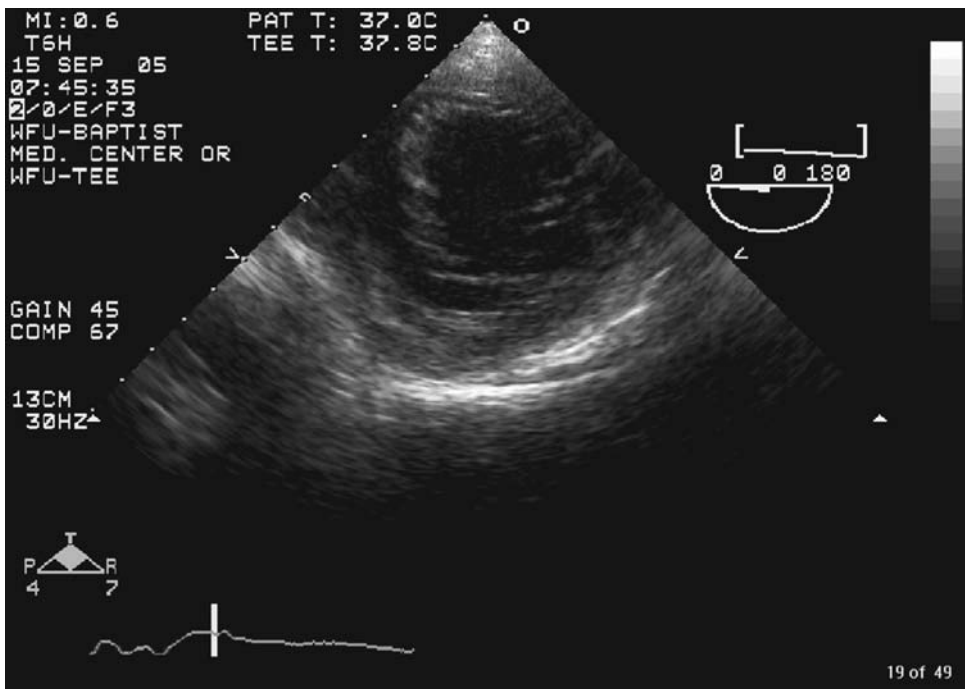


Figure 22 TG basal SAX view. The mitral valve is seen during diastole *en face*. Abbreviations: TG, transgastric; SAX, short axis.

distention. Increased LA pressures can lead to pulmonary hypertension with right ventricular dysfunction and tricuspid regurgitation. These are secondary signs seen on TEE in a patient with mitral stenosis.

Two-dimensional echocardiography of the stenotic mitral valve includes evaluation of the degree of thickening and fibrosis of the mitral valve leaflets, leaflet motion, the presence and severity of mitral annular calcification, and the extent of subvalvular structural involvement of the disease process. Because of commissural fusion, only the mid-portion of the mitral valve exhibits free diastolic motion. The restricted leaflet motion is often seen on 2D echo as a diastolic “doming” or “hockey stick” deformity of the anterior leaflet (Fig. 23).

The MVA can be estimated directly with planimetry in the TG basal SAX view (“fish-mouth” view) (Fig. 22). The stenotic mitral valve leaflets are often calcified and seen easily. Maximal valve opening is observed in early diastole. Scanning the valve superiorly to inferiorly (from annulus to valve orifice), the smallest orifice area in early diastole can be traced to determine the valve area. If the gain is set too high, the image may become oversaturated with a resulting underestimation of the valve area. Conversely, if the gain is set too low, the tips of the leaflets may not be accurately visualized with resulting overestimation of the MVA.

Use of the mitral valve PHT is probably the easiest and most commonly used method for calculation of the MVA. Assuming the rate of decline of the pressure gradient across the mitral valve is determined by the MVA, the smaller the MVA, the slower the rate of decline of the transmitral pressure gradient. The PHT is defined as the time interval (in milliseconds) required for the transmitral gradient to decline from its maximum pressure (in early diastole) to half of its maximum value. Transmitral pressure gradients

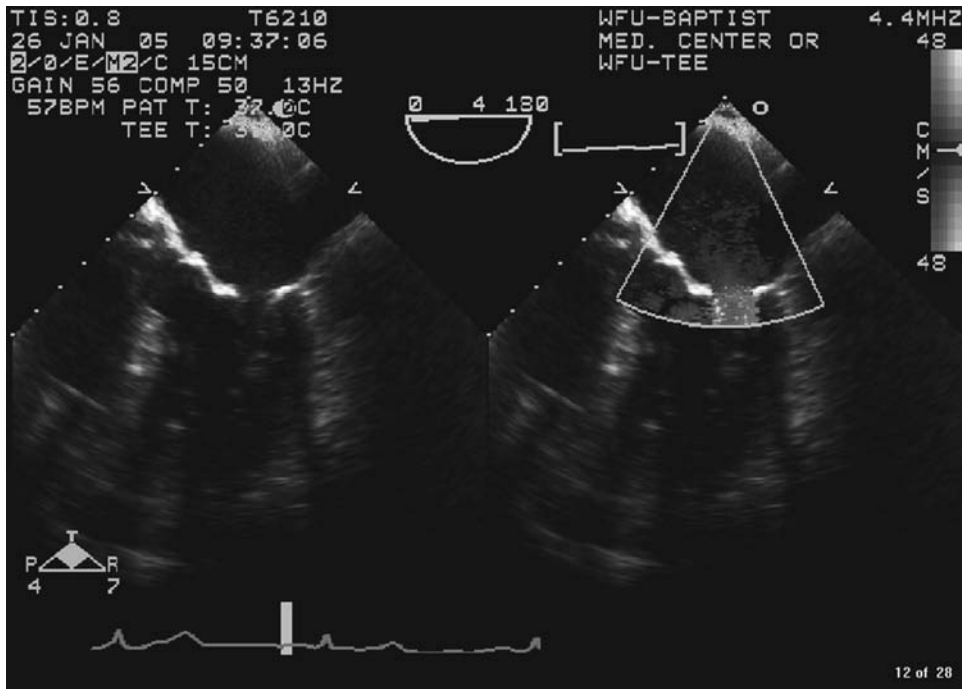


Figure 23 “Hockey stick deformity” of the anterior mitral valve seen in mitral stenosis.

can be obtained by applying the modified Bernoulli equation ($\Delta P = 4V^2$) to the spectral Doppler velocity curve of the mitral inflow. This velocity curve is obtained by applying pulse-wave Doppler (with a high pulse-repetition frequency) through the mitral valve orifice. Using the modified Bernoulli equation, the PHT will be equal to the time interval required for the mitral inflow velocity to decrease from V_{max} to $V_{max}/\sqrt{2}$. The relationship of the MVA to the PHT was first described by Hatle and Angelsen as follows (13):

$$MVA (cm^2) = 220/PHT (ms)$$

The derived constant of 220 corresponds to the PHT at which the MVA is equal to 1 cm^2 .

The PHT method assumes that the compliance of the left ventricle and left atrium is relatively stable and has minimal effect on the rate of transmitral pressure decline. This assumption may be incorrect in the first 24 to 48 hours after mitral valve commissurotomy or replacement. PHT can yield inaccurate estimates of MVA in conditions that acutely alter left atrioventricular compliance or in patients with rapid heart rates or severe aortic insufficiency (14). Severe aortic insufficiency will cause a rapid rise in the LV diastolic pressure, decreasing the PHT, resulting in an overestimation of the MVA (15).

The severity of mitral valve stenosis can be determined by measuring a mean pressure gradient across the mitral valve orifice. This is accomplished by tracing the diastolic mitral inflow velocity curve. Contemporary echocardiographic machines will calculate the area under the curve to determine the mean pressure gradient across the valve. This method is limited as estimated pressure gradients will vary with the flow across the valve. In atrial fibrillation, this limitation is compounded by the variable stroke volume seen with the irregular heartbeat. In conditions of increased cardiac output (i.e., exercise), there is an increase in transvalvular flow and thus a higher pressure gradient. Table 3 shows a grading of mitral stenosis with the various estimation techniques described.

Table 3 Severity Estimation of Mitral Stenosis (35)

| Grade | Mild | Moderate | Severe |
|------------------------|---------|----------|--------|
| Mean gradient (mmHg) | <6 | 6–10 | >10 |
| PHT (ms) | 100 | 200 | >300 |
| DHT (ms) | <500 | 500–700 | >700 |
| MVA (cm ²) | 1.6–2.0 | 1.0–1.5 | <1.0 |

Abbreviations: PHT, pressure half-time; DHT, deceleration half-time; MVA, mitral valve area.

As with the aortic valve, the continuity equation can be used to calculate the MVA. In a closed system, flow through one valve must equal flow through another valve. The blood flow through a valve can be calculated using the velocity of the blood flow through the valve and the area through which blood flows. The velocity of the blood is determined using the VTI, which is a mean value for the velocity of the blood measured. The VTI can be obtained by tracing the transvalvular velocity curve through a spectral Doppler interrogation of the reference or mitral valve. The continuity equation can then be used as follows:

$$Q (\text{Volumetric flow}) = \text{Area}_{\text{Mitral}} \times \text{VTI}_{\text{Mitral}} = \text{Area}_{\text{Ref}} \times \text{VTI}_{\text{Ref}}$$

$$\text{MVA} = \text{Area}_{\text{Mitral}} = \text{Area}_{\text{Ref}} \times \frac{\text{VTI}_{\text{Ref}}}{\text{VTI}_{\text{Mitral}}}$$

The continuity equation assumes that flow through the reference valve is equal to flow through the mitral valve. Shunting or regurgitation through the mitral or reference valve makes this assumption incorrect and would either overestimate or underestimate the MVA.

Mitral Regurgitation

MR has a number of causes, including myxomatous degeneration, rheumatic disease, endocarditis, Marfan syndrome, infiltrative diseases (amyloid, sarcoid, mucopolysaccharidosis), collagen-vascular disorders (i.e. lupus, rheumatoid arthritis), papillary muscle rupture or dysfunction, ischemia, and cardiomyopathies (16). General anesthesia can greatly affect the hemodynamic loading conditions and contractility of the heart, resulting in widely variable measurements of MR. It is not uncommon for a patient to have one set of measurements on TTE (in the awake state) and another (usually improved) set of measurements when under general anesthesia. Therefore, in certain circumstances, it is best to evaluate MR under physiologic conditions. Anesthesiologists can raise the blood pressure and the systemic vascular resistance if there is a question about the dynamic nature of the MR. Similarly, comparison of MR before and after surgical intervention should be performed under the same physiologic loading conditions.

The mechanism of MR can often be determined by 2D visualization of mitral leaflet motion. There can be excessive leaflet motion, restricted leaflet motion, or normal leaflet motion with poor coaptation (17). Excessive leaflet motion is classified as either billowing, prolapsed, or flail. A billowing mitral leaflet is seen with a bowing of part of the mitral valve leaflet above the level of the mitral annulus. The leaflet edge, however, still coapts well, without resultant MR. If the leaflet edge extends above the level of the annulus, the leaflet has prolapsed. The extreme case of leaflet prolapse, termed flail, is seen with papillary muscle or chordae tendineae rupture. A flail leaflet freely moves into the left atrium during systole. MR due to excessive leaflet motion will result in a regurgitant jet directed away from the affected valve leaflet (Fig. 24).



Figure 24 Posterior leaflet prolapse with a regurgitant jet directed over the anterior mitral valve leaflet and away from the affected leaflet.

Conversely, MR caused by restricted leaflet motion results in a regurgitant jet directed toward the affected valve leaflet (Fig. 25). Leaflet restriction is commonly caused by leaflet calcification or thickening or with ischemic papillary muscles. If the leaflets exhibit normal motion with failure to coapt, the cause is usually annular dilation or ischemia of the left ventricle or the LV-mitral valve apparatus. Leaflet perforation, as seen in infective endocarditis, can cause MR with normal leaflet motion on 2D interrogation.

Two-dimensional examination can also reveal indirect signs as to the severity of MR. MR results in a volume overloading of both the left atrium and the left ventricle. With chronic MR, the left ventricle and left atrium will dilate to accommodate this volume load. Early in the disease process of MR, the LV end-systolic volume does not change much; however, with time the LV end-diastolic volume and LA volume gradually increase. LA dimensions of greater than or equal to 5.5 cm and LV diastolic dimensions of ≥ 7 cm are suggestive of severe MR (18). With chronic increases in LA pressure, evidence of pulmonary hypertension (i.e., right ventricular hypertrophy and tricuspid regurgitation) can be seen. Pulmonary artery pressure can be estimated by adding the pressure gradient across the regurgitant tricuspid valve to the estimated right atrial pressure or central venous pressure. Acute MR leads to acute pressure overload of the left atrium without echocardiographic evidence of LA and LV dilatation; however, one can still see evidence of pulmonary hypertension with acute MR.

Color flow Doppler of the mitral valve regurgitant jet is one of the most frequently used parameters for the estimation of MR severity. The mitral valve is interrogated from 0° to 120° to find the largest regurgitant volume. A volume of less than 3 cm^2 corresponds to a mild degree of MR. Volumes of greater than 6 cm^2 correspond to a severe degree of MR. The ratio of the MR jet area to the area of the left atrium can also be used to estimate

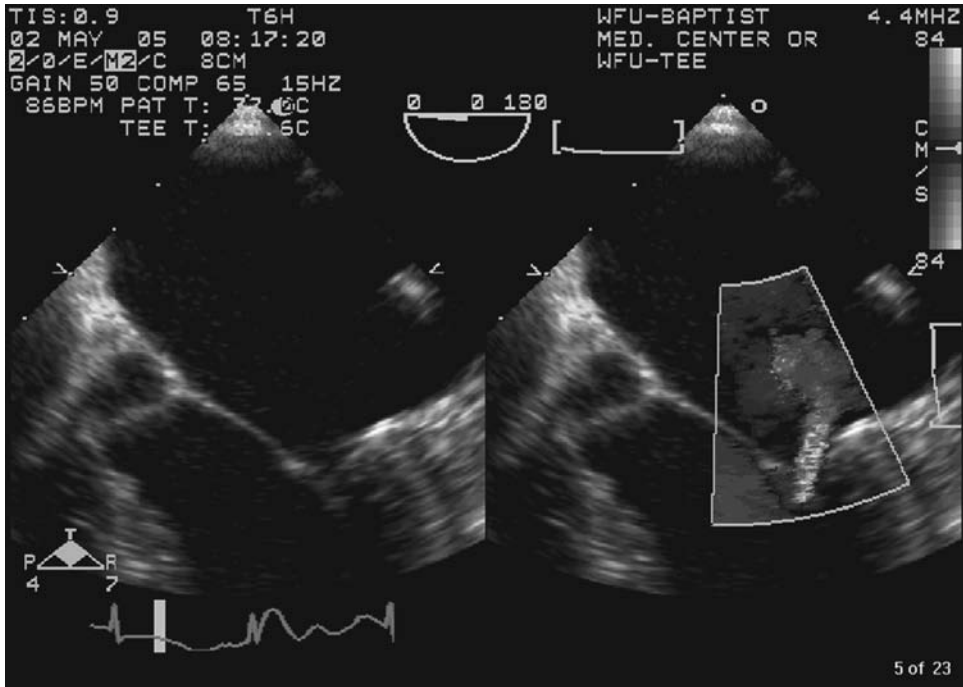


Figure 25 Restricted motion of the posterior leaflet, resulting in a regurgitant jet directed toward the affected leaflet.

MR severity. With mild MR, the MR jet area should be less than 30% of the LA area, whereas with severe MR, the MR jet area is greater than 50% of the LA area (19).

A measurement of the vena contracta is perhaps a more sensitive estimate of MR severity. The vena contracta is the narrowest portion of the regurgitant jet visualized on color flow Doppler. The vena contracta width corresponds to the size of the orifice through which the regurgitant volume flows. After interrogating the mitral valve regurgitant jet through 120° , the largest vena contracta is measured. A measurement of less than 0.3 cm corresponds to mild MR, while a measurement of greater than 0.55 cm corresponds to severe MR.

The use of the proximal isovolemic surface area (PISA) can be used to determine the orifice area through which the mitral regurgitant volume flows. An orifice area of less than 0.20 cm^2 corresponds to mild MR, while an area $\geq 0.4 \text{ cm}^2$ corresponds to severe MR. This method may not be as accurate with eccentric jets or when the isovelocity surface area is not hemispherical. In these instances, the mitral valve regurgitant orifice area can be calculated using the continuity equation. The mitral regurgitant volume (V_{MR}) can be calculated knowing the stroke volume through the mitral valve ($\text{SV}_{\text{Mitral}}$) and the stroke volume through any reference valve (SV_{Ref}), assuming no regurgitation at that reference valve, using the equation:

$$V_{\text{MR}} = \text{SV}_{\text{Mitral}} - \text{SV}_{\text{Ref}},$$

where $\text{SV}_{\text{Mitral/Ref}} = \text{VTI}_{\text{Mitral/Ref}} \times \text{Valve area}_{\text{Mitral/Ref}}$

The mitral regurgitant orifice can then be calculated by dividing V_{MR} by the regurgitant VTI (VTI_{MR}).

Table 4 Grading of MR Severity

| Method | Mild | Moderate | Severe |
|--|----------------------|--------------------------|----------------------|
| Jet area (cm ²) | <3 cm ² | 3–6 cm ² | >6 cm ² |
| Vena contracta (cm) | <0.3 cm | 0.3–0.55 cm | >0.55 cm |
| Regurgitant fraction (%) | <30% | 30–50% | >50% |
| Mitral orifice area (cm ²) | <0.2 cm ² | 0.2–0.39 cm ² | ≥0.4 cm ² |
| Regurgitant volume (mL) | <30 mL | 30–59 mL | ≥60 mL |
| Pulmonary vein flow | Blunted S wave | S wave < D wave | Systolic reversal |

Abbreviation: MR, mitral regurgitation.

$$\text{Mitral regurgitant orifice area} = \frac{V_{MR}}{VTI_{MR}}$$

The regurgitant volume itself can be used as an estimate of the severity of MR, with a volume of less than 30 mL corresponding to mild MR and a volume of ≥60 mL corresponding to severe MR.

Pulmonary venous flow is also affected by MR. With mild MR, there is blunting of the systolic wave of pulmonary venous flow. With severe MR, systolic reversal of pulmonary venous flow is commonly seen. A summary of the various methods of grading the severity of MR is provided in Table 4.

THE TRICUSPID VALVE

Anatomy

The tricuspid valve consists of anterior, posterior, and septal cusps tethered by chordae tendinae and papillary muscles all suspended by a fibromuscular annulus. The commissures of the tricuspid valve are not as well defined as those of the mitral valve. The orifice is larger than that of the mitral valve and is triangular in shape compared with the saddle shape of the mitral valve. The anterior leaflet is the largest and is tethered to the anterior papillary muscle, which arises from the moderator band. The moderator band is composed of muscular tissue arising from the intraventricular septum and can sometimes be seen on the echocardiogram. The posterior leaflet is the smallest and is anchored by the posterior papillary muscle. The septal leaflet attaches to the ventricular septum and is in very close proximity to the bundle of His (20).

Standard TEE Views

Midesophageal Four-Chamber View

This is sometimes referred to as the “opening shot” and will be the first view encountered after inserting the probe with the multiplane angle at 0°. The probe may need to be slightly retroflexed to fully develop the view. After optimizing the image, the right atrium, right ventricle, left atrium, and left ventricle are well visualized. The tricuspid valve appears on the left side of the display and the mitral valve to the right (Fig. 4). In this view, the septal leaflet of the tricuspid valve appears to the right of the display and a nonseptal leaflet to the left. The tricuspid annulus is measured in this view and should not exceed 28 mm. Tricuspid valve motion should be smooth with complete coaptation of the valve leaflets in systole. Leaflet mobility is assessed, and they are examined for

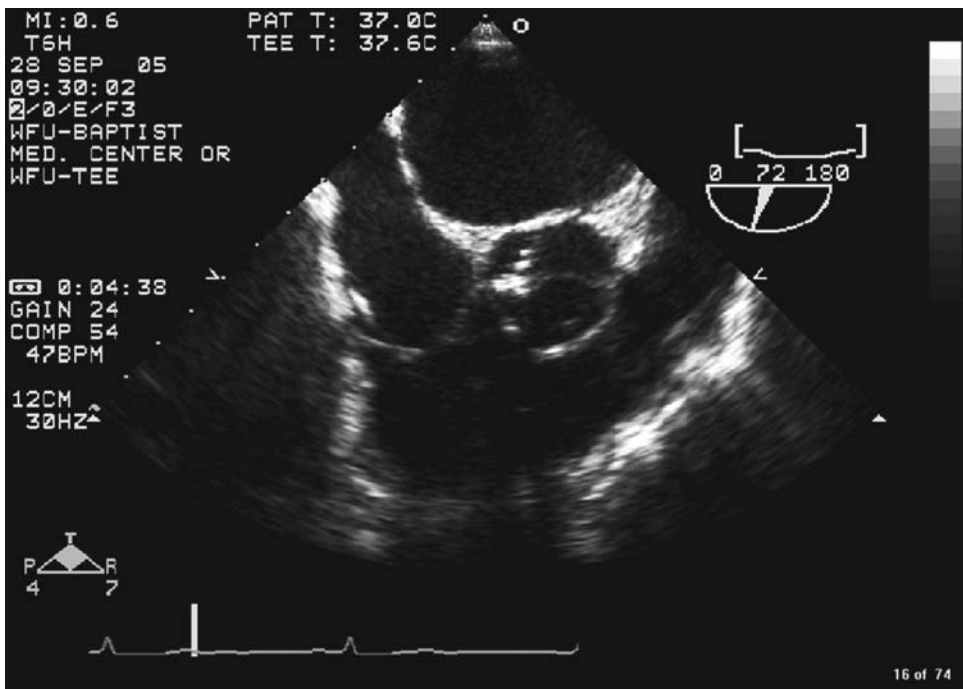


Figure 26 The ME RVOT view. A pulmonary artery catheter is seen in the right ventricle. *Abbreviations:* ME, midesophageal; RVOT, right ventricular outflow tract.

thickening or vegetations. Spectral Doppler is employed to interrogate the flow across the valve, and pulse- and continuous-wave Doppler can be used to determine pressure gradients and filling patterns in the right ventricle.

Midesophageal Right Ventricular Inflow-Outflow View

This view is developed by focusing on the tricuspid valve in the four-chamber view and then advancing the multiplane angle to approximately 45° to 90° until the tricuspid and pulmonic valves appear simultaneously (Fig. 26). The tricuspid valve appears with the posterior leaflet on the left side of the display and the anterior leaflet on the right. This view allows the most accurate determination of the tricuspid valve annular size (21). The annular size is important when evaluating the tricuspid valve for surgical repair of tricuspid regurgitation. An enlarged annulus may be easily repaired with a valvuloplasty procedure.

Transgastric Right Ventricular Inflow View

This view is developed by advancing the probe into the stomach with the multiplane angle at 0°, focusing on the right heart, and then advancing the multiplane angle to approximately 110° (Fig. 27). This view affords the best view of the chordae tendinae.

Tricuspid Regurgitation

Insignificant tricuspid insufficiency (TI) is very common and is often seen in patients with transvenous pacemaker leads and/or pulmonary artery catheters (22,23). Moderate to severe TI is most frequently the result of dilation of the right ventricle and the tricuspid

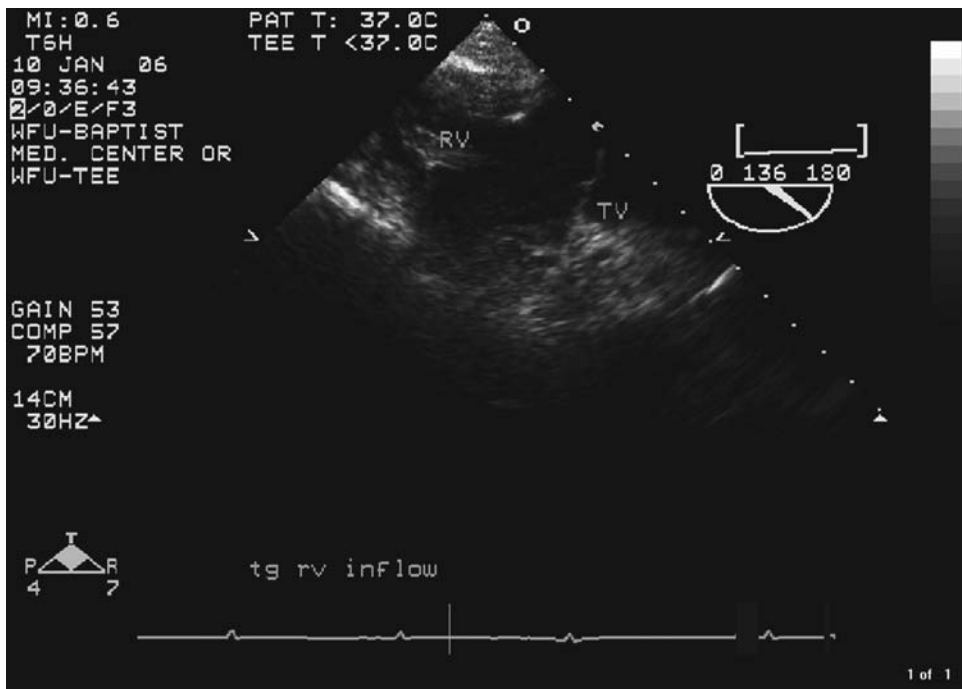


Figure 27 This view is developed by advancing the probe into the stomach with the multiplane angle at 0° , focusing on the right heart, and then advancing the multiplane angle to approximately 110° to 140° . This view affords the best view of the right ventricular chordae tendinae.

annulus. Any condition resulting in elevated right ventricular pressure (>55 mmHg) or right ventricular dilation can cause TI. Common causes observed in surgical patients include right heart ischemia, cor pulmonale, pulmonary embolism, left-heart failure, pulmonic valve stenosis, and pulmonary hypertension (24). Significant mitral insufficiency is a common cause of right ventricular dilation and secondary TI.

Primary TI is less commonly encountered, but is seen in intravenous drug users with infective endocarditis. Vegetations appear as mobile masses along leaflet edges and prevent proper coaptation of the valve leaflets. Both tricuspid and pulmonic valves are commonly involved.

Rheumatoid valvular disease typically involves both tricuspid and mitral valves and results in thickened, fused, and retracted leaflets that neither open nor close properly. Stenosis with insufficiency typically results.

Carcinoid syndrome is seen in patients with primary neuroendocrine tumors of the small intestine that have metastasized to the liver. Elevated levels of 5-hydroxytryptamine (serotonin) cause plaque formation on the right-sided heart valves. The valves appear thickened and immobile similar to that seen with rheumatic heart disease. Fenfluramine-phentermine (fen-phen) valvulopathy was commonly observed in patients taking this medication for weight reduction. Similar to carcinoid syndrome, this condition involves elevated serotonin levels and presents with shortened, thickened valves, which fail to properly coapt. In contrast to carcinoid syndrome, however, fen-phen valvulopathy affects both right and left heart valves.

Other causes of TI include blunt chest trauma, Ebstein's anomaly, and connective tissue disorders. Blunt chest trauma may cause an acute rise in right ventricular pressure

Table 5 Primary and Secondary Causes of TI

| Primary | Secondary (Functional) |
|------------------------------|-------------------------------------|
| Infective endocarditis | Myocardial ischemia/infarction |
| Carcinoid tumor | Cor pulmonale |
| Rheumatic heart disease | Pulmonary embolism |
| Trauma | Left-heart failure |
| Papillary muscle dysfunction | Pulmonic stenosis |
| Fen-phen valvulopathy | Pulmonary hypertension |
| Ebstein's anomaly | Mitral insufficiency |
| Connective tissue disorders | Pulmonary artery catheter/pacemaker |

Abbreviations: TI, tricuspid insufficiency; Fen-phen, Fenfluramine-phentermine.

Table 6 Estimating the Severity of TI

| | Mild | Moderate | Severe |
|--|---------------------------------|-----------------------------|---------------------|
| Regurgitant jet area | <5 cm ² | 5–10 cm ² | >10 cm ² |
| Regurgitant jet area/right atrial area | <30% | 30–60% | >60% |
| Jet mapping | Jet to level of tricuspid valve | Jet to half of right atrium | Jet past mid-atrium |
| Vena contracta | | <7 mm | >7 mm |
| Hepatic vein flow | Normal | Blunted | Reversed |
| Tricuspid annular dimension at end systole | | | >34 mm |

Abbreviation: TI, tricuspid insufficiency.

sufficient to cause a blowout in the tricuspid support apparatus and presents as flail leaflet on echocardiography. Ebstein's anomaly and connective tissue disorders such as Marfan's syndrome are less common causes of TI (Table 5) (25).

A standard system of evaluating the severity of TI is necessary to completely assess tricuspid valve function. Surgical and medical decision making is influenced by the severity of the lesion. There are varieties of measures used to estimate TI severity. No matter which measure is utilized, it is important not to rely on only one, but to make several measurements in several views, before making the diagnosis. For example, jet mapping in the four-chamber view may reveal moderate TI. However, additional views may reveal severe TI, and Doppler imaging may further demonstrate hepatic flow reversal in systole. The final assessment must reflect all the data, and a diagnosis of severe TI is appropriate.

Table 6 gives useful measurements in the determination of TI severity. The regurgitant jet area is easily measured in the four-chamber view, and jet area greater than 10 cm² is associated with severe TI. If the regurgitant jet area occupies less than 30% of the right atrium, the TI is usually mild. Regurgitant jets occupying 30% to 60% of the right atrium indicate moderate TI, and jets occupying greater than 60% usually indicate severe TI (Fig. 28). The size of the regurgitant jet is dependent on hemodynamics, with changes in the right ventricular afterload and contractility affecting the observed regurgitant jet size. General anesthesia is associated with a decrease in systemic vascular resistance and decreases the right ventricular afterload. This point gains clinical relevance when a patient with previously diagnosed severe TI is brought to the operating room and the intraoperative TEE now shows mild to moderate TI. Annular dilatation is often seen

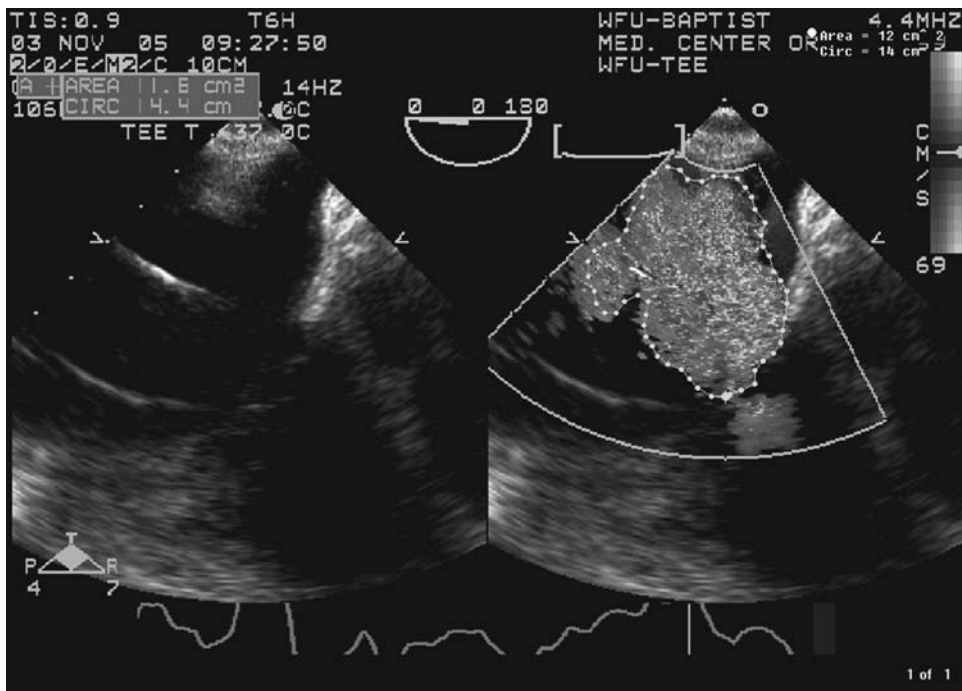


Figure 28 Severe tricuspid insufficiency diagnosed in the four-chamber view focused on the right heart. The regurgitant jet area occupies greater than 60% of the right atrial area. The volume of the jet is greater than 10 cm^2 . Both parameters are consistent with severe tricuspid regurgitation.

with severe TI and may be especially amenable to surgical correction with ring annuloplasty.

Measurement of the vena contracta provides an estimation of TI severity that is less dependent on hemodynamic conditions. The vena contracta is measured using Doppler color flow imaging at the narrowest point between the valve leaflets during ventricular systole (Fig. 29). A vena contracta greater than 7 mm indicates severe TI (26).

Interrogation of the hepatic vein flow using pulse-wave Doppler yields useful information in determining the severity of TI. Hepatic veins are located starting with the bicaval view and following the inferior vena cava down to the liver with a slight rightward rotation of the TEE probe. The pulse-wave Doppler sampling volume is placed within a hepatic vein and the waveform examined. Flow toward the probe appears as a positive deflection, and flow away from the probe appears as a negative deflection. Ventricular systole is normally associated with hepatic vein flow in the direction of the probe as blood fills the right atrium. In the setting of moderate TI, this flow is blunted. Systolic flow reversal in the hepatic veins indicates severe TI and is the only independent echocardiographic predictor of severe clinical TI (Fig. 30) (27,28).

Tricuspid Stenosis

Tricuspid stenosis is much less common than TI. Rheumatic heart disease is the most common cause of tricuspid stenosis and results in thickened, immobile valve leaflets with commissural fusion. Diastolic doming of the leaflets is usually present. In these cases, the mitral valve is usually also involved. Other causes of tricuspid stenosis, although rare,

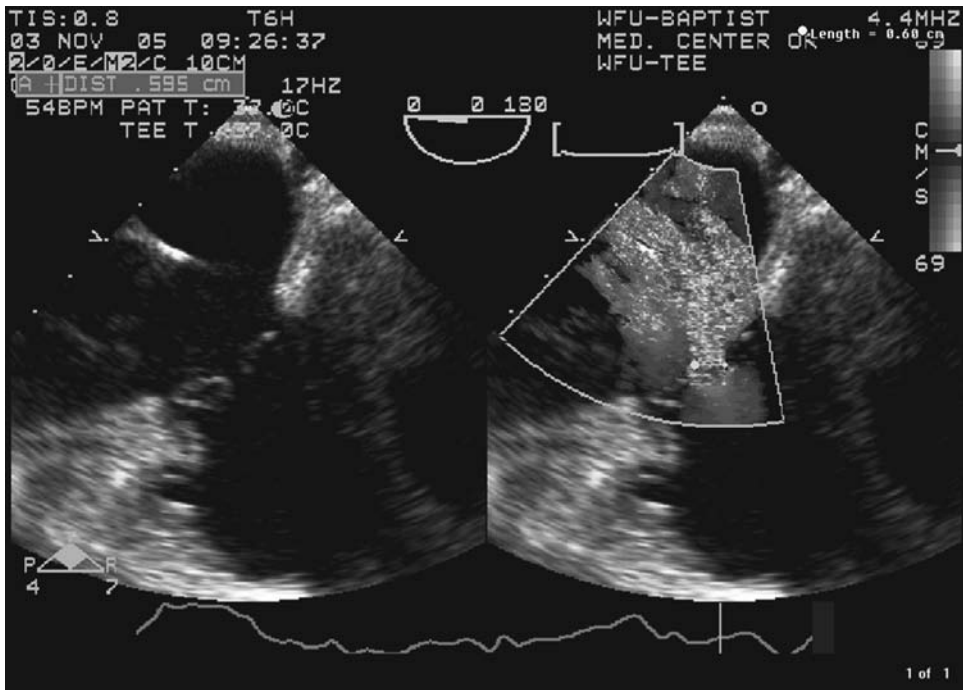


Figure 29 Measurement of the vena contracta (0.595 cm) in a patient with tricuspid insufficiency.

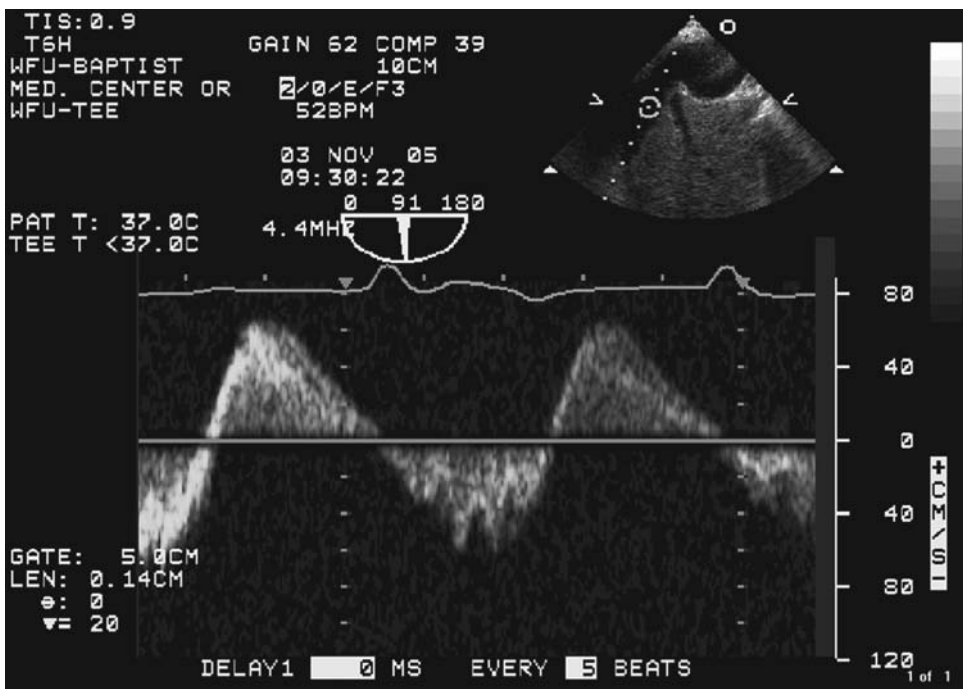


Figure 30 Hepatic flow reversal in the setting of severe TI. The pulse-wave Doppler sampling volume is placed within a hepatic vein (upper right of the screen). The negative deflection that follows the QRS complex represents flow away from the transducer during ventricular systole and is diagnostic of severe TI. *Abbreviation:* TI, tricuspid insufficiency.

include congenital anomalies, endocarditis, carcinoid heart disease, and endomyocardial fibrosis.

The area of the tricuspid valve is a useful measure of disease severity. As with the mitral valve, the tricuspid valve area (TVA) can be estimated by the PHT method or planimetry. The following equation is used to determine the TVA:

$$\text{TVA} = \frac{190}{\text{PHT}}.$$

Tricuspid stenosis is considered severe if the TVA is less than 1 cm² (29).

Transvalvular gradients are also useful in the quantification of tricuspid stenosis. The right side of the heart is a low-pressure system with the normal mean gradient across the tricuspid valve less than 2 mmHg. Mean gradients between 2 and 6 mmHg indicate moderate TS, and gradients greater than 7 mmHg indicate severe TS (30).

THE PULMONIC VALVE

Echocardiographic evaluation of the pulmonic valve is part of a complete examination. Unfortunately, the pulmonic valve is the most difficult valve to image owing to its thin leaflets and greater distance from the esophagus than the other valves (1). Epicardial scanning by the surgeon during the operation may yield high-quality images in a time-efficient manner (31). This technique can be used when TEE placement is contraindicated or when images are unsatisfactory (such as a patient who has had a Ross procedure and presents for reoperation).

Anatomy

The pulmonic valve is anterior and superior to the aortic valve. Similar to the aortic valve, it is tri-leaflet and semilunar, consisting of anterior, left, and right leaflets. The plane of the valve is roughly perpendicular in orientation to the aortic valve. The pulmonic valve is isolated from the other three heart valves by the infundibulum.

Standard TEE Views

Midesophageal Aortic Valve Short-Axis View

This view is obtained by rotating the multiplane angle to approximately 45° to 110° and focusing on the aortic valve on cross section. The pulmonic valve and the main pulmonary artery appear to the right of the aortic valve (Fig. 31). The main pulmonary artery can be followed to its bifurcation into the right and left pulmonary arteries by rotating the multiplane angle back toward 0° and withdrawing or anteflexing the probe slightly.

Midesophageal Right Ventricular Inflow-Outflow View

This view is developed by focusing on the tricuspid valve in the four-chamber view and then advancing the multiplane angle to approximately 45° to 90° until the tricuspid and pulmonic valves appear in the same image (Fig. 26). This view shows the pulmonic valve in the LAX view and is useful for evaluating pulmonary insufficiency with color flow Doppler (32). This is the best view for assessing leaflet motion. Systolic doming, when present, will be apparent in this view. This is a sign of nonpliable leaflets that dome outward in ventricular systole instead of opening smoothly like a normal valve.

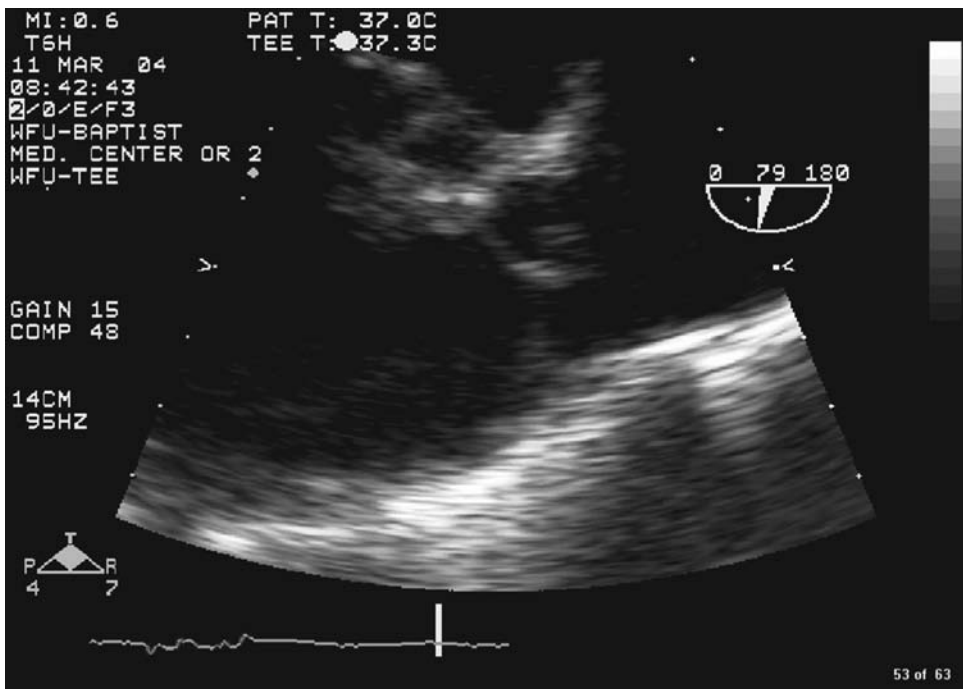


Figure 31 The pulmonic valve imaged in the aortic valve SAX view. *Abbreviation:* SAX, short axis.

Upper-Esophageal Aortic Arch Short-Axis View

This view is developed by withdrawing the probe with the multiplane angle at 90° until the aortic arch appears in the SAX view (Fig. 32). The main pulmonary artery and the pulmonic valve will appear to the left of the display. The view of the pulmonic valve may be improved by retroflexing the probe. This is the best view for measuring blood flow velocities across the pulmonic valve, as the Doppler beam can be aligned parallel to blood flow (33).

Pulmonary Regurgitation

Most patients have trivial pulmonary insufficiency, especially if a pulmonary artery catheter is in place. Severe pulmonary insufficiency is always pathologic and usually the result of dilation of the main pulmonary artery as observed in patients with pulmonary hypertension from any etiology. Primary causes of pulmonary insufficiency include fen-phen valvulopathy and carcinoid syndrome as previously described. These lesions result in short and thickened valves that fail to properly coapt. Carcinoid syndrome typically involves the tricuspid and pulmonic valves, and fen-phen valvulopathy affects all the valves. Infectious endocarditis can affect the tricuspid and pulmonic valves and presents as mobile masses attached to the valve leaflets.

The classification scheme for pulmonary insufficiency is less precise than that for mitral insufficiency or TI. In general, the larger the regurgitant jet and the farther the jet extends into the right ventricular outflow tract (RVOT), the more severe the pulmonic insufficiency (Fig. 33). The severity of pulmonic insufficiency can be estimated using the regurgitant jet height as a fraction of the RVOT height measured in the ME aortic valve

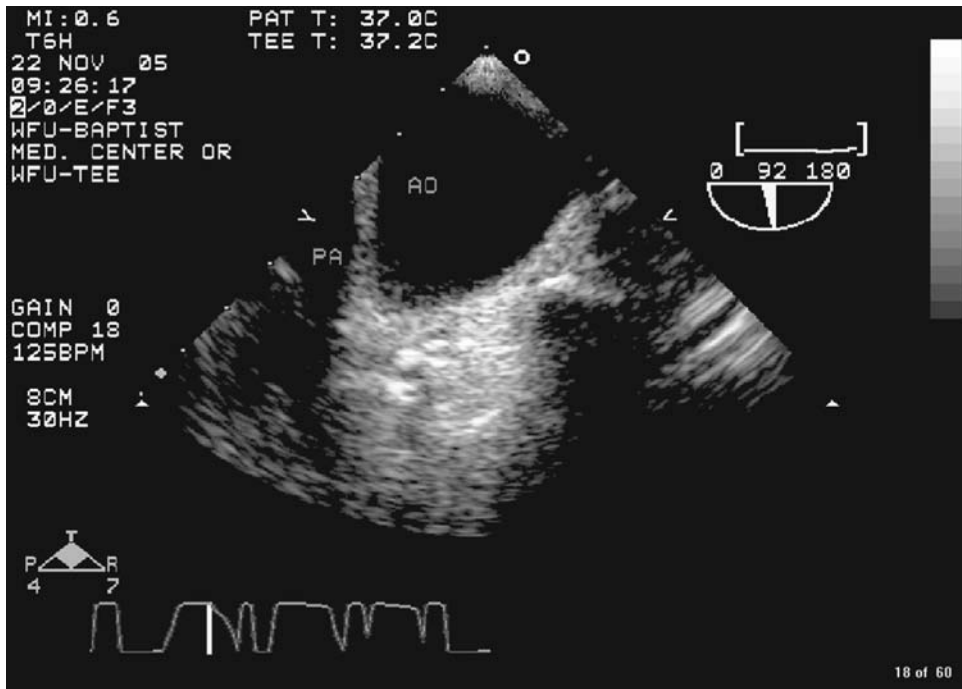


Figure 32 The UE aortic arch SAX view. *Abbreviations:* UE; upper esophageal; SAX, short axis.

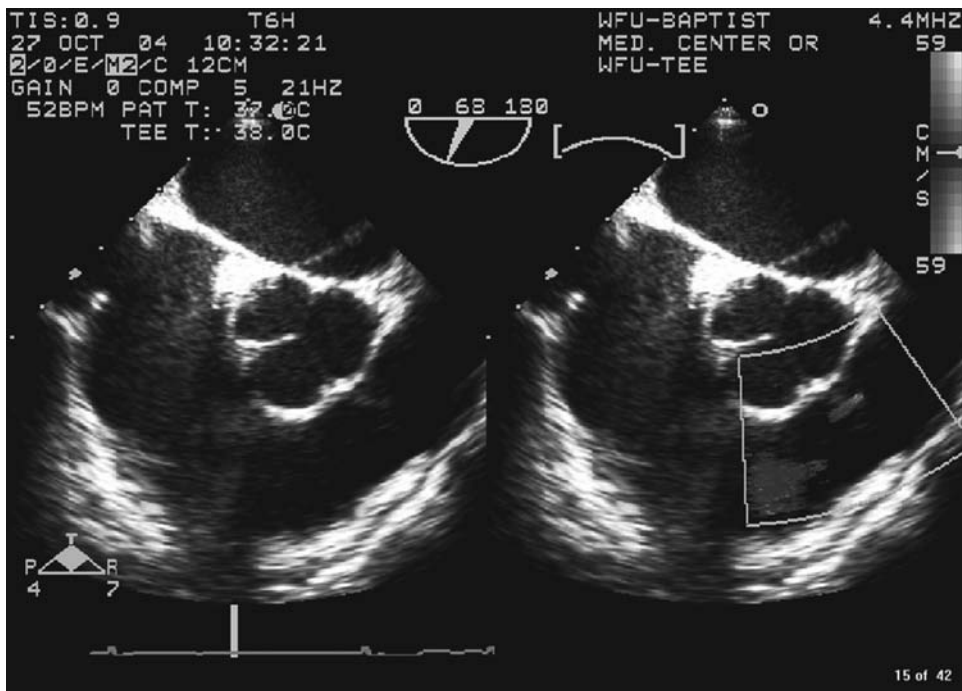


Figure 33 A small jet of pulmonary insufficiency is seen on this aortic valve SAX view. *Abbreviation:* SAX, short axis.

Table 7 Estimating the Severity of Pulmonic Stenosis

| | Mild | Moderate | Severe |
|---------------|----------|------------|----------|
| Peak gradient | <30 mmHg | 30–65 mmHg | >65 mmHg |

SAX view. If the jet occupies less than 25% of the RVOT, the pulmonary insufficiency is mild. Jets occupying 25% to 64% indicate moderate pulmonary insufficiency, and jets occupying greater than 65% indicate severe pulmonary insufficiency.

Pulmonic Stenosis

Pulmonic stenosis can be categorized as valvular, subvalvular, or peripheral (supra-valvular). Ninety percent of the lesions are valvular in nature, and the majority of pulmonary stenosis in the adult population is from untreated congenital heart disease. Pulmonary stenosis is more commonly seen as individuals with complex congenital heart disease increasingly survive into adulthood. Isolated valvular pulmonic stenosis comprises 10% of all congenital heart cases. The valve is usually tricuspid with pliable leaflets that are partially fused, creating a markedly narrowed orifice. In 15% of patients with isolated valvular pulmonic stenosis, the leaflets are not thin and fused but instead are markedly thickened from myxomatous tissue (34). Subvalvular pulmonic stenosis is often associated with a ventricular septal defect and presents as a narrowing of the infundibular region, usually with a normal pulmonic valve. Peripheral pulmonary stenosis is often associated with various acquired and congenital conditions such as rubella, tetralogy of Fallot, and Noonan, Ehlers-Danlos, and Williams syndromes. Obstruction can be at the level of the main pulmonary artery, the bifurcation, or at a more distal bifurcation. Less common causes of valvular pulmonic stenosis include carcinoid syndrome, which causes a combination of pulmonary insufficiency and stenosis, and rheumatic heart disease (although rheumatic heart disease rarely affects the pulmonic valve).

Pressure gradients across the stenotic valve give useful data about the severity of pulmonary stenosis (Table 7). To determine the pressure gradient across the pulmonic valve, continuous-wave Doppler is directed parallel to the pulmonic valve in the upper-esophageal aortic arch SAX view. Peak gradients less than 30 mmHg are associated with mild stenosis, peak gradients between 30 and 65 mmHg indicate moderate stenosis, and gradients greater than 65 mmHg indicate severe pulmonary stenosis. The continuity equation can be used to determine the area of the pulmonary valve to further assess disease severity.

CONCLUSION

TEE 2D and Doppler interrogation of cardiac valves is a powerful tool for evaluation pathology. By utilizing a systematic approach for each valve, appreciation of any pathology can be easily conveyed to the surgeon or referring physician.

REFERENCES

1. Shapira N, Fernandez J, McNicholas KW, et al. Hypertrophy of nodules of Arantius and aortic insufficiency: pathophysiology and repair. *Ann Thorac Surg* 1991; 51(6):969–972.
2. Stamm C, Li J, Ho SY, et al. The aortic root in supra-valvular aortic stenosis: the potential surgical relevance of morphologic findings. *J Thorac Cardiovasc Surg* 1997; 114(1):16–24.

3. Bonow R, Cheitlin MD, Crawford MH, et al. Task Force 3: valvular heart disease. *J Am Coll Cardiol* 2005; 45(8):1334–1340.
4. Rafferty T, Durkin MA, Sittig D, et al. Transesophageal color flow Doppler imaging for aortic insufficiency in patients having cardiac operations. *J Thorac Cardiovasc Surg* 1992; 104(2): 521–525.
5. Ekery D, Davidoff R. Aortic regurgitation: quantitative methods by echocardiography. *Echocardiography* 2000; 17(3):293–302.
6. Fang L, Hsiung MC, Miller AP, et al. Assessment of aortic regurgitation by live three-dimensional transthoracic echocardiographic measurements of vena contracta area: usefulness and validation. *Echocardiography* 2005; 22(9):775–781.
7. Reimold S, Maier SE, Aggarwal K, et al. Aortic flow velocity patterns in chronic aortic regurgitation: implications for Doppler echocardiography. *J Am Soc Echocardiography* 1996; 9(5): 675–683.
8. ACC/AHA guidelines for the management of patients with valvular heart disease: A report of the American College of Cardiology/American Heart Association Task Force on Practice Guidelines (Committee on management of patients with valvular heart disease). *J Am Coll Cardiol* 1998; 32(5):1486–1582.
9. Naqvi T, Siegel RJ. Aortic stenosis: the role of transesophageal echocardiography. *Echocardiography* 1999; 16(7, pt 1):677–688.
10. Richards KL. Assessment of aortic and pulmonic stenosis by echocardiography. *Circulation* 1991; 84(suppl 3):I182–I287.
11. Carpentier AF, Lessana A, Relland JY, et al. The “physio-ring”: an advanced concept in mitral valve annuloplasty. *Ann Thorac Surg* 1995; 60:1177–1185.
12. Shanewise J, Cheung A, Aronson S, et al. ASE/SCA guidelines for performing a comprehensive intraoperative multiplane transesophageal echocardiography examination: Recommendations of the American Society of Echocardiography Council for Intraoperative Echocardiography and Society of Cardiovascular Anesthesiologists Task Force for Certification in Perioperative Transesophageal Echocardiography. *J Am Soc Echocardiography* 1999; 12:884–898.
13. Hatle L, Angelsen B, eds. Pulsed and continuous wave Doppler in the diagnosis and assessment of various heart lesions. In: *Doppler Ultrasound in Cardiology: Physical Principles and Clinical Applications*. Philadelphia: Lea & Febiger, 1982:76–89.
14. Wranne B, Msee PA, Loyd D. Analysis of different methods of assessing the stenotic mitral valve area with emphasis on the pressure gradient half-time concept. *Am J Cardiol* 1990; 66: 614–620.
15. Thomas JD, Weyman AE. Doppler mitral pressure half-time: A clinical tool in search of theoretical justification. *J Am Coll Cardiol* 1987; 10:923–929.
16. Otto. Valvular regurgitation. In: *Textbook of Clinical Echocardiography*. 3rd ed. Philadelphia: Elsevier Inc., 2004:315–350.
17. Stewart WJ, Currie PJ, Salcedo EE, et al. Evaluation of mitral leaflet motion by echocardiography and jet direction by Doppler color flow mapping to determine the mechanisms of mitral regurgitation. *J Am Coll Cardiol* 1992; 20:1353–1361.
18. Oh J, Seward J, Tajik A. Valvular heart disease. In: *The Echo Manual*. 2nd ed. Philadelphia: Lippincott Williams & Wilkins, 1999:103–132.
19. Irvine T, Li X, Sahn D, et al. Assessment of mitral regurgitation. *Br Heart J* 2002; 88:11–19.
20. Netter FH. *Atlas of Human Anatomy*. 2nd ed. Rittenhouse Book Distributors, Inc., 1997.
21. Maslow A, Schwartz C, Singh A. Assessment of the tricuspid valve: a comparison of four transesophageal echocardiographic windows. *J Cardiothorac Vasc Anesth* 2004; 18(6):719–724.
22. Paniagua D, Alsrich HR, Lieberman EH, et al. Increased prevalence of significant tricuspid regurgitation in patients with transvenous pacemaker leads. *Am J Cardiol* 1998; 82(9):1130–1132.
23. Sherman SV, Wall MF, Kennedy DJ, et al. Do pulmonary artery catheters cause or increase tricuspid or pulmonic regurgitation. *Anesth Analg* 2001; 92:1117–1122.
24. Hinderlitter AL, Willis PW, Long WA, et al. Frequency and severity of tricuspid regurgitation determined by Doppler echocardiography in primary pulmonary hypertension. *Am J Cardiol* 2003; 91(8):1033–1037.

25. Braunwald E, Zipes DP, Libby P, eds. Braunwald's Heart Disease: A Textbook of Cardiovascular Medicine. 7th ed. Philadelphia: WB Saunders Co., 2004.
26. Tribouilloley CM, Enriquez-Sarano M, Bailey KR, et al. Quantification of tricuspid regurgitation by measuring the width of the vena contracta with Doppler color flow imaging: a clinical study. *J Am Coll Cardiol* 2000; 36:472–478.
27. Pennestri F, Loperfido F, Salvatori MP, et al. Assessment of tricuspid insufficiency by pulsed Doppler ultrasound of the hepatic veins. *Am J Cardiol* 1984; 54:363–368.
28. Shapira Y, Porter A, Wurzel M, et al. Evaluation of tricuspid regurgitation severity: echocardiographic and clinical correlation. *J Am Soc Echocardiography* 1998; 11:652–659.
29. Weyman AE. The Principles and Practice of Echocardiography. 2nd ed. Philadelphia: Lippincott Williams & Wilkins, 1994.
30. Fawzy ME, Mercer EN, Dunn B, et al. Doppler echocardiography in the evaluation of tricuspid stenosis. *Eur Heart J* 1989; 10(11):985–990.
31. Eltzschig HK, Kallmeyer IJ, Mihaljevic T, et al. A practical approach to a comprehensive epicardial and epiaortic echocardiographic examination. *J Cardiothorac Vasc Anesth* 2003; 17: 422–429.
32. Shanewise JS, Cheung AT, Aronson S, et al. ASE/SCA guidelines for performing a comprehensive intraoperative multiplane transesophageal echocardiography examination: recommendations of the American Society of Echocardiography Council for Intraoperative Echocardiography and the Society of Cardiovascular Anesthesiologists Task Force for Certification in Perioperative Transesophageal Echocardiography. *J Am Soc Echocardiogr* 1999; 12:884–900.
33. Klein AL, Murray RD, Grimm RA, et al. The effect of technical factors on the quality of pulmonary venous flow from the transverse and longitudinal imaging planes with transesophageal echocardiography. *J Am Soc Echocardiogr* 1995; 8:879–887.
34. Brickner ME, Hillis LD, Lange RA. Congenital heart disease in adults: first of two parts. *N Engl J Med* 2000; 342:256–263.
35. Savage RM, Aronson S. Assessment of the mitral valve. In: *Comprehensive Textbook of Intraoperative Transesophageal Echocardiography*. Philadelphia: Lippincott Williams & Wilkins, 2005:201.

9

Basic Echo Doppler

Mary Beth Brady

Department of Anesthesiology and Critical Care Medicine, Johns Hopkins Medical Institutions, Johns Hopkins Medical Center, Baltimore, Maryland, U.S.A.

Science becomes dangerous only when it imagines that it has reached its goal.

George Bernard Shaw, 1856–1950

INTRODUCTION

Echocardiography is a combination of complementary techniques. These techniques are two-dimensional echocardiography and Doppler ultrasound. Two-dimensional echocardiography displays three-dimensional structures in a two-dimensional format. It is an excellent method to interrogate anatomical structures. Fortunately, the high resolution of today's echocardiography technology enables very detailed examination of cardiac anatomy. Although two-dimensional echocardiography reveals much information about anatomy, it provides no information about blood flow and the forces associated with this flow. Doppler ultrasound provides this information. Doppler ultrasound is used to examine blood flow in terms of direction, velocity, and pattern of flow. It is a quantitative process and can be used as a means of grading disease severity. Two-dimensional echocardiography, on the other hand, can be used to diagnosis the disease itself. Two-dimensional echocardiography and Doppler ultrasound are complementary in that the first is used to evaluate structure and the second is used to evaluate function. Understanding the value and limitations of Doppler ultrasound is essential to understanding the diagnostic utility of ultrasound as a whole.

The objective of this chapter is to describe the fundamentals behind the technology of Doppler ultrasound, to describe its limitations, and to describe its utilization.

DOPPLER ANALYSIS: BEAM ORIENTATION

Doppler analysis provides information on the direction and velocity of a moving object. It is the same technology utilized by those patrolling the highways. In the case of the highway patrol, the moving objects are cars, and the patrol is interested in the velocities of

the cars for obvious reasons. In our case the moving object is the red blood cell. Our interest in the speed of the red blood cells at first glance may not be obvious but will be explained shortly.

The fundamentals of Doppler that we know today are based on the work of Christian Doppler, an Austrian physicist. His work on this was first published in 1842 in which he investigated the effect of movement of an object on sound frequency. He discovered that the frequency of sound is affected by its motion toward or away from the listener. Simply put, there are three possible scenarios: (i) if the source of sound is stationary, the frequency of that sound is constant; (ii) if the source of sound is moving toward the listener, the frequency of that sound increases; and (iii) if the source of sound is moving away from the listener, the frequency of that sound decreases.

In this way, we can compare the frequency transmitted to the frequency received and deduce some knowledge about the object's motion. "Doppler shift" is the term used to describe the difference between the frequency transmitted and that which is received (Fig. 1).

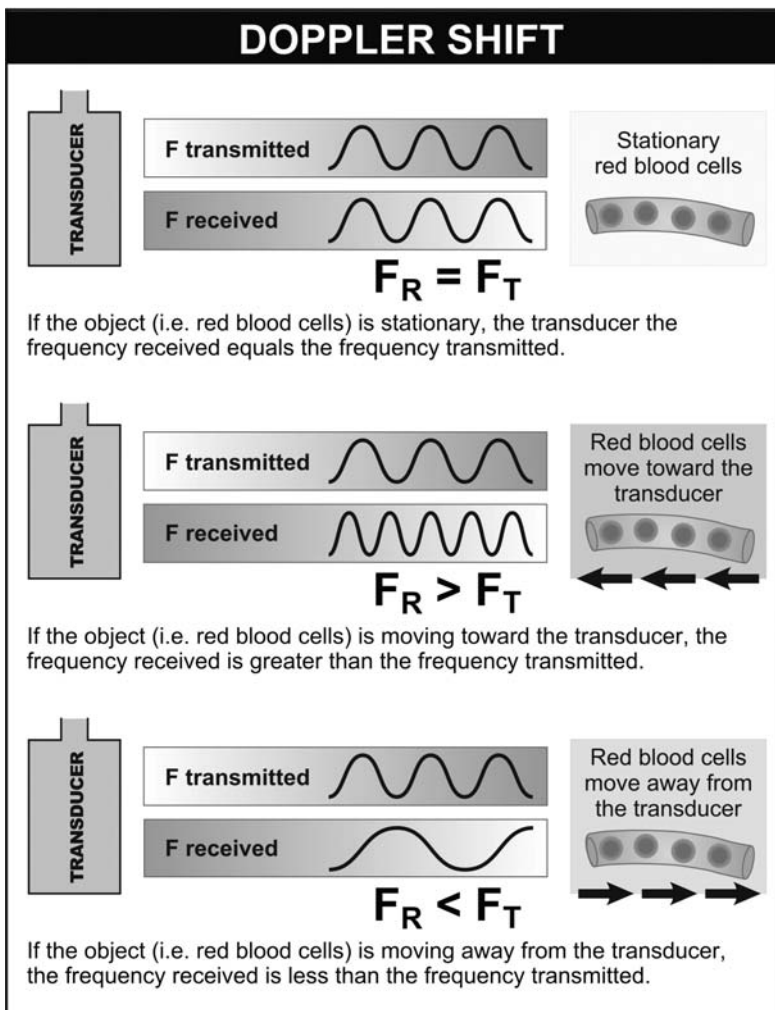


Figure 1 Doppler shift.

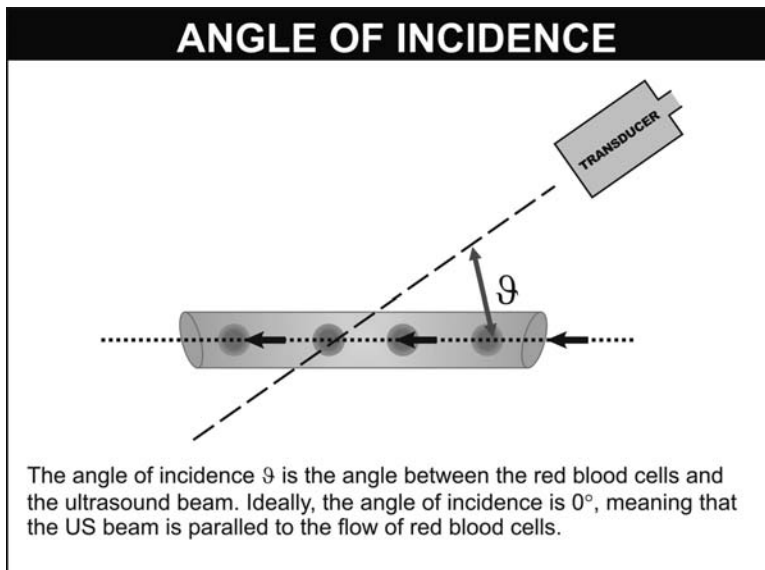


Figure 2 Angle of incidence.

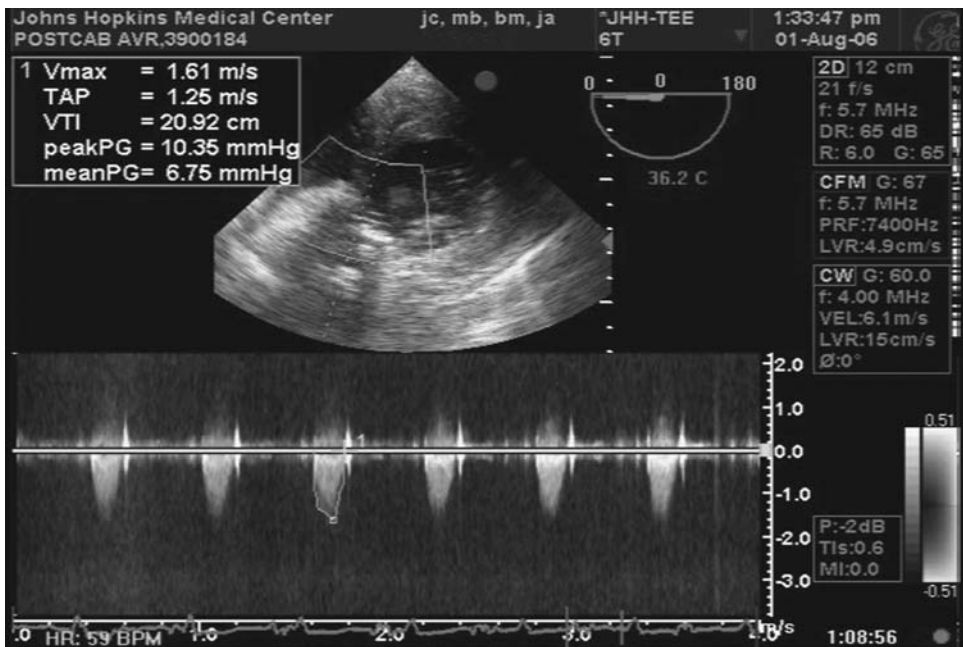
Doppler shift gives us information on frequency and therefore direction of flow of the red blood cell. Christian Doppler also described the “Doppler equation,” which relates the relationship between that “shift” and the velocity of the red blood cell.

$$\Delta f = \text{velocity} \times \cos \theta \times 2 (\text{transmitted frequency}) / c$$

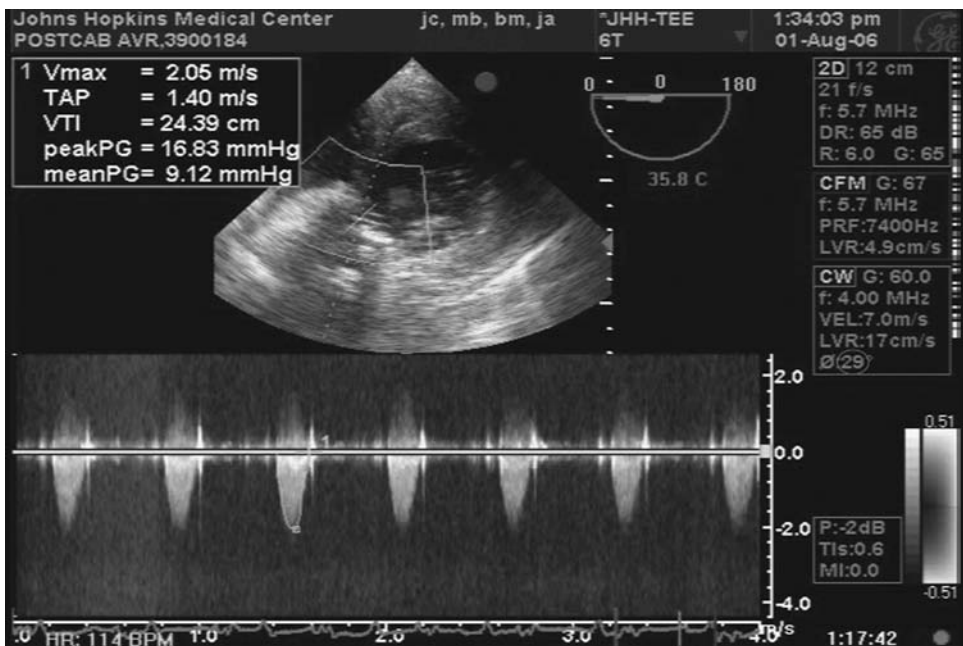
Δf is the difference between the frequency transmitted and the frequency received, v is the velocity of the red blood cell, and θ is the angle between the flow of red blood cells and the interrogating ultrasound beam. θ is referred to as the angle of incidence (Fig. 2). The transmitted frequency is the frequency transmitted, and c is the constant value of the speed of sound in blood, which is 1540 m/sec.

Noting that c , the speed of the sound of blood, and the transmitted frequency are constants, the equation can be simplified to reflect the fact that the Δf really depends on two variables, v and $\cos \theta$. If the flow of red blood cells and the interrogating ultrasound beam are parallel, the angle of incidence is 0° . Because $\cos 0^\circ = 1$, Δf will depend on blood velocity alone. In this way, if the ultrasound beam is parallel (angle is 0°), the Doppler equation will accurately reflect blood velocity. As the angle of incidence increases, the cosine of that angle decreases (Fig. 3), and Δf will be reduced, underestimating the true blood velocity. Finally if the ultrasound beam is perpendicular to the flow of red blood cells, the angle of incidence is 90° . Since $\cos 90^\circ = 0$, the Doppler system cannot appreciate any movement of blood. This concept of beam orientation is critical to understanding the basic Doppler technique. It has significant clinical implications, is often an area of confusion, and bears repeating. *If the angle of incidence is 0° , the measured velocity will be accurate. If the angle of incidence is anything other than 0° the measured velocity will be underestimated, never overestimated.*

As clinicians we are interested in the velocity of red blood cells because the velocity of red blood cells in a system reflects how that system is functioning. Therefore the velocity measured provides information on the structure being examined. Doppler



(A)



(B)

Figure 3 Angle of incidence. In this deep transgastric view of the AV, a gradient across the AV is measured at 0° (A) and at 29° (dark grey circle, B). The measured velocity results differ, not because the gradient has changed but because the angle of incidence has changed. If the ultrasound beam is not parallel to the blood flow, an underestimation of the blood flow velocity will occur. This, in turn, will underestimate the estimated gradient across the AV. *Abbreviation:* AV, aortic valve.

technology measures Doppler shift in order to calculate velocity. To solve for velocity, the Doppler equation is rearranged to become

$$v = \Delta f / \cos \theta \times c / 2(\text{transmitted } f)$$

Doppler technology assumes parallel blood flow, or an angle of incidence of 0° , and therefore $\cos \theta = 1$. If blood flow is not parallel, the angle of incidence is greater than 0° and the cosine of the angle will be less than 1. The true velocity will be higher than what is measured, because ultrasound technology defaults to an angle of 0° with a cosine of 1. For example, compare the following calculations. If Δf is 0.01 and the transmitted f is 7, the machine will assume that the angle of incidence is 0° and calculate velocity by the following equation:

$$v = \Delta f / \cos \theta \times c / 2(\text{transmitted } f)$$

$$v = 0.01 / \cos 0^\circ \times 1540 / 7$$

$$v = 0.01 / 1 \times 1540 / 7$$

$$v = 2.2 \text{ m/sec}$$

If blood flow is not parallel, let's say with an angle of incidence of 30° , the equation should be

$$v = \Delta f / \cos \theta \times c / 2(\text{transmitted } f)$$

$$v = 0.01 / \cos 30^\circ \times 1540 / 7$$

$$v = 0.01 / 0.87 \times 1540 / 7$$

$$v = 2.5 \text{ m/sec}$$

In this way, if blood flow is not parallel to the ultrasound beam, the default Doppler calculation (using an angle of 0°) will underestimate the true velocity (in our case calculating 2.2 m/sec instead of the true velocity of 2.5 m/sec). As the angle of incidence increases, the degree of underestimation increases. This underestimation is generally considered clinically acceptable if the angle of incidence is $\leq 30^\circ$.

DOPPLER TECHNIQUES

In the clinical arena, three Doppler techniques are commonly used to evaluate blood flow. They are pulse wave, continuous wave, and color flow. Each has its benefits and limitations. All are based on the concept of Doppler shift and the Doppler equation.

Pulse-Wave Doppler

Pulse-wave (PW) Doppler is used to interrogate blood velocity and the direction of blood flow at a specific point called the sample volume. For purposes of localization, the beam is superimposed on a two-dimensional image. The system is given the name pulsed because it repeatedly varies between transmitting and receiving ultrasound. It never transmits and receives at the same time, but repeatedly alternates (pulses) between transmitting and receiving. Simply, the system transmits a burst of ultrasound along the transmitted ultrasound beam. Multiple targets along the beam reflect this ultrasound, but the pulsed system only interprets information received after a fixed time interval. As the speed of sound in tissue is constant, the time delay from transmitting to receiving information is dependent only on the target's distance from the transducer. During PW Doppler, the system interprets signals only after a predetermined time. Therefore, signals at a specific

depth or location are the only signals that are evaluated. This process of selectively receiving and analyzing information from a specific distance away from the transducer is known as “range resolution.” Different depths or target sites can be interrogated by adjusting the timing between transmission and reception.

The PW Doppler system alternatively transmits and receives signals. The pulse repetition frequency refers to the rate at which the system repeatedly generates sound bursts. The term frequency here can be confusing. It does not refer to frequency as in “frequency and wavelength” but rather frequency in the sense of “how frequent.” The pulse repetition frequency will be low if the system waits a long time to transmit a pulse and high if it transmits the signal quickly. The pulse repetition frequency is directly related to the depth of the sample volume (the target being interrogated). One significant limitation to PW Doppler is that there is a limit to the maximal frequency or blood flow velocity that the system can accurately measure. The maximal frequency that can be accurately measured is known as the Nyquist limit. The Nyquist limit equals one half of the pulse repetition frequency. Above the Nyquist limit, analysis of returning information is inconclusive. If the Nyquist limit is exceeded, aliasing occurs and appears as a Doppler signal on the opposite side of the baseline. The signal appears to wrap around the baseline. If wraparound or aliasing occurs, velocity and direction of blood flow cannot be accurately interpreted (Fig. 4).

In summary, the advantage of PW Doppler is range resolution, which enables the system to interrogate blood flow and velocity at a specific location. The disadvantage of PW Doppler is that there is a maximal velocity that can be accurately measured. This velocity must be half of the pulse repetition frequency.

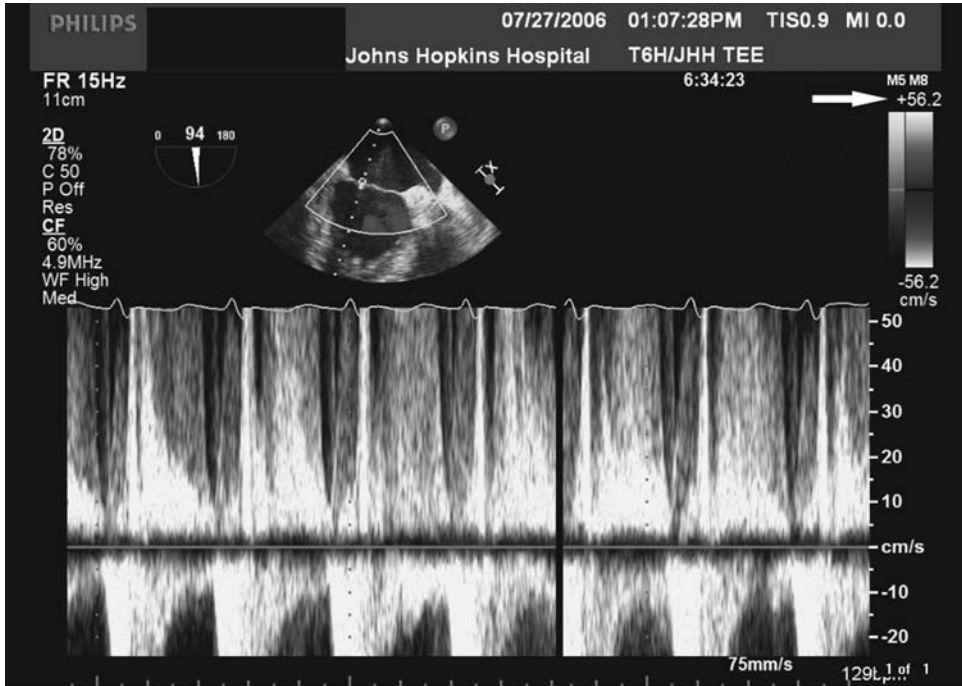
Continuous-Wave Doppler

As with PW Doppler, continuous-wave (CW) Doppler uses Doppler shift and the Doppler equation to measure the velocity of red blood cells. This technique differs from the pulsed technique in that it employs two crystals, one that continuously generates an ultrasound signal and one that continuously receives the reflected ultrasound signal. In this way, the Nyquist limit does not apply and aliasing does not occur. CW Doppler can measure much higher velocities compared with PW Doppler. In reality, CW Doppler can measure all velocities generated throughout the cardiac cycle. There is no physiological velocity that CW Doppler cannot measure. Although aliasing is not an issue, range ambiguity is. Range ambiguity refers to the fact that the exact location of the measured velocity is impossible to determine. All reflected signals along the ultrasound beam are simultaneously sampled. Direction and velocity of flow can be evaluated, but exact localization of blood flow is not possible.

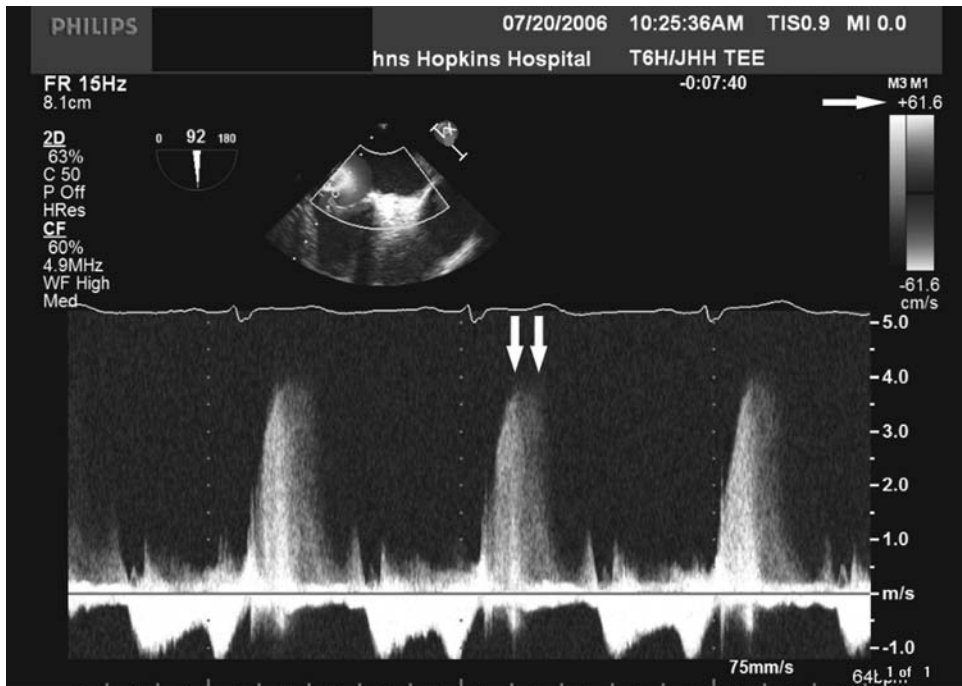
The display of CW Doppler also differs from that of PW Doppler in that CW Doppler incorporates a multitude of velocities and the spectral display is shaded throughout, while the PW Doppler spectral display reflects a more consistent velocity. As a result, the Doppler envelope of a pulse wave is generally cleaner in appearance compared with that of CW Doppler (Fig. 5). Comparing the specifics of CW Doppler with PW Doppler elucidates some of the advantages and disadvantages of the two techniques (Table 1).

Color Flow Doppler

Color flow Doppler is a third Doppler technique used to interrogate blood flow and direction. It is unique in that it provides both anatomical as well as blood flow information. This technique uses PW technology to evaluate blood flow and superimposes this information on a two-dimensional image. In order to do this, the system interrogates

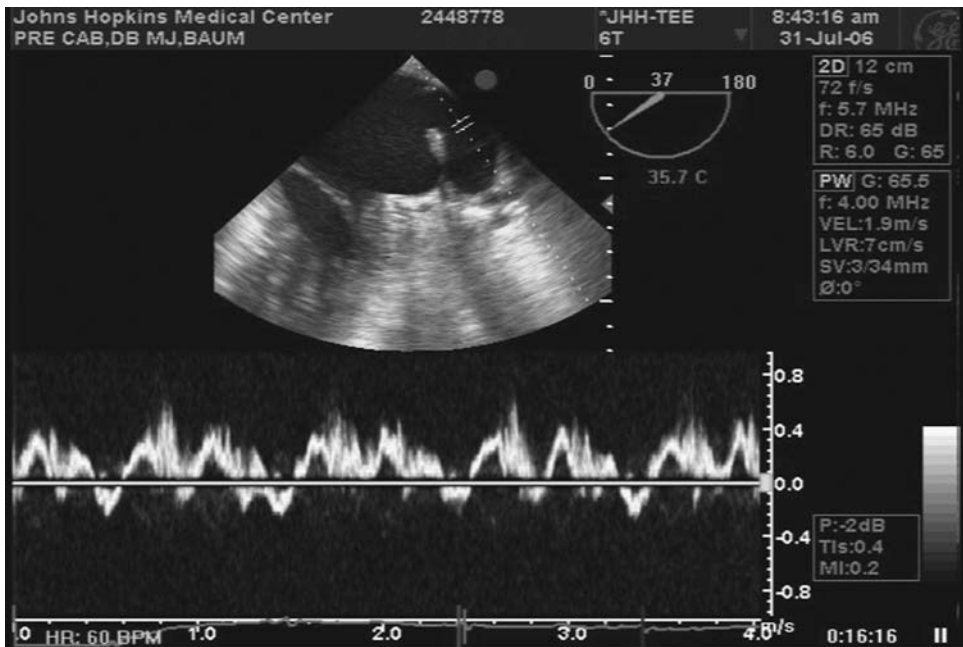


(A)

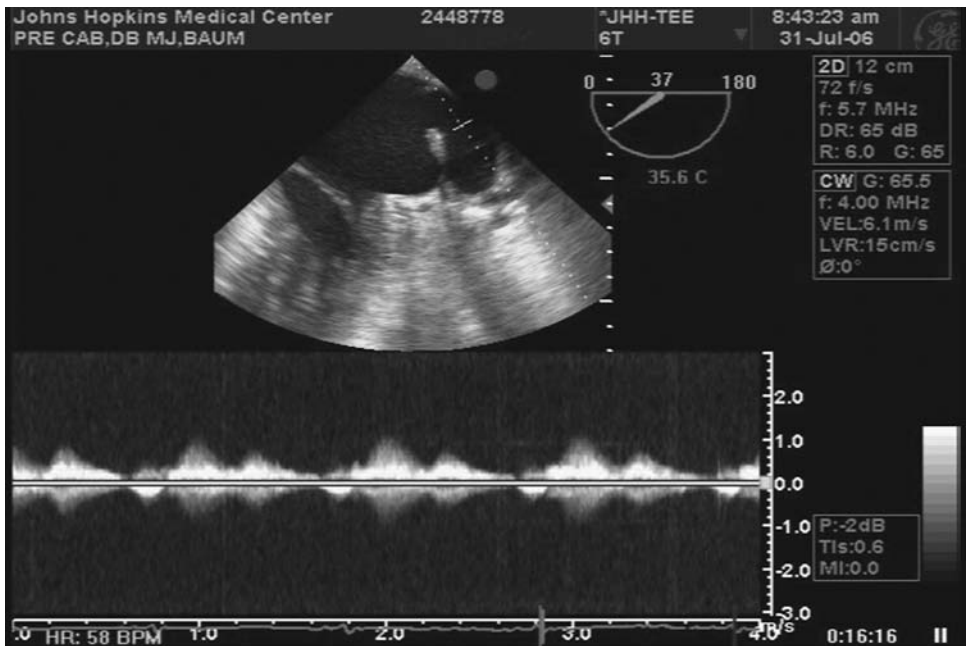


(B)

Figure 4 Aliasing. (A) In this view of the MV, the velocity measured exceeds the Nyquist limit (arrow) and aliasing occurs. Blood flow appears to wrap around the entire spectral display. (B) If the velocity scale is increased (arrow), the Nyquist limit is increased and aliasing no longer occurs. The spectral display no longer has the wraparound, and the velocity of blood flow can be appropriately measured (double arrows). Keep in mind that the velocity itself does not change. *Abbreviation:* MV, mitral valve.



(A)



(B)

Figure 5 PW and CW spectral display. (A) In this view of the LUPV, pulmonary venous blood flow is measured using PW Doppler. The spectral display is very clean. (B) In the same view of the LUPV, the pulmonary venous blood flow is measured using CW Doppler. All velocities along the axis of the ultrasound beam are measured. The resultant spectral display is much less crisp. *Abbreviations:* PW, pulse wave; CW, continuous wave; LUPV, left upper pulmonary vein.

Table 1 PW Doppler vs. CW Doppler

| Pulse wave | Continuous wave |
|--|---|
| Measures low velocities (usually <2 m/sec) | Measures high velocities (usually <9 m/sec; essentially all possible intracardiac velocities) |
| Measure velocities at a particular location | Measures all velocities along with axis of the ultrasound beam; records the highest velocity |
| No range ambiguity | Suffers from range ambiguity |
| Aliasing possible at high velocities | Intracardiac velocities too low for aliasing |
| Appropriate clinical uses | Appropriate clinical uses |
| LVOT and TVI | LVOT if a dynamic gradient |
| Mitral inflow velocities | Valvular pressure gradients (i.e., AV) |
| Evaluation of diastolic function | Evaluation of intracardiac pressures |
| Pulmonary and hepatic vein velocities | TR to evaluate RVSP |
| Locating a specific area of flow disturbance | VSD pressure gradients |

Abbreviations: LVOT, left ventricular outflow tract; TVI, time velocity integral; AV, aortic valve; TR, tricuspid regurgitation; RVSP, right ventricular systolic pressure; VSD, ventricular septal defect.

multiple sample volumes along the depth of each scan line. As the beam sweeps through the sector, multiple sample volumes are recorded. This, of course, differs from the above-mentioned pulse technique where the operator selects one specific sample volume. For each of these multiple sample volumes, direction and velocity of flow are calculated again utilizing principles of Doppler shift and the Doppler equation. The data regarding velocity and direction is then color coded. This color-coded result is superimposed on a two-dimensional image of the structure. Most often, blood flow away from the transducer is coded red and flow toward the transducer is coded blue. Velocity of blood flow plays a part in the color coding. As velocity increases, various color hues are displayed. High-velocity flow toward the transducer is often displayed as yellow, and high-velocity flow away from the transducer is often displayed as cyan. Areas of high turbulence result in directional variance and are encoded as green (Fig. 6).

Color flow Doppler is a great technique but has its own limitations. Because it uses the same technology as PW Doppler, it is susceptible to aliasing. Indeed, aliasing occurs at a lower velocity than that of PW Doppler because some of the technology is used to generate the two-dimensional image. One of the best uses of color flow Doppler is to first localize blood flow and then to quantify it more reliably than with PW or CW Doppler.

QUANTITATIVE DOPPLER: STROKE VOLUME CALCULATION

The above-mentioned Doppler techniques can be used to quantify cardiac flow, volume, and pressure. Some basic hemodynamic formulas are used for these calculations. These relatively noninvasive techniques correlate well with other more invasive methods. As in any Doppler measurement, proper parallel beam alignment is crucial.

In quantifying cardiac volumes, it is important to differentiate between blood flow velocity, volumetric flow, and stroke volume (SV). Often the units of measurement are helpful. Blood flow velocity is measured in cm/sec and is the speed at which blood travels. Volumetric flow is measured in cm^3/sec and is the amount of blood that is flowing per second. SV is expressed as cm^3/cycle and is the amount of blood flowing in a single cardiac cycle.



Figure 6 Color Doppler. In this view of the tricuspid valve, flow toward the transducer, flow away from the transducer, and turbulent blood flow is shown.

The flow rate through an orifice is the product of flow velocity and its cross-sectional area (CSA).

$$\text{Flow} = \text{Velocity} \times \text{CSA}$$

If flow is constant, the velocity measured at any point in time can be used for the equation. In the case of cardiovascular blood flow, flow is pulsatile and velocity varies throughout the cardiac cycle. To overcome this, individual velocities are sampled over one cardiac cycle and the sum of these velocities is integrated over time. This is known as the time velocity integral, or TVI. When velocity is integrated over time, the resulting units are a measure of distance; therefore the TVI units are expressed in centimeters. In this case the distance is termed stroke distance, which is the cumulative distance the red blood cells have traveled during a systolic ejection phase.

The second variable, CSA, is measured in square centimeters. When TVI and CSA are measured at the same point, their product equals SV.

$$\text{SV} = \text{TVI} \times \text{CSA}$$

SV quantifies the volume of blood ejected during one contraction and is measured in cubic centimeters. In the clinical setting, SV is an important parameter of cardiac performance.

SV and cardiac output (CO) are most reliably and easily measured at the left ventricular outflow tract (LVOT) or at the level of the aortic valve. Flow at the LVOT or aortic valve is most often laminar. Keep in mind that Doppler estimation is most accurate when measuring laminar flow. During the cardiac cycle, the CSA of some structures may vary but the CSAs of the LVOT and ascending aorta (because they are circular structures) change very little. Finally the entire stroke volume travels through these large structures.

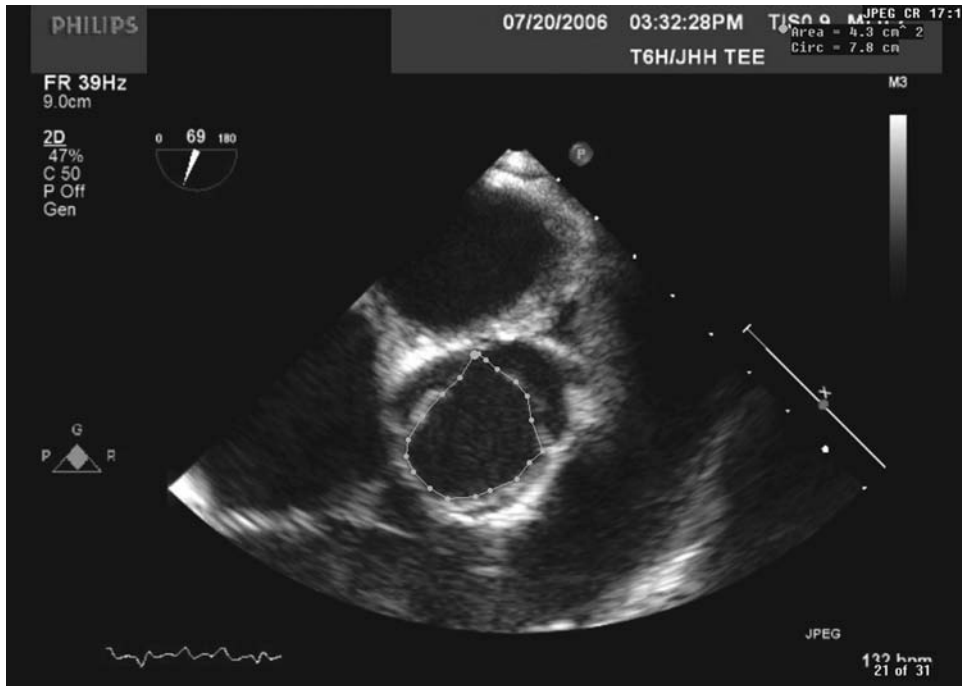


Figure 7 AV planimetry. The AV can be measured directly by planimetry. The valve opening is traced during systole in the ME AV short-axis view. This valve opens well and measures 4.3 cm². *Abbreviations:* AV, aortic valve; ME, midesophageal.

SV and CO can be measured at the level of the mitral valve or the pulmonary artery, but for the above reasons, this is less commonly done.

If measuring at the level of the aortic valve, the CSA of the valve can be measured using planimetry of a short-axis view of the aortic valve. In reality this is often easier said than done (Fig. 7). TVI is measured using CW Doppler with the Doppler beam directed through the valve orifice. Using transesophageal echocardiography, the transgastric or the deep transgastric long-axis views are the most helpful for this interrogation. If

$$\text{Flow} = \text{Velocity} \times \text{CSA}$$

the equation becomes

$$\text{Flow (SV)} = \text{TVI} \times \text{Aortic valve area}$$

Another approach is to measure the diameter of the LVOT and simply calculate its area. The area of a circle is

$$A = \pi r^2$$

The diameter of the LVOT is what is actually measured, so if $r = D/2$, the formula is simplified to

$$\begin{aligned} A &= \pi D^2 / 4 \text{ or} \\ A &= 3.14 / 4 (D^2) \text{ or} \\ A &= 0.785 (D^2) \end{aligned}$$

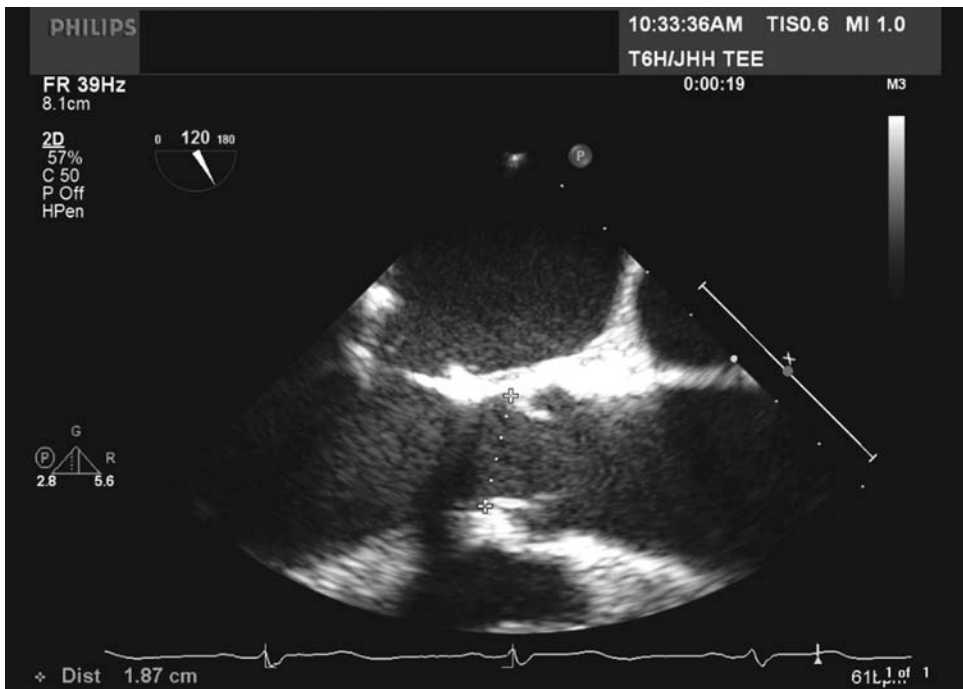


Figure 8 LVOT measurement. The diameter of the LVOT is measured in this long-axis view. Here the diameter measures 1.8 cm. In the formula for CO, the LVOT diameter is squared; therefore any error in this measurement greatly affects the calculated CO. *Abbreviations:* LVOT, left ventricular outflow tract; CO, cardiac output.

Multiple measurements of the LVOT diameter should be conducted. The largest diameter measured usually corresponds to the true diameter. The annular size does not vary much throughout the cardiac cycle, so the timing of this measurement is not crucial. The actual measurement is critical, in that the value is squared in the final formula. In this way, any error in measuring the LVOT will be exaggerated in the final outcome (Fig. 8).

If measuring at the level of the LVOT, TVI is measured using PW Doppler with the sample volume positioned in the LVOT just proximal to the aortic valve. The best transesophageal views for this measurement are the transgastric and deep transgastric long-axis views (Fig. 9). Therefore if measurements are taken at the level of the LVOT, SV is simplified by the following steps:

$$\text{Flow} = \text{Velocity} \times \text{CSA}$$

$$\text{Flow (or SV)} = \text{TVI} \times 0.785(D^2)$$

Of course, using either of these techniques, CO can be calculated by merely multiplying the product by heart rate.

INTRACARDIAC PRESSURE CALCULATIONS

Bernoulli Equation

The technology of both PW and CW Doppler provides measurement of the velocity of red blood cells. Once measured, this velocity can be used to provide an estimation of transvalvular pressure gradients and intracardiac pressures.

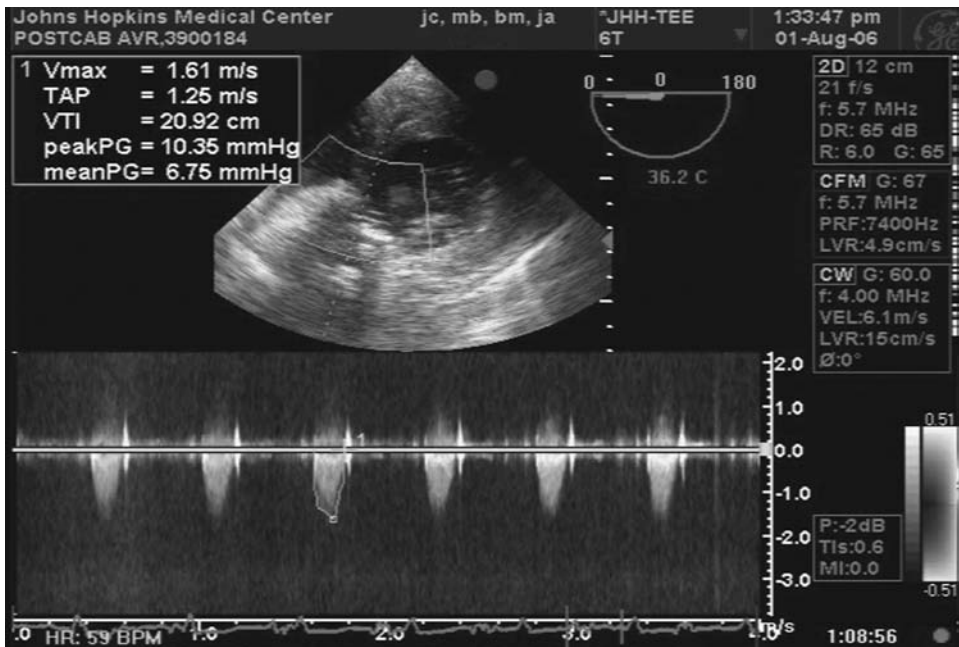


Figure 9 DTG LAX two-dimensional and TVI. TVI is traced and calculated in this DTG of the AV. Here TVI measures 20.9 cm and is used in the calculation of CO and SV. The maximal velocity across the AV is measured as 1.61 m/sec in this DTG view. Using the modified Bernoulli equation, $4v_2^2$, the peak gradient across this valve measures 10.35 mmHg. *Abbreviations:* DTG, deep transgastric view; LAX, long axis; TVI, time velocity integral; AV, aortic valve; CO, cardiac output; SV, stroke volume.

Generally, the velocity of blood traveling through a narrowed orifice depends on the size of the orifice. In simple terms, the narrower the orifice, the higher the velocity. In slightly more complicated terms, this is mathematically described by the Bernoulli equation:

$$\Delta P = 1/2\rho(v_2^2 - v_1^2) + \rho(dv/dt)dx + R(v)$$

where ΔP is the change in pressure, $1/2\rho(v_2^2 - v_1^2)$ refers to convection acceleration, $\rho(dv/dt)dx$ is flow acceleration, and $R(v)$ is viscous friction.

Flow acceleration, or $\rho(dv/dt)dx$, can be ignored in clinical settings. This is because our interest is in peak flows, and during peak flow, the flow acceleration is nonexistent. $R(v)$ represents the degree of energy lost due to viscous friction. Viscous friction is a function of blood viscosity and velocity. This term is insignificant for orifices with an area greater than 0.25 cm^2 in that blood flow is thought to be constant in that setting. Therefore, this term can also be ignored. Finally, convection acceleration, $1/2\rho(v_2^2 - v_1^2)$, can be simplified. The density of blood is $1.06 \times 10^3 \text{ kg/m}^3$ and is designated by the symbol ρ . The velocities distal and proximal to the area of interest are v_2 and v_1 respectively. With lesions of clinical significance, v_2 is far greater than v_1 . Keeping this in mind and noting that both terms are squared, the contribution of v_1 can be ignored, so that $v_2^2 - v_1^2$ can be simplified to merely v_2^2 .

In short, under most physiological conditions, both flow acceleration and viscous friction can be ignored. Convection acceleration can be simplified. In this way, the

Bernoulli equation then can be modified to what is known as the simplified Bernoulli equation, which is

$$\Delta P = 1/2\rho v_2^2$$

Converting to mmHg, the equation simplifies to

$$\Delta P = 4v_2^2$$

Thus, one of the most clinically significant applications of Doppler technology is the process of measuring the peak velocity of blood flow across a discrete lesion in order to estimate transvalvular gradients. This same technique can be used to measure intracardiac pressures.

There are a number of potential sources of error associated with this technique. These technical errors lead to an underestimation of the transvalvular pressure gradient. The most common error is inappropriate beam alignment. As previously discussed, aligning the ultrasound beam in any way that is nonparallel to blood flow results in an underestimation of velocity and therefore an underestimation of the pressure gradient. An angle of incidence greater than 30° underestimates the gradient significantly and is considered unacceptable. Color Doppler can first be used to visualize blood flow in order to optimize beam alignment. When possible, interrogating the area of interest in multiple views is suggested. Assessing multiple Doppler profiles, 5 for a regular rhythm and 10 for an irregular rhythm, is recommended.

The maximal velocity measured should be the velocity used for calculation of the pressure gradient. Assuming appropriate beam position, this maximal velocity can be measured by either PW or CW Doppler. If the maximal velocity is high and aliasing occurs with PW Doppler, CW Doppler should be utilized. Of course, CW Doppler carries with it the issue of range ambiguity, and there is the potential of interrogating the wrong flow signal.

The pressure gradients measured by Doppler technology are instantaneous gradients. The maximal velocity yields information about the maximum instantaneous gradient (Fig. 9). If the Doppler envelope is traced, the echocardiography machine can calculate the mean pressure gradient by averaging the Doppler-derived information over the period of flow. Discrepancies between Doppler-derived gradients and those gradients measured during cardiac catheterization can occur. Keep in mind that gradients are dynamic and may change over time and with varying clinical states. If the Doppler studies and catheterization measurements are not conducted at the same time, discrepancies may arise. Also, catheterization data often report peak-to-peak gradients. In aortic stenosis this pressure gradient is measured as the difference between the peak left ventricular pressure and the peak aortic pressure. These peak pressures occur at different times during the cardiac cycle. Doppler gradients, on the other hand, measure the gradient between the aorta and the left ventricle at the same time during the cardiac cycle, not necessarily at the points of peak pressure. As a result, the catheterization-derived gradient will be less than the Doppler-derived gradient.

Intracardiac Pressures

The simplified Bernoulli equation can also be used to evaluate intracardiac pressures.

$$\Delta P = 4v_2^2$$

Here ΔP is $P_1 - P_2$, the pressure difference between the proximal and distal cardiac chambers (Fig. 10). Doppler technology directly measures the velocity of flow between

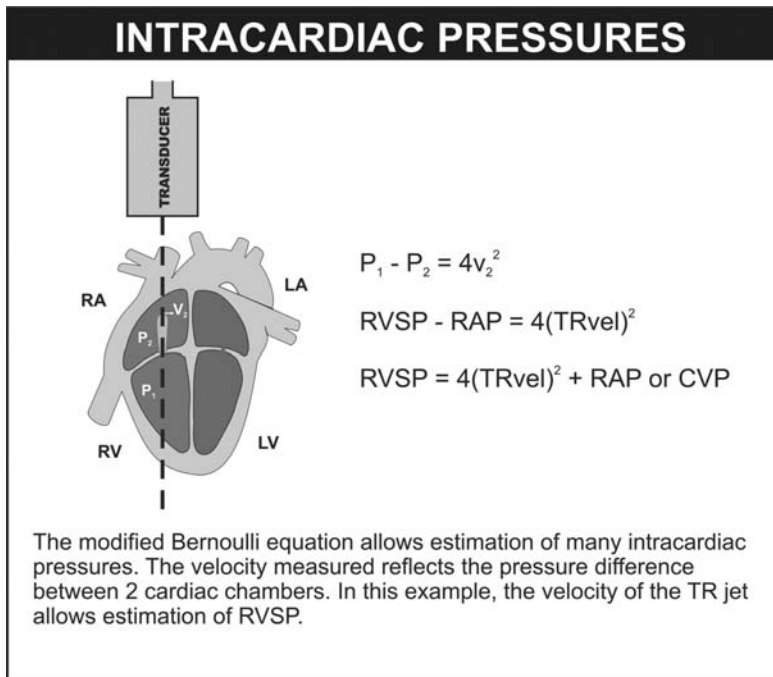


Figure 10 Intracardiac pressures.

the two cardiac chambers. If either P_2 or P_1 can be measured or estimated, the alternative pressure can be calculated using simple algebra. In this way, the right ventricular systolic pressure (RVSP), pulmonary artery mean pressure (PAMP), pulmonary artery diastolic pressure (PADP), left atrial pressure (LAP), and left ventricular end diastolic pressure (LVEDP) can all be estimated.

Right Ventricular Systolic Pressure

One common use of this calculation is estimating RVSP. The pressure gradient between the right atrium and the right ventricle is reflected by the velocity of the blood flowing through the tricuspid valve during systole. The higher the pressure difference between the right ventricle and the right atrium, the faster the velocity of the tricuspid regurgitation (TR) jet. Keep in mind there must be a regurgitant jet or the calculation cannot be made. The peak velocity of the TR jet is measured using CW Doppler. Right atrial pressure (RAP) or central venous pressure (CVP) is either measured or estimated. In this way, the simplified Bernoulli equation is expressed as

$$P_1 - P_2 = 4v_2^2$$

$$RVSP - RAP = 4(TR \text{ velocity})^2$$

By using simple algebra, RVSP can be calculated.

$$RVSP = 4(TR \text{ velocity})^2 + RAP$$

CVP can be used as an estimate of RAP, converting the equation to

$$RVSP = 4(TR \text{ velocity})^2 + CVP$$

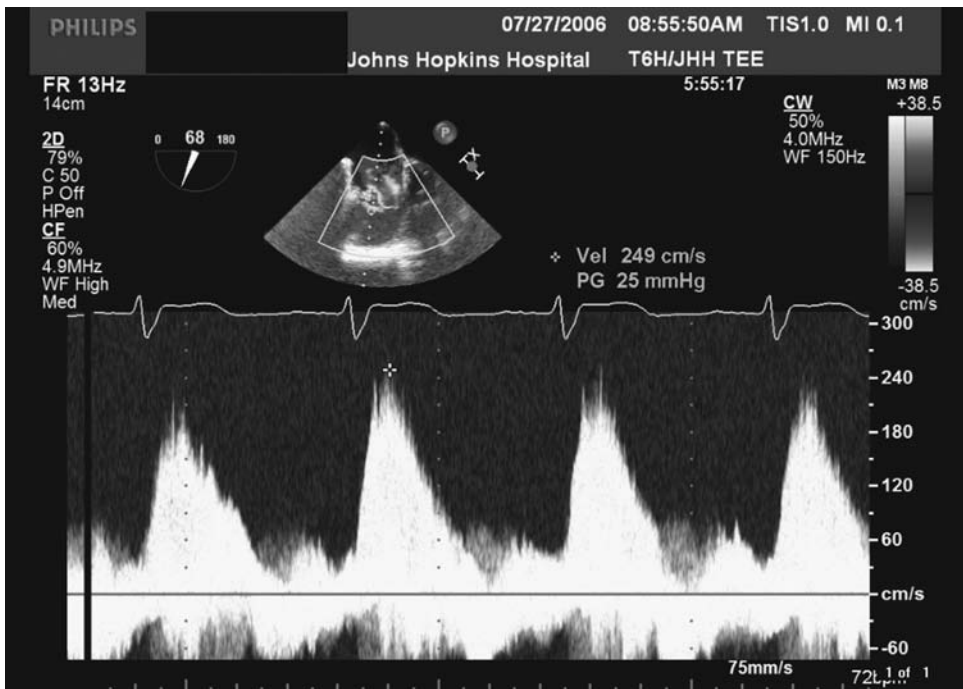


Figure 11 RVSP calculation. In this ME RV inflow-outflow LAX view, the velocity of the TR jet measures 249 cm/sec or 2.5 m/sec. The calculated gradient is 25 mmHg. Using the modified Bernoulli equation, $RVSP = 25 \text{ mmHg} + CVP$. *Abbreviations:* RVSP, right ventricular systolic pressure; ME, midesophageal; RV, right ventricular; LAX, long axis; TR, tricuspid regurgitation; CVP, central venous pressure.

RVSP and pulmonary artery systolic pressure (PASP) are essentially the same if there is no pulmonic valve stenosis or right ventricular outflow tract obstruction so that

$$RVSP \text{ or } PASP = 4(\text{TR velocity})^2 + CVP \text{ (Fig.11)}$$

Alternatively, RVSP can be estimated in patients with a left-to-right shunt by measuring the velocity of the ventricular septal defect (VSD) jet between the left ventricle and the right ventricle during systole. Left ventricular systolic pressure (LVSP) is assumed to be similar to the measured systolic blood pressure. Filling in the gaps in the simplified Bernoulli equation leads to

$$P_2 - P_1 = 4v_2^2$$

$$LVSP - RVSP = 4(\text{VSD velocity})^2$$

By using simple algebra, and assuming that LVSP is similar to systolic blood pressure, RVSP can be calculated as

$$RVSP = \text{Systolic blood pressure} - 4(\text{VSD velocity})^2$$

Pulmonary Artery Mean Pressure

The pressure gradient between the right ventricle and the pulmonary artery is reflected in the velocity of the pulmonic regurgitation jet during early diastole. This jet is measured

using CW Doppler. During diastole RVP and RAP are essentially the same. Again, RAP or CVP can be measured or estimated. Filling in the gaps in the simplified Bernoulli equation leads to

$$P_1 - P_2 = 4v_2^2$$

$$\text{PAMP} - \text{RVP} = 4(\text{Early PR velocity})^2$$

By using simple algebra, and assuming that RVP is similar to RAP or CVP during diastole, PAMP can be calculated as

$$\text{PAMP} = 4(\text{Early PR velocity})^2 + \text{CVP}$$

Pulmonary Artery Diastolic Pressure

At end diastole the velocity of the pulmonic regurgitation jet can be measured using CW Doppler. This velocity reflects the pressure difference between the pulmonary artery and the right ventricle at end diastole and can be used to calculate PADP. Again, right ventricular pressure is essentially the same as RAP during diastole. Filling in the gaps in the simplified Bernoulli equation leads to

$$P_1 - P_2 = 4v_2^2$$

$$\text{PADP} - \text{RVP} = 4(\text{Late PR velocity})^2$$

By using simple algebra, and assuming that RVP is similar to RAP or CVP during diastole, PADP can be calculated as

$$\text{PADP} = 4(\text{Late PR velocity})^2 + \text{CVP}$$

Keep in mind that with transesophageal echocardiography, parallel interrogation of the pulmonic regurgitation jet can often be technically challenging.

Left Atrial Pressure

Left atrial pressure can be estimated by interrogating flow across the mitral valve. The peak velocity of the mitral regurgitation (MR) jet reflects the pressure difference between the left atrium and the left ventricle. Assuming that left ventricular pressure is similar to systolic blood pressure, the simplified Bernoulli equation can be expressed as

$$P_1 - P_2 = 4v_2^2$$

$$\text{LVP} - \text{LAP} = 4(\text{MR velocity})^2$$

By using simple algebra

$$\text{LAP} = \text{Systolic blood pressure} - 4(\text{MR velocity})^2$$

If aortic stenosis or LVOT obstruction is present, systolic blood pressure will not approximate LVP and the formula cannot be used. CW Doppler is used to measure the MR jet from one of the midesophageal transesophageal echocardiography views. This enables parallel interrogation of blood flow (Fig. 12).

Left Ventricular End Diastolic Pressure

If aortic regurgitation (AR) is present, LVEDP can be estimated using the Doppler-measured velocity of the AR jet. The peak end diastolic velocity of the AR jet reflects the

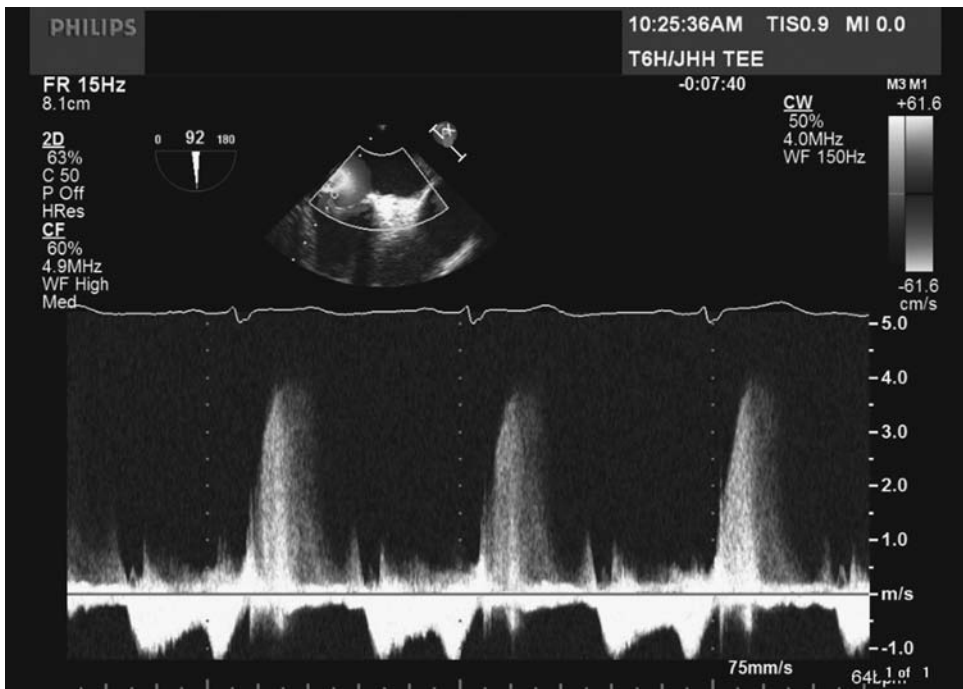


Figure 12 LAP. In this ME LAX view of the MV, the velocity of the regurgitant jet is 4 m/sec. The calculated gradient between the left atrium and left ventricle is therefore 64 mmHg. Using the modified Bernoulli equation, $LAP = SBP - 64$ mmHg. *Abbreviations:* LAP, left atrial pressure; ME, midesophageal; LAX, long axis; MV, mitral valve; SBP, systolic blood pressure.

pressure gradient between the aorta and the left ventricle during diastole. Filling in the gaps in the simplified Bernoulli equation leads to

$$P_1 - P_2 = 4v_2^2$$

$$\text{Systemic diastolic pressure} - \text{LVEDP} = 4(\text{AR velocity})^2$$

By simple algebra

$$\text{LVEDP} = \text{Systemic diastolic pressure} - 4(\text{AR velocity})^2$$

For all of the above calculations, Doppler technology is used to measure a velocity. This velocity is reflective of the pressure difference between the two cardiac chambers. One of the two pressures is either measured or estimated. The other pressure can then be calculated by using the simplified Bernoulli equation. Only simple algebra is required for this calculation.

CONCLUSION

Quantitative Doppler and two-dimensional echocardiography complement each other. Used in conjunction with one another, they provide quite an array of information on anatomy, blood flow, and valvular function. Understanding the principles of Doppler and recognizing its uses and its limitations is essential to appropriate ultrasound evaluation. There is much to understand about Doppler, but keep in mind some of these key elements.

1. Doppler technology allows measurement of blood flow velocity.
2. The velocity measured provides information on blood flow characteristics, pressure gradients, and anatomical abnormalities.
3. The interrogating ultrasound beam must be parallel to the flow of blood that is being interrogated. If the beam is nonparallel, the velocity measured will be underestimated, never overestimated.
4. PW Doppler measures velocity at one point along the ultrasound beam. If the velocity is very fast, aliasing can occur.
5. CW Doppler measures velocity at all points along the ultrasound beam. Aliasing does not occur, but range ambiguity is an issue.
6. Incorporating Doppler measurements into known and proven hemodynamic formulas provides much information on cardiac performance, valvular function, and intracardiac pressure gradients.

SUGGESTED READING

1. Feigenbaum H, Armstrong WF, Ryan T. Feigenbaum's Echocardiography. 6th ed. Philadelphia: Lippincott Williams & Wilkins, 2005.
2. Hatle L, Angelsen B. Doppler Ultrasound in Cardiology. Philadelphia: Lea & Febiger, 1985.
3. Nishimura RA, Miller FA, Callahan MJ, et al. Doppler echocardiography: theory, instrumentation, technique, and application. *Mayo Clin Proc* 1985; 60:321–343.
4. Perrino AC, Reeves ST. A Practical Approach to Transesophageal Echocardiography. Philadelphia: Lippincott Williams & Wilkins, 2003.
5. Quinones MA, Otto CM, Stoddard M, et al. Recommendations for the quantification of Doppler echocardiography: a report from the Doppler Quantification Task Force of the Nomenclature and Standards Committee of the American Society of Echocardiography. *J Am Soc Echocardiogr* 2002; 15:167–184.
6. Savage RM, Aronson S. Comprehensive Textbook of Intraoperative Transesophageal Echocardiography. Philadelphia: Lippincott Williams & Wilkins, 2005.
7. Yock PG, Popp RL. Noninvasive estimation of right ventricular systolic pressure by Doppler ultrasound in patients with tricuspid regurgitation. *Circulation* 1984; 70:657–662.

10

Transesophageal Doppler

Mark Hamilton

Department of Intensive Care, St. George's Hospital and Medical School, London, U.K.

Monty Mythen

*Anaesthesia and Critical Care, Institute of Child Health,
University College London, London, U.K.*

INTRODUCTION

The use of Doppler ultrasound to measure blood flow and cardiac output is not new. Originally, blood flow in the ascending aorta was measured at the suprasternal notch. The technique, however, was difficult to reproduce and the interindividual variability high. In the past 15 years, transesophageal Doppler monitoring measuring blood flow in the descending aorta has become more popular and reliable as a clinical tool, although some manufacturers have again started to produce suprasternal probes.

BASIC PRINCIPLES AND INSERTION METHOD

The technique of esophageal Doppler monitoring is based on measuring blood flow in the descending thoracic aorta and relies on the close anatomical relationship of the esophagus and the descending thoracic aorta.

Currently there are two major manufacturers of esophageal monitors, Deltex Medical Group plc, which produces CardioQ™, and Arrow International Inc., which produces the Hemosonic™ device. Both techniques involve the insertion of a flexible probe of small diameter into the esophagus. The CardioQ probe is equipped with a 4-MHz continuous-wave transducer, while the Hemosonic probe is a 5-MHz pulse-wave transducer, which is capable of measuring the aortic diameter using M-mode.

The probe is most commonly inserted orally in sedated/anesthetized patients who are being ventilated (see video 1). The probe of CardioQ is smaller in diameter and can be passed nasally, which has the advantage of improved stability for continuous cardiac output monitoring. A more flexible probe is also available for CardioQ, which may be inserted in awake patients under mild sedation and topical anesthesia (1) (see video 2). Once inserted the probe is gently advanced down the esophagus until the tip/transducer comes to rest at the midthoracic level T5-T6, approximately 35 to 40 cm from the teeth.

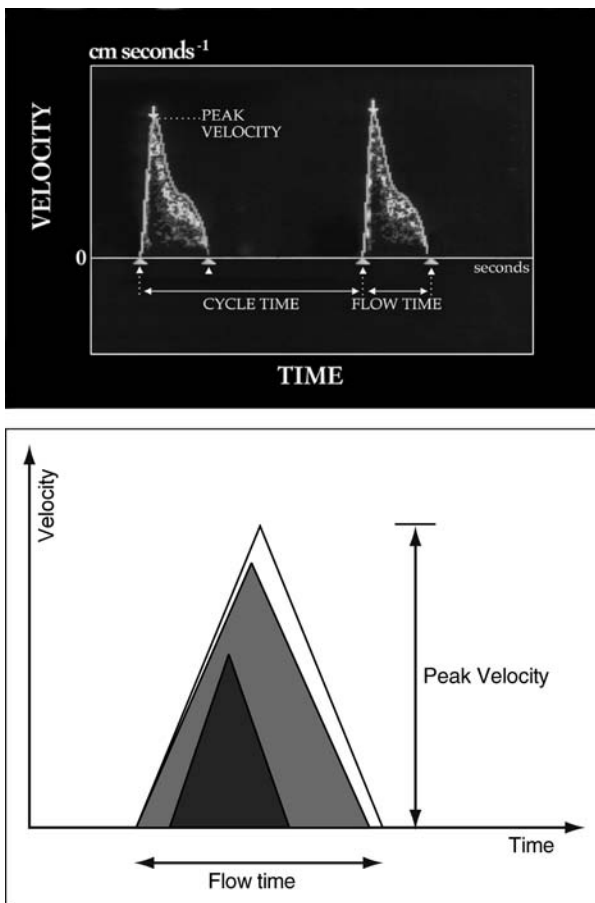


Figure 1 Schematic representation and screen shot of a “normal/characteristic waveform.” Visually there should be a dark/hollow center surrounded by red and then white in the trailing edge of the waveform. The waveform should be discrete and well contrasted with respect to the background.

The transducer needs to face posteriorly to insonate the descending aorta. This can be achieved by either slowly rotating the probe on its longitudinal axis or, more easily, by making sure it is facing the hard palate as it is being inserted. Once in approximately the right position, the characteristic Doppler velocity and sound waveform should be sought (Fig. 1). This will be the clearest signal with the highest peak velocity, which may need some adjustment to the depth of insertion of the probe. There are a number of characteristic waveforms that give some clue as to the position of the probe (Fig. 2). It is normal to have to adjust the gain control to get a sharp and clear waveform and eliminate any background interference; indeed if interference is marked due to low-frequency vessel wall motion (wall thump), a high-pass filter can be engaged. For the Hemosonic device a second transducer in the probe running at 10 MHz and insonating the aorta at right angles gives an M-mode echo from which the diameter of the aorta can be measured and the position of the probe checked.

Once in position and once a suitable waveform has been obtained, the measurement and calculation of stroke volume can be made. All techniques use the Doppler principle to calculate the velocity of aortic blood flow. The Doppler equation itself describes the

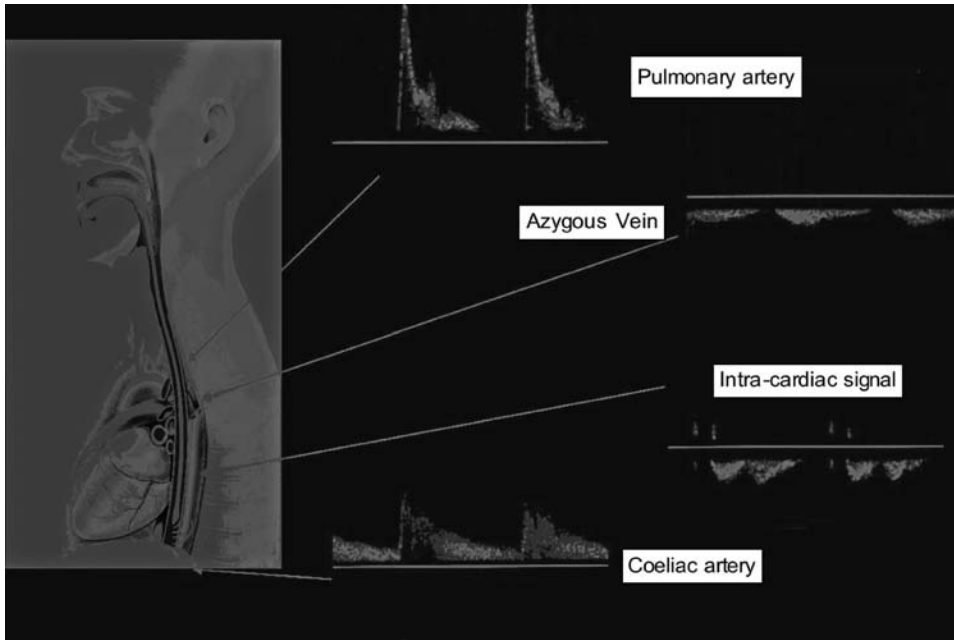


Figure 2 Some characteristic waveforms that give clues as to the position of the probe. Pulmonary artery showing a waveform very similar to the descending artery but often with the probe only 20–25 cm into the mouth. Intracardiac signal shows flow above and below the line, representing flow within the heart: as the probe is facing forward. It simply needs turning through 180° to face posteriorly for the correct signal. Celiac artery waveform looks and sounds very different and means the probe must be withdrawn a little.

relationship between the relative velocity of a moving object and the shift in frequency of sound waves either emitted by or reflected off that object—in this case the red blood cells. Doppler ultrasound is the technique whereby the Doppler effect is obtained using an acoustic carrier wave with a frequency exceeding the upper range of the human ear, i.e., greater than 20 KHz. By assuming a number of constants in the Doppler equation, the only unknown is the shift in frequency of the emitted ultrasound beam.

$$V = \frac{Cf_d}{2f_T \cos \theta}$$

- V = flow velocity
- C = speed of sound (in body tissue ~ 1540 m/sec)
- f_d = frequency shift (Hz)
- cos θ = cosine of angle between sound beam axis and velocity vector
- f_T = frequency of transmitted ultrasound (Hz)
- 2 = as using reflected ultrasound off a moving object

Note the equation has been rearranged to calculate velocity, which is primarily dependent on the frequency shift of the emitted ultrasound beam.

Measurement and calculation of stroke volume using esophageal Doppler is a derivation from principles used in transthoracic stroke volume measurement in the left ventricular outflow tract (2) (Fig. 3).

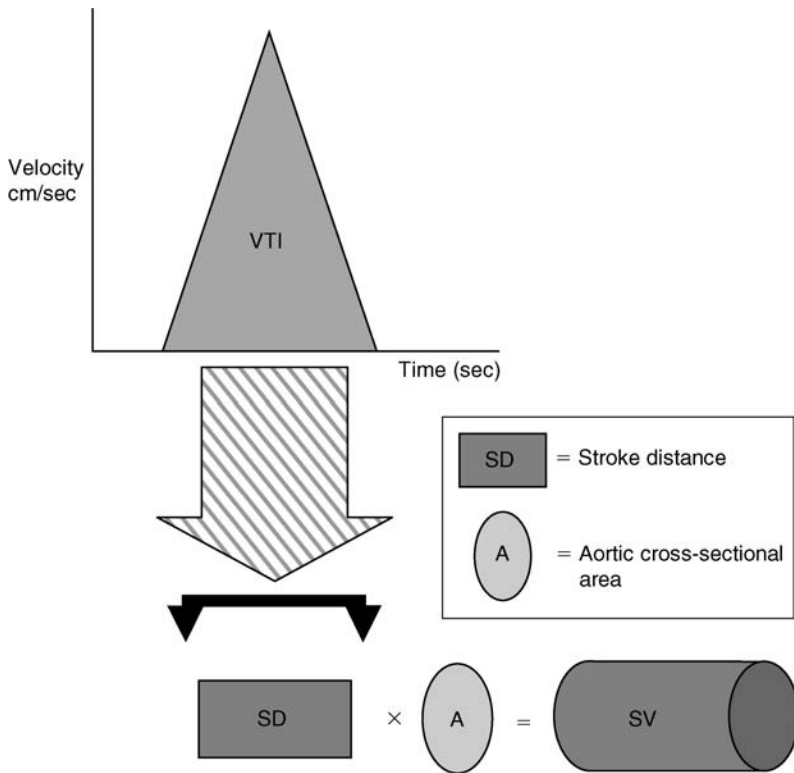


Figure 3 Principles of stroke volume calculation from aortic velocity measurements. Once integrated, the area under the maximum aortic velocity envelope (VTI) represents SD. Assuming little variation of aortic diameter (A) during systole and that all red blood cells are moving at maximum velocity, multiplying SD by the aortic cross-sectional area will give SV. *Abbreviations:* VTI, velocity time integral; SD, stroke distance; SV, stroke volume.

For the derivation to work, a number of assumptions have to be made.

1. The distribution of blood caudally to the descending aorta and rostrally to the great vessels and coronary arteries maintains a constant ratio of 70% to 30% (3).
2. A flat velocity profile exists within the aorta. The flow is in fact mildly parabolic; hence the ratio of the maximum velocity time integral (VTI) to envelope is used, which may inadvertently overestimate cardiac output (4).
3. The estimated cross-sectional area is close to the mean systolic diameter.
4. There is negligible diastolic blood flow.
5. The velocity of blood flow in the aorta is measured accurately.

The accuracy of the signal is best assessed subjectively through simultaneous visual inspection of the Doppler waveform and listening to the Doppler sound. The signal should be a well-defined triangle with a black center surrounded by red and then some white in the trailing edge of the waveform. This color spectrum displays the distribution of red blood cell velocities at a given point in time, i.e., a histogram of velocities over time. The brighter (whiter) the color in the display, the greater the number of red blood cells traveling at that given velocity. The angle of insonation is kept constant at 45° by its mounting angle on the probe, and this is corrected in the $\cos \theta$ portion of the velocity equation as the probe lies parallel to the aorta in the esophagus.

In order to find the cross-sectional area of the aorta, each manufacturer uses a different solution. The Hemosonic device uses M-mode echocardiography to measure the aortic diameter, while CardioQ uses a nomogram based on age, weight, and height to estimate the aortic diameter (5). One would expect that the direct measurement technique would result in a more accurate aortic cross-sectional area and hence stroke volume measurement.

INTERPRETATION OF WAVEFORM AND VARIABLES

Esophageal Doppler is a simple, easy, and reliable technique that most users can master after 12 or so uses (6), and most can obtain readings with minimal training. Although difficult to quantify, the shape of the VTI can be diagnostic in many cases (Fig. 4).

Transesophageal Doppler is capable of measuring a multitude of hemodynamic variables that add additional information to the shape of the waveform, as outlined below.

Contractility. Peak velocity (PV) of blood within the aorta gives a good estimate of contractility. PV is age dependent and behaves in a predictable manner, i.e., it is reduced with beta blockade and increased with positive inotropes (Table 1).

Stroke volume/cardiac output. Stroke distance is the area under the maximal velocity time curve/waveform and when multiplied by the aortic diameter gives a good estimate of stroke volume. Multiplying the stroke volume by the heart rate results in the cardiac output.

Preload. Blood flow during systole is measured as the flow time. Flow time is affected by heart rate, limiting its use. When divided by the square root of the heart rate, however, it becomes a useful index of preload and afterload,

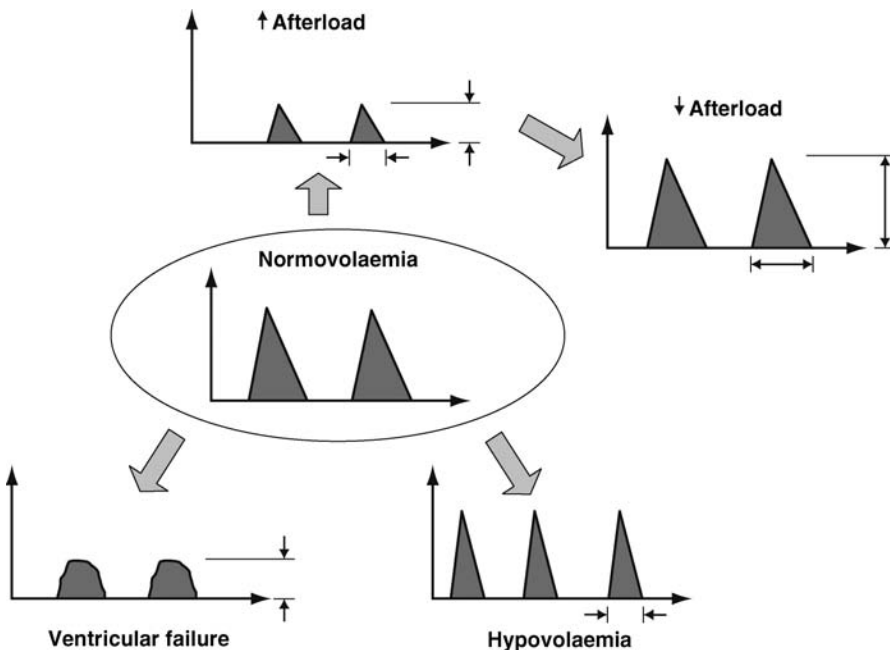


Figure 4 Characteristic shapes of VTI showing predominant changes in FTc and PV. Normal and decreased afterload of a little different shape and accentuated slightly. *Abbreviations:* VTI, velocity time integral; FTc, corrected flow time; PV, peak velocity.

Table 1 Normal Values

| | Age (yr) | Velocity (cm/sec) |
|----------------------|--------------|-------------------|
| Peak velocity | 20 | 90–120 |
| | 50 | 70–100 |
| | 70 | 50–80 |
| FTc | 330–360 msec | |

Abbreviation: FTc, corrected flow time.

termed the corrected flow time (FTc). Anything that impedes filling or emptying of the left ventricle will result in a low FTc (<330 msec). Most commonly this will be due to hypovolemia; however, obstruction from mitral stenosis or pulmonary embolism will give similar results.

As in interpreting electrocardiograms, there is a degree of pattern recognition that goes with interpretation and diagnosis from various waveforms and hemodynamic data. Figure 5 shows some example screen shots from a variety of clinical situations.

CLINICAL USE AS A HEMODYNAMIC MONITOR

To date there has been no mortality associated with the use of transesophageal Doppler. Morbidity is also astoundingly rare given the number of probe insertions per year. There are case reports of the probe inadvertently being inserted into the left or right main bronchus and episodes of nasal bleeding from nasal insertion, but no more so than conventional nasogastric tubes.

Suggested Action from Readings

A single reading may be diagnostic but most commonly is just a starting point from which to dynamically challenge/optimize the cardiovascular system.

Low stroke volume: Fluid is best given in boluses, e.g., 200–300 mL, to construct a Starling curve for that patient. One should look for a 5% to 10% improvement with each bolus and stop when the Starling curve begins to plateau (Fig. 6).

Low FTc: This most commonly represents hypovolemia, and the circulation should be challenged as above to achieve an FTc of 330 to 360 milliseconds. It should be remembered, however, that there are other, less common causes for a low FT_c, such as pulmonary embolism, which will not correct with fluid alone.

Low PV: Consider use of a positive inotrope.

Low PV and low FTc: Consider agents/maneuvers to decrease afterload, e.g., glyceryl trinitrate, peripheral warming, or reduction of vasoconstrictors.

PRACTICAL TIPS

1. When inserting the probe it is vital to lubricate the probe generously with an aqueous jelly, such as KY, prior to insertion. Not only does it make the probe far easier to insert but allows for a faster and more reliable signal acquisition. Air drastically attenuates the quality of ultrasound signals, but the lubricant provides good acoustic coupling between the probe and the esophageal wall.

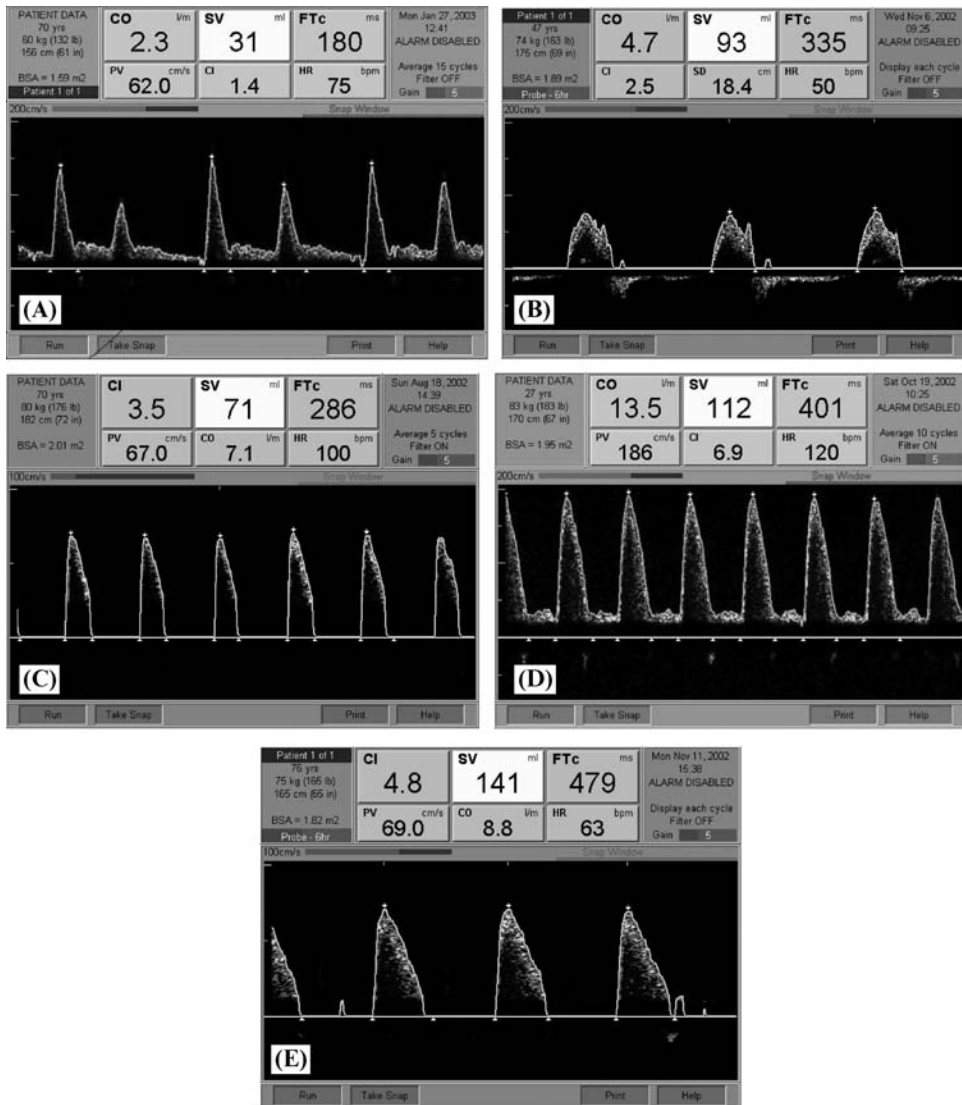


Figure 5 Example screen shots of various clinical conditions. (A) Atrial fibrillation: Note the two beats that do not take part in the cardiac output calculations (the ones without three little white arrows) and the long cycle length of 15 to average out the data more consistently. (B) Aortic regurgitation: Note the presence of flow below the baseline, which is greater than 50% of the diastolic period. (C) Hypovolemia: Note the narrow look to the waveform, which is confirmed by an FTc of 286. (D) Hyperdynamic pattern: Note the very high PV (186) for a 27 year old. (E) Sepsis: Note in particular the abnormally long FTc at 479. *Abbreviations:* FTc, corrected flow time; PV, peak velocity.

2. Orientating the probe so that the 45° angle is facing the hard palette prior to insertion will give a greater chance of correct positioning by maximizing the chances of the probe facing posteriorly and hence toward the aorta.
3. Transesophageal Doppler calculates velocity from the shift in frequency of a beam returning from the aorta, which it can translate into sound. By turning the volume up on the machine, it is easier to hear when a vessel is being insonated

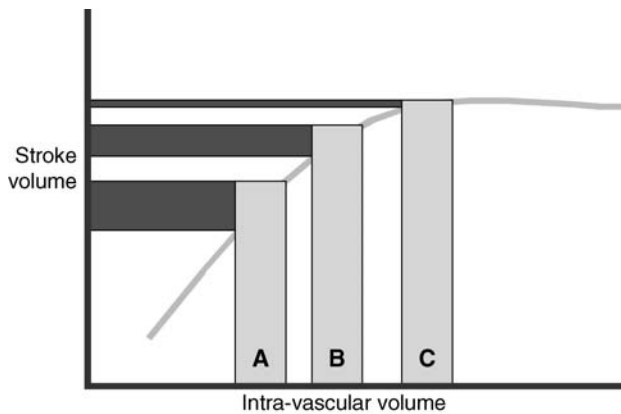


Figure 6 Starling curve showing the administration of three identical, i.e., 200 mL boluses of fluid. (A) Shows a large increase in stroke volume. (B) Shows a smaller but still significant increase in stroke volume. (C) As the plateau of the Starling curve is reached, there is little improvement in SV and would suggest optimal volume optimization. *Abbreviation:* SV, stroke volume.

and then allow more careful focusing of the probe. It is not uncommon to be able to hear the correct signal before seeing the waveform appear on the screen and consequently adjusting the gain. The sharpest sound with the best pitch is invariably the right waveform.

4. Adjusting the cycle length and gain:
 - a. Cycle length is essentially a measure of heart rate. By lengthening the “cycle length” in irregular rhythms, it is possible to increase accuracy. A cycle length of five is generally a good starting point.
 - b. Gain adjusts the contrast between background noise and the Doppler waveform. Aiming for a black background is important to sharply focus the Doppler waveform, which will allow the calculation software to more easily distinguish signal from artifact. A gain of five is again a good starting point.
5. The machines have a sensitivity algorithm built in that will attempt to identify artifact from true signal. If there is a great deal of variability in the cardiac output, e.g., in pulsus alternans or dropped beats, then the machine may inadvertently miscount the heart rate, leading to inaccurate cardiac output values. Always, therefore, visually check that each waveform is being counted, i.e., it has a small white triangle in each corner.
6. For the majority of patients, probe insertion and signal acquisition will be straightforward. For those in whom it is not, it is important to remain patient when focusing the probe. Some people have remarkable small acoustic windows through which the signal may be obtained.
7. Interference from diathermy is impossible to eliminate, but setting a cycle length of one will allow some useful information to be gained on a beat-to-beat basis when the opportunity allows.
8. Although the normal range for FTc is quoted as 330 to 360 milliseconds for patients under general anesthesia and particularly those with the addition of an epidural, an FTc approaching 400 milliseconds would be normal for a well-dilated and filled patient.

9. It is a dynamic monitor and as such must be refocused prior to each reading. Despite the fact that it is capable of giving a continuous cardiac output reading, it is important to maintain a well-focused signal for the technical reasons already outlined.

PERIOPERATIVE AND CRITICAL CARE STUDIES

Optimization of the High-Risk Surgical Patient

In the past 20 years numerous studies have shown that approaches at goal-directed hemodynamic therapy have improved mortality and morbidity (7–10). To date there have been eight peer-reviewed studies that have used esophageal Doppler to guide hemodynamic therapy and improve patient care (11–18).

The first study by Mythen and Webb in 1995 set out to reduce the incidence of gut mucosal hypoperfusion as judged by gastric tonometry in cardiac surgical patients (14). They followed a simple protocol aiming to maximize stroke volume with bolus colloid administration. Not only did they dramatically cut the incidence of mucosal hypoperfusion in the protocol group but they reduced the rate of major complications and the length of stay in the hospital and intensive care unit.

Sinclair et al. followed in 1997 with the only emergency study, which looked at orthopedic fractured neck of femur patients (16). They again used an algorithm-based approach to bolus colloid administration but used a combination of stroke volume and FTc in their algorithm. They showed a not unsurprising increase in stroke volume and cardiac output in the protocol group but also a significant decrease in the time patients were fit to be discharged.

Three studies then appeared in 2002 from Conway, Gan, and Venn. Conway et al. were the first to look exclusively at major bowel surgery patients, but did not show a significant difference in length of stay between groups (11). It should be noted, however, that the study was only powered to detect a difference in cardiac output between the two groups, not postoperative morbidity or mortality. Gan and colleagues used a combination of FTc and stroke volume–guided fluid administration algorithm to reduce length of stay and the incidence of nausea and vomiting and show an earlier return of bowel function in the active protocol group (12). Venn et al. studied a similar group of orthopedic patients as Sinclair did five years earlier. Only this time, they compared fluid resuscitation guided by central venous pressure (CVP) or Doppler and compared them to a control group. Outcome benefits were seen for both the CVP and Doppler groups. The Doppler group was, however, medically fit for discharge sooner, and the CVP group had a number of morbid events associated with CVP insertion (17).

The study by Wakeling et al. in 2005 compared outcomes from a well-resuscitated control group to a dynamically resuscitated Doppler group of colorectal patients in the largest randomized control study, to date, of 128 patients. Length of stay and morbidity were both significantly reduced in the protocol group (18).

The most recent study of 2006 by Noblett et al. from the Freeman Hospital in Newcastle looked at elective colorectal resection patients. They used a predominantly FTc-guided algorithm whereby patients in the protocol group were relatively aggressively resuscitated to achieve a normal FTc. Interestingly, despite receiving more fluid initially, the total volumes of fluid given to the protocol and control groups were similar. Consistent with previous studies, they were able to demonstrate reductions in the length of stay and complication rate, as well as a reduced level of IL 6 in the protocol group, suggesting a limited inflammatory response (15).

A systematic review and meta-analysis of clinical studies using Doppler supports the reduction in the length of hospital stay of nearly three days, but also suggests that patients tended to get less crystalloid and more colloid during surgery, 166 mL and 661 mL, respectively (19).

Validation and Comparison Studies

Inevitably there will always be debate as to the “accuracy” of a monitor and how it performs compared to other comparable technologies. Dark and Singer recently reviewed the validity of esophageal Doppler as a measure of cardiac output in the critically ill (20). They concluded that “*the oesophageal Doppler monitor has a high validity (no bias and high clinical agreement with pulmonary artery catheter thermodilution) for monitoring changes in cardiac output.*” From pooled data they found that the median bias for thermodilution pulmonary artery catheter versus esophageal Doppler was 0.19 L/min (range -0.69–2 L/min) for cardiac output and 0.6% (range 0–2.3%) for changes in cardiac output. There are fewer data with which to make such comparisons with other cardiac output monitors, but clinical experience shows little difference between comparable and clinically useful monitors.

CONCLUSION

There is a strong and expanding evidence base behind the clinical use of esophageal Doppler monitoring in both surgery and critical care. Its use has led to improvements in patient outcome through the use of algorithms based on measured and calculated Doppler data. It is a relatively simple technology that for the most part is easy to use and learn, is minimally invasive, and has a good safety profile. Real-time hemodynamic data acquisition is achievable within minutes, allowing both diagnostic and therapeutic treatment at the point of need.

REFERENCES

1. Walker D, Usher S, Hartin J, et al. Early experiences with the new awake oesophageal Doppler probe. *Br J Anaesth* 2004; 93(3):471.
2. Huntsman LL, Stewart DK, Barnes SR, et al. Noninvasive Doppler determination of cardiac output in man. Clinical validation. *Circulation* 1983; 67(3):593–602.
3. Boulnois JL, Pechoux T. Non-invasive cardiac output monitoring by aortic blood flow measurement with the Dynemo 3000. *J Clin Monit Comput* 2000; 16(2):127–140.
4. Daigle RE, Miller CW, Hstand MB, et al. Nontraumatic aortic blood flow sensing by use of an ultrasonic esophageal probe. *J Appl Physiol* 1975; 38(6):1153–1160.
5. Singer M, Clarke J, Bennett ED. Continuous hemodynamic monitoring by esophageal Doppler. *Crit Care Med* 1989; 17(5):447–452.
6. Lefrant JY, Bruelle P, Aya AG, et al. Training is required to improve the reliability of esophageal Doppler to measure cardiac output in critically ill patients. *Intensive Care Med* 1998; 24(4):347–352.
7. Bishop MH, Shoemaker WC, Appel PL, et al. Prospective, randomized trial of survivor values of cardiac index, oxygen delivery, and oxygen consumption as resuscitation endpoints in severe trauma. *J Trauma* 1995; 38(5):780–787.
8. Boyd O, Grounds RM, Bennett ED. A randomized clinical trial of the effect of deliberate perioperative increase of oxygen delivery on mortality in high-risk surgical patients. *JAMA* 1993; 270(22):2699–2707.

9. Rivers E, Nguyen B, Havstad S, et al. Early goal-directed therapy in the treatment of severe sepsis and septic shock. *N Engl J Med* 2001; 345(19):1368–1377.
10. Wilson J, Woods I, Fawcett J, et al. Reducing the risk of major elective surgery: randomised controlled trial of preoperative optimisation of oxygen delivery. *BMJ* 1999; 318(7191):1099–1103.
11. Conway DH, Mayall R, Abdul-Latif MS, et al. Randomised controlled trial investigating the influence of intravenous fluid titration using oesophageal Doppler monitoring during bowel surgery. *Anaesthesia* 2002; 57(9):845–849.
12. Gan TJ, Soppitt A, Maroof M, et al. Goal-directed intraoperative fluid administration reduces length of hospital stay after major surgery. *Anesthesiology* 2002; 97(4):820–826.
13. McKendry M, McGloin H, Saberi D, et al. Randomised controlled trial assessing the impact of a nurse delivered, flow monitored protocol for optimisation of circulatory status after cardiac surgery. *BMJ* 2004; 329(7460):258.
14. Mythen MG, Webb AR. Perioperative plasma volume expansion reduces the incidence of gut mucosal hypoperfusion during cardiac surgery. *Arch Surg* 1995; 130(4):423–429.
15. Noblett SE, Snowden CP, Shenton BK, et al. Randomized clinical trial assessing the effect of Doppler-optimized fluid management on outcome after elective colorectal resection. *Br J Surg* 2006; 93(9):1069–1076.
16. Sinclair S, James S, Singer M. Intraoperative intravascular volume optimisation and length of hospital stay after repair of proximal femoral fracture: randomised controlled trial. *BMJ* 1997; 315(7113):909–912.
17. Venn R, Steele A, Richardson P, et al. Randomized controlled trial to investigate influence of the fluid challenge on duration of hospital stay and perioperative morbidity in patients with hip fractures. *Br J Anaesth* 2002; 88(1):65–71.
18. Wakeling HG, McFall MR, Jenkins CS, et al. Intraoperative oesophageal Doppler guided fluid management shortens postoperative hospital stay after major bowel surgery. *Br J Anaesth* 2005; 95(5): 634–642.
19. Hamilton MA, Grocott MPW, Mythen M, et al. Does goal directed therapy using the oesophageal Doppler reduce surgical mortality and morbidity? *Intensive Care Med* 2006; 32(suppl 1):2060–2066 (abstr).
20. Dark PM, Singer M. The validity of trans-oesophageal Doppler ultrasonography as a measure of cardiac output in critically ill adults. *Intensive Care Med* 2004; 30(11):2060–2066.

11

Transcranial Doppler Ultrasonography

Alet Jacobs

Department of Anaesthesia, Nottingham University Hospital, Queen's Medical Centre, Nottingham, U.K.

Ravi P. Mahajan

University Division of Anaesthesia and Intensive Care, Queen's Medical Centre, Nottingham, U.K.

INTRODUCTION

Since its introduction by Aaslid and colleagues in 1982, transcranial Doppler (TCD) ultrasonography has rapidly evolved as a noninvasive technique for measuring blood flow velocity (FV) in the major intracranial arteries. TCD has been described as a stethoscope of the brain, allowing the clinician to “listen” for the changes in cerebral circulation. The main advantages are that it is safe, noninvasive, easy to use, portable, reproducible, and versatile; provides continuous online beat-to-beat information; and does not involve the use of radioactive substances. It is particularly useful in the investigation of vascular reactivity because it can detect rapid changes in FV instantaneously (1).

TCD was initially used for the detection of vasospasm following subarachnoid hemorrhage (SAH). Its applications have now expanded in critical care and research. In recent years, it has made immense contributions to our understanding of cerebral hemodynamics, including autoregulation and vascular reactivity.

The accuracy and interpretation of TCD is operator dependent. It requires a thorough knowledge of the basic principles and technique and the normal anatomy and physiology of the cerebral vasculature.

BASIC PRINCIPLES

TCD uses a 2-MHz probe—in this low-frequency range the ultrasound beam is able to penetrate thin areas of the skull. The probe emits an ultrasonic beam in a range-gated, pulsed-wave manner. The use of a range-gated Doppler beam allows selective sampling from cerebral arteries at specified depths. Pulse-wave Doppler implies that intermittent bursts of ultrasound waves are emitted followed by a period of “listening.” The interval between emission and reception of the beam allows calculation of the depth from which the reflected signal arose. Therefore, the depth of insonation can be adjusted by altering the interval between signal emission and reception.

The ultrasonic beam crosses the skull at points known as “windows” where the bone is thin enough to allow penetration of the beam. The ultrasonic beam, after having crossed the skull, is reflected back by the circulating red cells in its path. The change in frequency of the reflected beam is known as the Doppler frequency shift, and thus it is the difference between the transmitted and reflected frequencies. The frequency shift allows calculation of the blood flow velocity.

Frequency shift = Reflected frequency – Transmitted frequency

$$\text{Doppler frequency shift } (F) = \frac{2VF_t \cos \theta}{C}$$

$$\text{And therefore, } V = \frac{FC}{2F_t \cos \theta}$$

where F = Doppler frequency shift

V = Velocity of the red cells

F_t = Transmitted frequency (2 MHz)

C = Speed of sound in soft tissue (1540 m/sec)

$\cos \theta$ = correction factor for angle of incidence

In the above, F_t and C remain constant, and therefore the Doppler frequency shift depends mainly on the blood flow velocity (V) and the angle of incidence of the probe.

$\cos \theta$ is based on the angle of incidence between the ultrasound beam and the vessel, which is usually unknown, but is assumed to be less than 30° . If θ is 0° the cosine is 1. At an angle of 15° , the cosine remains more than 0.96, and therefore in this range an error caused by a change in angle is less than 4%. However, at an angle close to 30° , the measurement error becomes significant resulting in a difference of up to 15% between the real and the measured velocities. This should be taken into account when conclusions are based on absolute values of FV measured on different occasions. On the other hand, in order to use TCD reliably to make comparisons between repeated measurements of FV, it is vital that the angle of insonation be kept constant. In practice, this can be achieved by use of head bands to fix the probe to the skull (Fig. 1).



Figure 1 Use of a headband to fix the probe to the temporal window.

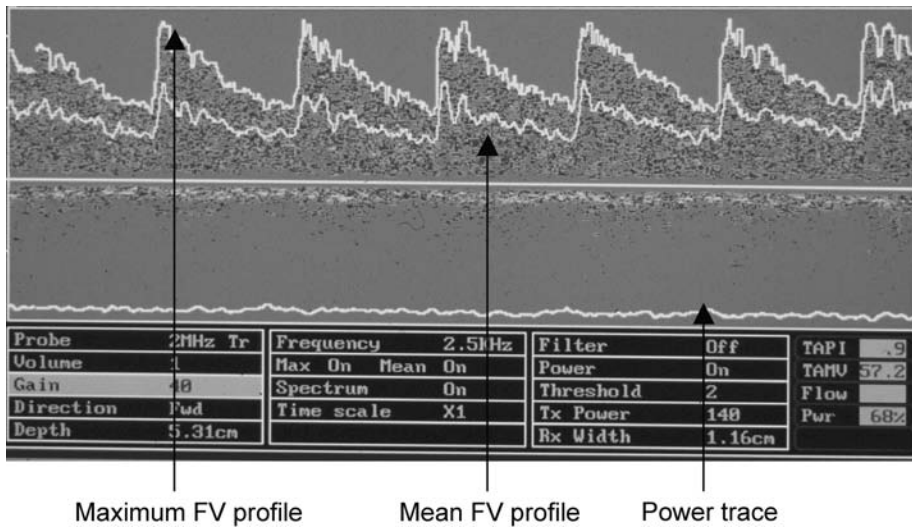


Figure 2 FV waveforms of the MCA. The outer pulsatile white line (outer envelope) represents maximal velocity, and the inner white line represents mean velocity. For the calculations of FV_s , FV_d , and FV_m , the outer envelope is usually selected. The lower white trace represents the power of the reflected Doppler signal. *Abbreviations:* FV, flow velocity; MCA, middle cerebral artery; FV_s , systolic flow velocity; FV_d , diastolic flow velocity; FV_m , mean flow velocity.

At any point in time, red blood cells move at a variety of speeds and in different directions within a vessel, and therefore the Doppler signal obtained from any sample volume within a vessel is a mixture of different frequency shifts, including different segments of the same vessel, branches, or surrounding arteries. The spectrum of different frequency shifts, which can be visually displayed by spectral analysis, provides a way of presenting three-dimensional data in a two-dimensional format. Time is represented on the horizontal scale, frequency shift (velocity) on the vertical scale, and signal intensity as the relative brightness or color (Fig. 2).

In order to calculate FVs during different phases of a cardiac cycle, a spectral envelope is created, corresponding to the maximum FV throughout the cardiac cycle. Each waveform is enveloped by the outer envelope that is drawn electronically to represent the maximum velocity profile of each cardiac cycle. In Figure 2, the outer white line represents such an envelope. The inner white line represents the mean velocity. Systolic, diastolic, and mean FV are all calculated from the maximum velocity profile. The lower white line represents the power of the reflected signal, relating to the total flow observed by the Doppler, accounting for the vessel area, hematocrit, and angle of incidence. During serial measurements, if the reflected power remains unchanged, the changes in velocity can be taken to represent changes in flow.

Several variables can be deduced from the spectral envelope, including peak systolic velocity, end diastolic velocity, and time-averaged mean (TAM) velocity. Of these, TAM velocity shows least variability and is normally used for routine evaluations. Once this envelope has been derived, the rest of the spectral analysis data is virtually ignored.

TECHNIQUE

Ultrasonic windows are areas in the skull where the bone is thin enough to allow penetration of an ultrasonic beam. Of the three windows (temporal, orbital, and foramen magnum), the temporal window is most commonly used. It is located just superior to the

zygomatic arch, defined as an area 2 cm above a line drawn from the lateral canthus of the eye to the tragus.

The temporal window allows insonation of the anterior, middle, and posterior cerebral arteries, the terminal segment of the internal carotid artery, and the anterior and posterior communicating arteries.

The identification of a vessel depends on several factors.

- Window used
- Depth of the sample volume
- Flow direction in relation to the probe
- Relation to other vessels
- Response to common carotid artery compression
- Anatomic variations of the circle of Willis

The middle cerebral artery (MCA) is commonly insonated, although the anterior cerebral artery (ACA) and posterior cerebral artery (PCA) can also be insonated. The probe faces perpendicular to the temporal bone to insonate the MCA, in an anterior direction for the ACA, and in a posterior direction for the PCA. The MCA is usually insonated at a depth of 35 to 55 mm, but the ACA and PCA are insonated at 60 to 70 mm. The distinguishing features on examination of the waveform are as follows:

- Direction of flow—It is toward the direction of the ultrasound beam (hence a positive deflection of the spectrum) in the MCA and PCA, but away from the direction of the beam in the ACA.
- Ipsilateral carotid artery compression—This would reverse the direction of flow in the ACA, reduce the flow in the MCA, and cause insignificant change in the PCA.
- Contralateral carotid artery compression—This would increase the flow velocity in the ACA and would produce no change in the MCA or PCA.

Of the different basal arteries, the MCA is easily accessible through the temporal window. It represents the bulk of blood flow to that hemisphere, carrying 50% to 60% of the ipsilateral carotid artery blood flow.

The patient should be in the supine position, although the semi-sitting position is also used. Acoustic gel is applied to the temporal area and the probe is applied with gentle force to the skin. Starting at a depth of 50 mm, a signal is searched by moving the probe slowly and systematically across the window. By making small adjustments in the probe position and angle, the best-quality audible signal can be obtained. Ample time should be allowed for correct vessel identification. Because of the error that can be introduced by the angle of insonation, the point of maximum deflection (representing the highest velocity) should be recorded and used for interpretation.

In the case of continuous monitoring, it is helpful to mark the probe position on the skin. It is vitally important to secure the probe position in order to maintain optimal Doppler signal throughout.

Once the best-quality audible signal is obtained, the quality of the spectral display can be verified on the screen. A skilled operator would be able to construct a mental image of the intracranial arteries. In order to verify identification of the MCA, the artery can be followed (by altering the depth of insonation) toward the bifurcation of the internal carotid artery into the MCA and anterior communicating artery, usually around a depth of 60 to 65 mm. At this point flow would become bidirectional, with flow direction toward (MCA) and away (ACA) from the probe. A slight anterior-superior orientation of the probe may aid the examiner in finding the bifurcation.

Further techniques for confirming identification of the MCA are the ability to follow the signal for at least 10 mm and reduction in the FV by compression of the ipsilateral carotid artery. In experienced hands, identification of the MCA is possible in 90% of cases.

DATA INTERPRETATION AND LIMITATIONS

Once the FV waveform is displayed, the systolic (FV_s), diastolic (FV_d), and mean (FV_m) flow velocities and flow direction can be calculated from the Doppler frequency shift. Most modern TCD devices calculate the FV_m automatically.

The mean or TAM FV shows least variability and dependence on heart rate, contractility, and systemic vascular resistance and is therefore the most commonly used variable. It correlates better with perfusion than systolic or diastolic velocity.

Although FV is taken to represent blood flow in the artery, it is worth remembering that a number of other factors may also influence its value (Table 1). These factors must be taken into account on comparing serial measurements within a subject.

In healthy adults, the mean MCA FV ranges from 35 to 90 cm/sec under normal physiological conditions. At birth the recorded values are lower (24 cm/sec), but they increase to 100 cm/sec at four to six years, after which they decrease steadily to 40 cm/sec in the seventh decade. All these factors, along with those in Table 1, should be considered when single values of flow velocities are documented.

Abnormally high FV_m could result from anemia, increased cerebral blood flow (CBF) (hyperemia), arteriovenous malformations, and arterial narrowing (e.g., atheromatous stenosis and vasospasm). Abnormally low FV_m could reflect a proximal flow-reducing lesion or occlusion, coma, or poor cardiac function.

In addition to the FV, a number of indices have been described that can aid the information obtained from the measurement of FV alone. Pulsatility index (PI) and resistance index (RI) are valuable for estimation of cerebral vascular resistance.

1. The pulsatility index of Gosling and King:

$$PI = \frac{FV_s - FV_d}{FV_m}$$

Table 1 Factors that Affect the Value of Measured FV

Technical factors

- Angle of insonation of the probe
- Side-to-side variability (can be up to 10%)
- Interobserver variability

Factors related to the subject

- Age
- Anatomical variations
- Hematocrit (lower hematocrit gives higher FV)
- Gender (females have higher FV)

Physiological factors

- State of arousal (decreased FV in depressed state)
- Pregnancy and menstrual cycle
- Arterial carbon dioxide (increased FV with increased carbon dioxide and vice versa)
- Temperature

Abbreviation: FV, flow velocity.

The PI is an index that relates systolic and diastolic velocities in an attempt to quantify the waveform. The greater the difference between the two, the greater the pulsatility. In addition to FV, PIs provide the examiner with information about the resistance of the cerebral vasculature. A higher-than-expected (e.g., >1.4) PI might result from a distal occlusion, raised intracranial pressure (ICP), or hypocarbia. A PI below 0.5 suggests a proximal flow-reducing lesion, such as an extracranial stenotic lesion, or a low intracranial resistance, e.g., arteriovenous malformation.

2. The resistance index of Pourcelot:

$$RI = \frac{FV_s - FV_d}{FV_s}$$

The RI is another estimate of vascular resistance: a low vascular resistance would be associated with increased FV_d , and a high vascular resistance would be characterized by a decreased FV_d .

The PI has been frequently used in the past. Normal PI ranges from 0.6 to 1.1. Its main advantage is that it is not affected by the angle of insonation. Both PI and RI may be influenced by a large number of factors, including systemic arterial pressure, distal resistance to flow, ICP, vascular compliance, and carbon dioxide, limiting their diagnostic value in clinical practice. However, these might have a qualitative role in assessing changes in resistance to flow in specific areas of the cerebral circulation.

It is important to note that TCD studies only provide a measure of cerebral blood velocity and not flow. The relationship between the two is as follows:

$$FV = \frac{\text{Blood flow volume}}{\text{Vessel diameter}}$$

Therefore, if flow remains constant while the diameter decreases, the FV will increase. Assumptions about changes in one factor will only hold if the other remains constant. There is currently no widely accepted reliable method of determining vessel diameter using TCD.

Limitations of TCD

- TCD provides global information on the FV in one major artery. Hence it may not be sensitive to the regional changes in cerebral perfusion.
- TCD does not provide direct information about blood flow, only flow velocity. Evidence from direct measurement of MCA diameter during craniotomy and magnetic resonance imaging (MRI) measurements, with changes in carbon dioxide and blood pressure, suggests that MCA diameter changes by less than 2% during modest changes in carbon dioxide and/or blood pressure. Therefore, during modest changes in blood pressure or carbon dioxide, MCA FV, as measured by TCD, can be used as a valid surrogate for changes in CBF.
- Accurate measurements depend on the angle of incidence and would therefore vary.
- Bone attenuates ultrasound energy by reflection, absorption, and scatter. In 8% of subjects the temporal bone is too thick to allow for an adequate ultrasonic window. This phenomenon is more common in older subjects, people of Afro-Caribbean origin, and women. It has resulted in the development of a 1-MHz ultrasound probe, which allows better penetration through bone.

ASSESSMENT OF CEREBRAL HEMODYNAMICS

TCD has been used in a number of ways to assess cerebral hemodynamics. Apart from static measurements of the FV profiles, dynamic tests have also been developed to assess cerebral vascular reactivity to carbon dioxide or cerebral autoregulation. In addition, information from the FV profile has also been processed to estimate cerebral perfusion pressure (CPP). Thus TCD is unique in that it allows assessment of many different aspects of cerebral hemodynamics.

Cerebral Blood Flow Measurement

A number of methods can give a direct measurement of CBF. These include the Kety-Schmidt method based on Fick's principle, xenon CT, and MRI. In comparison, TCD provides a cheaper, noninvasive, and more accessible method of estimating cerebral perfusion by measuring FV in the cerebral arteries.

Several studies have investigated the correlation between FV and blood flow measured by direct methods, to determine whether FV can be used to assess changes in CBF. The correlation between CBF and absolute values of FV has been poor. However, the correlation is strong when measuring relative changes in FV as a reflection of actual changes in CBF. This relationship is dependent on the diameter and perfusion territory of the artery remaining constant. In view of the fact that MCA diameter remains constant over a variety of physiological conditions (2), e.g., change in PCO_2 or arterial blood pressure, the changes in FV in most circumstances are more likely to reflect changes in blood flow.

Because of the factors described above, absolute values of FV cannot be taken to compare the CBF in two individuals. However, if all other factors are kept constant, the changes in FV on serial measurements within an individual can be taken to reflect changes in CBF. Hence, changes in FV in a patient undergoing an intervention (anesthesia) or in a patient undergoing treatment for cerebral vasospasm or head injury can be taken to indicate changes in CBF.

Cerebral Vascular Reactivity to Carbon Dioxide (1,3,4)

Vascular reactivity refers to the ability of the cerebral vasculature to constrict or dilate in response to various stimuli. Carbon dioxide affects cerebral vascular resistance by causing smooth muscle relaxation in the small distal arterioles. Vasodilatation of the distal arterioles decreases the cerebral vascular resistance, leading to an increase in CBF. On the other hand, hypocapnia causes vasoconstriction of the distal arterioles, leading to an increase in peripheral vascular resistance and a decrease in CBF. CBF is very sensitive to variations in arterial carbon dioxide, with a linear relationship between CBF and a $PaCO_2$ over a range of 3 to 9 kPa. Because carbon dioxide has a negligible effect on the diameter of the large proximal intracranial arteries, FV as measured by TCD can be used as an indirect measure of blood flow. This principle forms the basis of cerebrovascular reactivity testing.

In practice, a continuous measurement of FV using MCA is established. The subject is asked to hyperventilate to cause a modest decrease (1 kPa) in end-tidal carbon dioxide. In addition, rebreathing methods can be used to increase the end-tidal carbon dioxide by about 1 kPa. Normally, the FV should change by 15% to 40% per 1 kPa change in carbon dioxide. Hypertension and increased age decrease the reactivity. Decreases in carbon dioxide reactivity in younger patients indicate a decrease in cerebral vascular reserve; this may also be an indication of the severity of underlying disease.

Because the changes in FV can be measured instantaneously, the changes in carbon dioxide during assessment of reactivity need not be maintained for more than a minute. Hence the test is well tolerated by the subjects.

Cerebral Autoregulation (4–8)

This is the ability of the cerebral vasculature to maintain constant blood flow despite fluctuations in arterial pressures. This is valid over a range of mean arterial pressure (MAP), usually between 60 and 160 mmHg, although it may vary in certain disease states. Within this range the brain is protected from surges in arterial pressure caused by movement and change in posture. Beyond this range, flow becomes directly proportional to the perfusion pressure. This physiological mechanism protects the brain from potential hypoperfusion and ischemia at low arterial pressures and hemorrhage and edema at high perfusing pressures. Although the precise mechanism is unknown, it is possibly mediated by vasoconstriction and vasodilatation of precapillary resistance vessels in response to changes in arterial pressure.

Traditionally, to assess cerebral autoregulation, multiple measurements of CBF in response to changes in arterial blood pressure are made. This allows creation of an autoregulatory curve that can define the limits and the gradient of the plateau. This method is time-consuming and involves extreme changes in arterial blood pressure and administration of vasoactive drugs to manipulate arterial pressure. TCD offers a simpler, safer, and noninvasive alternative method of assessing cerebral autoregulation.

Although a number of different methods can be used to assess cerebral autoregulation, essentially, three different methods are commonly described in the literature related to anesthesia and intensive care. These are

- Test of static autoregulation
- Test of dynamic autoregulation
- Transient hyperemic response (THR) test

Test of Static Autoregulation

In this test the autoregulatory plateau is assessed over a small range of change in arterial pressure. A continuous record of baseline FV in the MCA is established. Once stable baseline measurements are reached, IV infusion of a vasopressor (phenylephrine) is started to cause a small increase in arterial blood pressure of 20 to 30 mmHg. Once a steady state has been reached, the FV measurement is repeated. The autoregulatory index is calculated as the percent change in cerebral vascular resistance ($CVR = MAP/FV$) per percent change in MAP. A negligible change in FV during increased blood pressure demonstrates intact autoregulation, and therefore the autoregulatory index should be 1. On the other hand a similar percent increase in FV during increased blood pressure would indicate lack of autoregulation. An index of less than 0.4 is taken to represent impaired autoregulation.

This method has been extensively used in the study of anesthetic agents and in critical care situations. It is simple and reproducible but is limited in that it requires the use of vasoactive agents.

Test of Dynamic Autoregulation

As the name suggests, the test assesses the dynamic aspect of autoregulation during a step change in blood pressure; essentially it assesses the speed of autoregulation.

The method was first described by Aaslid in 1989, and it has been extensively used in anesthesia and intensive care. One main advantage of this method over the test of static autoregulation is that the change in blood pressure is achieved without using pharmacological agents. Instead, bilateral thigh cuffs are used; these are inflated to a pressure above the subject's systolic arterial pressure and then suddenly deflated to cause a step decrease in blood pressure. MCA FV is continuously measured before, during, and after cuff deflation. With intact autoregulation, the FV recovers faster than MAP after an initial drop in both. With impaired autoregulation, there is delayed recovery of FV; it recovers at the same time as the blood pressure. An autoregulation index (ARI) is calculated based on comparing the observed speed of change in FV and predicted speed of change if autoregulation were as fast as possible ($ARI = 9$) or absent ($ARI = 0$). An ARI of 5 is considered normal. The changes in blood pressure are transient and are well tolerated by healthy subjects and patients. However, the measured values of ARI show high variability, and therefore repeated measurements should be made.

Transient Hyperemic Response Test

The THR test has been extensively used in testing cerebral autoregulation in clinical practice and research. To perform this test, continuous real-time measurement of FV in the MCA is established. Once a stable baseline measurement is reached, the ipsilateral common carotid artery is compressed for 10 seconds and then released. The compression should result in a sudden reduction in the MCA FV (as well as the pressure in the MCA) (Fig. 3). If autoregulation is intact, the vascular bed distal to the MCA undergoes vasodilatation to maintain CBF. Thus on the release of the compression, when the pressure in the MCA returns to normal, a transient increase in the MCA FV will be seen (Fig. 3); this hyperemic response is absent in impaired autoregulation.

In Figure 3, F_1 corresponds to the FV immediately before compression, F_2 indicates the FV immediately after compression, and F_3 reflects the FV on release of the

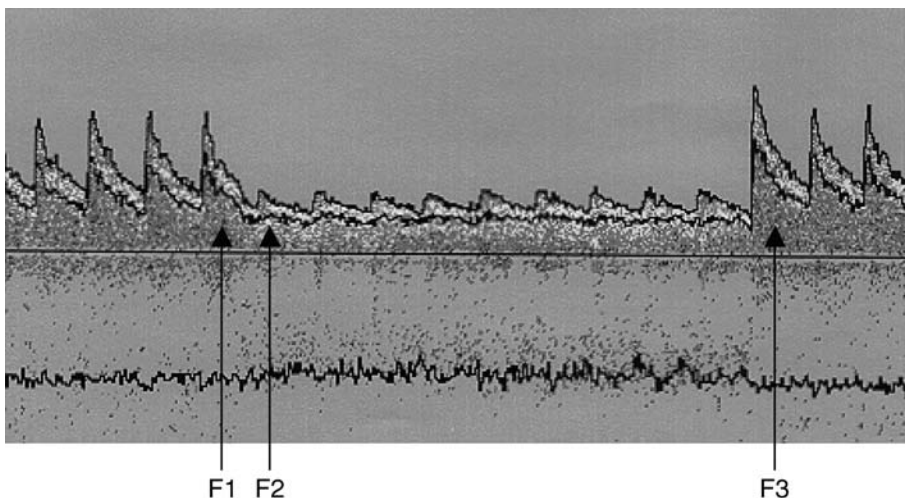


Figure 3 Changes in MCA FV during THR test. F_1 , FV immediately before the compression of ipsilateral common carotid artery; F_2 , FV immediately after the compression; F_3 , FV on release of the compression. The hyperemic response is assessed by the THR ratio, which is calculated as F_3/F_1 . *Abbreviations:* MCA, middle cerebral artery; FV, flow velocity; THR, transient hyperemic response.

compression. The ratio between FV before and after compression (F_3/F_1) is known as the THR ratio. A THR ratio of less than 1.09 could be an indication of impaired autoregulation. In addition to the THR ratio, the strength of autoregulation can be calculated by normalizing the THR ratio for changes in the MCA pressure at the onset of compression.

The THR test correlates well with tests of static and dynamic autoregulation. Its main advantages are that it is simple, noninvasive, and reproducible. It has been found to have a lower variability than the other tests. However, this test is contraindicated in patients with carotid artery disease because of the risk of embolization of carotid artery atheroma, although various studies have demonstrated its safety in this group of patients.

It is clear that different tests assess slightly different aspects of cerebral autoregulation. The test of static autoregulation assesses the gradient of the autoregulatory plateau, the test of dynamic autoregulation assesses the speed of autoregulation, and the THR test assesses the gradient of the plateau and the lower limit of autoregulation. All the tests are semiquantitative assessments of autoregulation, and whether or not they are interchangeable in different clinical situations is not clear.

Estimated Cerebral Perfusion Pressure and Zero Flow Pressure (9–13)

CPP is generally calculated as the difference between MAP and ICP:

$$\text{CPP} = \text{MAP} - \text{ICP}$$

Here, ICP is taken to represent the effective downstream pressure of the cerebral circulation. Recently, it has been shown that cerebral vascular tone, as assessed by measuring zero flow pressure (ZFP), also plays an important role in determining the effective downstream pressure; ZFP is defined as the arterial pressure at which CBF would cease. Hence the estimated cerebral perfusion pressure (eCPP) can be described as

$$\text{eCPP} = \text{MAP} - \text{ZFP}$$

Noninvasive measurement of eCPP and ZFP is a relatively new concept that has been applied to understand the effects of anesthetics on cerebral vascular tone and regulation of eCPP in a variety of clinical situations.

Aaslid described a method of estimating eCPP using TCD as follows:

$$\text{eCPP} = \text{FV}_m(A_1/F_1)$$

A_1 = amplitude of the fundamental frequency components of arterial pressure

F_1 = amplitude of the fundamental frequency components of FV

Fast Fourier analysis of the waveform was used to determine fundamental frequencies. The underlying principle was that

$$\text{Perfusion pressure} = \text{Flow} \times \text{Resistance}$$

In this formula, FV_m was taken to represent CBF and A_1/F_1 was taken to represent cerebral vascular resistance. Aaslid demonstrated a close correlation between eCPP and calculated CPP (MAP – ICP).

Belfort and colleagues used another formula to calculate eCPP.

$$\text{eCPP} = \text{FV}_m \times (\text{BP}_m - \text{BP}_d) / (\text{FV}_m - \text{FV}_d)$$

In this formula, BP_m and BP_d are mean and diastolic blood pressures, FV_m and FV_d are corresponding mean and diastolic flow velocities, and $(\text{BP}_m - \text{BP}_d) / (\text{FV}_m - \text{FV}_d)$ is taken to represent cerebral vascular resistance. The main advantage of this formula is that

eCPP can be calculated noninvasively using minimal routine equipment. In addition ZFP can be calculated as

$$\text{ZFP} = \text{MAP} - \text{eCPP}$$

Recent validation studies indicate that absolute values of ZFP show large variability; however, they are reliable in assessment of changes in effective downstream pressure in cerebral circulation as a consequence to changes in cerebral vascular tone and/or intracranial pressure.

In practice, it is unlikely that measurement of ZFP will replace measurement of ICP. However, the additional information on cerebral vascular tone can potentially be useful in assessing the severity of vasospasm and the effects of vasodilatory treatment. In addition, it can provide crucial information on interplay between perfusion pressure, vascular tone, and blood flow.

APPLICATIONS IN ANESTHESIA (1,14–17)

Assessment of cerebral hemodynamics in patients undergoing anesthesia has added a vast amount of knowledge regarding the effects of different agents. In addition, application of TCD in certain types of surgery can provide important information.

Anesthetic Agents

The effects of anesthetic agents on cerebral hemodynamics can be unpredictable due to ongoing changes in blood pressure, carbon dioxide, and use of accompanying agents.

IV Anesthetic Agents

TCD studies have shown that flow or metabolism coupling of cerebral circulation is maintained during infusion if IV anesthetic agents; the FV decreases in proportion to decreases in cerebral metabolic rate. These agents, in particular propofol, do not have significant effects on cerebral autoregulation or carbon dioxide reactivity.

Ketamine, when given alone, may increase MCA FV.

Inhalational Anesthetic Agents

TCD studies using nitrous oxide alone have shown that it increases FV, impairs autoregulation, and reduces ZFP. Thus its use in neuroanesthesia has declined. These vasodilatory effects of nitrous oxide are probably related to accompanying increases in cerebral metabolism. When given with propofol, it has no significant effects on cerebral hemodynamics.

Other inhalational agents can affect FV by two opposing mechanisms. Decrease in cerebral metabolism would tend to decrease FV, but the direct vasodilatory effect may tend to increase it. Overall isoflurane and desflurane tend to increase MCAFV and impair autoregulation. However, sevoflurane has minimal effects on FV and cerebral autoregulation, favoring its use in neuroanesthesia.

Other Agents

TCD studies have shown that muscle relaxants and moderate doses of opioids do not have significant effects on cerebral hemodynamics.

Vasoactive Agents

Norepinephrine, dobutamine, and dopexamine have been shown to have no effect on autoregulation or carbon dioxide reactivity. Norepinephrine has been shown to increase ZFP.

Glyceryl trinitrate increases MCA FV, has no effect on autoregulation, and decreases ZFP.

Detection of Emboli

Microembolism causes a characteristic distortion of the signal accompanied by a typical chirping sound as it passes through an insonated vessel. This property has been used to detect emboli during carotid endarterectomy and cardiac surgery. Either automatic software analysis or audiovisual inspection of the signal can be used. In carotid artery surgery, an association between embolic rates and the risk of clinical neurological events and/or changes on CT or MRI scans has been found. The presence of emboli detected during initial dissection and wound closure appears to be more predictable of adverse events than emboli during clamping or shunting. Emboli occurring during dissection and closure may be associated with excessive handling of the artery, which may be amenable to changes in surgical technique.

After fixing the TCD probe, the emboli monitoring mode is selected on the TCD machine. Emboli per hour are then calculated. Specific features of emboli are their short duration (0.1 sec), unidirectional movement, and signal strength of 6 to 60 dB above the background velocity spectrum.

Currently there is no reliable method of distinguishing air from particulate emboli. A consensus document for emboli detection has been published recently.

Carotid Endarterectomy

TCD has been suggested as a tool to assist selection of patients who may benefit from carotid endarterectomy and stenting. One study found that patients with asymptomatic carotid stenosis who presented with evidence of microemboli on TCD would benefit from endarterectomy or stenting as much as symptomatic patients, while asymptomatic patients without evidence of microemboli are best managed medically with delay of surgery until the occurrence of emboli. Preoperative assessment of carbon dioxide reactivity has been used to assess cerebral vascular reserve and the need for an intraoperative shunt.

MCA FV monitoring during carotid endarterectomy can detect cerebral ischemia during cross-clamping and microemboli on the release of the clamp. Also, it can indicate the requirement of a shunt. Severe reductions in FV (>90%) at the onset of clamping can predict intra- and postoperative stroke.

TCD may be useful in assessing the cause of postoperative neurological deterioration. The main differential diagnosis of postendarterectomy stroke is carotid occlusion or hemorrhage as a result of hyperperfusion (possibly as a result of autoregulation failure). TCD may be of value in distinguishing between them.

The main advantage of TCD is in providing some real-time feedback to the surgeon and anesthetist regarding hemodynamics and microemboli, which may direct alterations in technique and management.

Cardiac Surgery

TCD monitoring has contributed to improving our insight on mechanisms of brain injury during cardiac bypass. Extracorporeal circulation as well as hypothermia can impair

cerebral autoregulation. Reduced incidence of microemboli, as detected by TCD, has been correlated with improved outcome in terms of ICU stay and neuropsychological tests.

Neurosurgery

Apart from its use in detecting microemboli, TCD has been used postoperatively in monitoring MCA FV following neurosurgery, which may direct postoperative hemodynamic management. In cases where tumor and aneurysm surgery requires temporary occlusion or sacrifice of the carotid artery, changes in MCA FV in response to temporary manual occlusion of the carotid artery can be a good indicator of the collateral circulation and thus can predict tolerance to long-term occlusion.

Obstetrics

Pregnancy is associated with a decreased MCA mean FV. This is most marked in the third trimester as a result of a reduction in FV_s . FV_d remains unchanged. eCPP is increased over control values, and vascular reactivity remains unchanged. Epidural anesthesia reduces eCPP, but has no effect on MCA FV.

TCD has also been used in studies investigating pre-eclampsia. MCA FV is higher than in normal pregnancy.

APPLICATIONS IN INTENSIVE CARE (1,18–20)

Cerebral Edema and Brain Stem Death

Increased ICP physically increases the cerebral vascular resistance, resulting in decreased cerebral blood flow—the diastolic blood flow suffers earlier than the systolic. On TCD examination, the FV waveforms appear spiky, with reduced or absent diastolic blood flow (Fig. 4A). Eventually, reverberant flow may also be seen in severe cases (Fig. 4B). The calculated PI is markedly increased. These findings can aid the diagnosis of brain stem death, although TCD is not a formal requirement to confirm brain stem death.

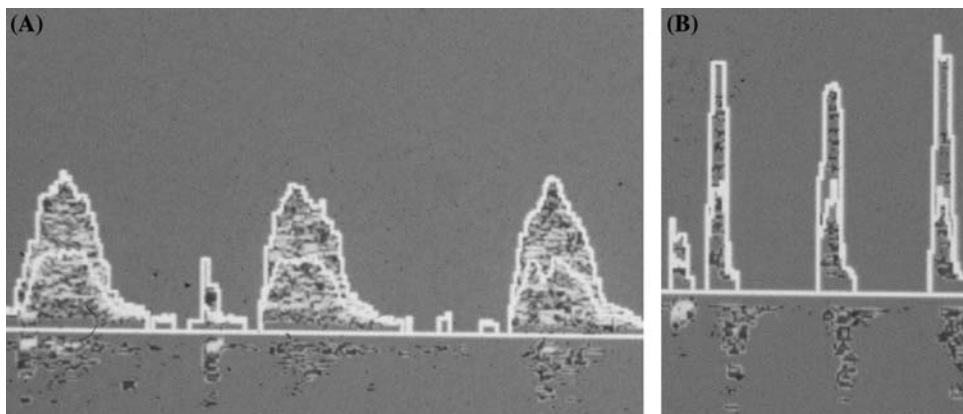


Figure 4 TCD traces in cerebral edema with loss of diastolic velocity (A). In severe cases reverberating flow may be seen (B). *Abbreviation:* TCD, transcranial Doppler.

Subarachnoid Hemorrhage

TCD examination can detect vasospasm of the large arteries of the circle of Willis, which is a major potentially treatable cause of morbidity and mortality following SAH. Typically, the FV waveforms become narrow and tall. An MCA FV of greater than 120 cm/sec is diagnostic of vasospasm. Using these criteria, TCD has a high specificity (85–100%) but low sensitivity (59–94%) compared to angiography in detecting vasospasm. Therefore, it is unlikely that TCD will replace angiography in confirming the diagnosis, but because it is noninvasive, serial measurements can be used to monitor the progress of vasospasm and the effects of treatment. MCA FVs greater than 200 cm/sec is associated with poorer CT grade of SAH and poorer outcome.

TCD can also be used to test autoregulation in SAH—loss of autoregulation assessed by THR is associated with poorer outcome.

Head Injury

A number of pathologies can coexist in head injury, and the nature of cerebral hemodynamics change continuously. TCD examination, along with other modalities, can

- Aid diagnosis
- Guide therapy
- Monitor progress
- Indicate severity
- Indicate prognosis

Changes in blood flow include those typical of raised ICP, vasospasm, or reduction in FV in the case of a mass lesion such as a hematoma (Fig. 5A). Hyperemia may be seen on the evacuation of hematoma (Fig. 5B). In ventilated patients with severe injury and complete loss of autoregulation, a cyclic flow pattern may be seen on the TCD display, as FV fluctuates with respiratory cycles of the ventilator.

Early loss of autoregulation as estimated by THR correlates with poor clinical state at presentation and outcome. Moderate hyperventilation may improve autoregulation (thigh cuff) in head injury. There is some evidence that hyperventilation and mannitol are only effective in lowering ICP when autoregulation is intact.

Others

Cerebral autoregulation and metabolism may be compromised in sepsis and in patients with fulminant hepatic failure. In patients with liver failure, TCD findings of cerebral edema and loss of autoregulation can predict poor neurological outcome.

SUMMARY

The main advantage of TCD is its simplicity, portability, cost-effectiveness, and noninvasiveness. The information is real time, with beat-to-beat display of the FV profile in major intracranial arteries. Information can be reliably gained regarding serial changes in the FV waveform. Apart from the changes in the FV, TCD can be used to assess eCPP, cerebral vascular tone, cerebral vascular reactivity, and cerebral autoregulation. Together, these variables have been used to gain knowledge about the effects of anesthetics. In patients with neurological diseases, knowledge and continuous assessment of these variables can help in diagnosis, assessment of severity, monitoring the progress and determining the prognosis.

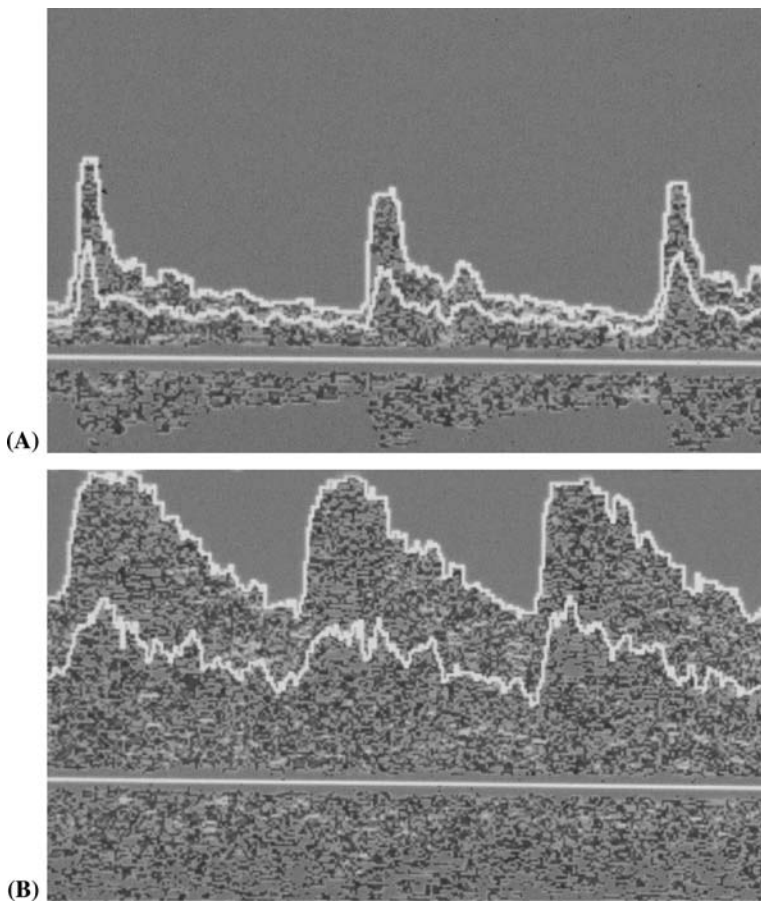


Figure 5 Decreased FV may be seen on the side of subdural hematoma (A). Evacuation of hematoma leads to hyperemia (B) followed by normalization of FV. *Abbreviation:* FV, flow velocity.

ACKNOWLEDGMENT

Many thanks to Dr. R. Winter for his help in obtaining the TCD traces.

REFERENCES

1. Moppett IK, Mahajan RP. Transcranial Doppler ultrasonography in anaesthesia and intensive care. *Br J Anaesth* 2004; 93:710–724.
2. Giller CA, Matthews D, Purdy P, et al. Cerebral arterial diameters during changes in blood pressure and carbon dioxide during craniotomy. *Neurosurg* 1993; 32:737–741.
3. Lipsitz LA, Mukai S, Hammer J, et al. Dynamic regulation of middle cerebral artery flow velocity in aging and hypertension. *Stroke* 2000; 31:1897–1903.
4. Matta BF, Lam AM, Sterbel S, et al. Cerebral pressure autoregulation and carbon dioxide reactivity during propofol-induced EEG suppression. *Br J Anaesth* 1995; 74:159–163.
5. Panerai RB. Assessment of cerebral pressure autoregulation in humans—a review of measurement methods. *Physiol Meas* 1998; 19:305–338.

6. Aaslid R, Lindegaard K-F, Sorteberg W, et al. Cerebral autoregulation dynamics in humans. *Stroke* 1989; 20: 45–52.
7. Mahajan RP, Cavill G, Simpson EJ. Reliability of the transient hyperaemic response test in detecting changes in cerebral autoregulation induced by graded variations in end-tidal carbon dioxide. *Anesth Analg* 1998; 87:843–849.
8. Cavill G, Simpson EJ, Mahajan RP. Factors affecting the assessment of cerebral autoregulation using the transient hyperaemic response test. *Br J Anaesth* 1998; 81:317–321.
9. Aaslid R, Lunder T, Lindegaard K-F, et al. Estimated cerebral perfusion pressure from arterial blood pressure and transcranial Doppler recordings. In: Miller JD, Teasdale GM, Rowan JO, et al. eds. *Intracranial Pressure VI*. Berlin: Springer Verlag, 1986:226–229.
10. Weyland A, Buhre W, Grund S, et al. Cerebrovascular tone rather than intracranial pressure determines the effective downstream pressure of the cerebral circulation in the absence of intracranial hypertension. *J Neurosurg Anesth* 2000; 12:210–216.
11. Sherman RW, Mahajan RP. Estimation of critical closing pressure and cerebral perfusion pressure using transcranial Doppler. *Br J Anaesth* 2003; 90:396–397.
12. Athanassiou L, Hancock SM, Mahajan RP. Doppler estimation of zero flow pressure during changes in downstream pressure in a bench model of a circulation using pulsatile flow. *Anaesthesia* 2005; 60:133–138.
13. Hancock SM, Mahajan RP, Athanassiou L. Effects of changes in end tidal carbon dioxide on estimated cerebral perfusion pressure and zero flow pressure in healthy volunteers. *Anesth Analg* 2003; 96:847–851.
14. Hancock SA, Eastwood JR, Mahajan RP. Effects of inhaled nitrous oxide 50% on estimated cerebral perfusion pressure and zero flow pressure in healthy volunteers. *Anaesthesia* 2005; 60: 129–132.
15. Bedforth NM, Girling KJ, Harrison JM, et al. The effects of sevoflurane and nitrous oxide on middle cerebral artery blood flow velocity and transient hyperemic response. *Anesth Analg* 1999; 89:170–174.
16. Harrison JM, Girling KJ, Mahajan RP. Effects of propofol and nitrous oxide on middle cerebral artery flow velocity and cerebral autoregulation. *Anaesthesia* 2002; 57:27–32
17. Ackerstaff RG, Moons KG, van de Vlasakker CJ, et al. Association of intraoperative transcranial Doppler monitoring variables with stroke from carotid artery endarterectomy. *Stroke* 2000; 31:1817–1823.
18. Smielewski P, Czosnyka M, Kirkpatrick P, et al. Evaluation of transient hyperaemic response test in head-injured patients. *J Neurosurg* 1997; 86:773–778.
19. Muizelaar JP, Lutz HA III, Becker DP, et al. Effect of mannitol on ICP and CBF and correlation with pressure autoregulation in severely head-injured patients. *J Neurosurg* 1984; 61:700–706.
20. Steiger HJ, Aaslid R, Stooss R, et al. Transcranial Doppler monitoring in head injury: relations between type of injury, flow velocities, vasoreactivity and outcome. *Neurosurgery* 1994; 34:79–85.

12

The Respiratory System

Daniel A. Lichtenstein

*Medical Intensive Care Unit, Hôpital Ambroise-Paré,
Faculté Paris-Ouest, Boulogne, France*

INTRODUCTION

Thoracic ultrasound provides an alternative imaging tool for the pleura, lung, and associated structures. Recognition of this role was slow in part due to the belief that air would not allow useful ultrasound images to be generated (1). The reality is that this application—regarding this largest and vital organ—was accessible since the early days of ultrasound imaging.

A historical perspective is interesting. Ultrasound arose from the works of Langevin on sonar (1915). A medical use for this discovery was forecast by Dénier (2). The advent of real-time imaging in 1974 initiated current applications (Henry & Griffith). The 1980s technology (ADR-4000) was sufficient to exploit lung signals—and develop nearly all fields of emergency ultrasound. More recently, ultrasound has emerged as a useful tool in critical care medicine (3). This occurred after a prolonged silent period—the critical care community had been informed as early as 1991 of the potential of this “sleeping giant” (4). François Jardin realized early the role of cardiac ultrasound in the ICU (5). We were in a privileged place to develop clinical ultrasound for the critically ill, performed by the intensivist with a book to follow in 1992 (6). At this time, the accepted field of thoracic ultrasound was limited to the diagnosis of pleural effusion (7) if it was used at all (8,9). Lung (and general) ultrasound has lost years compared to the heart, but this period is now behind us.

Interest in lung ultrasound arose from the inadequacies of other investigations: Auscultation, recognized since 1810 (10), has low accuracy (11). Plain X rays available since 1895 (12) give limited information (11,13–17). Computed tomography (CT), available increasingly since 1972 (18), overcomes many of these flaws, but not without other drawbacks. This chapter aims to show that, provided current dogma is revisited, lung ultrasound should be added to the classical armamentarium. A standardized analysis of artifacts—usually indefinite structures—provides information that will allow initiation of emergency care in many critical situations.

PART I

REQUIRED MATERIALS, BASIC TECHNIQUES, AND NORMAL PATTERNS

The Principles of Lung Ultrasound

The concept of lung ultrasound is based on seven principles (19).

1. Unsophisticated ultrasound devices are perfectly adequate.
2. Intrathoracic air and water are intimately mixed. From this mingling arise artifacts. Water-rich disorders (pleural effusion and consolidation) and air-rich disorders (pneumothorax and interstitial syndrome) have opposite behavior in respect to gravitational effects.
3. The basis of ultrasound lung signals arises from the pleural line.
4. Lung ultrasound is mainly based on artifact analysis.
5. Ultrasound signals are largely dynamic.
6. Nearly all acute pulmonary disorders about the pleura and chest wall, explaining the potential of lung ultrasound.
7. The lung is the most voluminous organ. Precise areas can be defined.

The Choice of the Ultrasound Unit: A Critical Step

Guidelines for materials are available in chapter 2. We would like, however, to share with the reader a personal view of ultrasound.

Physicians usually try to purchase the most up-to-date technologies. In critical care, for the past 18 years we have done the opposite as explained below.

For assessing the lung, resolution was fully satisfactory since 1991 (see Figures 2–12 throughout the chapter). Such performance is not, paradoxically, present in up-to-date echocardiographic or ultraminiature units in ICUs and ERs. Manufacturers have not included lung imaging in their specifications. Analog devices provide better image resolution than digital.

For hospital use, our device has a 30 × 38-cm footprint with cart, allowing bed-to-bed and floor-to-floor use. The weight (>13 kg) is unattractive to thieves. Simple-to-use devices are required as they are destined to be used around the clock. Handheld devices, once on a cart, are paradoxically more cumbersome than ours. Very small units are not mandatory in the hospital (where space is not a big problem). We believe it was unnecessary to wait for ultraminiaturization to develop whole-body ultrasound in the critically ill. For those who really need ultrasmall units, some less well known products have interesting quality/cost ratios.

We don't use Doppler imaging for the lung, veins (20,21), or cervicofacial applications (6). We only ask for Doppler imaging from other departments on rare occasions. Ultrasound devices without Doppler have better resolution and lower cost and emit lower-energy ultrasound waves (22–24). Other modes to enhance images (e.g., tissue harmonic imaging) are also unnecessary. The aim of some manufacturers to suppress artifacts should be resisted in this area of practice. We will soon see the role of a simple approach for hemodynamic assessment.

We use only one probe (Fig. 1). This 5-MHz microconvex probe allows satisfactory analysis of the lungs, abdomen, heart, veins, and sinuses.

Our microconvex probe studies, in addition, areas like the lung apex, subclavian vein, or lower femoral vein, which are usually hard to analyze using other types of probe. Linear or abdominal probes cannot be applied in such areas, and phased-array probes are unsuitable for

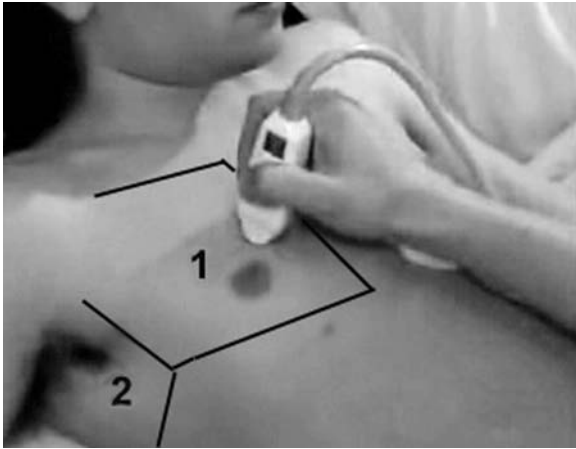


Figure 1 Main stages of investigation. This stage defines investigation of the anterior chest wall (zone 1) in a supine patient at earth level. Extension to zone 2 (lateral wall) defines stage 2.

superficial structures. All the images in our book were acquired using this single probe (25). In addition, relevant interventional procedures can be performed using this probe.

Asepsis is a critical issue in ICUs. With keyboards full of buttons and handheld units without carts or with more than one probe, asepsis is difficult to achieve. The disinfectant product (which should remain with the machine, reducing the interest of ultraminiaturization) should be compatible. Some products used for other applications progressively destroy the probes.

The unit should switch on immediately. Analogic systems can, but most laptops cannot—a hindrance in this setting. The coupling product, gel (whose volume also reduces the interest of miniaturization), can be replaced by a self-vanishing product allowing ultrarapid whole-body investigation.

If the above model is followed, then blurred images, large-size devices impairing access to patients, keyboards crowded with microbes, probes sometimes sticky with dry gel, complicated Doppler curves, and long minutes of switching on should all be avoidable. As regards the future, the perspective of wireless probes or holographic visualization is interesting, but today simpler imaging of areas such as the lung is more clinically relevant and important.

The Normal Lung

To obtain the best of ultrasound, we follow the seven principles one by one. The patient's position and area where the probe is applied should be specified through a gravitational axis. Critically ill patients are usually supine.

Analysis can be standardized using definite landmarks [anterior and posterior axillary lines, and the nipple line]. We scan directly through intercostal spaces using longitudinal views with the ribs at each side of the long axis of the probe (Fig. 1). We avoid imaging the thorax via the abdominal route, which can generate errors.

Stage 1 investigates the anterior chest wall (zone 1) in supine patients and gives information on pneumothorax, interstitial syndrome, and complete atelectasis. Stage 1 defines half-sitting patients.

Stage 2, the lateral wall (zone 2), is added to the anterior, informing on substantial pleural effusions, alveolar consolidation, and diaphragm function.

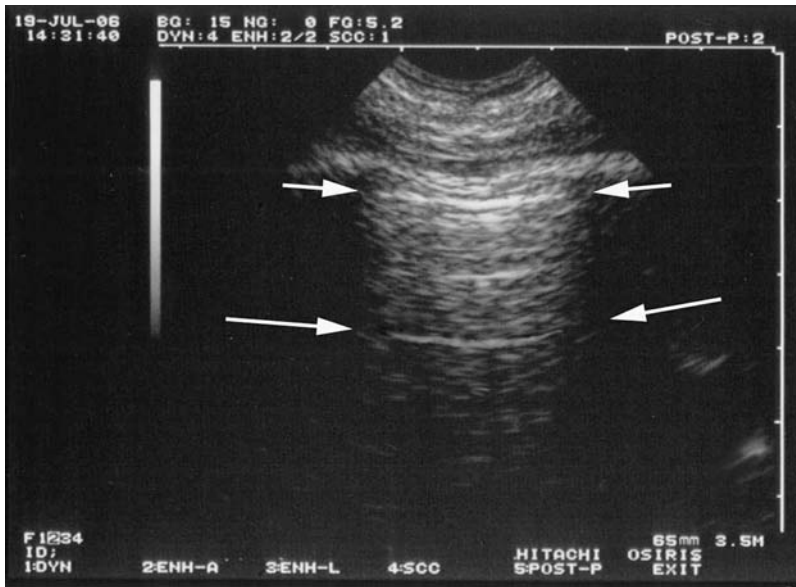


Figure 2 Normal lung. Longitudinal scan of an intercostal space. A rib on either side casts an acoustic shadow behind it leading to an area of black (where arrows are located). Between the two ribs, half a centimeter below in an adult, the pleural line is located (*short arrows*). Upper rib, pleural line and lower rib outline the bat sign. The horizontal line (*long arrows*) that arises from the pleural line, separated by a skin-lung distance, is an artifact representing a repetition of the pleural line. This is termed the A line and has clinical applications.

Stage 3 is defined by slightly raising the ipsilateral back of supine patients, inserting the probe as posterior as possible (zone 3). Short probes (cable to transmitting surface) are mandatory. Small disorders not detected by previous approaches are detected.

Stage 4 is a comprehensive analysis with lateral decubitus positioning, complete study of the posterior wall, and apex analysis.

The probe is applied on an intercostal space, searching for the pleural line (Fig. 2). The upper and lower ribs cast posterior acoustic shadows. Between the two ribs, 0.5 cm deeper, a roughly horizontal, usually hyperechoic line is visible—the pleural line, which indicates the parietal and visceral pleura (the lung surface). The lung line is an ultrasound description of the visceral pleura. The lung line is normally virtual, i.e., indistinct from the pleural line, and is only visualized in the case of pleural effusion (Figs. 4 and 5). The ribs and pleural line outline a characteristic pattern, the so-called bat sign, a permanent landmark that it is mandatory to recognize at each examination.

From the pleural line, static and dynamic signs arise.

1. Static sign: The A line, arising from the pleural line. Only air artifacts are visible. Alphabetic classifications avoid long descriptions (19). This physiologic artifact is a horizontal, hyperechoic reverberation artifact recurring at regular intervals (the skin-pleural line distance) called the A line (Fig. 2).

2. Dynamic sign: Lung sliding. This dynamic sign is visible at the pleural line, synchronized with respiration, corresponding to the visceral pleura sliding over the fixed parietal pleura during lung displacement along its craniocaudal axis. M-mode imaging yields the so-called seashore sign, confirming lung sliding (Fig. 3). More detail on lung sliding is available elsewhere (25). Many probes supplied on echocardi-Doppler

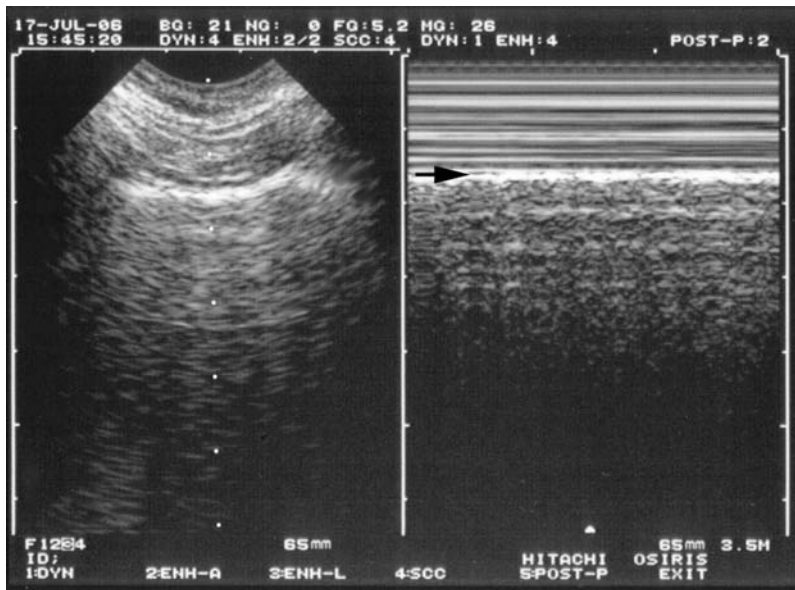


Figure 3 Lung sliding. On the left is the conventional B-mode image as in Figure 2. On the right, in time motion, an obvious difference in pattern appears on either side of the pleural line (*arrow*). The motionless superficial layers generate horizontal lines—the so-called waves. The deep artifacts follow the lung sliding—hence this sandy pattern. The whole image designates the seashore sign. The seashore sign, an all-or-nothing rule, shows that lung sliding is a relative movement of the lung alongside superficial tissues.

devices have insufficient resolution. Most filters must be bypassed as they can mask lung sliding. In dyspneic patients, muscular contractions make analysis difficult (unless M-mode is used). Lung sliding is abolished by many disorders (see the “Pneumothorax” section).

Normal lungs exhibit A lines plus lung sliding. Vertical artifacts can be visible: Z lines are present in 80% of cases (26) and B lines in 27% of cases, but confined to the lower intercostal space (27) or isolated at the anterior wall (described in the “Interstitial Syndrome” section). In ventilated patients without respiratory disease, the cupolas of the diaphragm are located one to two spaces below the nipple line, moving toward the abdomen at inspiration, with amplitude 10 to 15 mm.

Other artifacts (I, S, N, O, W . . . lines) have been described (25).

PART II

COMMON ACUTE DISORDERS: PATTERNS OF IMAGES—CLINICAL APPLICATIONS

According to the second principle, patterns of images are a function of the air-water ratio. This varies from the two extremes—a pleural effusion containing pure liquid to a pneumothorax containing pure air. All described patterns were assessed using CT as the gold standard.

Pleural Effusion

We begin with this familiar application, predicted since 1946 (2), and under assessment since 1967 (7). The prevalence is 62% in medical ICUs (28). Paradoxically, even nowadays, ultrasound use depends on local habits. New image patterns can reinforce old ones, and skilled use of ultrasound proves nearly as accurate as CT for this diagnosis.

Image Patterns

The traditional subcostal routes yield unsettling ghost artifacts. We insert our small footprint probe directly through intercostal spaces. Stage 2 at the level of the bed will demonstrate substantial effusions. If none is visible, a move to stage 3 can detect minimal effusions.

Apart from obvious criteria of a dependent image separating the pleural layers above the diaphragm, there are two signs, one static and one dynamic, that will greatly help in difficult cases. A static sign, the “quad sign,” is the label highlighting that the effusions’ borders are regular (Fig. 4). A dynamic sign, the sinusoid sign, is the label given to inspiratory decrease of effusion thickness, indicating centrifugal inspiratory shift of the lung toward the wall, along a “core/surface” axis, confirmed in M-mode (Fig. 5). Considering these signs provides 93% sensitivity and specificity with CT as gold standard (11). When the gold standard is withdrawal of pleural fluid, specificity is 97% (29).

Echogenicity may not be a reliable sign of effusion, since the classically anechoic pattern may be absent in more complicated cases—e.g., pyothorax, hemothorax. Fluid may collect both in dependent and nondependent areas if pleural pathology is present.



Figure 4 Pleural effusion (quad sign) intercostal approach. The quad sign is a basic static sign. The four borders of the effusion are regular. The pleural line, from where it arises (*upper arrow*). Upper and lower shadows of the ribs (*lateral arrows*). Mostly, the deep border designates the visceral pleura (the lung line), regular (*lower arrow*). There is associated alveolar consolidation.

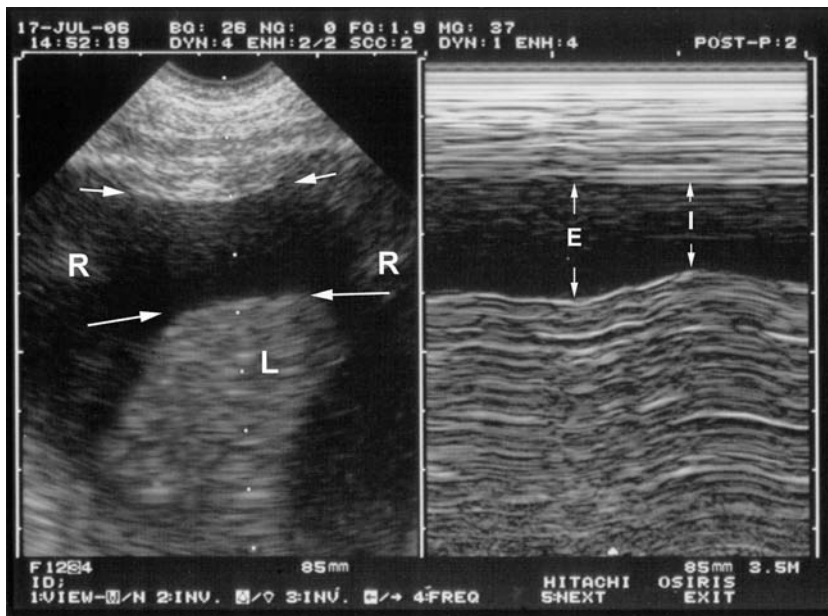


Figure 5 Pleural effusion (sinusoid sign) (*Left*): Static approach. R, shadow of ribs. (*Upper short arrows*): Pleural line. (*Lower long arrows*): Lung line. L, consolidated lung. (*Right*): Dynamic approach. The centrifugal inspiratory shift is demonstrated using the time-motion mode. The sinusoid sign, a sign specific to liquid pleural effusion, and indicating a low viscosity. I, inspiration, E, expiration.

Applications

Ultrasound detects the presence of an effusion, evaluates its volume, provides information on its nature, and indicates the optimum location for thoracentesis.

Positive Diagnosis

Bedside plain radiography has only 39% sensitivity (11), missing effusions up to 525 mL (30). False-positive cases are numerous. Plain radiography at the bedside misses one-third of ultrasound-visible and easy-to-puncture effusions in ventilated patients (29). Ultrasound is acknowledged as an imaging method of choice (31).

Volume of Effusion

Bedside plain radiography does not provide valuable information, particularly with supine films. Ultrasound roughly estimates this volume. With experience we can estimate a large effusion of 500–1000 mL, or a very small collection of 15–30 mL. This approximation is sufficient in clinical practice. More sophisticated approaches are available (32). A 1-mm thick effusion can be detected, provided the probe is applied over an adequate area.

Nature of Fluid

Ultrasound provides noninvasive information (33). Transudates are supposedly anechoic, exudates echoic. Yet when assessing an anechoic effusion, it seems more prudent to

perform ultrasound-assisted thoracentesis whenever detection of exudate is likely to alter management. This simple procedure bypasses sophisticated discussions and other more complex tests. Mobile particles (the plankton sign) or septa suggest a hemothorax or pyothorax.

Interventional Ultrasound

The risk of blind thoracentesis is significant in ventilated patients. Using visual approach rules described below, thoracentesis allows routine safe puncture, even in the presence of effusions not visible on plain X rays (29). Among mandatory criteria, one checks for inspiratory interpleural distance greater than or equal to 15 mm, an effusion visible at adjacent intercostal spaces, and the absence of inspiratory interposition of the lung, heart, liver, or spleen. Thoracentesis should be performed immediately after ultrasound localization, the patient remaining in the same position (supine position is often possible). The presence of the sinusoid sign indicates low effusion viscosity, with drainage possible with fine needles or catheters, i.e., minimal trauma. The success rate in ventilated patients is 97% (29), and complications between nil (29) and 1.3% (34). Less than 10 seconds are needed to obtain liquid in 88% of cases (29). Withdrawal of significant volumes of effusion liquid improves ventilatory conditions (35) and weaning from ventilators (25).

Alveolar Consolidation

This daily concern in the ICU is imperfectly detected by plain radiography. Auscultation sometimes has better accuracy (11). 98.5% of cases about the pleura, a mandatory condition for ultrasound detection (36). This application is not new (2,37). Here again, imaging patterns can be improved.

As opposed to pleural effusion, pneumothorax, or interstitial syndrome, which are rapidly detected, small locations need to be searched for—a worthwhile effort each time positive detection alters management (25). We avoid subcostal approaches, which access only limited areas of the lung and yield ghost artifacts.

Image Patterns

Apart from obvious criteria (a tissue-like intrathoracic image arising from the pleural line—or a pleural effusion), two criteria are valuable in difficult cases (Fig. 6).

1. Static criterium: Anatomic shape. Unlike the quad sign, the deep boundary is usually irregular unless the whole lobe is consolidated (shred sign).
2. Dynamic criterium: The absence of any sinusoid dynamic allows distinction from pleural effusion (sometimes associated). Craniocaudal inspiratory movement is present or impaired (in severe cases), but no inspiratory centrifugal shift occurs. Considering these patterns, sensitivity is 90% and specificity 98% (36).

Subtle findings are accessible. There is correlation with lobar anatomy—often the lower lobe in critically ill patients. The volume can be roughly measured. Lung sliding is often abolished. Necrotizing areas can be seen within the consolidation. Air bronchograms yield hyperechoic punctiform or linear images (37). An inspiratory centrifugal movement of the air bronchograms is called a dynamic air bronchogram. This sign, when present, allows distinction between nonretractile (pneumonia) and retractile (atelectasis) consolidation with 60% sensitivity and 100% specificity for diagnosing nonretractile ones (38,39).



Figure 6 Alveolar consolidation. Infectious alveolar consolidation of the left lower lobe. Basic criteria are the tissue-like patterns located in the thorax, separated from the abdomen by the cupola of the diaphragm, a basic landmark in any thoracic examination (S, spleen). The static criterium is the irregular deep boundary of the image, in connection with the aerated lung (*shred sign, arrows*). The dynamic criterium (not demonstrated here) is the immobility of the image during respiration. Note minimal associated pleural effusion between lung and chest wall and lung and diaphragm. Note small hyperechoic air bronchograms, whose dynamics have clinical implications.

Atelectasis is a basic application. This change is more physiopathologic than anatomic (40). Early signs occur immediately following atelectasis (e.g., one-lung intubation), when the lung is still aerated. The immediate sign is abolition of lung sliding. Cardiac pulsatility can be seen through the motionless lung—a sign called the “lung pulse,” which has 90% sensitivity for early diagnosis of complete atelectasis (40). Late signs occur when the lung collapses, including alveolar changes, absence of a dynamic air bronchogram (static air bronchograms are possible), loss of volume, and mediastinal and diaphragmatic shift. Other signs and figures will not be described in order to save space (25).

Applications

Ultrasound applications are increasing as the limitations of plain radiography are realized (11,13–17). The diagnosis of pneumonia can be immediate. Alveolar recruitment can be managed in acute respiratory distress syndrome (ARDS) patients. Applications like needle sampling for culture from within consolidation are still experimental (25).

Interstitial Syndrome

Here, air is mingled with small amounts of water. The diagnosis is exclusively based on artifact analysis, and we must take a step toward abstract concepts. No clinical sign of interstitial syndrome has been described, and bedside radiography is rarely expected to

detect the interstitial component. In practice, the intensivist has got used to doing without this information. We expect to see increasing interest in an application that has proved perfectly accessible to ultrasound since 1994 (27,41).

Patterns of Images

The basic sign is a comet-tail or ring-down artifact having specific features. It arises from the pleural line. It is well defined, laser like. It erases the A lines. It spreads out without fading. It depends on lung sliding. This artifact was called the B line. Several B lines visible in a single view have been dubbed “lung rockets” (Fig. 7). If lung rockets disseminated all over the anterolateral wall are assumed to define diffuse interstitial syndrome, and if the test is defined negative when B lines are absent, isolated, or confined to the lower intercostal space, ultrasound has 93% sensitivity and 93% specificity when compared to bedside radiography, and the concordance is complete when CT is the gold standard (27).

The reflection pattern detected by ultrasound devices is generated by elements with a high acoustic impedance gradient with surrounding structures: water (high impedance) surrounded by air (low impedance) (see chap. 1, “Applied Physics of Medical Ultrasound”). They are under the limits of resolution for ultrasound, present at and all over the lung surface, separated from each other by 7 ± 1 mm or less, present in cardiogenic pulmonary edema, and resolved with the use of diuretics. Thickened subpleural interlobular septa perfectly fulfill this description, a hypothesis confirmed by CT correlations. Normal septa, 300 microns wide, cannot be seen using ultrasound.

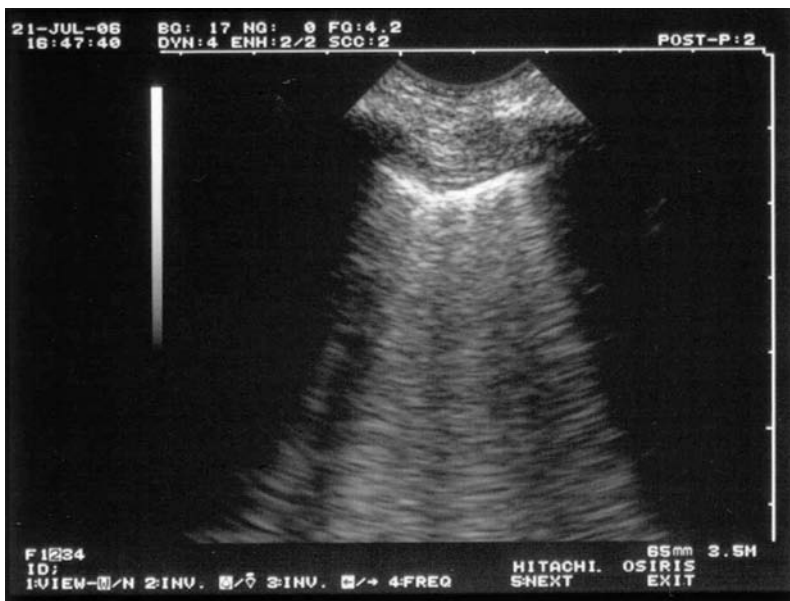


Figure 7 Interstitial syndrome. These vertical comet-tail artifacts have specific peculiarities, strictly arising from the pleural line, laser like echoic, spreading to the edge of the screen without fading, erasing normal A lines and (in real time) moving with the lung sliding. This pattern defines B lines. Several B lines in a single view are reminiscent of a rocket at lift-up. Diffuse lung rockets indicate interstitial syndrome. This patient has cardiogenic pulmonary edema.

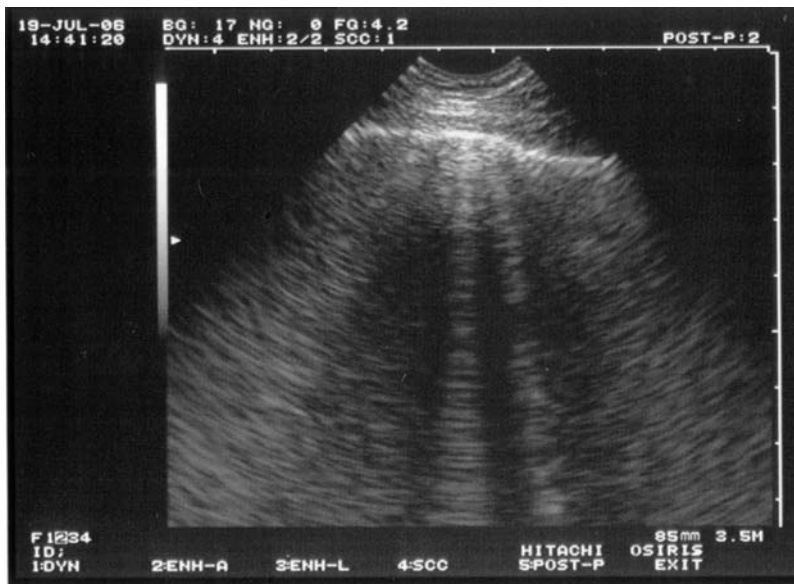


Figure 8 E lines. Two well-defined comet tails descend to the edge of the screen. However, no rib is visible, and the bat sign is absent—compare with Figure 2. This pattern cannot be due to B lines. The patient has parietal emphysema with collections of gas between superficial tissues—above the pleural line. The proposed term is E lines.

Thickened septa, 700 microns wide, remain under ultrasound resolution—but this subtle change generates the artifact. Ultrasound B lines can be considered an equivalent of Kerley’s B lines on plain chest X ray (42). Superficial septa alone are accessible, but observation shows that they behave like deeper ones. As the acute interstitial syndrome is usually diffuse, the diagnosis is immediate from the moment the probe is applied to the thorax. Artifacts separated by 7 ± 1 mm (called B7) indicate interlobular septa thickening and 3 ± 1 mm (B3 lines) ground-glass lesions (27).

As ultrasound B lines have clinical implication, they should be distinguished from other artifacts. E lines (E for emphysema), generated by subcutaneous emphysema, don’t arise from the pleural line. An absence of the bat sign allows immediate distinction (Fig. 8). Z lines (Z for the last letter) arise from the pleural line, but are ill defined, short, independent from lung sliding and don’t erase A lines (Fig. 9). Z lines, present in 80% in normal subjects, should not be considered pathological (26).

Clinical Applications

At first sight, the intensivist may question the relevance of detecting the interstitial syndrome (using ultrasound or any method). Here are some examples of clinical impact for immediate care. In emergency situations it is virtually equivalent to diagnosing acute pulmonary edema (cardiogenic or noncardiogenic). Screening for B lines is part of the diagnosis of pneumothorax (43). B lines allow immediate distinction between pulmonary edema and exacerbation of chronic obstructive pulmonary disease. Sensitivity in diagnosing pulmonary edema is 100%, specificity 92% (44). Diffuse B lines are unusual in pulmonary embolism (45). Other applications are available (25).

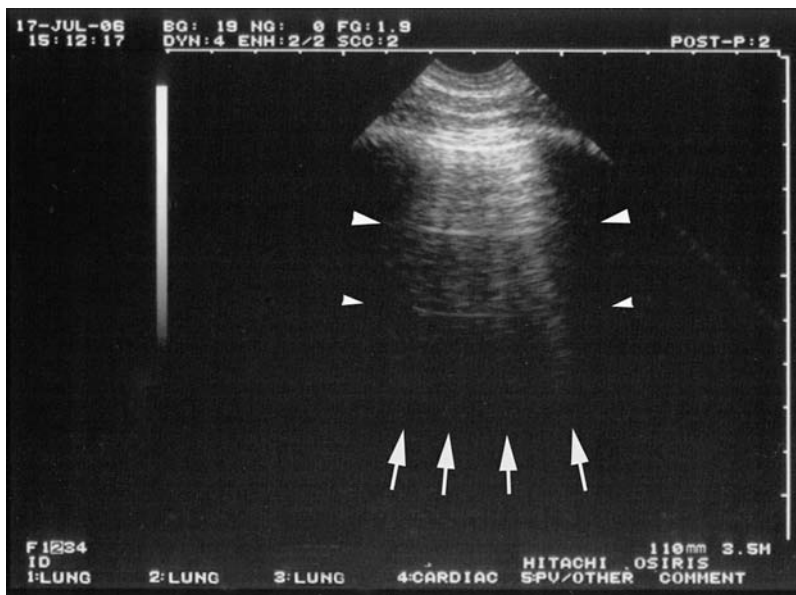


Figure 9 Z lines. These three or four ill-defined comet-tail artifacts (vertical arrows) do not erase the physiologic A lines (*arrowheads*) and quickly vanish without reaching the edge of the screen. These are Z lines. In actual fact, the feature that must be considered here for clinical purpose is an A-line pattern.

Pneumothorax

This pleural collection contains gas and no water. Can ultrasound detect gas (the main hindrance to ultrasound) within a gas-containing organ? Yes, with a better accuracy than radiography, provided one more step is made toward abstract concepts. Patterns are standardized and reproducible. Any correctly trained intensivist will rule out pneumothorax in some seconds and rule it in less than one minute. CT remains the gold standard for comparison.

Pneumothoraces raise familiar problems in emergencies. Some are life threatening (46). Many are radio-occult on plain films (47,48), even if under tension (49). Excessive search leads to overirradiation and extra costs, whereas an overlooked pneumothorax is a clinical risk. Ultrasound provides a solution.

Image Patterns

This refers exclusively to artifact analysis. Pneumothorax should be sought first at the anterior and lower area, 98% of cases being at least anterior and inferior in supine patients (50). Usefully this is an easy location to scan.

Many signs are available, three covering most situations.

1. Abolition of lung sliding: It should be sought for in stage 1. A complete absence of this dynamic sign is observed instead of the familiar lung sliding. Sensitivity and negative predictive value are 100% (51). Lung sliding allows pneumothorax to be confidently discounted in a matter of seconds. M-mode confirms abolished lung sliding, yielding the stratosphere sign (Fig. 10). Doppler imaging is not of major interest. A linear probe can be used, but our microconvex probe always gives the answer and allows analysis of deeper lung structures and in passing other areas in the whole body.

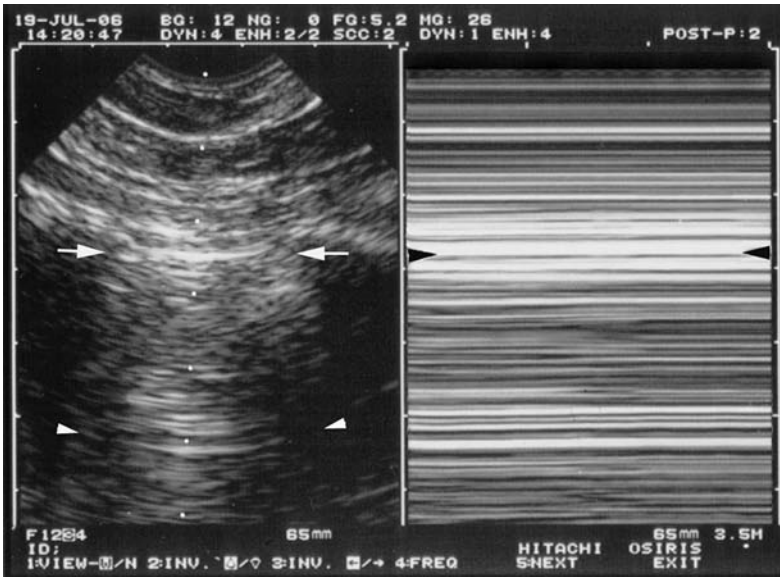


Figure 10 Pneumothorax (A line and stratosphere sign). (Right) The abolition of lung sliding can be confirmed using time-motion M-mode. Exclusively horizontal lines are displayed, indicating complete absence of dynamics at the level of, and below, the pleural line (dark arrowheads): the so-called stratosphere sign. (Left) Note the basic absence of any B line, with a frank A line (white arrowheads). Arrows: location of the pleural line.

Interestingly, we discovered that this sign had been noticed, long ago, in horses (52) and taken up by other teams (53).

The belief that lung sliding abolition is pathognomonic of pneumothorax seems widespread but is untrue. Countless situations abolish lung sliding—particularly in patients at high risk for pneumothorax, including massive atelectasis (including one lung intubation), acute or chronic pleural symphysis, severe fibrosis, phrenic nerve palsy, jet ventilation, cardiac arrest, and simple apnea. Equally technical issues may cause errors, e.g., misuse of filters on an inappropriate probe. Severe asthma generates quasi-abolition. Specificity, which is 91% in healthy subjects (51), falls to 78% in critically ill (54) and up to 60% in ARDS patients. *We must reiterate that abolished lung sliding is not specific to pneumothorax.*

The use of other ultrasound signs easily bypasses this “issue.”

2. The A-line sign: This label implies that no B line is visible. From the pleural line, in stage 1, exclusive A lines arise (Fig. 10). Lung rockets are never visible. The A-line sign is 100% sensitive for the diagnosis of complete pneumothorax, with a 60% specificity (43). The slightest B line allows discounting of pneumothorax (43). As B lines arise from the lung alone, this finding is logical. This helps in the numerous cases with abolished lung sliding. Z lines are visible in 84% of cases of pneumothorax (26).

3. The lung point: This sign allows pneumothorax to be confirmed with certainty, i.e., the patient is likely to benefit from chest drain. When patterns suggestive of pneumothorax (absent lung sliding, plus A lines, stage 1) are detected, the probe moves laterally until it finds a location showing sudden inspiratory visualization of lung sliding or B lines. This is an all-or-nothing law, whether the lung abuts the wall or not (Fig. 11). Specificity is 100%. The overall sensitivity of 66% falls when there is complete retraction (54) but increases to 79% in occult pneumothorax (26). A very posterior or absent lung

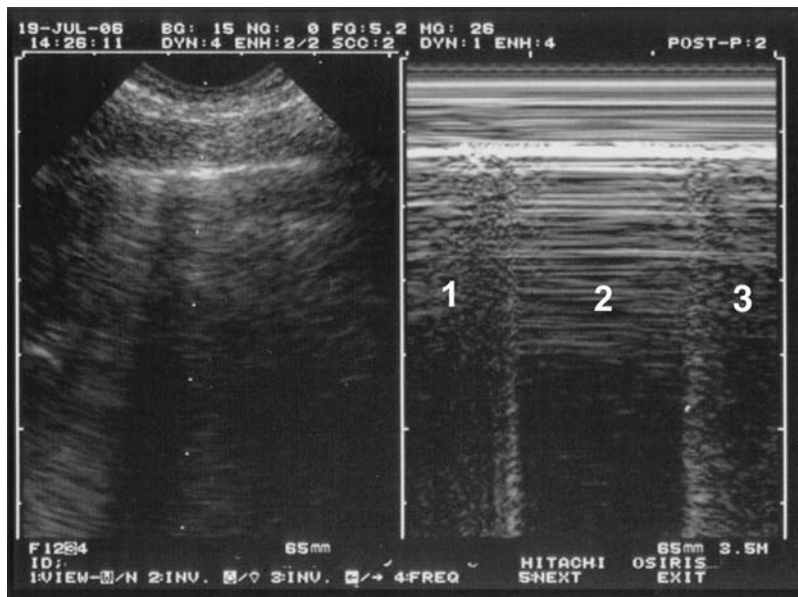


Figure 11 Pneumothorax (lung point). (*Left*) Static image, not fully informative. (*Right*) Time-motion acquisition. The collapsed lung slightly increases its volume on inspiration. Fleeting changes are objectified at the precise location where the lung is, or is not, in contact with the chest wall, yielding sudden change between “seashore” and “stratosphere” pattern. From the left to the right, (1) shows the seashore pattern corresponding to the inspiratory phase, (2) shows the stratosphere pattern corresponding to the expiration phase, and (3) corresponds to a new inspiratory phase.

point characterizes pneumothoraces with complete retraction. The lung point is mandatory for confident management, since it confirms that the image patterns are not due to the use of unsuitable devices or technical errors. In addition, the lung point location indicates the pneumothorax volume. Indication for drainage of occult pneumothoraces is 8% if anterior, 90% if lateral (26).

Clinical Applications

The immediate recognition of pneumothorax is now readily available, from ICU to prehospital medicine (55). Life-saving drainage is now performed after such ultrasound imaging. Inside hospitals, ultrasound competes with or replaces plain radiography and decreases the use of CT.

Immediate discounting of pneumothorax allows cost and time savings when managing acute dyspnea, cardiac arrest, routine procedures (subclavian catheterization and thoracentesis). An elegant application is the possibility of using ultrasound alone (25). Pneumothoraces can be monitored if intensivists believe a chest drain is not required clinically. This logic can be used when X rays are undesirable (e.g., pregnant woman, child).

Other Applications

Pulmonary Embolism

A normal pattern in dyspneic patients is expected from pulmonary embolism, as is the familiar normal radiography. The absence of B lines is found with a sensitivity of 91%

(B7 lines) to 100% (B3) (45). Pulmonary infarction, sometimes described (56), seems rarely observed in severe pulmonary embolism, maybe because time is required to develop significant areas of infarction.

Airway Control

The lung pulse immediately indicates one-lung intubation. Among other signs, the cupola of the diaphragm on the nonventilated side becomes motionless whereas the ventilated one has increased amplitude. The endotracheal tube position within the trachea gives a variant of the “seashore sign” using subtle to-and-fro movements of the tube (<2 mm for avoiding mucosal damage). Doppler is not of major interest: visual perception is sufficient, and M-mode confirms it. Ultrasound can guide surgical or percutaneous tracheostomy (57,58).

Diaphragm Function

The diaphragm is located on stage 2. Location, amplitude, direction, and inspiratory thickening are accessible to ultrasound (25).

Maxillary Sinuses

If one considers they are part of the respiratory system, there is a place for ultrasound here. A normal, empty sinus gives reverberation air artifacts very similar to the image of a normal lung. When there is total radiological opacity of the sinus, from the presence of fluid in the sinus, the walls of the sinus are depicted using a transversal paranasal approach (Fig. 12). A sinusogram indicates a sinus anomaly (sinusitis or mucosal thickening). All sinusites with total X-ray opacification yield a sinusogram. A complete sinusogram always indicates sinusitis with total opacity. An incomplete sinusogram can be due to mucosal thickening or fluid level. Absence of a sinusogram when lifting the



Figure 12 Maxillary sinusitis. Typical image of a sinusogram in the case of sinusitis. On X ray there would be complete opacification of the maxillary sinus.

head ahead rules out sinusitis. By following these simple rules, transfer of febrile ICU patients to CT can often be avoided (59).

Miscellaneous

Several signs, e.g., swirl sign and plankton sign, are, on occasion, valuable for detecting pneumothorax, or pleural effusion. Interventional ultrasound is a major field for thoracentesis, drainage of pneumothorax, and abscess. Assessment of ARDS, including alveolar recruitment, lung water, PEEP, ventral decubitus, distinction between lesional and cardiogenic pulmonary edema, managing fluid therapy, and others measurements, is possible (25).

PART III

THORACIC ULTRASOUND IN DAILY PRACTICE

The number of applications as seen in Part II is large. To limit space we will only cover basic applications.

Thoracic Ultrasound: An Answer to the Traditional Quandary “Radiography or CT in the ICU”?

The choice is usually restricted between these examinations (18). The place of ultrasound is near to CT, with 90% to 100% success rates (19). Plain bedside radiography, although easy to perform, provides limited information. CT provides a correct overview but has many drawbacks, including the need for transportation of sick patients, delays in performing scans, time spent (even with ultrarapid systems), and high irradiation (equivalent to 100–200 plain X rays) (60–62). The high cost of CT is a significant issue.

For a balanced view, weak points of ultrasound with respect to CT should be compared with strong ones. Septations within pleural effusions, necrotizing areas within consolidations (63), real-time information (lung sliding, dynamic air bronchograms, phrenic function) are not seen on CT. By assessment of strong and weak points, the correct choice of imaging can be made for the individual patient.

The Approach to Dyspneic Patients

The traditional approach includes analysis of radiography, blood tests, and often a spiral CT. Ultrasound data alone (lung, venous, and simple cardiac items) have accuracy superior to the traditional approach: 85% versus 52% (64). For instance, an ultrasound approach immediately solves the challenge of COPD versus pulmonary edema (44). Physical examination and thorough analysis of X rays remain necessary—time permitting—but as experience grows, ultrasound data will take an increasing place, resulting in prompt relief of dyspnea.

Who Should Benefit from Thoracic Ultrasound?

Critically ill patients in the ICU first, but also those in emergency rooms, should benefit (65). In prehospital medicine, lung (and general) ultrasound has proven feasible long ago (55).

Lung ultrasound is not officially claimed by radiologists until now. It is not a simple transfer of competences from other areas of practice, but rather a new discipline with added value; it will belong to those who first develop expertise in this area—a development opportunity for intensivists (66).

A Place for Simplicity

Concerns about the operator dependency of ultrasound has delayed progress of ultrasound. Such considerations are equally true for other imaging like CT and plain films but are less well acknowledged. What is true for obstetrics or cardiac echography is paradoxically untrue for vital emergencies. B lines and the stratosphere sign are amongst the simpler signs one can imagine in ultrasound—or even in medicine. Simplicity also concerns the equipment used. Thoracic ultrasound is feasible in more than 98% patients (67) and its potential applications are widening (68–71).

Versatility

A small shift of our microconvex probe allows heart analysis, i.e., prompt life-saving diagnoses like pericardial tamponade, right cavities enlargement, and left heart failure. Lung combined with heart results in the thorax being considered as a whole. Thorax added to the abdomen, using familiar and less familiar applications (pneumoperitoneum, mesenteric infarction), veins, head (including maxillary sinusitis), and all interventional procedures, results in a whole-body approach (25).

A Control of Costs

If the physician decides to stop test escalation once the clinical problem is solved, dramatic cost savings are possible. Countless studies can be performed. For example, the “lung pulse” sign alone allows standard ICUs to purchase devices in three years (40). Overcost due to complications (e.g., pneumothorax following thoracentesis) decrease.

Limitations of Thoracic Ultrasound

A mastery of its limitations will make ultrasound the high-precision tool it is. The wise user will promptly recognize them and turn to traditional techniques. One critical limitation is purchase of unsuitable devices. Operator skill is a classical limitation. Other pitfalls are avoidable: use of an inadequate probe, use of the subcostal route, nonlongitudinal scans, ignorance of diaphragm location, disregard of gravitational axis, confusion between B, Z, and E lines, and lack of knowledge of filters.

Real hindrances are natural (parietal emphysema, pleural calcifications, body habitus, deep lesions like abscesses, pneumatoceles) or artificial (dressings, drains). Obese patients are usually suitable candidates for thoracic ultrasound since the air/water impedance gradient enables satisfactory analysis. Problems with air emphysema in the chest wall can be overcome in certain cases (25).

Each application has limitations (that can be usually solved using correct training). Encysted pleural effusions will not yield the sinusoid sign. The “dark ultrasound lung” is a finding corresponding to white radiologic lungs, but without a discriminative feature allowing distinction between consolidation and effusion. Posterior pneumothorax escapes anterior analysis (25). Any interstitial syndrome, either acute or chronic, yields B lines.

Training

We learned medicine step by step during long studies. Why should we expect to master lung ultrasound in a few hours? Its future will lie in earlier training of students and junior doctors. Note that training in thoracic and emergency ultrasound is easier than in other areas of traditional ultrasound (66). Currently, one realistic way is bedside teaching during residency. Training structures should be developed in authorized centers. Ultraminature devices can give the illusion that ultrasound is easy. Young operators must first use a small percentage of the applications—always, at the very beginning, in parallel with conventional techniques. They can begin by focused applications (e.g., discounting pneumothorax). They will increase knowledge step by step, turning back to conventional methods if in doubt. If ultrasound routinely needs a confirmation test, ultrasound will be useless as it will result in loss of time.

CONCLUSIONS

Added to other clinical assessments, thoracic ultrasound provides an imaging tool in the acutely ill for the detection of life-threatening disorders. Provided minor limitations and rigorous training are accepted, in addition to the well-known advantages of ultrasound, one can add the major advantage of lung ultrasound—simplicity.

Each time the diagnoses of pleural effusion, pneumothorax, alveolar consolidation, and interstitial syndrome are raised, ultrasound provides the answer using standardized tools (72). Symbolizing for some the stethoscope of tomorrow, if we refer to the Greek origin, ultrasound is nothing but a stethoscope of today: *scopein* (to observe) and *stethos* (the chest wall).

REFERENCES

1. Weinberger SE, Drazen JM. Diagnostic procedures in respiratory diseases. In: Harrison's Principles of Internal Medicine. 16th ed. New York: McGraw-Hill, 2005:1505–1508.
2. Dénier A. Les ultrasons, leur application au diagnostic. Presse Méd 1946; 22:307–308.
3. Hatfield A, Bodenham A. Ultrasound: an emerging role in anaesthesia and intensive care. Br J Anaesth 1999; 83(5):789–800.
4. Lichtenstein D, Axler O. Intensive use of general ultrasound in the intensive care unit, a prospective study of 150 consecutive patients. Intensive Care Med 1993; 19:353–355.
5. Jardin F, Dubourg O. L'exploration échocardiographique en médecine d'urgence. Paris: Masson, 1986:3–154.
6. Lichtenstein D. General ultrasound in the intensive care unit. 1st ed. Paris: Springer-Verlag, 1992.
7. Joyner CR, Herman RJ, Reid JM. Reflected ultrasound in the detection and localisation of pleural effusion. JAMA 1967; 200:399–402.
8. Desai SR, Hansel DM. Lung imaging in the adult respiratory distress syndrome: current practice and new insights. Intensive Care Med 1997; 23:7–15.
9. Wyncoll DL, Evans TW. Acute respiratory distress syndrome. Lancet 1999; 354(9177): 497–501.
10. Laënnec RTH. Traité de l'auscultation médiate, ou traité du diagnostic des maladies des poumons et du cœur. Paris: J.A. Brosson & J.S. Claudé, 1819; New York: Hafner, 1962.
11. Lichtenstein D, Goldstein I, Mourgeon E, et al. Comparative diagnostic performances of auscultation, chest radiography and lung ultrasonography in acute respiratory distress syndrome. Anesthesiology 2004; 100:9–15.

12. Williams FH. A method for more fully determining the outline of the heart by means of the fluoroscope together with other uses of this instrument in medicine. *Boston Med Surg J* 1896; 135:335–337.
13. Greenbaum DM, Marschall KE. The value of routine daily chest X-rays in intubated patients in the medical intensive care unit. *Crit Care Med* 1982; 10:29–30.
14. Janower ML, Jennas-Nocera Z, Mukai JI. Utility and efficacy of portable chest radiographs. *Am J Roentgenol* 1984; 142:265–267.
15. Peruzzi W, Garner W, Bools J, et al. Portable chest roentgenography and CT in critically ill patients. *Chest* 1988; 93:722–726.
16. Wiener MD, Garay SM, Leitman BS, et al. Imaging of the intensive care unit patient. *Clinics in Chest Medicine* 1991; 12:169–198.
17. Ivatury RR, Sugerman HJ. Chest radiograph or computed tomography in the intensive care unit? *Crit Care Med* 2000; 28:1033–1039.
18. Hounsfield GN. Computerized transverse axial scanning. *Br J Radiol* 1973; 46:1016–1022.
19. Lichtenstein D. Lung ultrasound in the critically ill. *Yearbook of intensive care and emergency medicine*. Heidelberg: Springer, 2004:625–644.
20. Lichtenstein D, Jardin F. Diagnosis of internal jugular vein thrombosis. *Intensive Care Med* 1997; 23:1188–1189.
21. Cronan JJ. Venous thromboembolic disease: the role of ultrasound, state of the art. *Radiology* 1993; 186:619–630.
22. Taylor KJW. A prudent approach to Doppler ultrasonography. *Radiology* 1987; 165:283–284.
23. Miller DL. Update on safety of diagnostic ultrasonography. *J Clin Ultrasound* 1991; 19: 531–540.
24. Guidelines of the British Medical Ultrasound Society, 2000.
25. Lichtenstein D. *General ultrasound in the critically ill*. 3rd Ed. Heidelberg; New York: Springer-Verlag, 2005.
26. Lichtenstein D, Mezière G, Lascols N, et al. Ultrasound diagnosis of occult pneumothorax. *Crit Care Med* 2005; 33:1231–1238.
27. Lichtenstein D, Mezière G, Biderman P, et al. The comet-tail artifact: an ultrasound sign of alveolar-interstitial syndrome. *Am J Respir Crit Care Med* 1997; 156:1640–1646.
28. Mattison LE, Coppage L, Alderman DF, et al. Pleural effusions in the medical ICU: prevalence, causes and clinical implications. *Chest* 1997; 111:1018–1023.
29. Lichtenstein D, Hulot JS, Rabiller A, et al. Feasibility and safety of ultrasound-aided thoracentesis in mechanically ventilated patients. *Intensive Care Med* 1999; 25:955–958.
30. Collins JD, Burwell D, Furmanski S, et al. Minimal detectable pleural effusions. *Radiology* 1972; 105:51–53.
31. Doust B, Baum JK, Maklad NF, et al. Ultrasonic evaluation of pleural opacities. *Radiology* 1975; 114:135–140.
32. Vignon P, Chastagner C, Berkane V, et al. Quantitative assessment of pleural effusion in critically ill patients by means of ultrasonography. *Crit Care Med* 2005; 33:1757–1763.
33. Yang PC, Luh KT, Chang DB, et al. Value of sonography in determining the nature of pleural effusion: analysis of 320 cases. *Am J Roentgenol* 1992; 159:29–33.
34. Mayo PH, Goltz HR, Tafreshi M, et al. Safety of ultrasound-guided thoracentesis in patients receiving mechanical ventilation. *Chest* 2004; 125(3):1059–1062.
35. Talmor M, Hydo L, Gershenwald JG, et al. Beneficial effects of chest tube drainage of pleural effusion in acute respiratory failure refractory to PEEP ventilation. *Surgery* 1998; 123:137–143.
36. Lichtenstein D, Lascols N, Mezière G, et al. Ultrasound diagnosis of alveolar consolidation in the critically ill. *Intensive Care Med* 2004; 30:276–281.
37. Weinberg B, Diakoumakis EE, Kass EG, et al. The air bronchogram: sonographic demonstration. *Am J Rontgenol* 1986; 147:593–595.
38. Lichtenstein D, Mezière G, Seitz J. The dynamic air bronchogram - an ultrasound sign of nonretractile alveolar consolidation. *Réanimation* 2002; 11(suppl 3):98s (abstract).
39. Lichtenstein D, Mezière G. Ultrasound diagnosis of atelectasis. *Int J Intensive Care* 2005; 12:88–93.

40. Lichtenstein D, Lascols N, Prin S, et al. The lung pulse: an early ultrasound sign of complete atelectasis. *Intensive Care Med* 2003; 29:2187–2192.
41. Lichtenstein D. Diagnostic échographique de l'œdème pulmonaire. *Rev Im Med* 1994; 6: 561–562.
42. Kerley P. Radiology in heart disease. *Br Med J* 1933; 2:594.
43. Lichtenstein D, Mezière G, Biderman P, Gepner A. The comet-tail artifact, an ultrasound sign ruling out pneumothorax. *Intensive Care Med* 1999; 25:383–388.
44. Lichtenstein D, Mezière G. A lung ultrasound sign allowing bedside distinction between pulmonary edema and COPD: the comet-tail artifact. *Intensive Care Med* 1998; 24:1331–1334.
45. Lichtenstein D, Loubière Y. Lung ultrasonography in pulmonary embolism. *Chest* 2003; 123(6):2154.
46. Steier M, Ching N, Roberts EB, et al. Pneumothorax complicating ventilatory support. *J Thorac Cardiovasc Surg* 1974; 67:17–23.
47. Hill SL, Edmisten T, Holtzman G, et al. The occult pneumothorax: an increasing diagnostic entity in trauma. *Am Surg* 1999; 65:254–258.
48. McGonigal MD, Schwab CW, Kauder DR, et al. Supplemented emergent chest CT in the management of blunt torso trauma. *J Trauma* 1990; 30:1431–1435.
49. Gobien RP, Reines HD, Schabel SI. Localized tension pneumothorax: unrecognized form of barotrauma in ARDS. *Radiology* 1982; 142:15–19.
50. Lichtenstein D, Holzapfel L, Fria J. Projection cutanée des pneumothorax et impact sur leur diagnostic échographique. *Réan Urg* 2000; 9(suppl 2):138s (abstract).
51. Lichtenstein D, Menu Y. A bedside ultrasound sign ruling out pneumothorax in the critically ill: lung sliding. *Chest* 1995; 108:1345–1348.
52. Rantanen NW. Diseases of the thorax. *Vet Clin North Am* 1986; 2:49–66.
53. Targhetta R, Bourgeois JM, Balmes P. Ultrasonographic approach to diagnosing hydro-pneumothorax. *Chest* 1992; 101:931–934.
54. Lichtenstein D, Mezière G, Biderman P, et al. The lung point: an ultrasound sign specific to pneumothorax. *Intensive Care Med* 2000; 26:1434–1440.
55. Lichtenstein D, Courret JP. Feasibility of ultrasound in the helicopter. *Intensive Care Med* 1998; 24:1119.
56. Bitschnau R, Mathis G. Chest ultrasound in the diagnosis of acute pulmonary embolism. *Radiology* 1999; 211:290.
57. Hatfield A, Bodenham A. Portable ultrasonic scanning of the anterior neck before percutaneous dilatational tracheostomy. *Anaesthesia*. 1999; 54(7):660–663.
58. Sustic A, Kovac D, Zgaljardic Z, et al. Ultrasound-guided percutaneous dilatational tracheostomy: a safe method to avoid cranial misplacement of the tracheostomy tube. *Intensive Care Med* 2000; 26:1379–1381.
59. Lichtenstein D, Biderman P, Mezière G, et al. The sinusogram, a real-time ultrasound sign of maxillary sinusitis. *Intensive Care Med* 1998; 24:1057–1061.
60. Kalra MK, Maher MM, Toth TL, et al. Strategies for CT radiation dose optimization. *Radiology* 2004; 230(3):619–628.
61. Brenner DJ, Elliston CD, Hall EJ, et al. Estimated risks of radiation-induced fatal cancer from pediatric CT. *Am J Roentgenol* 2001; 176:289–296.
62. Berrington de Gonzales A, Darby S. Risk of cancer from diagnostic X-Rays. *Lancet* 2004; 363:345–351.
63. Lichtenstein D, Peyrouset O. Lung ultrasound superior to CT? The example of a CT-occult necrotizing pneumonia. *Intensive Care Med* 2006; 32:334–335.
64. Lichtenstein D, Mezière G. Ultrasound diagnosis of an acute dyspnea. *Crit Care* 2003; 7(suppl 2): S93 (abstract).
65. Rose JS, Levitt MA, Porter J, et al. Does the presence of ultrasound really affect computed tomographic scan use? A prospective randomized trial of ultrasound in trauma. *J Trauma* 2001; 51:545–550.
66. Lichtenstein D, Mezière G. Training of general ultrasound by the intensivist. *Réan Urg* 1998; 7(suppl 1):108s (abstract).

67. Lichtenstein D, Biderman P, Chironi G, et al. Feasibility of general ultrasound in the ICU. *Réan Urg* 1996; 5(6):788:SP 50 (abstract).
68. Maury E, Guglielminotti J, Alzieu M, et al. Ultrasonic examination: an alternative to chest radiography after central venous catheter insertion? *Am J Respir Crit Care Med* 2001; 164: 403–405.
69. Beckh S, Bolcskei PL, Lessnau KD. Real-time chest ultrasonography: a comprehensive review for the pulmonologist. *Chest* 2002; 122(5):1759–1773.
70. Rowan KR, Kirkpatrick AW, Liu D, et al. Traumatic pneumothorax. Detection with thoracic US: Correlation with chest radiography and CT. *Radiology* 2002; 225: 210–214.
71. Blaivas M, Lyon M, Duggal S. A prospective comparison of supine chest radiography and bedside ultrasound for the diagnosis of traumatic pneumothorax. *Acad Emerg Med* 2005; 12(9): 844–849.
72. van der Werf TS, Zijlstra JG. Ultrasound of the lung: just imagine. *Intensive Care Med* 2004; 30:183–184.

Index

- Absorption, in image creation, 9–10
- ACA. *See* Anterior cerebral artery (ACA)
- Accreditation in TEE, Europe, 108–109
- Acoustic gel, 182
- Acoustic impedance, 8, 28–31
- Acoustic reflection, 28–31
- Acoustic refraction, 28–31
- Acoustic shadowing, 31–34
- Acute respiratory distress syndrome (ARDS), 203, 207
- Airway control, 209
- Alveolar consolidation, 202–203
- American Society of Echocardiography (ASE), 89, 125
- Anatomy, 63–67
 - arteries, 66–67
 - of brachial plexus blocks, 74
 - lymphatics, 66
 - veins, 63–66
 - arm and leg, 66
 - axillary/subclavian, 63
 - femoral, 64–65
 - internal jugular vein, 63
- Anesthesia, TCD in, 189–191
 - agents, 189–190
 - cardiac surgery, 190–191
 - carotid endarterectomy, 190
 - emboli detection, 190
 - neurosurgery, 191
 - obstetrics, 191
- Anesthetic agents, 189–190
 - in anesthesia, 189–191
- Angles
 - of incidence, 149
 - of insonation, 180, 182
- Anterior cerebral artery (ACA), 182
- Aortic aneurysm pathology, 113
- Aortic regurgitation (AR), 119–122, 163
- Aortic stenosis, 122–125
- Aortic valve, TEE of, 111–125
 - anatomy, 111–113
 - aortic regurgitation, 119–122
 - aortic stenosis, 122–125
 - deep transgastric long-axis view, 117
 - midesophageal aortic valve long-axis view, 116
 - midesophageal aortic valve short-axis view, 114–115
 - midesophageal four-chamber view, 113–114
 - transgastric long-axis view, 117
 - upper-esophageal aortic arch long-axis view, 116
- Aortic valve area (AVA), 124
- Apical four-chamber view, TTE, 105
- Apical LAX view, TTE, 105
- Apical two-chamber view, TTE, 105
- AR. *See* Aortic regurgitation (AR)
- ARDS. *See* Acute respiratory distress syndrome (ARDS)
- ARI. *See* Autoregulation index (ARI)
- Arrays
 - curvilinear arrays, 6
 - linear arrays, 6
 - phased arrays, 6
- Arrow International Inc., 167
- ASE. *See* American Society of Echocardiography (ASE)
- Asepsis, 197
- Association of Cardiothoracic Anaesthetists, 47
- Asthma, 207
- Atelectasis, 203
- Attenuation, 31–34
- Autoregulation index (ARI), 187

- AVA. *See* Aortic valve area (AVA)
- Axillary approach, to brachial plexus blocks, 78
- Beam spreading and focusing, in image creation, 7–8
- Bernoulli equations, 124, 131, 158–160
- Bernoulli principle, 121
- Beta blockade, 171
- B-mode, 4
- Brachial plexus blocks, 74–78
 - anatomy, 74
 - approaches, 75
 - axillary approach, 78
 - infraclavicular, 77–78
 - interscalene, 76–77
 - supraclavicular, 75–76
- Brain stem death, and cerebral edema, 191
- British Medical Ultrasound Society, 49
- British Society of Echocardiography, 47
- Bronchograms, 202
- Calipers, 19
- Cannulation, 58
 - of central veins, 60
- Canthus, 182
- Carbon dioxide (CO₂), cerebral vascular reactivity to, 185–186
- Carcinoid syndrome, 137, 142
- Cardiac echography, 211
- Cardiac output (CO), 156
- Cardiac surgery, TCD in, 190–191
- CardioQ™, 167
- Carotid endarterectomy, 190
- Carpentier classification, 125
- Cart-based system, 14–15
- CASE. *See* Consortium for the Accreditation of Sonographic Education (CASE)
- Catheter tip misplacement, 60
- Cavitation, in safety concerns, 11
- CBF. *See* Cerebral blood flow (CBF)
- CEM. *See* College of Emergency Medicine (CEM)
- Central venous catheters (CVC), 14, 47
- Central venous pressure (CVP), 161, 175.
 - See also* Right atrial pressure (RAP)
- Cerebral autoregulation, TCD in, 186–188
 - dynamic autoregulation, 186–187
 - static autoregulation, 186
 - transient hyperemic response test, 187–188
- Cerebral blood flow (CBF), and TCD, 183, 184
 - measurement, 185
- Cerebral edema, and brain stem death, 191
- Cerebral hemodynamics, TCD in, 185–189
 - CBF, measurement, 185
 - cerebral autoregulation, 186–188
 - CPP, 188–189
 - vascular reactivity, to CO₂, 185–186
 - ZFP, 188–189
- Cerebral perfusion pressure (CPP), 188–189
- Cerebral vascular reactivity, to CO₂, 185–186
- Certification, of TEE
 - in Europe, 108–109
 - in US, 108
- Cervical plexus block, 79
- Cine-loop, in ultrasound machine, 20
- Circle of Willis, 192
- CO. *See* Cardiac output (CO)
- College of Emergency Medicine (CEM), 50
- Color Doppler, 34, 72, 114, 116
 - aortic regurgitation, 119, 120
- Color flow Doppler, 90, 152, 155
 - mitral valve regurgitant, 92, 94, 133–134
- Color gain control, 25
- Compound imaging, 24
- Computed tomography (CT), 64, 195, 210
- Consortium for the Accreditation of Sonographic Education (CASE), 50
- Continuous-wave (CW) Doppler, 152
 - vs. PW Doppler, 152
- Control panel, in ultrasound machine, 19
- CPP. *See* Cerebral perfusion pressure (CPP)
- Craniocaudal inspiratory movement, 202
- Crosssectional area (CSA), 156
- CSA. *See* Crosssectional area (CSA)
- CT. *See* Computed tomography (CT)
- CVC. *See* Central venous catheters (CVC)
- CVP. *See* Central venous pressure (CVP)
- CW. *See* Continuous-wave (CW) Doppler
- Dark ultrasound lung, 211
- Data interpretation, of TCD, 183–184
- Deep transgastric long-axis view, 117
- Deep transgastric view, of TEE, 98
- Deltex Medical Group plc, 167
- Depth control
 - in transducers, 35
 - in ultrasound machine, 23
- Descending aorta LAX view, of TEE, 101
- Descending thoracic aortic SAX view, of TEE, 98
- Diaphragm function, 209
- Diathermy, 174
- Doppler, Christian, 148

- Doppler effect
 analysis, 147–151
 angle of incidence, 149
 equation, 149
 shift, 148
 ultrasound technology, 147, 151
 controls, in ultrasound machine, 24–25
 curves, 197
 echocardiography, 111
 frequency shift, 180
 signals, 9, 181
 sound, 170
 techniques, 151–155
 color flow Doppler, 152, 155
 continuous-wave (CW) Doppler, 152
 pulse-wave (PW) Doppler, 151–152
 velocity, 168, 170, 174
 Dynamic air bronchogram, 202
- ECG. *See* Electrocardiogram (ECG)
- Echocardiographer, 113
- Echocardiography, 147
 TEE. *See* Transesophageal echocardiography (TEE)
 TTE. *See* Transthoracic echocardiography (TTE)
- Echo Doppler
 Doppler analysis, 147–151
 Doppler shift, 148–149, 151
 Doppler techniques. *See* Doppler techniques
 intracardiac pressure calculations. *See*
 Intracardiac pressure calculations
 overview, 147
 stroke volume (SV) calculation, 155–158
- Echo-tip needles, 44
- ECPP. *See* Estimated cerebral perfusion pressure (eCPP)
- Effectiveness assessment, of ultrasound, 61–62
- EFSUMB. *See* European Federation of Societies for Ultrasound in Medicine and Biology (EFSUMB)
- Electrocardiogram (ECG), 28
- Emboli detection, TCD in, 190
- Emphysema, 211
- Epidural analgesia, 81–82
- Epidural space visualization, 82
- Equipment settings, of ultrasound machine
 application presets, 18–19
 cine-loop, 20
 color gain control, 25
 compound imaging, 24
 control panel, 19
 depth/zoom control, 23
 [Equipment settings, of ultrasound machine]
 Doppler controls, 24–25
 focus control, 23
 freeze, 19
 frequency control, 23
 high resolution zoom, 23
 overall gain, 20–21
 patient data, 18
 select key, 20
 switching on/off, 18
 TGC, 22
 tissue harmonic imaging, 23–24
 tracker ball, 20
 transducer selection, 18
 velocity scale control, 25
 wall filter, 25
- Ergonomics, 15
- Esophageal Doppler, 171
 monitor, 167
- Estimated cerebral perfusion pressure (eCPP)
 and zero flow pressure, 188–189
- Europe, accreditation of TEE, 108–109
- European Federation of Societies for Ultrasound in Medicine and Biology (EFSUMB), 49
- Examination of Special Competence in Perioperative Transesophageal Echocardiography (PTEeXAM), 108
- FAST. *See* Focused assessment with sonography in trauma (FAST)
- Femoral nerve block, 79–80
- Fenphen valvulopathy, 142
- Fick's principle, 185
- First-pass venipuncture, 60
- Flow time (FTc), 172, 174, 175
- Flow velocity (FV), 179, 181
 factors, 183
- Focus control, 23
- Focused assessment with sonography in trauma (FAST), 52
- Fourier analysis, 188
- Freeze, in ultrasound machine, 19
- Frequency control, in ultrasound machine, 23
- FTc. *See* Flow time (FTc)
- FV. *See* Flow velocity (FV)
- Gain control, in transducers, 35
- Gastric tonometry, 175
- Handheld systems, 14–15
- Hands-free ultrasound probes, 43

- Head injury, 192
- Heart valves, TEE of
 aortic valve. *See* Aortic valve, TEE of
 mitral valve. *See* Mitral valve, TEE of
 pulmonic valve, 141–144
 tricuspid valve, 135–141
- Heating, in ultrasound safety concerns, 12
- Hemodynamic monitor, clinical use, 172–175
- Hemodynamic therapy, 175
- Hemosonic™, 167
- Hepatic veins, 139
- High resolution zoom, in ultrasound
 machine, 23
- Hyperechogenic reflection, of epineurium, 73
- Hyperemia. *See* Cerebral blood flow (CBF)
- Hypocapnia, 185
- Hypocarbia. *See* Intracranial pressure (ICP)
- Hypothermia, 190
- Hypovolemia, 58, 172
- ICP. *See* Intracranial pressure (ICP)
- ICU. *See* Intensive care unit (ICU)
- ILook, 36
- Image creation, 4–10
 absorption, 9–10
 beam spreading and focusing, 7–8
 reflection, 8–9
 scatter, 9
- Infraclavicular brachial plexus block, 77–78
- Inotropes, 171
- Insertion method, 167–171
- Intensive care, TCD in, 191–192
- Intensive care unit (ICU), 210
- Interactive online learning materials, 55
- Internal jugular vein, 61
- Interpretation of waveform, 171–172
- Interscalene brachial plexus blocks, 76–77
- Interstitial syndrome, 203–206
 clinical applications, 206
 patterns of image, 204–206
- Interventional ultrasound, 202
- Intracardiac pressure, 160–164
 calculations, 158–164
 Bernoulli equation, 158–160
 intracardiac pressure, 160–164
 left atrial pressure, 163
 left ventricular end diastolic pressure,
 163–164
 pulmonary artery diastolic pressure, 163
 pulmonary artery mean pressure, 162–163
 right ventricular systolic pressure, 161–162
- Intracranial pressure (ICP), 184
- Kety- Schmidt method, 185
- LA. *See* Left atrial (LA)
- LAP. *See* Left atrial pressure (LAP)
- Laryngoscopy, 87
- Left atrial pressure (LAP), 163
- Left ventricular end diastolic pressure
 (LVEDP), 163–164
- Left ventricular (LV) septal wall thickness, 114
- Left ventricular outflow tract (LVOT), 113,
 156, 158
- Left ventricular systolic pressure (LVSP), 162
- Levels of training, for ultrasound, 49
- Longitudinal approach, for needle visualization
 hybrid approach, 42
- Lungs
 analysis, 197–199
 pulse, 203
 rockets, 204
 ultrasound, principles, 196
- LV. *See* Left ventricular (LV)
- LVEDP. *See* Left ventricular end diastolic
 pressure (LVEDP)
- LVOT. *See* Left ventricular outflow tract
 (LVOT)
- LVSP. *See* Left ventricular systolic pressure
 (LVSP)
- Magnetic resonance imaging (MRI), 184, 185
- MAP. *See* Mean arterial pressure (MAP)
- Maxillary Sinuses, 209
- MCA. *See* Middle cerebral artery (MCA)
- ME. *See* Midesophageal (ME)
- Mean arterial pressure (MAP), 186
- Microstreaming, in ultrasound safety
 concerns, 11
- Middle cerebral artery (MCA), 182
- Midesophageal aortic valve
 long-axis view, 116
 of TEE, 93–94
 short-axis view, 114–115
 of TEE, 92
- Midesophageal bicaval view, of TEE, 92
- Midesophageal four-chamber view, 113–114
- Midesophageal four-chamber view, of TEE,
 89–90
- Midesophageal imaging (ME), 89, 111
- Midesophageal long-axis view, of TEE,
 91–92
- Midesophageal mitral commissural view, of
 TEE, 90

- Midesophageal right ventricular inflow-outflow view, of TEE, 92
- Midesophageal two-chamber view, of TEE, 90
- Mirror-type systems, 44
- Mitral regurgitation (MR), 132–135, 163
- Mitral valve, of TEE, 125–135
 - anatomy, 125
 - mitral regurgitation, 132–135
 - mitral stenosis, 129–132
 - standard TEE views, 125–129
- Mitral valve area (MVA), 125
- M-mode, 6
 - echocardiography, 167, 168, 171
- Morbidity, 172
- MR. *See* Mitral regurgitation (MR)
- MRI. *See* Magnetic resonance imaging (MRI)
- Mucosal hypoperfusion, 175
- MVA. *See* Mitral valve area (MVA)
- Nasogastric tubes, 172
- National Board of Echocardiography, 108
- National Electrical Manufacturers Association (NEMA), 12
- National Institute for Clinical Excellence (NICE), 47, 62
- Needle
 - position assessment, 36–39
 - tips, 43
 - visualization, 41–44, 73
 - longitudinal hybrid, 42
 - transverse, 42
- Needle guidance techniques, 40–41
 - direct ultrasound, 40–41
 - free-hand puncture, 41
 - needle guidance devices, 40–41
 - indirect ultrasound, 40
- NEMA. *See* National Electrical Manufacturers Association (NEMA)
- Nerve block, ultrasound-guided, principles, 73
- Nerves, ultrasound imaging, 72–73
- Neurosurgery, 191
- NICE. *See* National Institute for Clinical Excellence (NICE)
- Normal lung, analysis, 197–199
- Nyquist limit, 152
- Obstetrics, 191
- Orientation marker, 35
- Overall gain, in ultrasound machine, 20–21
- PADP. *See* Pulmonary artery diastolic pressure (PADP)
- Palm top, 14
- PAMP. *See* Pulmonary artery mean pressure (PAMP)
- Parasternal long-axis view, TTE, 101–102
 - of right ventricle, 102
- Parasternal short-axis view, TTE
 - of left ventricle, 104
 - of mitral valve, 102
 - of right ventricle outflow tract, 102
- PASP. *See* Pulmonary artery systolic pressure (PASP)
- Patient details, in ultrasound machine, 18
- PCA. *See* Posterior cerebral artery (PCA)
- Peak velocity (PV), 171
- Perioperative care, 175–176
- Phantoms, 36
- PHT. *See* Pressure half-time (PHT)
- Physics of ultrasound, 28
- PI. *See* Pulsatility index (PI)
- PISA. *See* Proximal isovolemic surface area (PISA)
- Planimetry, 157
- Plankton sign, 201
- Pleural effusion, 200–202
 - applications, 201–202
 - imaging pattern, 200–201
- Pneumothorax
 - clinical application, 208
 - image pattern, 206–208
- Popliteal fossa block, 81
- Posterior cerebral artery (PCA), 182
- Power Doppler ultrasound, 39
- Practicalities, vascular access, 68–69
 - needle tip placement verification, 69
 - needle visualization, 69
 - transducer and display setup, 68–69
- Practical training, for ultrasound, 50–51
- Pressure half-time (PHT), 121, 131
- PRF. *See* Pulse repetition frequency (PRF)
- Proximal isovolemic surface area (PISA), 134
- PTEeXAM. *See* Examination of Special Competence in Perioperative Transesophageal Echocardiography
- Pulmonary artery diastolic pressure (PADP), 163
- Pulmonary artery mean pressure (PAMP), 162–163
- Pulmonary artery systolic pressure (PASP), 162
- Pulmonary Embolism, 208–209
- Pulmonary regurgitation, 142–144
- Pulmonary stenosis, 144

- Pulmonic valve, 141–144
 anatomy, 141
 pulmonic stenosis, 144
 standard TEE views, 141–142
- Pulsatility index (PI), 183
- Pulse-echo
 principle, 1–2
 ultrasound, 2–3
- Pulse repetition frequency (PRF), 25, 152
- Pulse-wave (PW) Doppler, 151–152
vs. CW Doppler, 155
- PV. *See* Peak velocity (PV)
- PW. *See* Pulse-wave (PW) Doppler
- Radiologists, 211
- Range resolution, 152
- RAP. *See* Right atrial pressure (RAP)
- Rationale, for ultrasound
 limitations, 60–61
- RCOG. *See* Royal College of Obstetricians and Gynaecologists (RCOG)
- RCR. *See* Royal College of Radiologists (RCR)
- Real-time moving display, 6
- Red blood cell, 148, 149, 158
- Red cells, 180
- Reflection, in image creation, 8–9
- Regional anaesthetic techniques,
 ultrasound-guided, 73
- Resistance index (RI), 183
- Resolution, image
 axial, 34
 slice thickness, 34
 transverse, 34
- Respiratory system
 alveolar consolidation, 202–203
 interstitial syndrome, 203–206
 lung ultrasound
 normal lung, 197–199
 principles of, 196
 unit selection, 196–197
 overview, 195
 pleural effusion
 applications, 201–202
 image patterns, 200–201
 pneumothorax, 206–210
 thoracic ultrasound, 210–212
- Reverberation, 29
- Rheumatic heart disease, 139
- RI. *See* Resistance index (RI)
- Right ventricular outflow tract (RVOT), 142
- Right ventricular systolic pressure (RVSP),
 161–162
- Robot-assisted devices, 44
- Royal College of Obstetricians and Gynaecologists (RCOG), 51
- Royal College of Radiologists (RCR), 47
- RVOT. *See* Right ventricular outflow tract (RVOT)
- RVSP. *See* Right ventricular systolic pressure (RVSP)
- Safety, with ultrasound, 10–12
- SAH. *See* Subarachnoid hemorrhage (SAH)
- SAX. *See* Aortic valve short axis (SAX);
 Short-axis view (SAX)
- SCA. *See* Society of Cardiovascular Anesthesiologist (SCA)
- Scatter, in image creation, 9
- Sciatic nerve block, 80–81
 popliteal fossa, 81
 subgluteal, 81
- Select key, in ultrasound machine, 20
- SFA. *See* Superficial femoral artery (SFA)
- Short-axis view (SAX), 92
- Society of Cardiovascular Anesthesiologists (SCA), 89, 125
- Sonographer, 113
- SonoSite™, 36
- Standards for Ultrasound Equipment*, 15
- Starling curve, 172, 174
- Sternocleidomastoid muscle, 79
- Stratosphere sign, 206
- Stroke volume (SV), 155, 156
 calculation, 155–158
- Subarachnoid hemorrhage (SAH), 179, 192
- Subcostal four-chamber view, of TTE, 105–108
- Subgluteal sciatic nerve block, 81
- Superficial femoral artery (SFA), 66
- Superior vena cava (SVC), 61
- Supervision, ultrasound training, 53–54
 local training program, 53
 skill maintenance, 54
- Supraclavicular brachial plexus blocks, 75–76
- SV. *See* Stroke volume (SV)
- SVC. *See* Superior vena cava (SVC)
- Swept gain, 3. *See also* Time gain compensation (TGC)
- Switching on/off, ultrasound machine, 18
- TAM. *See* Time-averaged mean (TAM)
 velocity
- TCD. *See* Transcranial Doppler (TCD)
 ultrasonography
- TEE. *See* Transesophageal echocardiography (TEE)
- TG. *See* Transgastric (TG) imaging
- TGC. *See* Time gain compensation (TGC)

- Thoracentesis, 201
 Thoracic paravertebral block, 82–83
 Thoracic ultrasound
 in daily practice, 210–212
 limitations, 211
 THR. *See* Transient hyperemic response test (THR)
 Three-dimensional probes, 43
 TI. *See* Tricuspid insufficiency (TI)
 Time-averaged mean (TAM) velocity, 181
 Time gain compensation (TGC), 3, 22.
 See also Swept gain
 Time velocity integral (TVI), 156
 Tissue acoustic impedance, 31
 Tissue harmonic imaging, 23–24
 Tracker ball, in ultrasound machine, 20
 Tragus, 182
 Training
 duration, 51–53
 importance, 48
 levels, 49
 requirements, 49–51
 for senior staff, 54–55
 supervision, 53–54
 local training program, 53
 skill maintenance, 54
 Transcranial Doppler (TCD)
 ultrasonography
 in cerebral hemodynamics, 185–189
 data interpretation, 183–184
 in intensive care, 191–192
 limitations, 184
 principles, 179–181
 techniques, 181–183
 Transducers, 5, 16
 cleaning, 16
 probes, 34–35
 selection, 18
 Transesophageal Doppler, 171
 as hemodynamic monitor, 172–175
 insertion method, 167–171
 perioperative studies, 175–176
 principles, 167–171
 waveform, 171–172
 Transesophageal echocardiography (TEE), 15, 49
 examination technique, 89–101
 deep transgastric view, 98
 descending aorta LAX view, 101
 descending thoracic aorta view, 98
 ME aortic valve LAX view, 93–94
 ME aortic valve SAX view, 92
 ME ascending aortic LAX view, 94
 ME ascending aortic SAX view, 94
 [Transesophageal echocardiography (TEE) examination technique]
 ME bicaval view, 92
 ME four-chamber view, 89–90
 ME LAX view, 91–92
 ME mitral commissural view, 90
 ME right ventricular view, 92
 ME two-chamber view, 90
 TG basal SAX view, 98
 TG LAX view, 96–97
 TG mid-SAX view, 94
 TG right ventricular inflow view, 97
 TG two-chamber view, 95
 UE aortic arch LAX view, 100
 UE aortic arch SAX view, 100
 heart valves. *See* Heart valves, TEE of
 inpatient procedure, 85–86
 outpatient procedure, 85–86
 overview, 85
 probe insertion, 86–87
 probe manipulation, 87–88
 safety and complications, 85
 Transgastric (TG) imaging, 94–95, 117
 basal SAX view, of TEE, 98
 long-axis view, 117
 TEE, 96–97
 mid-short-axis view, of TEE, 94
 right ventricular inflow view, of TEE, 97
 two-chamber view, of TEE, 95
 Transient hyperemic response test (THR), 187–188
 Transthoracic echocardiography (TTE), 111
 apical four-chamber view, 105
 apical LAX view, 105
 apical two-chamber view, 105
 parasternal LAX view, 101–102
 of right ventricle, 102
 parasternal SAX view
 of left ventricle, 104
 of mitral valve, 102
 of right ventricle outflow tract, 102
 subcostal four-chamber view, 105–108
 Transverse approach, for needle visualization, 42
 Tricuspid insufficiency (TI), 136
 Tricuspid regurgitation, 136–139
 Tricuspid stenosis, 140–141
 Tricuspid valve, 135–141
 anatomy, 135
 insufficiency, 139–141
 regurgitation, 136–139
 standard TEE views, 135–136
 tricuspid stenosis, 139–141
 Tricuspid valve area (TVA), 141

- TTE. *See* Transthoracic echocardiography (TTE)
- TVA. *See* Tricuspid valve area (TVA)
- TVI. *See* Time velocity integral (TVI)
- Ultrasonic beam, 180
- Ultrasonography, 179
- Ultrasound
- advantages of, 72
 - echoes, 32
 - gel, 35, 68
 - intensity, 9
 - unit, choice of, 197–198
- Ultrasound-guided nerve block, principles, 73
- Ultrasound-guided regional anaesthetic techniques, 73
- United States, certification of TEE, 108
- Upper esophageal aortic arch LAX view, of TEE, 100
- Upper-esophageal aortic arch long-axis view, 116
- Upper esophageal aortic arch SAX view, of TEE, 100
- V. *See* Blood flow velocity (V)
- Vascular access, ultrasound-guided, 57–69
- applied ultrasound anatomy, 63–67
 - practicalities, 68–69
 - venous system, 57–58
- Vascular examinations, 15
- Vasodilatation, 185
- Vasospasm, 179, 185
- Velocity scale control, in ultrasound machine, 25
- applied physics, 62–63
- Velocity time integral (VTI), 124, 170, 171
- Vena contracta, 139
- Ventricular septal defect (VSD), 162
- Visualization, of epidural space, 82
- Visualization, of superficial vessels, 62
- Voice activation packages, 15
- Volume of Effusion, 201
- VSD. *See* Ventricular septal defect (VSD)
- VTI. *See* Velocity time integral (VTI)
- Wall filter, in ultrasound machine, 25
- WFUMB. *See* World Federation for Ultrasound in Medicine and Biology (WFUMB)
- Windows, 180, 181
- foramen magnum, 181
 - orbital, 181
 - temporal, 181
- World Federation for Ultrasound in Medicine and Biology (WFUMB), 12
- Xenon CT, 185
- X rays, 208, 209
- Zero flow pressure (ZFP), TCD, 188–189
- ZFP. *See* Zero flow pressure (ZFP)
- Zygomatic arch, 182

about the book...

Practical Ultrasound in Anesthesia for Critical Care and Pain Management is a stand-alone comprehensive reference that covers important aspects of ultrasound for the practicing anesthesiologist. Beginning with a background on the physics of equipment and practical applications, this text takes the specialist through subjects like needle visualization, teaching, training, accreditation, and getting the best out of your ultrasound equipment.

With high-resolution ultrasound photographs ***Practical Ultrasound in Anesthesia for Critical Care and Pain Management*** covers topics that explore:

- vascular access
- nerve blockade
- echocardiography
- transesophageal echocardiography - evaluation of the valves
- basic echo Doppler
- transesophageal Doppler
- transcranial Doppler
- the respiratory system

Also included is a fully developed CD, that includes high-resolution video clips of actual ultrasound examples, organized in an easy cross-referenced fashion for the busy clinician.

about the editors...

PHILIP M. HOPKINS is Professor of Anesthesia, University of Leeds, Director, UK National Malignant Hyperthermia Investigation Unit, and Honorary Consultant Anesthetist, Leeds Teaching Hospitals Trust, Leeds, UK. Dr. Hopkins received his M.D. from the University of Leeds, Leeds, UK. Dr. Hopkins currently serves as an Editorial Board member of the British Journal of Anaesthesia and is a member of the ESA Research Committee. Dr. Hopkins's research consists primarily of anesthesia and intensive care medicine in relation to malignant hyperthermia, exertional heat illness and stroke, as well as drug reactions and allergies, and the use of ultrasound-guided techniques in regional anesthesia.

A. R. BODENHAM is Director of Intensive Care and Consultant in Anesthesia, Leeds General Infirmary, Leeds, UK. Dr. Bodenham obtained his M.D. from St. Bartholomew's Hospital in London, UK. Dr. Bodenham specializes in anesthesia and intensive care, with an interest in interventional procedures, as well as vascular surgery and access procedures. Dr. Bodenham continues to perform studies on the airway, as well as central venous access, ultrasound guided procedures, and sepsis management.

SCOTT T. REEVES is the John E. Mahaffey, MD Endowed Professor and Chair of the Department of Anesthesia and Perioperative Medicine at the Medical University of South Carolina, Charleston, South Carolina, USA. Dr. Reeves received his M.D. from the Medical University of South Carolina, Charleston, South Carolina, USA. He did his residencies in Internal Medicine and Anesthesiology at Baylor College of Medicine and advance training in pediatric cardiothoracic anesthesiology at the Texas Heart Institute, in Houston, Texas, USA. Dr. Reeves is a fellow of the American Society of Echocardiography and the American College of Cardiology and is very active as program chair for the Society of Cardiovascular Anesthesiology. Dr. Reeves's research concentrates on scardiac anesthesiology, perioperative transesophageal echocardiography and pain perception in surgery patients.

Printed in the United States of America

DK3560

